UNIVERSITY OF SOUTHAMPTON

FACULTY OF MEDICINE

Cancer Sciences Division

Volume 1 of 1

The Role of Eps8 in Myofibroblast Transdifferentiation

by

Steven James Frampton

Thesis for the degree of Doctor of Philosophy

September 2016

ABSTRACT

Background

Myofibroblasts are central to the pathogenesis of fibrotic disease, but their presence in a range of solid tumours is also an important prognostic factor predicting poorer patient outcome. This specialised, highly contractile cell develops as a result of increases in intracellular and extracellular matrix tension and the activity of the cytokine TGFβ1. It is characterised in fibroblasts by the *de novo* expression of alpha smooth muscle actin (αSMA) stress fibres. Myofibroblasts have been shown to promote many of the 'hallmarks of malignancy' in neighbouring cancer cells including dysregulated growth, resistance to apoptosis, tumour cell invasion and metastasis.

Eps8 is a widely expressed adapter protein that has been identified as a critical regulator of actin organisation and cell motility in a range of cell types. In this study we have assessed the role of Eps8 in fibroblast-to-myofibroblast transdifferentiation.

Methods

Western blotting, quantitative real-time PCR, and RNA-seq techniques were used to assess alterations in expression profiles in cultured human fibroblasts as a result of TGFβ1 treatment or Eps8 downregulation. Immunocytochemistry was used to assess the formation of stress fibres, while gel contraction; Transwell migration; xCELLigence proliferation and TGFβ activation assays were used to assess effects on cell function. Tissue microarrays of a range of fibrotic human organs or oral cancer specimens were used to validate the *in vitro* findings and a mouse xenograft model was used to assess the effect of fibroblast Eps8 expression on human tumour development *in vivo*.

Results

We identified a novel role of Eps8 as a regulator of fibroblast-to-myofibroblast transdifferentiation and demonstrated that Eps8 is downregulated during myofibroblast transdifferentiation induced by TGFβ1 treatment or senescence-inducing stimuli. Suppression of Eps8 by the use of siRNA augments TGFβ1-induced myofibroblast transdifferentiation, and augments cancer cell migration *in vitro* and tumour growth *in vivo*. Eps8 knockdown upregulated SMAD2 expression and augmented TGFβ1-dependent SMAD2 phosphorylation and Nox4 induction. Although Eps8 has several known functions our investigations indicate that the formation of a tricomplex with its binding partners Abi1 and SOS1 is necessary for the regulation of myofibroblast transdifferentiation.

Table of Contents

List of tables

List of figures

DECLARATION OF AUTHORSHIP

I, Steven James Frampton, declare that this thesis and the work presented in it are my own and has been generated by me as the result of my own original research.

The Role of Eps8 in Myofibroblast Transdifferentiation

I confirm that:

1. This work was done wholly or mainly while in candidature for a research degree at this University;
2. Where any part of this thesis has previously been submitted for a degree or any other qualification at this University or any other institution, this has been clearly stated;
3. Where I have consulted the published work of others, this is always clearly attributed;
4. Where I have quoted from the work of others, the source is always given. With the exception of such quotations, this thesis is entirely my own work;
5. I have acknowledged all main sources of help;
6. Where the thesis is based on work done by myself jointly with others, I have made clear exactly what was done by others and what I have contributed myself;
7. None of this work has been published before submission

Signed: .....

Date: .....

Acknowledgements

There are numerous people that I would like to thank for their help and support, enabling me to complete this project. Cancer Research UK generously supported the work and invested in my academic and professional development over the past three years. I would especially like to thank my supervisors Professor Gareth Thomas and Dr Emma King for their invaluable advice and guidance over the last 4 years. I knew that I could trust their experience when difficult decisions concerning the direction of the project needed to be made and that their door was always open whenever I needed them, irrespective of other pressures.

I also owe a particular debt of gratitude to Drs Veronika Jenei, Massimiliano Mellone, and Christopher Hanley for their technical help and support throughout the project. As a medic joining the laboratory, many of the technical procedures were completely new to me and their experience, patience demonstrating new skills or equipment, and advice when I was trouble-shooting, was invaluable. James Clarke and Oliver Wood were also great sources of guidance on bioinformatics and helped to make the subject both manageable and enjoyable.

Four years have passed extremely quickly, but I have made a great many friends not only within the Experimental Pathology group, but the wider Somers Building and WISH laboratory. I wish all that I have met the best of luck for the future in all of their scientific endeavours…

Finally, most importantly, I would like to thank my wife, parents, and the rest of my family for their unquestioning support over the past four years. The unexpected delays leaving the laboratory of an evening, the extra visits at the weekend, and the evenings and weekends spent writing this thesis in full time clinical practice have all had a cost, and I very much appreciate that it has not just been me that shouldered the burden. Thank you, and I hope after all that, you still think it was worth it….

Definitions and Abbreviations

αSMA – αsmooth muscle actin

Abi1 – Abelson interactor 1

ANOVA – analysis of variance

BMP – bone morphogenetic protein

BSA – bovine serum albumin

CAF – cancer-associated fibroblast

CCL4 – carbon tetrachloride

CDK – cyclin-dependent kinase

CTD – C-terminal domain phosphatases

CTGF – connective tissue growth factor

DAPI – 4,6-diamidino-2-phenylindole

DMEM – Dubecco's Modified Eagle's Medium

ECM – extra-cellular matrix

ED-A/B – extra-domain A/B

EGF(R) – epidermal growth factor (receptor)

EndoMT – endothelial to mesenchymal transition

EMT – epithelial to mesenchymal transition

Eps8 – epidermal growth factor receptor kinase substrate 8

Erk – extracellular signal-related kinase

EMT – epithelial – mesenchymal transition

FAK – focal adhesion kinase

FBS – fetal bovine serum

FEP – fibroepithelial polyp

FGF – fibroblast growth factor

GSK – glycogen synthase kinase

FSP-1 – fibroblast-specific protein 1

Grb2 – growth factor receptor binding protein 2

HAT – histone acetylases

HDAC – histone deacetylases

HGF – hepatocyte growth factor

HNSCC – head and neck squamous cell carcinoma

HPV – human papilloma virus

HSC – hepatic stellate cells

IGF – insulin-like growth factor

IHC – immunohistochemistry

IPF – idiopathic pulmonary fibrosis

JNK – c-Jun N-terminal kinase

LAP – latency associated peptide

LLC – large latent complex

LTBP – Latent TGFβ-binding protein

LOX – lysyl oxidase

MLC – myosin light chain

MMP – matrix metalloprotease

MRTF – myocardin-related transcription factor

mTOR – mammalian target of rapamycin

NMSC – non-melanomatous skin cancer

NO synthase – nitric oxide synthase

OSCC – oral squamous cell carcinoma

PARP1 – poly (ADP-ribose) polymerase I

PDGF – platelet-derived growth factor

PDK-1 – phosphoinositide-dependent kinase 1

PI3K – phosphoinositide 3 kinase

PKC – protein kinase C

qRT-PCR – quantitative real-time polymerase chain reaction

R-SMAD – receptor-regulated SMAD

ROS – reactive oxygen species

RTK – receptor tyrosine kinase

SARA – SMAD anchor for receptor activation

SCC – squamous cell carcinoma

SD – standard deviation

SD-1 – stromal cell derived factor 1

SEM – standard error of the means

SLC – Small latent complex

SRF – serum response factor

TAK1 – TGFβ-activated kinase I

TGFβ1 – transforming growth factor β type 1

TIMP – tissue inhibitor of matrix metalloprotease

TMA – tissue microarray

USP – ubiquitin-specific proteases

UVR – ultraviolet radiation

VEGF – vascular endothelial growth factor

Chapter 1: Introduction

1.1 The myofibroblast

1.1.1 Definition

The loose connective tissue that lines and supports epithelial structures in the body has been demonstrated to be critically influential in determining the fate of the epithelial tissues (Pietras & Ostman 2010; Stover et al. 2007). One of the key cell types orchestrating the activity of this tissue stroma is an activated cell called a myofibroblast.

Initial identification of these cells in granulation tissue highlighted some fibroblast-like features, including the presence of a developed endoplasmic reticulum, coupled with features common to smooth muscle cells such as contractile actin microfilament bundles (Gabbiani et al. 1971). The term 'myofibroblast' therefore reflected the combination of the secretory and contractile phenotypes of these cells.

No single marker has been identified that can be used to define a myofibroblast and exclude it from all other cell types. A fully developed myofibroblast displays a collection of features, and some argue that they can only be definitively identified by combining light microscopy, electron microscopy and immunostaining techniques (Eyden 2008). In many circumstances the presence of alpha smooth muscle actin (αSMA) arranged into functional stress fibres is sufficient to identify myofibroblasts, particularly when combined with other information such as a stromal location in tissue sections, or when derived from a known precursor cell population *in vitro*.

The ultrastructural features that help define myofibroblasts reflect their function. The prominent rough endoplasmic reticulum indicates the up-regulation of secretory activity. Myofibroblasts are particularly recognised for secreting cytokines, growth factors, extra-cellular matrix proteins (including type I and III collagen, ED-A and ED-B fibronectin) and tissue remodelling enzymes such as matrix metalloproteases (Vedrenne et al. 2012). Bundled stress fibres containing αSMA underlie the ability of these cells to effect enhanced contractility compared to non-transdifferentiated fibroblasts and are

important for their role in wound repair (Gabbiani et al. 1971; Boris Hinz et al. 2001). Dense fibronexuses, mechanically linking the intracellular contractile apparatus with the extracellular matrix, enable the transmission of cell tension to the extracellular matrix (ECM) but also 'sense' changes in mechanical stress in the micro-environment and transduce the changes into intracellular signalling pathways (Hinz & Gabbiani 2003).

Histological features:

- Spindle-cell or stellate morphology
- Abundant peri-cellular matrix
- Palely eosinophilic cytoplasm

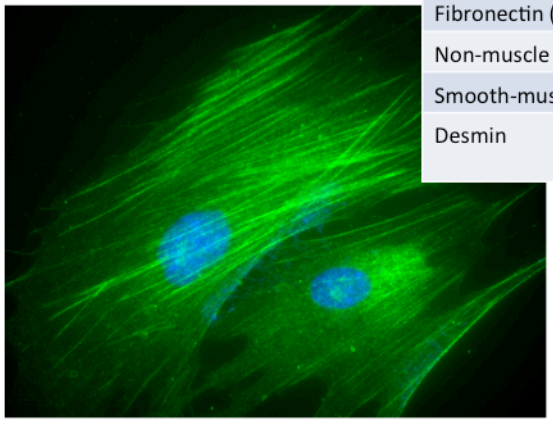

Immunophenotype:

Protein	negative	positive
Vimentin		✓
αSMA		✓
Fibronectin (inc ED-A)		✓
Non-muscle myosin		✓
Smooth-muscle myosin	✓	
Desmin	✓ (or v little)	

Ultrastructure:

- Prominent rough endoplasmic reticulum (ER)
- Golgi apparatus with collagen-secreting granules
- Peripheral myofilaments
- Fibronexus junctions
- Gap junctions

Figure 1-1 Characteristic features of myofibroblasts

Myofibroblasts display a collection of features that facilitate their distinction from both their precursors and from other differentiated cell types such as smooth muscle cells. Although the use of a single marker to assess myofibroblast characterisation can be inaccurate in some circumstances, the *de novo* expression of αSMA in a population of fibroblasts is used by many as an adequate marker of myofibroblast transdifferentiation. αSMA stress fibres are immune-labelled here in green.

1.1.2 Origin

Myofibroblasts are rarely present in tissues in the absence of either tumour, inflammation, or trauma (Eyden et al. 2009) but are recruited to or generated locally in response to these insults.

The cellular lineage from which myofibroblasts are derived remains the subject of much debate and investigation (Kramann et al. 2013). Evidence exists for the differentiation of myofibroblasts from local precursors such as mesenchymal stromal cells, fibroblasts (Rønnov-Jessen & Petersen 1993),

ADAM12+ perivascular cells (Dulauroy et al. 2012) and pericytes (Kramann et al. 2013). Additionally, circulating progenitor cells such as fibrocytes and circulating mesenchymal stromal cells have been implicated (Ishii et al. 2003) while other theories include the de-differentiation of local endothelial or epithelial cells, otherwise known as endothelial (EndoMT) or epithelial to mesenchymal transition (EMT) respectively (Kalluri & Weinberg 2009).

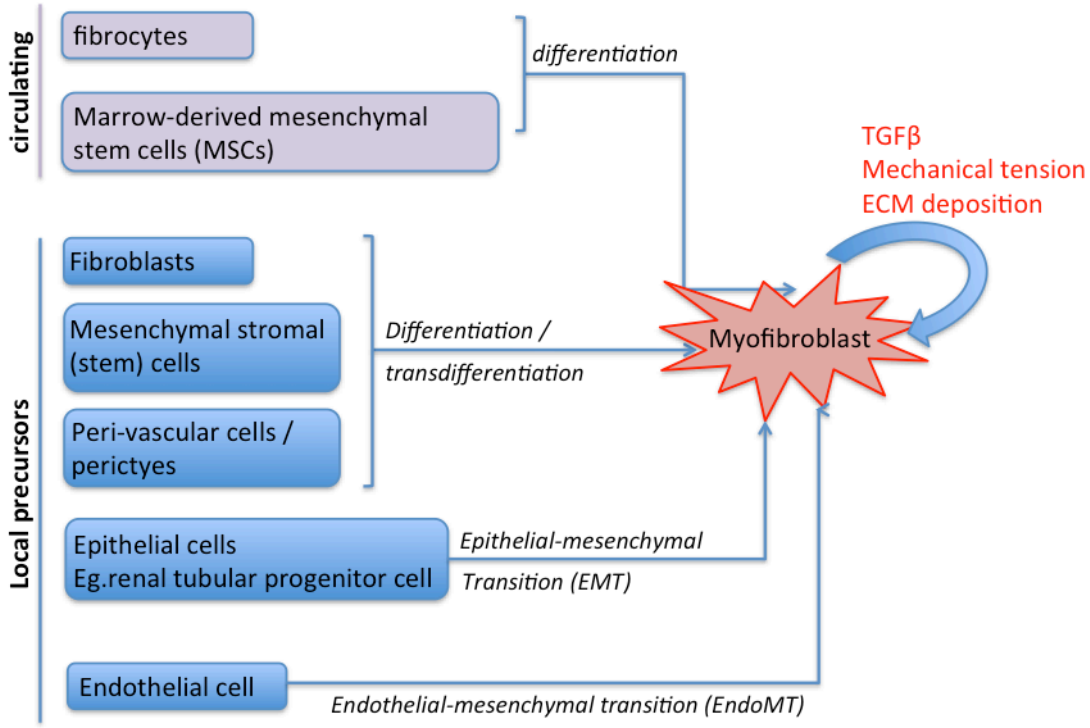

Figure 1-2 Myofibroblasts can differentiate from differing cells of origin

Evidence exists supporting myofibroblast development from a range of precursor cells including differentiation from local interstitial fibroblasts, pericytes or adipocytes; local endothelial and epithelial cells via Endo / epithelial-mesenchymal transition (Endo / EMT); as well as from circulating bone-marrow derived precursors. A number of cytokines are responsible for recruitment of these cells, which combine with tissue tension to drive myofibroblast transdifferentiation.

There is likely to be variation in the source of myofibroblast precursors depending on the tissue type in question and the nature of the tissue injury (LeBleu et al. 2013; Kidd et al. 2012; Hinz et al. 2012), but more complex cell fate studies coupled with advancing knowledge of specific molecular marker combinations, may help to clarify this.

Myofibroblast recruitment, differentiation and proliferation are complex processes mediated by the combined action of cytokines (such as TGFβ),

growth factors (like EGF, FGF, VEGF), intracellular contractility and matrix tension but the immune system also has a critical role in orchestrating the duration of the response. The innate immune system is involved in initial recruitment but mast cells, neutrophils, eosinophils, macrophages and T cells have all been shown to contribute to myofibroblast recruitment and proliferation in the early stages of excessive fibrotic responses (Wick et al. 2013)

1.1.3 Overview of myofibroblast differentiation

The activation of progenitor cells, whatever their origin, into fully contractile myofibroblasts is thought to be a two-stage process (Gabbiani et al. 2012).

Initial activation of the cells by a variety of factors including cytokines or growth factors (including TGFβ), or small increases in extracellular matrix tension initially result in the polymerisation of actin monomers into “F-actin” microfilaments (B Hinz et al. 2001), thought to have sufficient contractile ability to commence extracellular matrix (ECM) remodelling and facilitate cell migration. This phenotype has been coined the ‘proto-myofibroblast’ (Gabbiani et al. 2012). Critically, a particular isoform of actin not normally expressed in non-muscle cells, αSMA, is not incorporated into the contractile filaments at this stage. For the subsequent second stage, to which other appropriate cytokine signals (including TGFβ1) can contribute, mechanical stress is both necessary and sufficient to facilitate complete differentiation of the proto-myofibroblast into a myofibroblast (Olsen et al. 2011). This is accompanied by the incorporation of αSMA into bundled stress fibres, significantly increasing cell contractility (B Hinz et al. 2001).

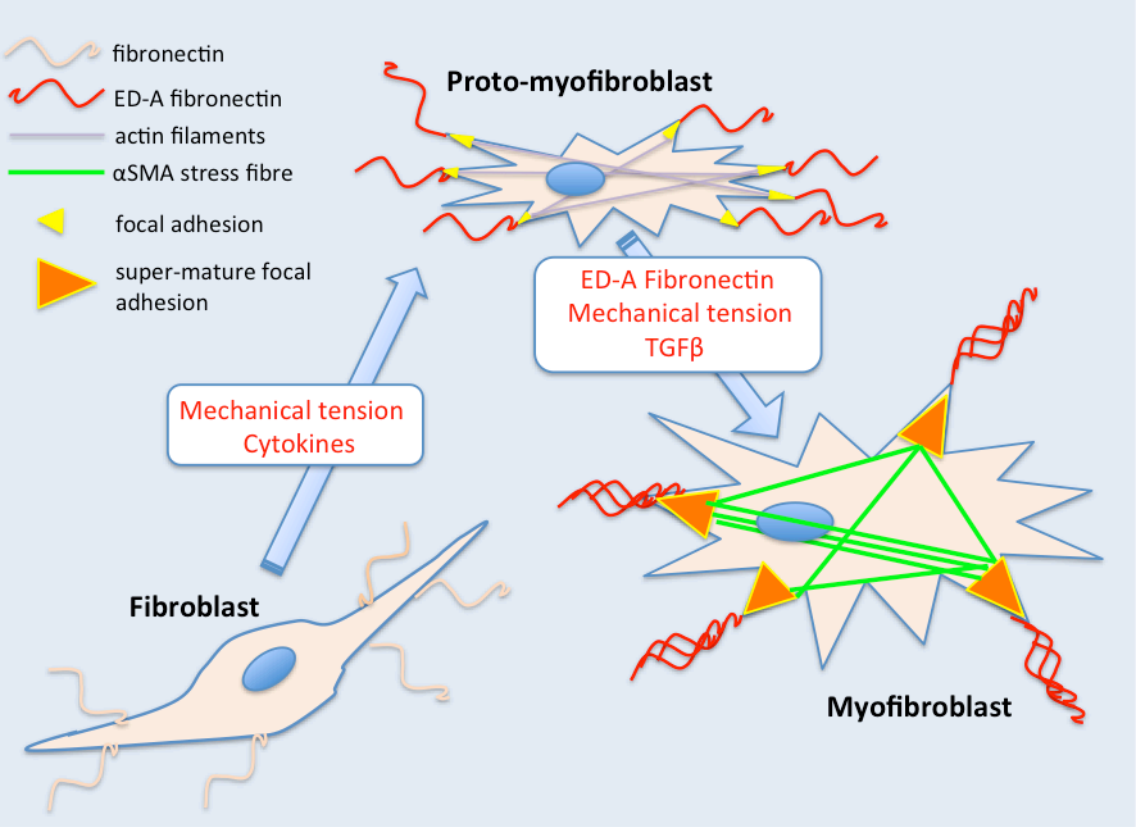

Figure 1-3 The two-stage process of fibroblast-to-myofibroblast transdifferentiation.

Early intracellular tension is required for the expression and secretion of the ED-A splice-variant of fibronectin, and the assembly of an F-actin contractile apparatus with small focal adhesions transmitting tension to the ECM. Further tension, often with the additional effect of cytokines such as TGFβ1, is required for expansion and maturation of the adhesions, enabling the generation of greater tension and incorporation of αSMA into the stress fibres.

1.1.4 Role of tension in differentiation

The ability of the cells to effect and respond to mechanical tension in the surrounding ECM results from the linear connectivity of ECM proteins, via integrins and focal adhesion molecules at the cytoplasmic surface, with the cytoskeleton and contractile apparatus within the cell.

Focal adhesions are membrane-bound multi-molecular anchors between the cell cytoskeleton and the ECM consisting of integrins, integrin-activator proteins (e.g. Talin or Kindlins), structural proteins (e.g. Palladin) and proteins linking the focal adhesion to the actin cytoskeleton (e.g. Focal Adhesion Kinase (FAK) or Integrin Linking Kinase (ILK)) (Karaköse et al. 2010). The focal adhesion not only acts as a mechanical scaffold facilitating cell-ECM and cell-

cell adhesion but also functions as a complex cell signalling *nidus* between the cell and its environment, with conformational changes transmitting 'inside-out' and 'outside-in' signalling. Various cytoplasmic kinases (including Src and phosphatidylinositol-3 kinase) interact with integrins and transmit signals that can facilitate myofibroblast transdifferentiation (Legate et al. 2009).

Focal adhesions are dynamic structures, which augment in response to cell tension. Under low-tension conditions the component integrins are dispersed across the cell surface, rather than forming focal complexes. Intracellular contractility is required for the clustering of integrins to promote formation of focal adhesions, and inhibition of contractility conversely results in their disaggregation (Chrzanowska-Wodnicka & Burridge 1996). The necessary contractility is produced by the force-generating interaction between actin filaments and myosin. This can be promoted by phosphorylation of the regulatory protein myosin light chain (MLC), which in turn has been shown to be modulated by the activity of Rho GTPases (Chrzanowska-Wodnicka & Burridge 1996). Actin-myosin contractility is also required for the development of F-actin stress fibres and proto-myofibroblast development, since inhibition of the actin-myosin interaction by the use of antibodies (Höner et al. 1988) or inhibitors (Chrzanowska-Wodnicka & Burridge 1996) has been shown to prevent their development.

As intracellular and extracellular tension further increases, multiple focal adhesions can fuse together. This expansion of the focal adhesion is thought to re-equilibrate the force per unit area exerted on the intracellular apparatus and allows greater contractile force to subsequently be communicated from the cell to the ECM (Van De Water et al. 2013). It has been shown that only when focal adhesions become longer than 8μm can αSMA be recruited to stress-fibres, suggesting that there is a minimum tissue tension for myofibroblastic differentiation (Goffin et al. 2006). Once this threshold has been exceeded accumulation of αSMA into pre-made stress fibres produces a step-change in cell contractility and augments the feed-forward cycle of tension generation.

As discussed previously the fibronexus, where intracellular stress fibres are mechanically coupled to the ECM, is an ultrastructural marker of the myofibroblast phenotype and fibronectin is an essential component of the

fibronexus. A particular splice variant, ED-A fibronectin, is expressed and secreted by cells only when they develop a protomyofibroblast phenotype (Tomasek et al. 2002). The use of extracellular antibodies against it have shown that it is required for subsequent αSMA expression, collagen type I expression (Serini et al. 1998), and the formation of a sufficiently large focal adhesion to allow myofibroblast transdifferentiation (Dugina et al. 2001). Notably the presence of monomeric rather than polymeric ED-A fibronectin fails to produce the same effect (Serini et al. 1998) implying that the effect results from the interaction of ED-A fibronectin with its environment.

Increasing cell tension not only promotes a more contractile phenotype but also up-regulates the expression of a number of genes essential for the myofibroblast phenotype (Sun et al. 2006; Wang et al. 2002). Serum-response factor (SRF) is a constitutively expressed transcription factor that gains significantly more activity when joined by cofactors of the myocardin-related transcription factor (MRTF) family. A particular member of the family, MRTF-A, is bound to and inactivated by monomeric G-actin in the resting state (Miralles et al. 2003; Van De Water et al. 2013). When intracellular contractility increases and G-actin is encouraged to polymerise to form F-actin, MRTF-A dissociates and translocates to the nucleus where it binds with SRF to target promoter regions (Miralles et al. 2003). As a result of experiments over-expressing MRTF-A or knocking down MRTF-A/B it has been shown that these transcription factors are both necessary and sufficient for myofibroblast differentiation (Crider et al. 2012).

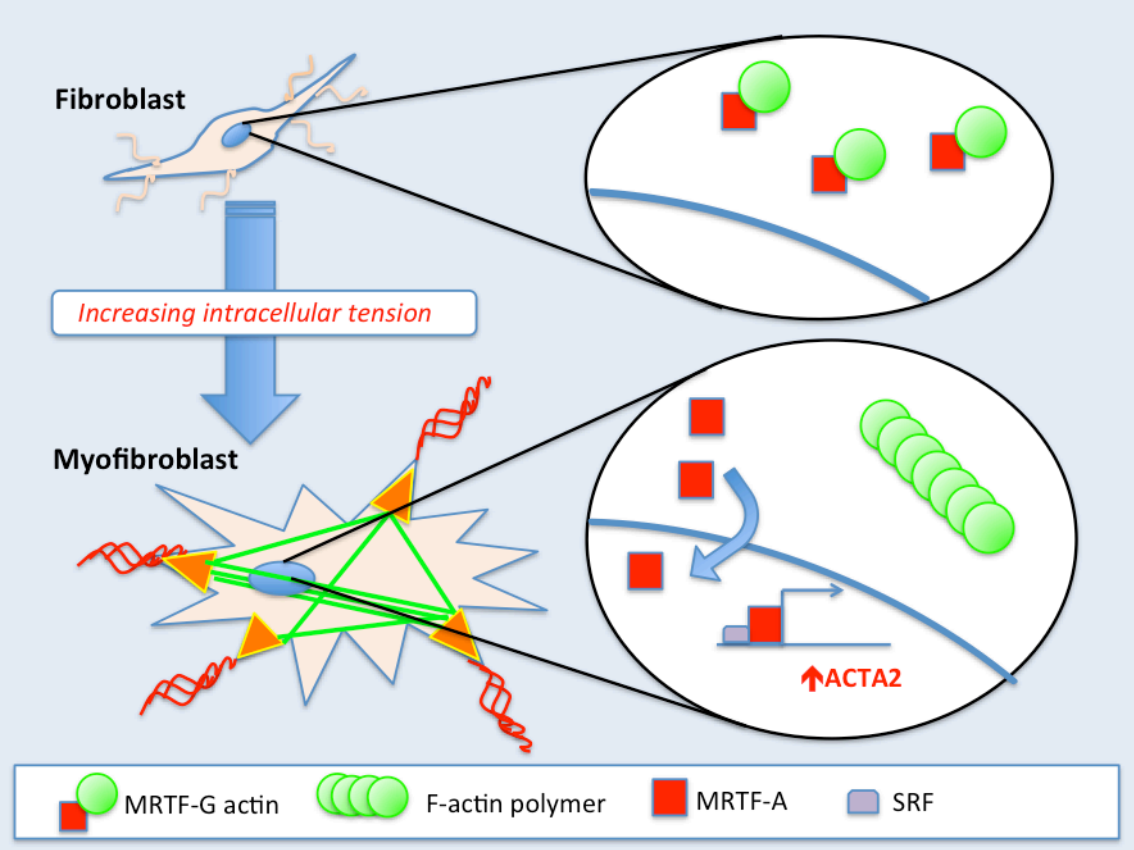

Figure 1-4 Increased intracellular tension drives expression of myofibroblast genes.

Binding to monomeric G-actin sequesters MRTF-A in the cytoplasm. As actin polymerises into filamentous (F) actin MRTF-A is released and translocates to the nucleus where it binds as a co-activator with SRF to up-regulate the transcription of a number of genes contributing to the myofibroblast phenotype.

Given that there is some actin-myosin mediated intracellular contractility within non-activated, migrating fibroblasts it is currently unclear whether a migrating fibroblast creates sufficient tension, combined with cytokine / growth factor signalling, to trigger protomyofibroblast development (Van De Water et al. 2013). Other causes of increased tissue tension that could potentially trigger myofibroblast differentiation have been identified. Increased flow of interstitial fluid through the extra-cellular matrix, as occurs with the inflammatory milieu following tissue injury, has been shown to provide sufficient mechanical force to trigger differentiation (Ng et al. 2005). Induction of collagen type I cross-linking in the extracellular matrix, catalysed by lysyl oxidase (LOX) enzymes has been shown in some models of fibrosis to increase tissue stiffness prior to myofibroblast development or the up-regulation of collagen secretion (Georges

et al. 2007). Antibody-mediated inhibition of LOX-L2 reduces myofibroblast differentiation, the extent of fibrosis, and settling of metastases in a variety of models of cancer and fibrosis (Barry-Hamilton et al. 2010). Such small increases in ECM tension may therefore be sufficient to send myofibroblast precursors on a path towards protomyofibroblast and subsequent myofibroblast development.

The importance of avoiding tissue tension, and so myofibroblast induction, in surgically repaired wounds to minimise scar formation is well recognised and modern surgical techniques minimise wound tension. In vivo models of skin wounds placed under external separating tension show earlier expression of myofibroblastic markers (ED-A fibronectin and αSMA) than controls (B Hinz et al. 2001). Furthermore, tension-free wounds, unlike splint-separated wounds, demonstrate a gradual reduction of myofibroblastic markers commencing at around day 10 and a greater number of apoptotic figures, suggesting that myofibroblast deactivation is at least partly achieved through apoptosis (Carlson et al. 2003).

As will be shown in later sections, TGFβ1 signalling is critically important for myofibroblast development, tissue fibrosis, and tumour-stroma cross-talk. It was initially felt that TGFβ1 signalling and mechanical tension were distinct mechanisms necessary for myofibroblast differentiation but it has subsequently been shown that mechanical tension can cause activation of latent TGFβ1 that has been previously secreted into the extracellular matrix (Gabbiani et al. 2012).

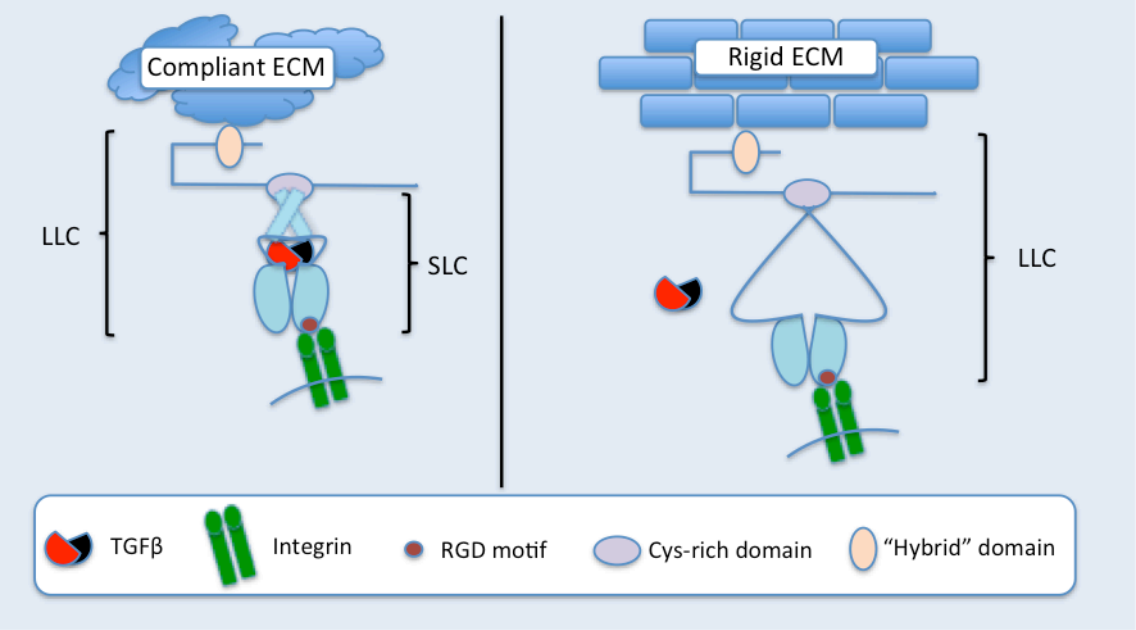

Figure 1-5 TGFβ1 is bound in an inactive state on the ECM and released by mechanical tension.

In the absence of mechanical tension through the Large Latent Complex (LLC), inactive TGFβ1 is restrained by the closed conformation of the "straitjacket" module of the Latency Associated Peptide (LAP) within the Small Latent Complex (SLC). When the LLC experiences an adequate increase in tension, as a result of binding to a rigid extracellular matrix and intracellular force transmitted through activated integrins binding via RGD domains, a conformational change occurs in LAP. This unfolds the straitjacket domain and releases active TGFβ1 to act on nearby cell-surface TGFβ receptors.

TGFβ1 is synthesised in a number of cell types as a pro-peptide, and once cleaved from its N-terminal sequence, it remains attached to the remaining 'Latency-Associated Peptide' (LAP) by non-covalent bonds to form a unit termed the Small Latent Complex (SLC). Prior to secretion of the SLC from the cell it is bound to a member of the fibrillin protein family called 'Latent TGFβ-Binding Protein' (LTBP) to form the 'Large Latent Complex' (LLC). The LTBP tethers TGFβ1 to the extracellular matrix and LAP restrains TGFβ1 preventing access to its interactive domains (Annes 2003).

A number of integrins have been demonstrated to mediate TGFβ release and activation by binding to LAP at RGD (Arg-Gly-Asp) motifs. Integrins αvβ3, αvβ5, and αvβ6 (the latter only expressed by epithelial cells) all activate TGFβ via the transduction of mechanical force to the LLC but αvβ8 activates TGFβ purely by guiding proteases to the complex (Mu et al. 2002). Release of TGFβ requires integrin-binding and tension on LAP, co-incident with counter traction via a

stiffened extracellular matrix and LTBP. The resulting conformational change in LAP releases TGFβ1 which can act in conjunction with tissue tension to effect further myofibroblast differentiation (Gabbiani et al. 2012). In this way a positive feed-forward loop of force-dependent TGFβ-driven transdifferentiation is created. Release of TGFβ1 from its restraining proteins can also result from enzymatic cleavage by plasmin (Lyons et al. 1988) or matrix metalloproteases (MMPs) (Yu & Stamenkovic 2000). In addition, Thrombospondin-1 can bind to the LLC producing a conformational change and subsequent TGFβ1 release (Murphy-Ullrich & Poczatek 2000).

TGFβ1is also transferred to myofibroblast precursor cells within exosomes (Webber et al. 2010). Cancer cells from a range of tissues produce such exosomes, which entrain myofibroblast transdifferentiation in their target precursors (Cho et al. 2012; Cho et al. 2011; Chowdhury et al. 2015). Exosomal TGFβ1 has been observed to generate a phenotype distinct from that induced by secreted TGFβ1 with, in some cases, greater inferred ability to induce angiogenesis and tumour invasiveness (Chowdhury et al. 2015).

1.1.5 Mechanism of prolonged tissue tension

The mechanism of delivery of the longstanding contraction of myofibroblasts, which outlasts the longevity of both skeletal and smooth muscle contraction is not fully understood. One theory is that of a ratchet-type mechanism, where the strong and far-reaching RhoA/ROCK-mediated contraction of the myofibroblast is followed and reinforced by weak and repeated calcium-dependant contractions (Castella et al. 2010). The latter are proposed to straighten and remodel the collagen matrix from which the tension has been released by the stronger initial force, maintaining the tissue tension when the RhoA/ROCK dependant force is removed. Thus the effective tension within tissue stroma is maintained not only by intracellular contractility but by functional remodelling of the ECM, resulting in a positive feed-forward increase in tissue tension and myofibroblast transdifferentiation.

1.1.6 Role of cytokines and growth factors in differentiation

Many growth factors and cytokines have been shown to contribute to myofibroblast differentiation, including components of hedgehog (Hh)–Gli; platelet-derived growth factor (PDGF); connective tissue growth factor (CTGF); epidermal growth factor (EGF); transforming growth factor (TGFβ1); Wnt; and Notch signalling pathways (Kramann et al. 2013). TGFβ1 is widely accepted to be the most potent of these (De Wever et al. 2008) and is the most frequently used in *in vitro* myofibroblast models.

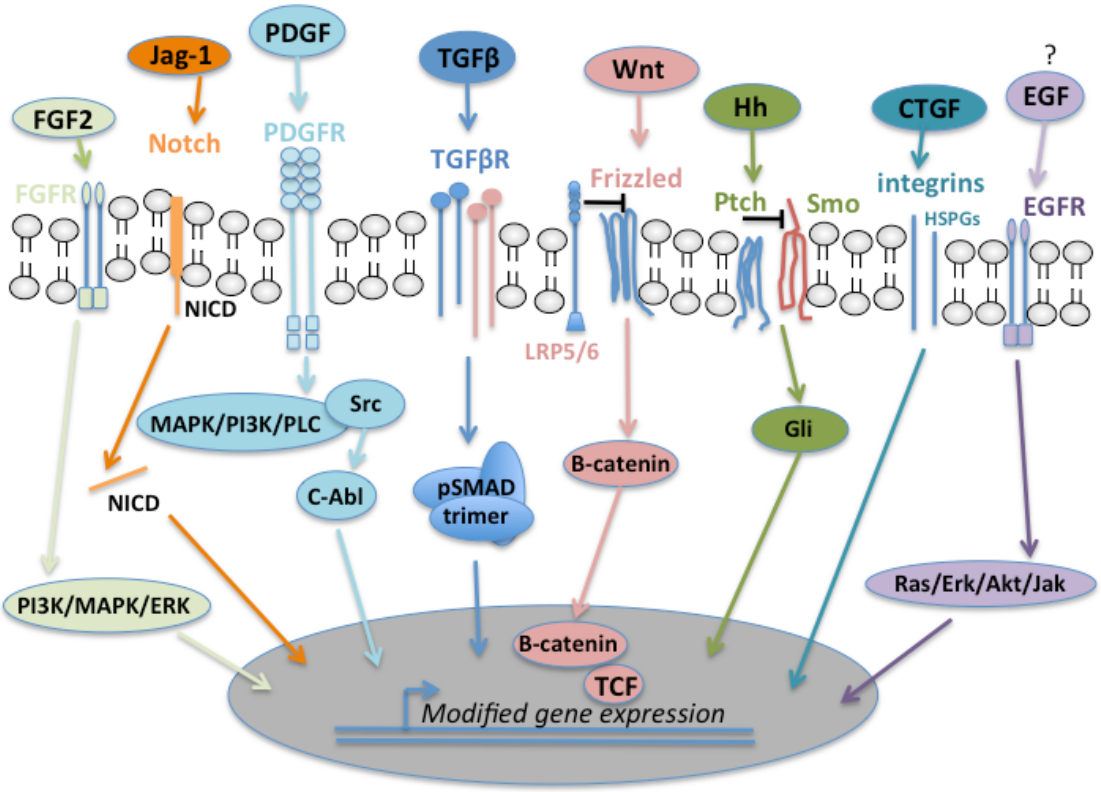

Figure 1-6 Multiple cytokines and growth factors contribute to myofibroblast differentiation

Current understanding of the interplay between different signalling pathways involved in myofibroblast differentiation is limited, but members of multiple signalling pathways contribute to myofibroblast differentiation. The best characterised of these pathways are shown above. While FGF2 promotes transdifferentiation FGF1 & 9 inhibit transdifferentiation (Zhang et al. 2016; Joannes et al. 2016). Although EGFRs are only sparsely located on fibroblasts they are more prominent on other myofibroblast precursors and can promote transdifferentiation (Kramann et al. 2013).

1.1.6.1 TGFβ1 signalling

TGFβ signalling has a key role in maintaining homeostasis and regulating a number of activities during development, in health and in the development of disease (Stover et al. 2007). In health and during early tumorigenesis autocrine and stromal-derived TGFβ is normally growth-suppressive to epithelial cells. As tumorigenesis proceeds the effect of TGFβ is considerably more complex. The growth-inhibitory effect of TGFβ on epithelial cells wanes as TGFβ levels in the tumour microenvironment increase (Roberts & Wakefield 2003). This is felt to be commonly due to downregulation, silencing or inactivating mutations developing in the TGFβ signalling cascade (Bierie & Moses 2006). As tumorigenesis progresses TGFβ signalling becomes able to promote metastatic behaviour through the induction of epithelial to mesenchymal transition (EMT), but a complete absence of TGFβ signalling may also promote metastatic behaviour (Bierie & Moses 2006).

TGFβ also targets multiple cell types in the tumour stroma contributing to many critical processes including inflammation, angiogenesis and immune evasion (Bierie & Moses 2006). TGFβ is the best characterised and most potent secreted factor influencing myofibroblast development and has been the focus of much research (De Wever et al. 2008).

It is thought that the most effective TGFβ signal is transmitted through the 'canonical' SMAD signalling pathway but additional signals are transmitted through several other ('non-canonical') pathways (Massagué 2012; Bierie & Moses 2006). The overall effect of a positive TGFβ signal is determined by modulation of the core signal at a number of levels by a number of different mediators, in some cases enabling a reversal of the signal's effect. In the following sections I will first discuss the best characterised 'canonical' pathway and then its modulation.

1.1.6.1.1 The core signal of the canonical SMAD pathway

From analysis of the human genome there are up to 42 members of the TGFβ superfamily, of which eight Bone Morphogenetic Proteins (BMPs), five Activins and three TGFβ proteins have been identified and characterised (Feng & Derynck 2005). Of the TGFβ subfamily TGFβ1 is considered the most

significant and best characterised in myofibroblast differentiation (De Wever et al. 2008).

On ligand binding, the receptors for the TGFβ family form a tetrameric configuration composed of a homodimer of a type II receptor, with constitutive serine/threonine kinase activity, and a homodimer of a type I receptor (Derynck & Zhang 2003). The type I receptor is phosphorylated by the type II receptor, the resultant conformational change activating its kinase activity and producing a binding site for receptor-regulated SMAD proteins (R-SMADs) (Huse et al. 2001). The receptor tetramer has strong serine/threonine kinase activity. There are seven type I and five type II receptors identified in humans but the TGFβR1/TGFβR2 combination carries most of the TGFβ signal from TGFβ1,TGFβ2 or TGFβ3 ligands (Massagué 2012).

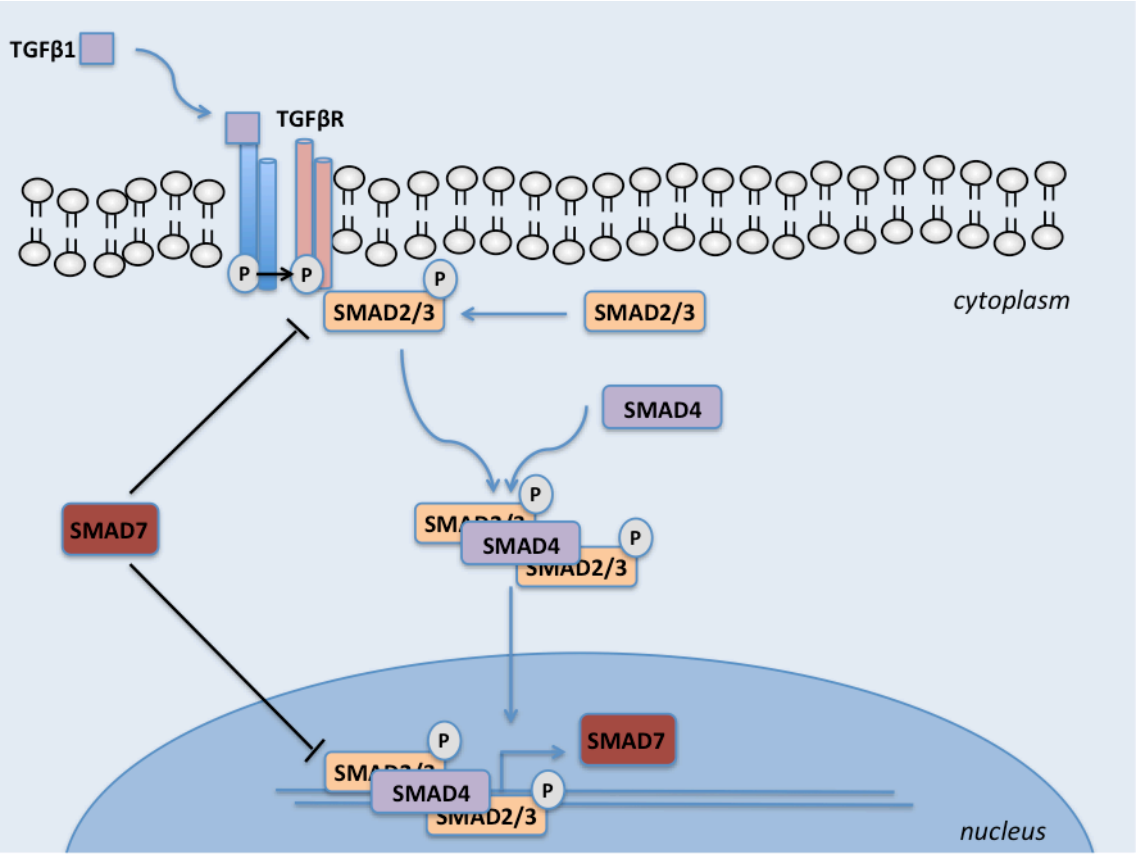

Figure 1-7 Canonical signalling pathway for TGFβ

TGFβ binds to the TGFβR1-R2 receptor tetramer resulting in its autophosphorylation, and the subsequent binding and phosphorylation of SMAD2 or SMAD3. Phosphorylated SMAD2/3 forms a trimer with SMAD4 and translocates to the nucleus, binding with co-activators or co-repressors to regulate transcription. SMAD7 expression is upregulated by SMAD2/3 phosphorylation and acts at multiple levels to provide negative feedback to the signal.

The R-SMAD family comprises of SMAD1,2,3,5 and 8. Initially, it was thought that SMADs 2 and 3 only bind to, and are phosphorylated by, signalling through the TGFβR1/TGFβR2 receptor tetramer. SMADs 2 and 3 however, are also activated by Activin and Nodal signalling through a different type I/II receptor combination, while SMAD1,5 and 8 are activated by BMP signalling and by high TGFβ concentrations via ALK I/TGFβRII tetramers (Feng & Derynck 2005; Pardali et al. 2010).

Phosphorylation of SMAD2 and 3 by type I TGFβR subunits is at an *SXS* motif in their C-terminal domain. An accessory protein termed 'SMAD Anchor for Receptor Activation' (SARA) has been shown to be important for the efficient recruitment and phosphorylation of SMADs 2 and 3 to the receptor subunits and truncated versions of SARA impair TGFβ signalling (Wu et al. 2000; Tsukazaki et al. 1998). Phosphorylation of the R-SMAD tail region by the receptor complex causes dissociation from the TGFβR and formation of a trimer with the co-SMAD, SMAD4. This trimeric complex is then translocated to the nucleus and interacts with a variety of transcription factors, co-activators and co-repressors to modulate the transcription of various genes (Chen & Xu 2010; Hill 2009; Massagué 2012).

SMAD proteins contain two conserved domains, the N-terminal Mad homology 1 (MH1) and the C-terminal Mad homology 2 (MH2) domains. Of these, the MH2 domain is mainly responsible for SMAD oligomerisation, recognition by type I receptors and binding to cytoplasmic adaptors and transcription factors. The MH1 domain plays a crucial role in the nuclear localisation of R-SMADs via importin-α and β, which is mainly driven by the gradient of RanGTP (Kurisaki et al. 2001; Moustakas et al. 2001).

In the nucleus the R-SMAD trimers bind to SMAD-binding-elements (SBEs) on DNA to effect the activation or repression of target genes. The additional binding of co-activators or repressors and other DNA-binding partners provides both specificity and flexibility to the signal outcome (Massagué 2012).

1.1.6.1.2 Modulation of the canonical SMAD signal

A particular cell's response to TGFβ1 signalling is time and situation specific and modulation of the signal occurs at many levels.

Even before the TGFβ receptor is activated there are several potential modifying influences on the TGFβ signal. Firstly, there are three different isoforms of TGFβ – 1,2, and 3. TGFβ1 is the most potent activator of the TGFβ signalling pathway, predominantly due to higher affinity of the receptor for this ligand (Cheifetz et al. 1990) and TGFβ1 expression and secretion is regulated and known to increase with myofibroblast transdifferentiation and to be up-regulated in the tumour microenvironment. The storage of TGFβ1 in a latent state bound to the ECM, as shown in earlier sections, provides an additional level of regulation (Gabbiani et al. 2012). TGFβ1 bound to the Large Latent Complex requires either enzymatic cleavage or a threshold level of ECM stiffness to release the active TGFβ1. Additionally, pH shifts and reactive oxygen species (ROS), potentially resulting from tissue trauma, radiotherapy and even the presence of local tumour are known to cause increased TGFβ1 activation (Barcellos-Hoff & Dix 1996). Finally, there are cell surface accessory proteins, including betaglycan that have been noted to enhance TGFβ affinity for its receptor and receptor responsiveness although their purpose in the modulation of TGFβ signalling has not been fully elucidated (Feng & Derynck 2005; Wiater et al. 2006).

Alternative type I TGFβ receptor subunits including ALK 1,2 and 3 have been shown to interact with the TGFβ-selective type II receptor subunit TGFβRII and transmit TGFβ1 signals. The relative quantity of different type I receptors depends critically on the species and cell type (Goumans et al. 2003; Daly et al. 2008). Endothelial cells, for example have been shown to preferentially express the ALK1 type I subunit, whereas the metastatic breast line EpH4 expresses ALK2, and MDA-MB-231 express ALK2 and ALK3. Kinase activity of the TGFβR1 (ALK5) receptor subunit has been shown to be required for activation of the ALK1/2/3 subunit by TGFβ1 and the ensuing phosphorylation of SMAD1 and SMAD5. This has led to the proposition of a TGFβRII + TGFβRI + ALK1/2/3 receptor complex, which may explain the phosphorylation of SMAD1/5 in NIH-3T3 mouse fibroblasts in response to TGFβ1 (Daly et al. 2008). The mix of R-SMADs resulting from ALK5 and ALK1/2/3 activation produce additional mixed

SMAD complexes containing both SMAD2/3 and SMAD1/5 monomers bound to SMAD4. This pool of transcriptional complexes resulting from TGFβ1 activation initiate a broader range of responses with transcription at novel elements as well as canonical SMAD2/3-SMAD4 TGFβ-responsive elements but they do not bind to traditional BMP-responsive elements. Differential affinity of alternative type I receptors for TGFβ1 can effectively create a dose-dependant response to TGFβ1 treatment. Signalling may be predominantly down the canonical pathway at low TGFβ1 concentrations, but as it increases low affinity ALK1/2/3 receptors are activated and additional non-canonical SMAD signalling ensues (Daly et al. 2008). In endothelial cells TGFβ signalling through ALK1 and ALK5 receptors transmits opposing effects on proliferation and migration and the outcome for the cell depends on the ratio of these two signals (Goumans et al. 2003).

Activities of R-SMADs are influenced by interacting factors from other signalling pathways and negative feedback affecting the degradation of TGFβ receptors and activation and degradation of R-SMADs. R-SMADs structurally contain two globular MH domains joined by a linker region. In addition to their phosphorylation by TGFβRI at their C-terminal tail region, SMADs also contain multiple phosphorylation sites within the linker region, activation of which modifies their function. Cyclin-dependent Kinase 8 and 9 (CDK8 and CDK9) are components of the DNA binding complex called 'mediator' and, in the presence of SMAD4 and tail-phosphorylation of the R-SMAD they phosphorylate, in a TGFβ-dependant manner, sites in the linker region on SMAD1,2 or 3. This results in increased transcriptional activity of the SMAD complex and may depend on the recruitment of additional factors such as YAP, a transcriptional co-activator in the hippo signalling pathway (Chen & Wang 2009). CDK4, which is normally involved in progression from G1 of the cell cycle, also phosphorylates these linker regions, but this immediately targets them for ubiquitin-mediated degradation. While small C-terminal domain phosphatases (CTDs) can de-phosphorylate these linker regions, thereby dissociating linker-binding proteins and recycling the complex, continued linker phosphorylation can result in further linker phosphorylation by glycogen synthase kinase 3 (GSK3). This creates binding sites for E3 ubiquitin-ligases, which facilitate R-SMAD ubiquitylation followed by proteasome-mediated degradation. In the case of SMAD2/3 the responsible E3-ubiquitin ligase is

'Neural precursor cell Expressed Developmentally Down-regulated protein 4-Like' (NEDD4L), which has been shown to restrict the amplitude and duration of TGFβ-induced responses (Gao et al. 2009). NEDD4L is regulated by phosphorylation by 'Serum/Glucocorticoid regulated Kinase I' (SGKI), itself modulated by a range of inflammatory cytokines including TGFβ and the same factors that stimulate PI3K signalling (Lang & Cohen 2001).

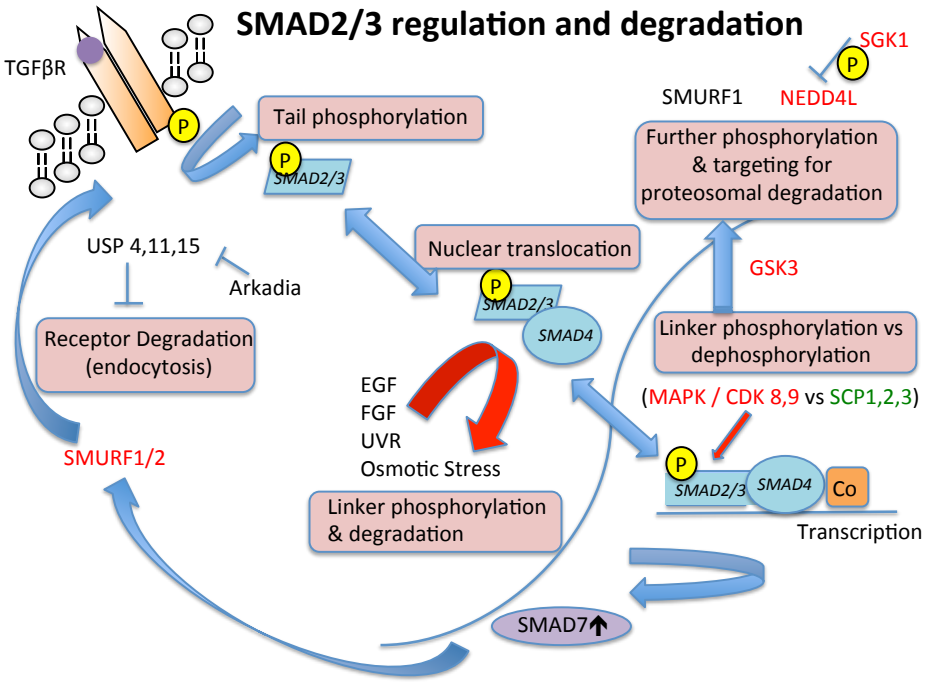

Figure 1-8 Receptor SMAD regulation and degradation

Ligand activation of the TGFβ receptor complex results in binding and tail phosphorylation of SMAD2 and SMAD3 facilitating formation of an oligomeric complex with SMAD4 and transportation into the nucleus. SMAD7 transcription is induced by the subsequent formation of a SMAD3-dependent DNA-binding complex. SMAD7 provides negative feedback on TGFβ signalling by competing with SMAD2/3 for receptor binding and activation and by recruiting E3 ubiquitin ligases to the TGFβ receptor facilitating their degradation. Phosphorylation of the linker region on SMAD2/3 may increase their activity but further phosphorylation by glycogen synthase kinase 3 or linker phosphorylation by growth factors, UV radiation or osmotic stress targets the R-SMADs for proteosomal degradation.

Tail phosphatases remove the C-terminal phosphate from activated R-SMADs, returning them to their basal state and terminating signalling through them (Bruce & Sapkota 2012). SMAD6 and SMAD7 are 'inhibitory' SMADs and their expression is induced by TGFβ1 signalling and R-SMAD-activated transcription. SMAD7 is more potent in this regard than SMAD6 (Miyazono 2000) and has been shown to act by migrating from the nucleus to the cytoplasm: (1)

competing with R-SMADs for binding to TGFβRs and (2) recruiting SMURF2 to the TGFβ receptor to facilitate ubiquitination and degradative endocytosis, limiting ongoing TGFβ signalling (Kavsak et al. 2000; Ebisawa et al. 2001). Ubiquitin specific proteases 4, 11 and 15 counteract this activity. Interestingly USP15 is also recruited by SMAD7 creating a balance between receptor survival and degradation (Massagué 2012). Further limitation of TGFβ1 signalling is provided by Poly (ADP-Ribose) polymerase 1 (PARP1), which triggers SMAD complex dissociation by ADP-ribosylating SMAD3 and SMAD4 (Lönn et al. 2010), and the induction of Ski/SnoN (nuclear oncoproteins which bind to R-SMADs and SMAD4 and disrupt their interaction) (Stroschein 1999; Wu et al. 2002). Both Ski and SMAD7 are themselves ubiquitinated by another E3 ubiquitin ligase termed Arkadia (Levy et al. 2007; Koinuma et al. 2003). It can therefore be seen that there is significant complexity to regulation of signalling within the TGFβ pathway.

1.1.6.1.3 Regulation of canonical transcription by SMADs

The R-SMAD-co-SMAD complex in isolation only has weak transcriptional activity, but its binding of DNA binding partners that target specific DNA sequences, provide specificity and increased binding affinity (Massagué 2012). Clearly modification of the binding partners available for the SMAD complex has a profound effect on the effect of the transmitted TGFβ1 signal.

The epigenetic environment provides a further level of regulation, limiting the DNA that is available for transcription at any point in time (Massagué 2012). Regulation of transcription occurs through the recruitment to the SMAD complex of histone acetylases (HATs) such as p300 or CBP, which stimulate transcription, or deacetylases (HDACs) such as C-terminal binding protein (CTBP), which repress transcription (Massagué et al. 2005). While methylation status has potential to influence the repertoire of transcribed genes in response to a TGFβ1 signal, focal, signal-directed DNA demethylation has also been demonstrated in response to TGFβ signalling allowing the transcription of a CDK4 inhibitor and repression of cell proliferation (Thillainadesan et al. 2012).

1.1.6.1.4 Non-canonical signalling through TGFβ receptors and external influences on TGFβ1 signalling

TGFβ1 is known to cause activation of several non-canonical TGFβ signalling pathways including those involving small GTPases RhoA and Rac1, Protein Kinase C (PKC), Phosphoinositide-3-Kinase (PI3K), TGFβ-associated Kinase 1 (TAK1) and Extracellular signal-related Kinase (Erk) (see Figure 1-9) (Mu et al. 2012). Similarly, members of numerous pathways have been shown to impact on TGFβ1-dependent SMAD signalling. Some of the better-understood interactions of TGFβ receptors are highlighted below.

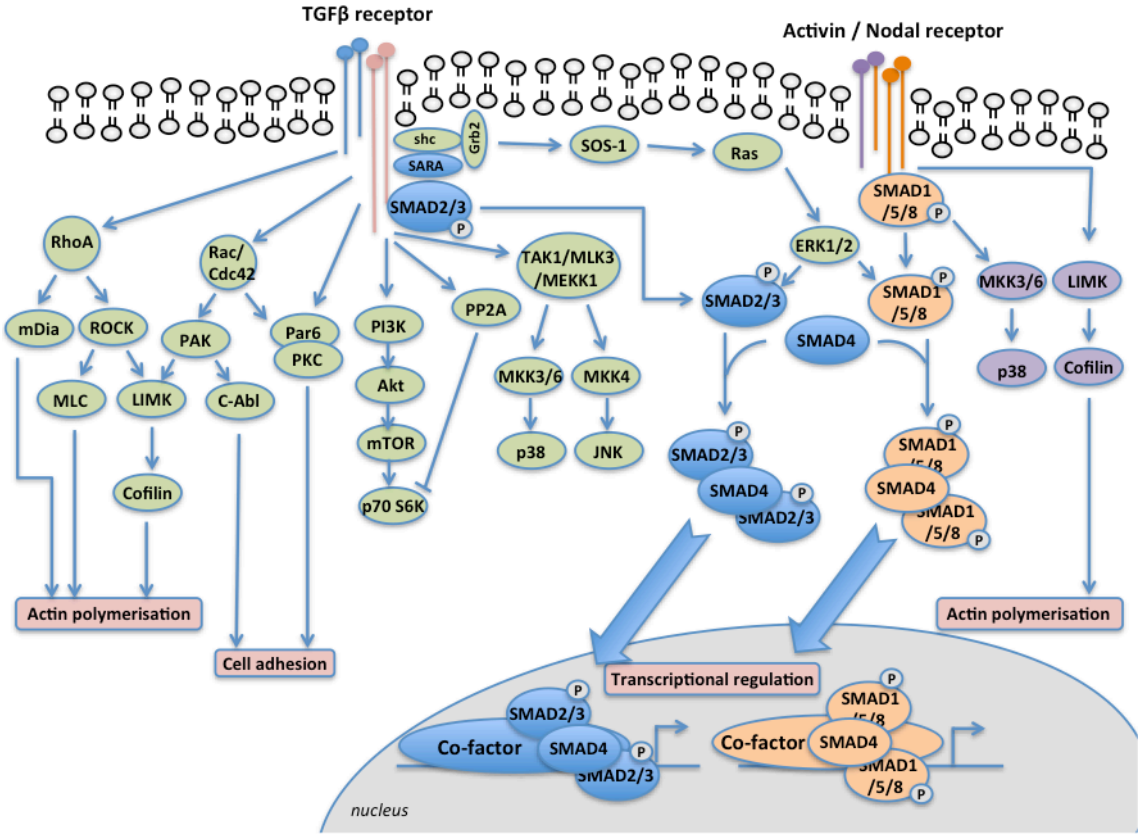

Figure 1-9 Canonical and non-canonical signalling pathways activated by TGFβ and BMPs.

Canonical TGFβ pathway is shown in blue, while non-canonical signalling pathways connected to TGFβ receptors are shown in green. Activin / nodal-mediated SMAD signalling is demonstrated in orange, while non-SMAD dependent pathways are shown in purple.

The ability of TGFβR subunits to phosphorylate tyrosine as well as serine/threonine residues in fibroblasts, underlies their ability to activate the Ras-Raf-Erk-MAPK pathway. Following TGFβ activation the TGFβRI subunit can

phosphorylate the Shc1 adaptor, triggering recruitment of Growth Factor Receptor Binding protein 2 (Grb2) and binding of Ras guanine nucleotide exchange factor Son of Sevenless (SOS-1). This catalyses the removal of GDP from Rac1, allowing GTP-binding and activation of the Erk-MAPK signalling cascade, triggering cell proliferation and migration (Lee et al. 2007). In addition, in mammary epithelial cells, Src can phosphorylate a tyrosine residue in the TGFβRII subunit, also recruiting Shc and Grb2 and activating the p38 MAPK pathway (Galliher & Schiemann 2007). It is possible that the inherent tyrosine kinase activity of the TGFβRII receptor may be sufficient, in the absence of TGFβ1, to activate non-canonical signalling (Mu et al. 2012). It has been shown that the relative expression of the TGFβRII subunit on the cell surface may help to regulate activity through Erk1/2 signalling, with high expression of this subunit in dermal fibroblasts causing greater Erk1/2 activation via TGFβ compared to epithelial cells (Bandyopadhyay et al. 2011).

Tumour necrosis factor α receptor-associated factor 6 (TRAF6) is a ubiquitin ligase which, following TGFβ activation is recruited to the cytoplasmic domain of TGFβRI. Via ubiquitylation, TRAF6 activates itself and TGFβ-activated kinase I (TAK1) leading to activation of p38 (via MKK3/6), and c-Jun N-terminal kinase (JNK) cascades promoting apoptosis and cell migration in HEK 293 cells (Sorrentino et al. 2008; Yamashita et al. 2008). TAK1 has also been shown to activate the NF-κB pathway potentially influencing inflammatory responses, and survival signalling (Adhikari et al. 2007). JNK itself, often activated by stress or mitogenic signals, has been shown to phosphorylate SMAD3 at a non-SXS motif, enhancing both its activation and nuclear translocation in lung epithelial cells (Engel et al. 1999). In endothelial cells MAPK kinase kinase kinase I (MEKK-I), which activates JNK and Erk MAPK, has also been shown to phosphorylate and activate SMAD2 leading to increased SMAD complex formation and target transcription (Brown et al. 1999).

The PI3K-AKT pathway is also activated by TGFβ and can transmit signals effecting EMT in epithelial cells (Bakin et al. 2000). Although the mechanism by which the TGFβ signal is transduced into the Akt pathway is not well understood both TGFβRI and TGFβRII appear to be required and TGFβRI has been shown to indirectly associate with the p85 subunit of PI3K to cause activation (Yi et al. 2005). Interestingly, the overexpression of SMAD7 abrogated this TGFβR-dependant PI3K activation (Yi et al. 2005). SMAD7

expression is also induced via Jak/STAT signalling in response to interferon γ and via NF-κB signalling in response to inflammatory cytokines and lipopolysaccharide in fibroblasts (Bitzer et al. 2000). TGFβ-induced PI3K signalling to mTOR is thought to have a central role in epithelial-mesenchymal transition so further understanding this form of non-canonical signalling is important in the study of cancer metastasis (Lamouille & Derynck 2011).

PAR6 is a polarity protein in epithelial cells which, when activated, recruits the ubiquitin-ligase SMURF1to degrade the RhoA small GTPase responsible for the intercellular tight junction assembly. TGFβ activation of the TGFβRII subunit causes phosphorylation of PAR6 and can contribute to cell dissociation and epithelial to mesenchymal transition (EMT).

Inhibitory interactions of other pathways with TGFβ signalling have also been observed. Protein Kinase C (PKC) has been shown to phosphorylate the MH1 globular domain of SMAD3 preventing it from binding DNA (Yakymovych et al. 2001). In addition, Akt has also been shown to bind to non-phosphorylated SMAD3 preventing TGFβ1-induced activation and nuclear translocation and this has been proposed as a mechanism by which insulin and Akt can inhibit apoptosis (Conery et al. 2004; Remy et al. 2004). MAPK signalling has been shown to negatively feedback on TGFβ canonical signalling. Oncogenic Ras, has been shown to reduce the expression of SMAD4 in intestinal epithelial cells, resulting in a reduction in SMAD complexes and TGFβ-induced protein expression (Saha et al. 2001). Activation of the Erk-MAPK pathway also reduces canonical SMAD signalling in epithelial and cancer cells by TGFβRI ectodomain shedding via activation of tumour necrosis factor-α-converting enzyme (Liu et al. 2009). MAPK, through its serine/threonine kinase activity has also been shown to bind SMAD2 and SMAD3 on their linker region in epithelial cells, preventing transport into the nucleus and targeting them for degradation, inhibiting the TGFβ signal (Kretzschmar et al. 1999). Given that TGFβ1 signalling is a key mechanism of myofibroblast differentiation, this potential inhibition of myofibroblast differentiation by MAPK signalling may help to explain why use of the EGFR inhibitor ZD1839 resulted in enhanced fibrosis in a bleomycin model of interstitial pulmonary fibrosis (Suzuki et al. 2003), while the use of an EGFR ligand named amphiregulin had the opposite effect (Fukumoto et al. 2010).

Numerous microRNAs have also been shown to regulate myofibroblast transdifferentiation via interference with mRNA translation or degradation (Hu & Phan 2013). Depending on their targets, including members of the TGFβ signalling pathway, their effects can either promote or suppress myofibroblast transdifferentiation (G. Liu et al. 2010; Liu et al. 2012).

1.1.7 Role of free radicals and Reactive Oxygen Species (ROS) in myofibroblast transdifferentiation

Reactive oxygen species (ROS) are chemically reactive molecules containing oxygen. They are produced in a tightly regulated way within normally-functioning cells, serving as a second messenger for intracellular signalling (Forman et al. 2008). They are also a by-product of mitochondrial metabolism and are produced at higher levels in rapidly proliferating, highly metabolically active cancer cells (Costa et al. 2014). While ROS are normally regulated at low levels, significant environmental stresses on the cell (e.g. UV radiation) can produce much higher levels, resulting in *oxidative stress* (Trachootham et al. 2008). This can be damaging to the cell by causing unchecked oxidation of amino acids and fatty acids, inactivation of enzymes via oxidation of co-factors, and can cause DNA damage via several mechanisms (Trachootham et al. 2008). Cells retaining normal apoptotic function can sense excessive presence of ROS and undergo apoptosis and this is utilised in radiotherapy where ionising radiation also generates significant intracellular oxidative stress (Hubenak et al. 2014).

The NAPDH oxidase family of enzymes (NOX1-7) are the main intracellular producers of endogenous ROS and are located on a variety of cell membranes and organelles including the mitochondria where they power the electron transport chain (Muller 2000). Conversely, the scavenging of oxygen free radicals is effected by small molecule antioxidants such as vitamins C&E, uric acid and glutathione, and enzymes including superoxide dismutase, glutathione peroxidase and catalase.

NOX4 is constitutively active within most cells, and its activity is therefore primarily regulated at the transcriptional level (Serrander et al. 2007). Although it initially passes an electron to an oxygen molecule generating a superoxide molecule, this highly reactive molecule almost instantly reacts to form a more

stable ROS signalling molecule of hydrogen peroxide. This causes reversible oxidation of thiol groups on cysteine residues on a variety of proteins and transcription factors modifying their activity (Trachootham et al. 2008).

NOX4 expression in fibroblasts is up-regulated by a number of signalling molecules recognised as important in fibrotic conditions including TGFβ1, angiotensin II and platelet-derived growth factor (Barnes & Gorin 2011), while SMAD2/3 and PKC have been identified as intermediates in the pathway (Bondi et al. 2010; Cucoranu et al. 2005; Wei et al. 2009). Evidence for an association between NOX4 expression and fibrosis arises from biopsies of patients with idiopathic pulmonary fibrosis (IPF), which show elevated levels of NOX4, and correlate with elevated markers of myofibroblast differentiation (Amara et al. 2010). NOX4 expression has subsequently been shown to drive myofibroblast differentiation in a variety of organs including the heart, lung, kidney, and liver (Cucoranu et al. 2005; Bondi et al. 2010; Amara et al. 2010; Jiang et al. 2012), with NOX4 siRNA, inhibitors and gene deletion able to attenuate fibrosis in rodent models (Aoyama et al. 2012; Gorin et al. 2005; Hecker et al. 2010; Jarman et al. 2014; Jiang et al. 2012). This has also highlighted the potential for therapeutic NOX4 targeting in fibrotic conditions.

The targets of TGFβ1-induced NOX4-mediated ROS production include SMAD2/3, which are phosphorylated to a greater extent in the presence of NOX4 (Cucoranu et al. 2005). In addition, mitogen-activated protein kinase phosphatase 1(MKPI) is inactivated by ROS oxidation, resulting in increased activation of JNK and p38 (R. Liu et al. 2010). JNK oxidation has been shown to be necessary for TGFβ1-mediated myofibroblast differentiation in prostatic tissue (Sampson et al. 2011). Other targets of NOX4-derived ROS include ERK1/2 and Src, while the action of ROS on LAP releases active TGFβ1 from sequestration in the extracellular matrix (Bondi et al. 2010; Block et al. 2008; Jobling et al. 2006). All of these intermediates result in increased expression of the traditional markers of the myofibroblast.

Scavengers of ROS include a number of enzymes dependent on the incorporation of the element selenium. In tumour stroma and in association with myofibroblast differentiation the expression of these enzymes and selenium transporters is reduced while exogenously applied selenium rescues their expression and activation, and reduces myofibroblast transdifferentiation

(Sampson et al. 2011). Clearly the balance between ROS production and ROS scavenging is important in determining fibroblast/myofibroblast fate.

In addition to ROS, nitrogen-centred radicals, such as nitric oxide (NO) and peroxynitrite are also important for intracellular signalling and are produced by the action of Nitric Oxide Synthase (NOS) in conjunction with NAPDH. NO primarily signals via the induction of soluble Guanylyl Cyclase (sGC) and the production of cGMP, which in turn regulates the activity of a population of kinases and phosphodiesterases (Murad 2006). They appear to act in the opposite manner to NOX4, namely that TGFβ causes a down-regulation of NOS activity and NO levels, while inhibition of NOS augments TGFβ1-induced collagen production (Chu & Prasad 1999). In addition, the use of nitric oxide donors prevents TGFβ-induced collagen production and myofibroblast differentiation *in vitro* and fibrosis in *in vivo* models (Vercelino et al. 2010; Zenzmaier et al. 2010). The effector molecule in the signalling pathway appears to be, or exists downstream of cGMP since exogenous synthetic cGMP mimics the effects of upstream activation of the pathway (Chu & Prasad 1999). Phosphodiesterase 5 (PDE5), which is not only a target of cGMP, but negatively feeds back hydrolysing its phosphodiester bond and deactivating it, itself became a treatment target. PDE5 inhibitors have subsequently been shown to not only be useful in pulmonary hypertension, benign prostatic hypertrophy and erectile dysfunction but also reduced myofibroblast differentiation *in vitro* and fibrosis severity *in vivo* in various models (Valente et al. 2003; Ferrini et al. 2006).

ROS signalling clearly has an important role in myofibroblast differentiation and the development of fibrosis in a range of tissues. There appears to be a balance between opposing effects of NOX4 and NO pathways, although NO appears to be downstream of NOX4. Potential interventions in order to reduce or reverse fibrosis therefore involve inhibiting the NOX4 arm or activating the NO arm, or alternatively boosting free radical scavenging.

1.1.8 Epigenetic regulation of myofibroblast transdifferentiation

All of the cell signalling and transcription factor complex interactions that rely on gene transcription to elicit an effect are dependant on the DNA being accessible. The cell's environmental circumstances influence its epigenetic

signature and resultantly the areas of DNA that can be read. Some of these changes are heritable and can exist in cells for several passages, or even the life of a cell when explanted *in vitro*, while other changes more readily revert.

DNA methylation is a well-recognised form of epigenetic regulation and mostly occurs on CpG islands at which cytosine residues become methylated. Densely methylated areas of DNA can be transcriptionally silenced in fibrotic conditions: hypermethylation and silencing of the THY1 gene in fibroblasts correlates with extent of lung fibrosis (Sanders et al. 2011), and SMAD7 and Fli-1 genes are hypermethylated in scleroderma fibroblasts (Wang et al. 2006). Depending on the particular profiles of genes that are silenced, however, the effect of DNA methylation can potentially be anti or pro-fibrotic (Hinz et al. 2012).

Histone modification also affects the ability of target DNA to be accessed and read. Histone deacetylases 4, 6, and 8 (HDACs 4/6/8) have been identified as the main histone modifiers responsible for ongoing fibrosis and are thought to produce their effect via suppression of gene expression (Hinz et al. 2012). In human lung fibroblasts the use of siRNA against HDAC4 markedly reduced TGFβ1-induced αSMA and phosphorylation of Akt suggesting that its mechanism of action includes the Akt pathway (Guo & Shan 2009).

1.1.9 Termination of myofibroblast function

In a cutaneous wound the duration of myofibroblast presence is known to vary depending on the animal species, the size of the wound, the nature of the injurious agent, tissue tension, and the vascular and immunological status of the individual (B Hinz et al. 2001; Van De Water et al. 2013; Brem & Tomic-Canic 2007). There is considerable evidence however, that once sufficient myofibroblasts have been recruited, early myofibroblast removal can reduce the extent of scarring and fibrosis. Techniques such as reducing wound tension or covering wounds with tissue grafts can cause more rapid resolution of granulation tissue and the earlier disappearance of cells bearing the hallmarks of myofibroblasts (B Hinz et al. 2001).

Most chronic scars or areas of chronic fibrosis eventually become relatively acellular once significant amounts of extracellular matrix have been laid down and remodelled, and it is possible that reducing myofibroblast numbers at this

late stage may have little impact on the resultant extent of fibrosis (Liu et al. 2013). Many anti-fibrotic therapies are therefore focused on the active stage of fibrosis where myofibroblasts are present in large numbers and are actively secreting ECM. At this stage, treatments are aimed at removing the causative agent triggering myofibroblast recruitment and proliferation, reducing myofibroblast signalling or differentiation, or reducing the myofibroblast load by either apoptosis or phenotype reversal.

The initial observation of an increasing number of apoptotic figures in a healing wound as myofibroblast numbers declined provided evidence that apoptosis plays a significant role in the termination of myofibroblast function (Desmouliere et al. 1995). Many authors, however, have reported increased apoptosis resistance as a result of increased TGFβ1 and Akt signalling during myofibroblast differentiation (Horowitz & Lee 2004).

The balance between NOX4 expression and antioxidant Nrf2 has been shown to be an important determinant of lung myofibroblast apoptosis and the extent of reaction to a fibrotic stimulus. Tissue samples from lungs of patients with idiopathic pulmonary fibrosis (IPF) have demonstrated an imbalance in the expression of the two proteins, and targeting NOX4 expression in mouse models reduced the extent of established fibrosis (Hecker et al. 2014). This highlights the potential of ROS balance in future treatment strategies.

A technique to augment myofibroblast apoptosis in the CCL4-induced liver fibrosis model involves administering Gliotoxin, linked to an antibody to the myofibroblast protein synaptophysin. Gliotoxin is thought to mediate apoptosis via inhibition of NF-κB signalling and through increasing mitochondrial membrane permeability (Wright et al. 2001; Orr et al. 2004). Anti-synaptophysin targeting reduces inadvertent associated macrophage and kuppfer cell destruction by Gliotoxin, and prevents associated MMP13 reduction. Following 7 weeks of CCL4 application, but prior to a final dose of CCL4, synaptophysin-linked Gliotoxin caused a significant increase in active caspase-3, reduction in αSMA expression, and reduction in ECM collagen compared to controls suggesting effective myofibroblast apoptosis (Douglass et al. 2008). The potential systemic side effects of such treatment have not as yet, however, been fully evaluated.

In some models, myofibroblasts appear capable of genuinely reversing their phenotype, reducing αSMA expression and contractility without evidence of myofibroblast apoptosis or overgrowth of a non-differentiated subpopulation (Guyot et al. 2010). Using the same rodent model of liver fibrosis, evidence has arisen for the ability of specific sub-populations of myofibroblasts in certain situations to revert from their full myofibroblast phenotype without undergoing apoptosis. In the liver two resident populations of progenitor cells predominantly contribute to the myofibroblast pool in response to pro-fibrotic stimuli - peri-sinusoidal hepatic stellate cells and portal fibroblasts. In the CCL4-induced model of liver injury 40-45% of activated myofibroblasts have been shown to survive in a de-activated 'quiescent' form following removal of the fibrotic stimulus and fibrosis resolution. When quiescent they revert to lying in peri-sinusoidal areas typical of HSCs, suggesting this to be their cell of origin. Although non-productive for αSMA, these cells when explanted *in vitro* express more αSMA and collagen IαI in response to fibrogenic stimuli, suggesting that though 'quiescent' they remain primed for a fibrotic response (Troeger et al. 2012).

A variety of cell signalling molecules and inhibitors have been cited as influencing myofibroblast reversibility. Water-soluble extracts from the amniotic membrane have been shown, when added to *in vitro* culture medium, to reverse the cellular shape, αSMA and ED-A fibronectin expression, and actin filament assembly of myofibroblasts (Li et al. 2008). αSMA expression and contractility can also be reversed in explanted myofibroblastic tissue from heart valves by the application of poly-unsaturated fatty acids (Witt et al. 2014).

The PDE5 inhibitor Vardenafil has been shown to inhibit myofibroblast differentiation and reverse the expression of αSMA in prostate cells *in vitro* and using *in vivo* models. Analysis has shown that this may be due to an alteration of REDOX balance, with increased expression of SOD2 and unchanged expression of NOX4, or due to reduced activity through the PI3K-Akt pathway (Zenzmaier et al. 2012).

Corneal fibroblasts and myofibroblasts have been shown to arise from EMT from corneal keratinocytes in response to corneal injury. In an *in vitro* model, the extent of collagen type III and αSMA secretion by corneal fibroblasts in response to TGFβ1 was reversed if after 2 weeks the treatment was switched

from TGFβ1 to TGFβ3 (Karamichos et al. 2014). Another *in vitro* study has shown an ability of FGF and heparin to reduce the percentage of myofibroblasts in the fibroblast population, but it is unclear whether this is due to a growth rate differential between the two cell types rather than genuine reversal of the myofibroblast phenotype (Maltseva et al. 2001).

The addition of PGE_2 24hours after TGFβ1 treatment has been shown to reduce the subsequent expression of αSMA in primary lung fibroblasts grown from some patients with IPF. PGE2 was shown to dephosphorylate FAK, while FAK inhibition also reduced αSMA expression and the generation of stress fibres containing αSMA (Garrison et al. 2013). However, given that αSMA fibres typically develop 48-72hrs post TGFβ1 treatment it is likely that this represents prevention rather than reversal of myofibroblast development.

Finally, the matrix on which myofibroblasts are cultured *in vitro* appears critical in influencing potential reversibility. Differentiated myofibroblasts plated on amniotic membrane, rather than plastic plate coated with type I collagen, return to an αSMA-negative progenitor-like state, while hepatic myofibroblasts explanted from cirrhotic liver and plated *in vitro* on matrigel-coated plates down-regulate ColIαI, ColIα2 and αSMA expression compared to uncoated plates (Sohara et al. 2002; Li et al. 2008). It is likely that tissue tension between the myofibroblasts and their ECM is a key determinant of ongoing fibrotic behaviour.

1.1.10 Role of myofibroblasts

1.1.10.1 Tissue injury and repair

Damage to tissue can result from numerous insults. Whatever the tissue type, its continuity is restored by a combination of regeneration and repair, although the balance between the two processes varies with tissue type and the mode of injury. Tissue regeneration involves the proliferation of neighbouring cells to replace damaged cells with cells of the same type in the same configuration. Unless tissue damage is particularly minor, regeneration is accompanied to a greater or lesser extent by the process of repair where the previous functional parenchyma is replaced with scar tissue. This ensures tissue continuity more rapidly but the resulting scar tissue lacks the function of the pre-existing parenchyma.

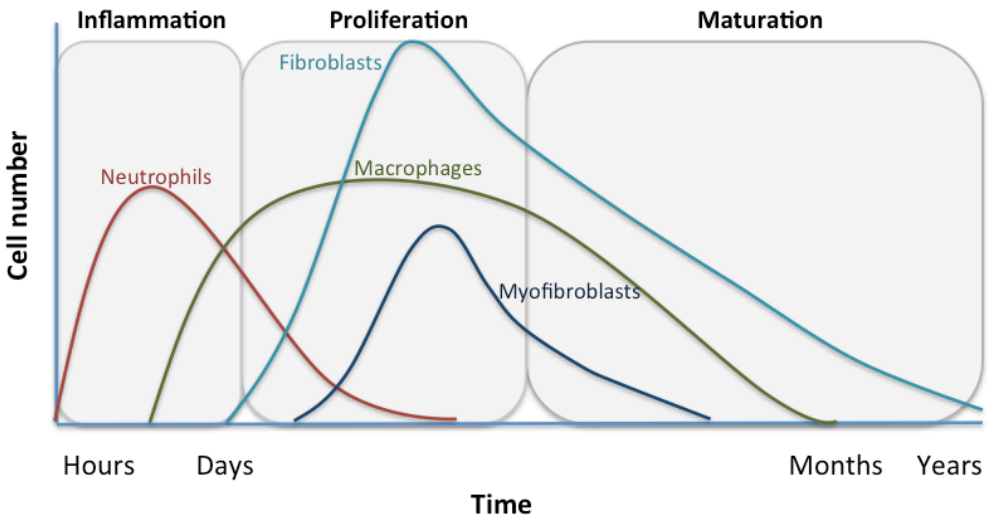

Figure 1-10 Recruitment of cell types to an acute wound.

Fibroblasts are recruited to a wound after a few days following an influx of inflammatory mediators – mainly neutrophils and macrophages. Fibroblasts proliferate and differentiate until epithelial integrity is reformed and then numbers reduce, at least partially by apoptosis, as the scar matures.

Immediately following an injury platelet derived growth factor (PDGF) and other plasma proteins, released from blood vessels by direct trauma or increased permeability, flood the extracellular matrix. Within 24 hours neutrophils are additionally recruited to the edges of the wound, attracted by factors released by these cells and any fibrin clot that has formed. While epithelial regeneration is occurring at the surface of the tissue over the first 48 hours, macrophages, fibroblasts and other myofibroblast precursors are also recruited to the wound (Larson et al. 2010). Over the next 7-14 days stromal proliferation and angiogenesis, forming granulation tissue, is accompanied by an enhanced secretion of extracellular matrix proteins by activated myofibroblasts (Van De Water et al. 2013). This is essential to restore tissue continuity, particularly if the defect is large. Myofibroblasts also contract to bring the wound edges together, minimising the size of the defect, and the requirement for extracellular matrix secretion.

Wound perfusion and oxygen tension appear to be an important determinant of the speed of healing and the balance of regeneration versus repair. αSMA expression is markedly reduced, *in vitro*, when myofibroblasts are subjected to hypoxic conditions (2% O_2), and prolonged ischaemia has been shown to

decrease myofibroblast formation and wound contraction in a rodent experimental model of wounding (Modarressi et al. 2010; Alizadeh et al. 2007). Over the following weeks the vascularisation and inflammatory infiltrate in the injured area recedes and deposited ECM is gradually remodelled to increase its tensile strength. The presence of myofibroblasts gradually diminishes to finally leave an acellular, remodelled scar.

In contrast to wounds in adults and late gestation fetuses, dermal wounds in early gestational fetuses heal in a 'scarless' fashion (Colwell et al. 2003). This results in the regeneration of a loose reticular mesenchymal network identical to the pre-injured tissue along with newly regenerated dermal structures (Beanes et al. 2002). As gestation progresses, and throughout adult life, injuries of the dermis and many other tissues heal with a greater degree of repair and scarring. The full explanation for the differences between wound healing in the adult versus early fetus is currently unclear but the differences in the recruitment, secretory pattern, and pattern of collagen remodelling by fibroblasts have all been implicated (Larson et al. 2010).

1.1.10.2 Dermal fibrosis - Scleroderma, Hypertrophic and Keloid Scarring

Fibrotic skin conditions have been a focus for fibrosis research given the ease of access of tissues for biopsy and analysis. Clear differences occur between the pathologies but there are some striking similarities. All of the conditions listed above demonstrate excessive deposition of collagen and extracellular matrix, elevated tissue inhibitor of metalloproteinase 1 (TIMP1) expression, and expression of particular HLA molecules (Canady et al. 2013). In addition, fibroblasts in all three conditions demonstrate down-regulation of the micro RNA miR-196a, which has been shown to be an important inhibitor of collagen deposition (Canady et al. 2013).

Systemic sclerosis is a chronic autoimmune fibrotic condition of unknown aetiology with an annual incidence of 0.45-1.9 per 100 000 people (Canady et al. 2013). It can occur in a form limited to the skin where it is known as scleroderma or can have systemic involvement including heart, lung and kidneys. Current treatments are only of very limited efficacy and are restricted to immunosuppressants and generic, organ-preserving treatments such as Elanoprost or ACE inhibitors which limit the deterioration in perfusion and function. Systemic involvement carries an average 5-year survival of between

34 and 73% (Canady et al. 2013), with most of the mortality resulting from organ fibrosis.

Consistent with the theory of exaggerated myofibroblast activity, analysis of skin from scleroderma patients reveals excessive secreted collagen (types I, III, V and VII), fibronectin, and TGFβ1 while circulating blood levels of TIMPs, which generally act to inhibit ECM remodelling were also found to be higher in patients with limited or diffuse systemic sclerosis compared to controls (Beeton et al. 2001). Fibroblasts from patients with scleroderma also showed elevated SMAD2/3 phosphorylation, nuclear SMAD3/4 localisation and variable augmentation of SMAD3 expression (Mori et al. 2003), while authors have seen either increases in non-functional or decreases in functional SMAD7 expression (Dong et al. 2002; Asano et al. 2004). Microarray data demonstrates increases in the transcription of integrins known to be involved with the activation of TGFβ1 (Rudnicka et al. 1994; Rajkumar et al. 2005; Sargent & Whitfield 2011). Fibroblasts explanted from patients with scleroderma were also shown, in comparison to controls, to demonstrate higher basal levels of reactive oxygen species (ROS), via a NADPH-oxidase-like pathway, although this was shown to be TGFβ-independent (Sambo et al. 2001). During the development of fibrosis in scleroderma increased proliferation of biosynthetically-active fibroblasts is observed, but *in vitro* clonal analysis of explanted cells shows heterogeneity in secretory patterns, supporting the hypothesis of myofibroblast precursors being recruited from multiple sites (Hinz et al. 2012). Explanted cells from scleroderma skin also have a greater predilection for myofibroblast differentiation than control cells and a greater Akt-mediated resistance to apoptosis (Jun et al. 2005).

Keloid scarring occurs more commonly in young people with darkly pigmented skin, and the fibrotic tissue overgrows the margin of the scar rarely regressing (Satish et al. 2006; Canady et al. 2013). Keloid scars show a marked increase in the type I: type III collagen ratio compared to normal scars (Verhaegen et al. 2009) and decreased hyaluronan secretion (Meyer et al. 2000). Like scleroderma fibroblasts they exhibit resistance to apoptosis and secrete elevated levels of TGFβ1 (Canady et al. 2013).

Hypertrophic scars are also are excessive in their extent compared to normal scars but occur in people of all races, do not overgrow the margin of the scar

and often regress (Canady et al. 2013). Myofibroblasts are commonly seen in tissue sections (Gabriel 2011) and explanted fibroblasts express higher levels of TGFβ1 than controls (Bock et al. 2005). As with keloids, tissue from hypertrophic scars express high levels of TIMPs 1 & 2 and high levels of MMP2 suggesting abnormal tissue remodelling in these conditions (Ulrich et al. 2010).

Clearly there is need of an improved understanding of myofibroblast biology that can help to identify treatments with potential to improve the poor survival in diffuse systemic sclerosis and the poor cosmetic effects of excessive scarring.

1.1.10.3 Organ fibrosis

45% of deaths in the Western world can reportedly be attributed to chronic fibroproliferative diseases (Wynn 2009) and in all of these conditions, whatever the initial trigger, the myofibroblast is the key effector of fibrosis.

Renal fibrosis appears to be a common final pathway following injury from a range of triggers to the kidney. The cross-talk between the epithelium and the stroma is felt to be critical and the loss of homeostasis in the renal tubulo-interstitium, resulting in abnormal signalling (including the secretion of TGFβ1), is the trigger for precursor recruitment and myofibroblast differentiation (Koesters et al. 2010).

In the lung, fibrosis can occur in differing patterns depending on the nature and source of the injurious agent. Asthma and Chronic Obstructive Pulmonary Disease (COPD) result in fibrosis surrounding the small airways, while pleural fibrosis affects the pleural space and pulmonary hypertension the vasculature. Idiopathic Pulmonary Fibrosis (IPF) is a progressive fibrotic disease affecting the interstitium surrounding the alveolar air sacs, but its aetiology is poorly understood. Nonetheless, IPF demonstrates all of the same hallmarks of fibrosis as other fibrotic conditions – ROS-dependency, increased myofibroblast cytokine, growth factor and ECM secretion (including TGFβ1); reduced myofibroblast sensitivity to inhibitory signals (reduced TNFα and PGE2 receptors); and resistance to apoptosis due to TGFβ1-driven phosphorylation of Akt (Vancheri et al. 2010). Without treatment IPF carries a 20-40% 5-year mortality (some quote as high as 50% 3 year mortality (Vancheri et al. 2010))

but the drug treatment Pirfenidone, in stage III clinical trials, delivers improved lung function tests, progression-free survival and all-cause mortality (King et al. 2014). Pirfenidone's mechanism of action is not clear but *in vitro* studies have demonstrated that it reduces primary lung myofibroblast proliferation, TGFβ-induced differentiation, collagen deposition, and TGFβ-induced SMAD3, Akt and p38 phosphorylation (Conte et al. 2014). In addition, Pirfenidone has been shown to improve fibrosis in animal models of cardiac, renal and liver fibrosis (Shimizu et al. 1998; Mirkovic et al. 2002; Salazar-Montes et al. 2008).

The study of liver fibrosis offers potentially unique insights into myofibroblast functional reversibility. Up to a threshold, hepatic parenchyma can regenerate from quite significant injury as long as the injurious agent e.g. alcohol or viral infection is removed (Hinz et al. 2012). Current evidence indicates that myofibroblasts governing liver fibrosis are derived from two local pools – Hepatic Stem Cells (HSCs) and portal fibroblasts, possibly with an additional contribution from circulating precursors. When fibrotic liver specimens containing HSCs and portal fibroblasts are treated in an identical fashion HSCs can lose their αSMA expression (effectively de-differentiate) and survive while portal fibroblasts undergo apoptosis (Guyot et al. 2010). Furthering our understanding of these differences, why myofibroblasts in other organs show comparative resistance to apoptosis, and clarifying the origins of myofibroblast precursors in different circumstances may help us to influence myofibroblast reversibility.

1.1.10.4 Cancer

1.1.10.4.1 Head and neck cancer and cancer of the upper digestive tract

Head and neck cancers are a diverse group of tumours that arise from the lip, oral cavity, nose, paranasal sinuses, pharynx or larynx. Although there is a range of subtypes reflecting the cells of origin, 90% are squamous cell carcinomas arising from the epithelium of the mucosal lining of these structures.

Table 1 UK Cancer statistics for Head & Neck and upper aerodigestive tract tumours (www.cancerresearchuk.org).

Body site	UK Annual Incidence (*year*)	UK 5yr DFS (*year*)	UK Annual Cancer Deaths (*year*)
Skin (BCC/SCC)	**102,628** (*2011*)	n/a	**638** (*2012*)
Oral	**6,767** (*2011*)	**50%** (2010)	**2,119** (*2012*)
Oropharyngeal	**1,066** (*2006*)	**52%** (2007)	**292** (*2006*)
Oesophageal	**8,332** (*2011*)	**13%** (2010)	**7,701** (*2012*)

From WHO data the worldwide annual incidence of head and neck squamous cell carcinoma (HNSCC) in 2002 was approximately 600 000. While there is significant geographical variation in the incidence at various anatomical subsites, in the UK alone there are over 7500 new cases of oral or oropharyngeal squamous cell carcinoma each year. Alcohol and smoking are the most universal and significant risk factors for HNSCC while betel nut chewing, wood dusts, Epstein Barr (EBV) and Human Papillomavirus (HPV) infection are additional site-specific risk factors.

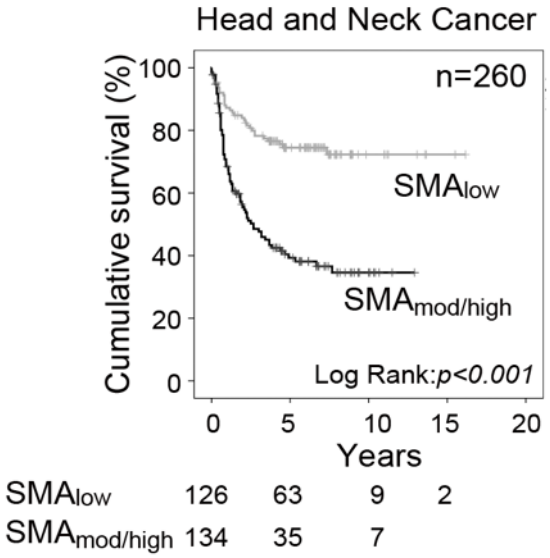

Figure 1-11 Stromal αSMA expression inversely correlates with disease-specific survival in Head and Neck cancer.

Kaplan-Meier curves demonstrate cumulative disease-specific survival stratified by αSMA-staining status. Lower figures display the total number of participants remaining under follow-up, subdivided by initial tumour αSMA status, with the timescale correlating with the graph.

Depending on the tumour site and stage treatment modalities include surgery, radiotherapy and chemotherapy with an additional developing role for monoclonal antibody therapies. Despite these treatments, population outcomes are still relatively poor with 5-year disease-free survival remaining at around 50%. The presence of αSMA positive myofibroblasts surrounding oral squamous cell carcinoma has been shown to correlate with more aggressive tumour behaviour and to predict prognosis more accurately than the classical TNM classification (Kellermann et al. 2007; Marsh et al. 2011). Furthermore, given the intricate anatomy and physiology of the head and neck region, even patients who are successfully treated often carry significant morbidity from their treatments including altered sense of hearing, smell or taste, dry mouth, altered voice, impaired swallowing and reduced mobility of the jaw and neck. Some of these are directly related to fibrosis resulting from therapeutic interventions.

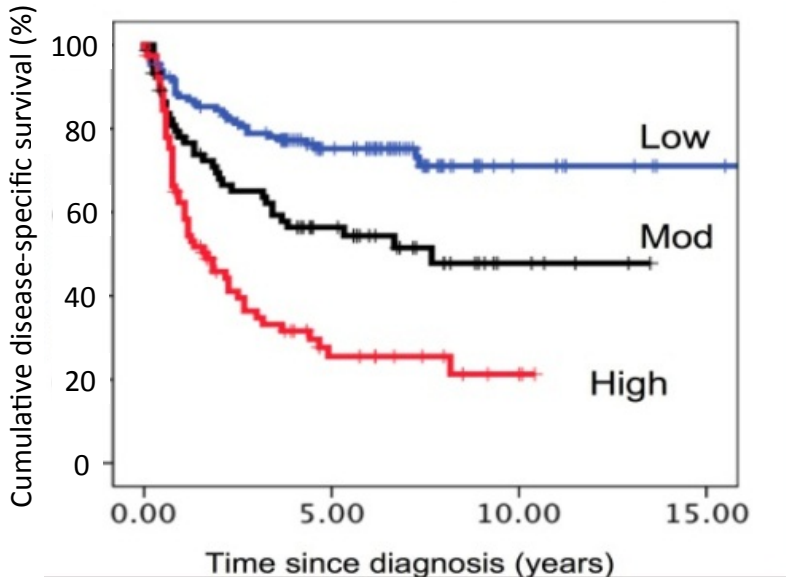

Figure 1-12 Stromal αSMA expression inversely correlates with disease-specific survival in Oral Squamous Cell carcinoma.

Kaplan-Meier curve demonstrates cumulative disease-specific survival stratified by αSMA-staining status; n=282. Derived from Marsh et al., 2011.

Skin cancer is the most common human malignancy and results primarily from exposure to ultraviolet radiation (Armstrong & Kricker 2001). During much of our sun exposure clothing covers most of the body, so a large proportion of skin cancer arises in the typically uncovered head and neck region, and metastases are in the first instance primarily to lymph nodes in the parotid gland and neck. Malignant melanoma is a particularly aggressive variety of skin cancer that affects younger individuals and is usually considered separately from non-melanomatous skin cancer (NMSC), which itself comprises mainly Basal Cell carcinoma (BCC) and Squamous Cell carcinomas (SCC). The incidence of NMSC has been increasing since the 1960s (de Vries et al. 2005) and in the UK in 2008 there were almost 100 000 new cases registered. Within the UK the south coast experiences the highest UV exposure, which, coupled with a rapidly expanding retirement population, results in a high local incidence of skin tumours. BCCs rarely metastasise and are normally cured by local treatment while cutaneous SCCs metastasise in 1.5% of cases. Although this percentage is small, cutaneous SCCs are the second most common malignancy in humans (second only to BCCs), so the incidence of malignant disease is significant. Furthermore, the tumours that do metastasise are very aggressive and so cutaneous SCCs still cause approximately 600 deaths per year in the

UK, twice as many as those resulting from oropharyngeal tumours. The presence of a desmoplastic stroma, generated by the myofibroblast, has been recognised as a high-risk pathological feature in the primary tumour which is associated with increased patient mortality (Samarasinghe et al. 2011).

Oesophageal carcinoma is the eighth most common malignancy worldwide and as a result of particularly poor survival rates (15% 5-year disease-free survival) has been identified as an area of unmet need by Cancer Research UK. Squamous cell carcinoma usually arises in the upper oesophagus but adenocarcinoma arising in the lower oesophagus is the most common variety in the Western world. Alcohol, smoking and gastro-oesophageal reflux disease are the risk factors with the strongest association. Patients commonly only present once the tumour is of a sufficient size to cause obstructive symptoms and by this time it has commonly invaded local structures making curative treatment unlikely. Treatment options again include, alone or in combination, surgery, chemotherapy and radiotherapy.

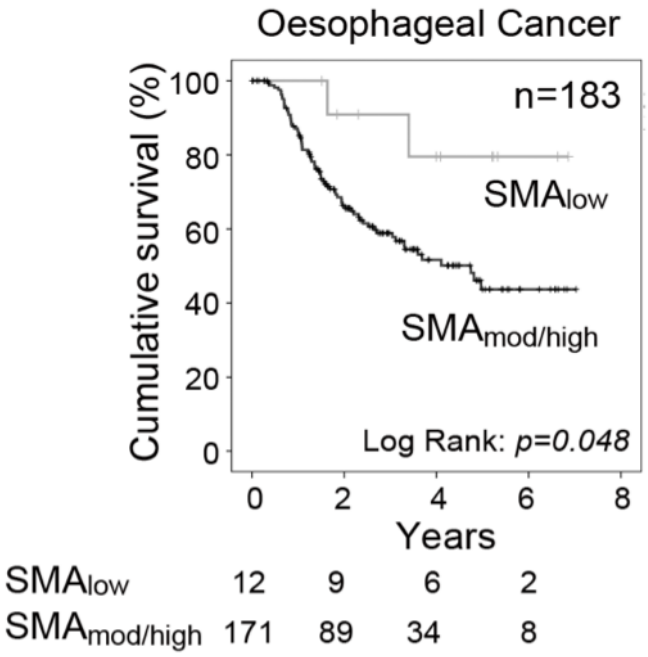

Figure 1-13 Stromal αSMA expression inversely correlates with disease-specific cumulative survival in oesophageal cancer.

Kaplan-Meier curves demonstrate cumulative disease-specific survival stratified by αSMA-staining status. Lower figures display the total number of participants remaining under follow-up, separated by initial tumour αSMA status, with the timescale correlating with the graph.

It was originally thought that carcinogenesis at all these sites resulted solely from mutations in the epithelial compartment. Dysregulated epithelial proliferation, disordered cell-cell adhesion and subsequent metastasis were thought to be the sole abnormalities that were targets for treatment. The active role of the myofibroblast and the stromal compartment in tumorigenesis was first recognised when the stromal response to tumours was likened to “a wound that never heals” (Dvorak 1986). It was subsequently discovered that the supposedly healthy stromal tissue surrounding the tumour, otherwise known as the tumour microenvironment, plays a critical role in tumorigenesis at numerous sites in the body. It is now appreciated that the cross-talk between tumour epithelium and peri-tumoural stroma, triggered initially by loss of epithelial homeostasis, is critical to tumour biology (Gabbiani et al. 2012).

1.1.10.4.2 The role of Cancer Associated Fibroblasts (CAFs)

The prognostic importance of αSMA-expressing fibroblasts within the tumour stroma has been demonstrated in a number of different tissues (including the oral cavity) with increased expression correlating with poorer patient outcomes (Marsh et al. 2011; Chen et al. 2014; Horn et al. 2013). A highly desmoplastic stroma, indicative of active myofibroblast activity, is also recognised as a risk factor for more aggressive behaviour and higher risk of recurrence in cutaneous squamous cell carcinoma (Samarasinghe et al. 2011).

The cancer-associated fibroblast (CAF) appears to be a heterogenous group of cells comprised of true myofibroblasts (containing αSMA-positive stress fibres), non-activated fibroblasts, and αSMA-negative ‘activated’ fibroblasts (Polanska & Orimo 2013; Sugimoto & Mundel 2006). The fibroblastic population appears to not merely serve as a pool for myofibroblastic differentiation but also to possess its own tumour-promoting activity. For example, genetic ablation of FSP-1 (fibroblast-specific protein -1) positive fibroblasts significantly reduces tumorigenesis in animal models but also reduces the seeding of metastases at distant sites (Grum-Schwensen et al. 2005; O’Connell et al. 2011). A proportion of fibroblasts at any time are also senescent, unable to apoptose, but irreversibly committed to withdrawal from proliferation (Macieira-Coelho 1998). While senescent fibroblasts are similar to other myofibroblasts in that they possess functional αSMA stress fibres and secrete factors that promote tumour

cell invasion, they generate a modified gene expression profile, with differences in a number of extracellular matrix genes (Mellone et al. 2016). The precise role of these different sub-populations with differing expression profiles is currently unclear but may at least partially result from differences in the cell types from which they originate.

Hannahan and Weinberg categorised cancer biology by identifying a more expansive set of behaviours that cancer cells acquire beyond the earlier recognition of dysregulated proliferation and metastatic potential. Their 'Hallmarks of Cancer' model was recently updated to incorporate further new concepts in cancer cell biology and they also stressed the importance of the tumour microenvironment. CAFs have been shown to contribute to many of the features known to contribute to tumour development as shown in figure 1-14 (Hanahan & Coussens 2012).

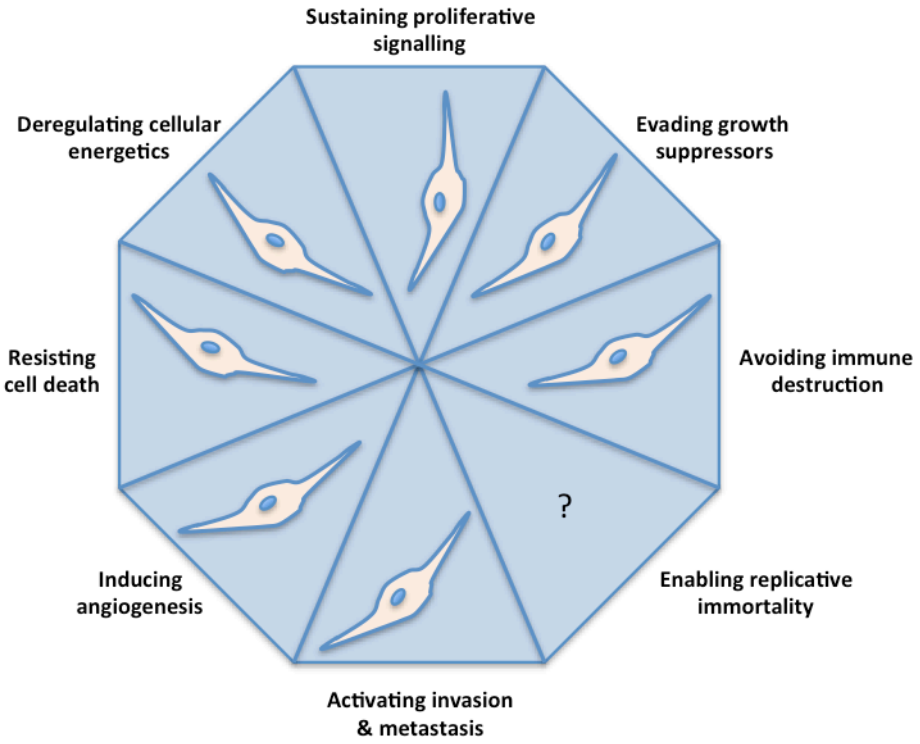

Figure 1-14 The role of Cancer Associate Fibroblasts (CAFs) in supporting the 'updated' hallmarks of cancer.

While infiltrating inflammatory cells and angiogenic vascular cells also contribute to a number of processes supporting tumour proliferation and metastasis, evidence is accumulating for a role for CAFs in all of the hallmarks of cancer, with the exception of 'enabling replicative immortality'.

CAFs have been shown to influence cancer cell development and proliferation. In both *in vivo* and *in vitro* systems CAFs have been shown to influence 'initiated' prostate epithelial cells to form tumours, while normal fibroblasts do not (Olumi et al. 1999). Co-culture experiments of human CAFs with breast tumour cells produced significantly more growth than tumour cells co-cultured with normal fibroblasts from the same patient (Orimo et al. 2005). Co-injection of pancreatic stellate cells (fibroblast equivalents that reside in the pancreas) with pancreatic tumour cells, in an orthotopic model, caused larger and more numerous tumours than when epithelial cancer cells were injected without fibroblasts. Cell-cell contact may not however be necessary for the effect since addition of the conditioned medium from pancreatic stellate cells to pancreatic tumour cell cultures increased cell proliferation in a dose-dependant manner (Hwang et al. 2008). CAFs are able to secrete numerous proteins including a number of recognised mitogenic growth factors such as Hepatocyte growth factor (HGF), along with members of the Epidermal and Fibroblast growth factor families including Insulin-like growth factor 1 (IGF-1) and Stromal cell-derived factor-1 (SDF-1/CXCL12), and these are known to have proliferative effects on cancer cells. Cell contact between CAFs and cancer cells is, however, still important. Normal quiescent dermal fibroblasts, via cell-cell contact with tumour cells generally inhibit their proliferation. This effect is reduced or reversed when tumour-derived fibroblasts are used, suggesting that CAFs lose their ability to limit cancer cell growth (Flaberg et al. 2011). Finally, CAFs may also be able to inhibit apoptosis of tumour cells. This may be achieved through increased secretion of soluble pro-survival factors such as IGF-1 and IGF-2, or through secretion and remodelling of extracellular matrix providing increased pro-survival signalling through cell-matrix interactions (Hanahan & Coussens 2012).

Cancer-associated fibroblasts have also been proposed to metabolically support the survival and growth of the epithelial tumour compartment. It has been proposed that reactive oxygen species, generated by oxidative stress in cancer cells, promotes aerobic glycolysis in stromal fibroblasts via NFκB activation (Guido et al. 2012; Martinez-Outschoorn, Balliet, et al. 2012). This process results in diversion of ATP synthesis from mitochondrial oxidative phosphorylation to cytosolic lactic acid fermentation and results in augmented generation and secretion of lactate as well as ketone bodies and glutamine.

These can be used as metabolic fuels or as organic building blocks for the proliferating tumour compartment. Preferential expression of enzymes associated with ketone body production has been shown in the stromal compartment of breast cancer, while enzymes associated with mitochondrial metabolism of ketone bodies are up-regulated preferentially in the tumour compartment (Martinez-Outschoorn, Lin, et al. 2012). Furthermore, profiling of the stroma from the most aggressive breast tumours has revealed, amongst other traits, a transcriptional shift towards aerobic glycolysis (Pavlides et al. 2010). In orthotopic mouse experiments, co-injection of fibroblasts expressing increased ketone body production more than doubled tumour size while breast cancer cells over-expressing enzymes required for ketone utilisation showed marked increases in cancer cell proliferation and metastasis (Martinez-Outschoorn, Lin, et al. 2012; Salem et al. 2012).

Cancer-associated fibroblasts are thought to promote tumour angiogenesis by both direct and indirect routes. They are known to secrete a number of pro-angiogenic factors including VEGF, FGFs, PDGF-C and SDF-1 which can act directly on endothelial precursor cells and pericytes (Räsänen & Vaheri 2010; Orimo et al. 2005; Crawford et al. 2009). In addition, the increased secretion of proteolytic enzymes in CAFs compared to quiescent fibroblasts is likely to release latent angiogenic factors that have been trapped in the extracellular matrix. Finally CAFs are also know to secrete a range of chemoattractants (including SDF-1) for macrophages and neutrophils which themselves can deliver a pro-angiogenic signal (Orimo et al. 2005).

Chronic inflammation is known to promote the development of tumours at numerous sites including the skin and oesophagus. Some have proposed that CAFs secrete a pro-inflammatory signature of proteins, which, depending on the particular immune cells recruited, can support tumour progression. In particular the mRNA expression levels of secreted proteins CXCL-1, which acts as a chemoattractant for neutrophils and macrophages, and IL-6 (amongst others) have been shown to be elevated in CAFs associated with SCCs at numerous different tumour sites (Erez et al. 2010). However, CAF-secreted TGFβ also appears to have a tumour-inhibiting role in T-cell dependent tumour surveillance and destruction. Genetic abrogation of SMAD-dependant signalling in CD4 and Lck-expressing T cells in a mouse model resulted in the tendency

to a TH2 phenotype and increased frequency of spontaneous oral and gastrointestinal tumours (Kim et al. 2006).

CAFs have for some time been shown to influence the invasiveness of tumours. Early observations noted that colonic carcinoma cells injected into wounds behaved more invasively than when injected into normal skin suggesting that the differing tissue environments must be responsible (Dingemans et al. 1993). TGFβ and MMP secretion from CAFs have a role in stimulating epithelial-mesenchymal transition in the cancer cells, dissociating their cell-cell adhesions and enhancing their migratory ability (Giannoni et al. 2010; Chaffer & Weinberg 2011). However, the effect of CAFs does not seem to be solely due to the induction of EMT. An extracted epithelial tumour cell line from rats only showed invasive behaviour in in vitro models when co-suspended with tumour-associated myofibroblasts and this was shown to occur despite continued E-cadherin expression - therefore in the absence of epithelial-mesenchymal transition (Dimanche-Boitrel et al. 1994). An additional study imaging the migration of a co-culture of SCC cells and CAFs showed the epithelial cells to maintain epithelial characteristics but to invade through a three dimensional in vitro model following tracks created by CAFs, while CAFs are also visible at the invasive fronts in some tumours (Gaggioli 2008; Hanahan & Coussens 2012). There is emerging evidence that in some cases CAFs metastasise along with tumour epithelial cells, and thereby prime the recipient environment to enhance the survival potential of the metastatic tumour cells (Duda et al. 2010). The pro-migratory effect of CAFs on cancer cells can also be mediated by secreted soluble factors, since in pancreatic cancer models conditioned media alone from pancreatic stellate cells can increase the degree of migration of pancreatic cells (Hwang et al. 2008). It is very likely that CAFs influence cancer cells via a combination of secreted factors, direct cell-cell interactions and modification of the extracellular matrix to make it more favourable for cancer cell migration.

It is notable that CAFs are not only potential treatment targets as a result of their tumour promoting activities but also as a result of their interference with treatment regimes. Deposition of collagen extracellular matrix, which is increased in CAFs and myofibroblasts, markedly inhibits the penetrance of chemotherapeutic drugs to the central tumour. Targeting the CAFs for destruction in a murine model improved chemotherapy uptake markedly,

prolonging lifespan (Loeffler et al. 2006). Targeting the stroma with inhibitors of hedgehog signalling in a mouse pancreatic tumour model was also shown to improve the penetration of gemcitabine via transiently increased tumour perfusion (Olive et al. 2009). The benefit of potential combination treatments, with stromal modulation alongside tumour targeting, is highlighted by the use of stromal HGF inhibitors alongside Raf inhibitors in co-culture experiments of melanoma cell lines with stromal cells from treatment-resistant patients (Straussman et al. 2012).

Although we consider the stroma as genetically normal it has been shown to often harbour its own genetic mutations. TP53 or PTEN mutations in breast tumour stroma are common while loss of heterozygosity or allelic imbalance in p53 in the stroma correlates significantly with rates of tumour metastasis (Patocs et al. 2007; Kurose et al. 2002). The mechanism and role of mutations in the stroma are currently unclear but a prostate cancer model has suggested that the epithelial compartment can induce clonal expansion of a small fraction of fibroblasts that lack p53, generating a proliferative, desmoplastic stroma and helping to drive tumorigenesis (Hill et al. 2005).

1.2 Eps8 Structure, function and binding partners

1.2.1 Eps8

Epidermal growth factor receptor kinase substrate factor 8 (Eps8) was initially identified in 1993 in a screen of phosphorylated targets resulting from the overexpression of epidermal growth factor receptor in NIH-3T3 fibroblasts (Fazioli et al. 1993). Eps8 is expressed widely in humans while having homologues in *Drosophila* and the nematode *C elegans*, suggesting a core role in cell physiology (Wong et al. 1994).

A 92kDa protein was predicted by the 3550 nucleotide cDNA, and generation of an antibody against the protein identified a major 97kDa and less prevalent 68kDa protein (Fazioli et al. 1993). Due to sequence similarity between these proteins they were felt to both derive from the same species, but the detection of two separate mRNAs and the failure of expression of the 68kDa isoform when the full length cDNA was virally expressed suggest that they do not arise

from the same mRNA or from post-translational modification of the 97kDa isoform (Fazioli et al. 1993). Instead it is likely that the 97kDa and 68kDa isoforms arise from alternatively spliced mRNAs (Fazioli et al. 1993).

Eps8 was shown in immunoprecipitation assays to bind to EGFR in a manner independent of its tyrosine phosphorylation although the functional relevance of this interaction still remains unclear (Fazioli et al. 1993). Although the initial detection of Eps8 was by the use of EGFR, it has been recognised that fibroblasts often express very few EGF receptors, and that PDGF receptors are more numerous (Fazioli et al. 1993). Consistent with this observation PDGF-BB, but not EGF, stimulation of fibroblasts resulted in Eps8 phosphorylation but the only phosphorylated Eps8 isoform was that generated related to the higher, 97kDa band (Fazioli et al. 1993). Due to the predominance of the 97kDa variant and its more thorough characterisation we have only considered this protein in our study, and from now on will refer to this as Eps8.

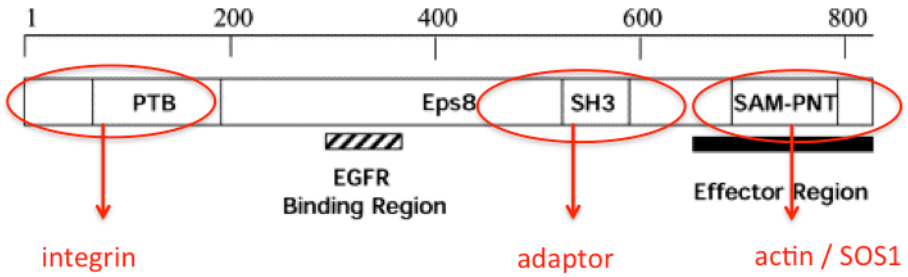

Figure 1-15 Eps8 is composed of functional subunits

The c-terminal region (right side of above figure) of Eps8 is responsible for its actin bundling and capping functions, and can tether Eps8 to the actin cytoskeleton. It is also responsible for the binding of SOS-1. The SH3 'adaptor' domain is the subject of competitive competition between Abi1 and Rn-Tre, while the N terminus (left side of the above figure) has been associated with the binding of integrins.

Examining the sequence of Eps8 provided some information as to its function and interactions. A 50 amino acid stretch of the protein showed sequence homology with the SH3 domain of other proteins known to interact with RTKs. Although there was additionally some sequence homology with SH2 domains, by which proteins such as Src interact with phosphotyrosine groups including those on RTKs (Fazioli et al. 1993), this was shown not to be responsible for Eps8 binding to EGFR (Castagnino et al. 1995). Finally a potential nuclear

targeting sequence, rich in basic amino acids was also identified (Fazioli et al. 1993), although its relevance is unclear at present.

1.2.2 Functions of Eps8

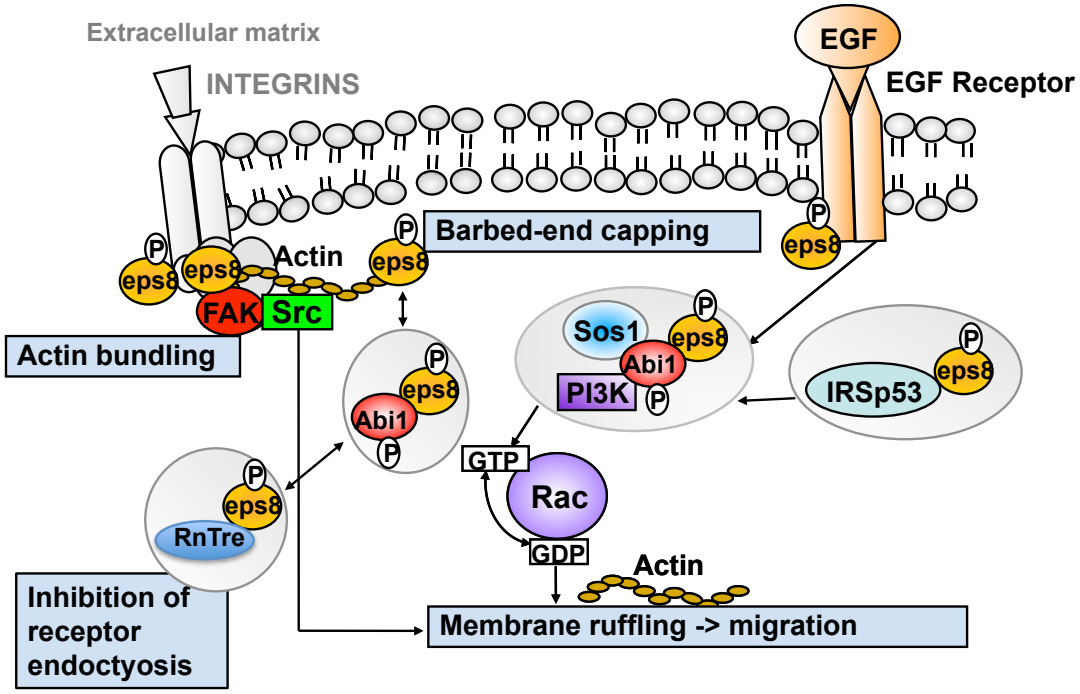

Figure 1-16 Recognised functions of Eps8

Active competition between Rn-Tre and Abi1 exists for binding to Eps8 and determines the relative activity of Eps8 in the inhibition of endocytosis versus roles in actin bundling, capping and cell migration. Eps8 is known to form a Rac1-activating 'tricomplex' in association with Abi1 and SOS-1 (and also PI3K), the formation of which is enhanced by the binding of IRSp53. The N-terminus of Eps8 is also involved in integrin-binding, while integrins are crucial to developing cell-ECM tension required for myofibroblast transdifferentiation.

Further knowledge of the sequence and structure of Eps8 have facilitated an improved understanding of its interactions and functions (Tocchetti et al. 2003). Two particularly important regions are the C-terminal effector region, responsible for binding to either actin or a guanine nucleotide exchange factor called SOS-1, and an SH3 domain that interacts with a number of other proteins. Utilising a portion of its C-terminal subunit, Eps8 can function as an actin capping protein, binding to the barbed end of extending actin polymers to prevent further extension of targeted filaments. This may help to produce a meshwork of actin, as occurs at the advancing lamellipodia of a migrating cell, where a broad front is required. Localised inhibition of actin capping may also

facilitate local extension of actin polymers to generate projections such as filopodia but the mechanisms that govern this are not well understood (Disanza et al. 2004). Barbed end-capping activity has been shown to be crucial for neuronal plasticity, and Eps8 knockout mice demonstrate cognitive impairment and immature synaptic spines which fail to potentiate with stimulation (Menna et al. 2013).

Eps8 also has a role in the physical *bundling* of actin polymers. This property is also facilitated by the C-terminal domain, but by a distinct segment to that which confers end-capping activity. Separation of these two activities by the creation and testing of truncated segments of Eps8 indicate that Eps8's role in lamellipodia function and motility is conferred through the end-capping activity, while actin bundling is responsible for early filopodia / microspike extension (Hertzog et al. 2010). The contextual interaction of Eps8 with other molecules is thought to determine whether the end-capping or bundling function of Eps8 predominates, allowing Eps8 to effectively serve as a molecular switch (Vaggi et al. 2011). The actin binding property of the c-terminal domain may also subtend an important role in providing subcellular localisation of Eps8 at areas where actin turnover is highest (Scita et al. 2001).

In addition to actin bundling and capping, Eps8 also influences the dynamics of the actin cytoskeleton, and cell motility, by activating the small Rho-GTPase Rac-1. Rac-1 is thought to have an important role as a molecular switch favouring lamellipodia extension. This produces the earliest morphological feature of cell migration otherwise known as 'membrane ruffling' (Boyde & Bailey 1977). Eps8 has been shown to be critical for membrane ruffling since it localises at growth factor-induced actin-rich ruffles, while stimulated Eps8-null fibroblasts fail to form membrane ruffles (Offenhauser et al. 2004). The C-terminal effector region of Eps8 is sufficient to activate Rac1 (via an interaction with Son-of-sevenless homologue 1 (SOS-1)), but optimal Rac1 activation requires other associations via Eps8's SH3 domain including with Abelson Interactor 1 (Abi1 or E3b1) to form a tricomplex. Despite involvement of other molecules in the 'tri'complex including PI3K, Eps8 remains necessary for Rac1-activating function, demonstrating its importance in actin-modelling and cell migration (Scita et al. 1999).

Abi1 is an adapter protein, recognised as a member of the WAVE complex, and therefore involved in the regulation of actin polymerisation (Steffen et al. 2004). Abi1 is also important in regulating Eps8-mediated barbed-end capping by effecting a necessary conformational change in the actin-binding c-terminal domain of Eps8. Binding of Abi1 to Eps8 may also help to localise Eps8 activity since Abi1 is localised at areas of actin polymerisation and turnover (Disanza et al. 2004). The importance of Abi1 in cell migration is indicated by the abrogation of PDGF-induced membrane ruffling in mouse fibroblasts following microinjection of antibody to Abi1 (Scita et al. 1999).

SOS1 is a guanine nucleotide exchange factor, a protein, which possesses the ability to catalytically activate Rac-1 by enhancing the rate of dissociation of inactivated GDP, allowing GTP to bind in its place. SOS1 is in fact a *dual specificity* guanine nucleotide exchange factor as it is capable of activating either Rac-1 or Ras depending on the circumstance. On stimulation of the EGF receptor, Grb2 is recruited and binds SOS1, localising it to the plasma membrane and facilitating Ras activation. Abi1 competes with Grb2 for binding to SOS1 and when successfully bound, recruits Eps8, forming the Rac-1-activating tricomplex (Bhat et al. 2014). Furthermore, the presence of the adapter protein p66shc inhibits the interaction of SOS1 with Grb2 and along with elevated levels of SNTA1 promotes formation of the tricomplex (Khanday et al. 2006; Bhat et al. 2014). CIIA is another adapter protein that in epithelial cells inhibits SOS1–Grb2 interactions and promotes tricomplex signalling. Interestingly in epithelial cells, TGFβ1signalling has been shown, via NF-κB signalling, to up-regulate CIIA levels, tricomplex activation, and Rac1 activity, resulting in increased migration in epithelial cell lines (Hwang et al. 2011). PIP3, resulting from phosphoinositide 3-kinase (PI3K) activity, may be required for SOS1 activation, and this could explain why PI3K, via its p85 subunit, is recruited to the tricomplex by Abi1 (Vanhaesebroeck et al. 2001; Katso et al. 2006). Indeed the absence of p85 PI3K has been shown to abrogate Abi1-dependent Rac1 activation (Innocenti et al. 2003). SOS1 mutations in humans are recognised to produce Noonan's syndrome and hereditary gingival fibromatosis type I (Roberts et al. 2007; Hart et al. 2002).

An additional adapter protein, IRSp53, augments the actin-bundling activity of Eps8, and enhances tricomplex formation and Rac1 activation. Resultantly, Eps8-IRSp53 complexes have been shown to localise at the leading edge of

migrating NIH3T3 fibroblasts (Funato et al. 2004). IRSp53 is also known to act downstream of the tricomplex serving as an intermediary between Rac1 and the WAVE2 complex to effect the Rac1 signal on membrane ruffling (Miki et al. 2000). More recent insights have revealed that in V-Src-transformed cells IRSp53, via necessary Eps8 binding, promotes PI3K and STAT3 activation and Cyclin D1 expression resulting in increased cell proliferation. Meanwhile, in Hela cells, EGFR binding and Src activation results in IRSp53/Eps8 interaction and STAT3 activation, resulting in mitogenic signalling and cell proliferation (P. S. Liu et al. 2010).

Eps8 also has an important role in the regulation of receptor endocytosis. Stimulation of FGF receptors by FGF causes Src-mediated phosphorylation of Eps8, which results in enhanced receptor endocytosis and trafficking (Auciello et al. 2013). Following EGFR activation a 'GTPase activating protein' (GAP), named Rn-Tre, competes with Abi1 for binding to the SH3 subunit of Eps8. The resulting Eps8-RnTre complex inhibits the GTPase activity of the GTP-ase Rab5, preventing receptor endocytosis (Lanzetti et al. 2000). This mechanism is postulated to serve to prolong the duration of cell signalling through a number of membrane-bound receptors including EGFR (P. P. Di Fiore & Scita 2002; Lanzetti et al. 2000). It is currently debated as to whether Eps8 is required for the inhibitory effects of Rn-Tre on receptor endocytosis (P. Di Fiore & Scita 2002; Martinu et al. 2002). The balance between the two potential fates of Eps8 (tricomplex versus R-Tre binding) appears to be modulated by JNK2 expression levels. Higher JNK2 levels favour tricomplex formation and lower levels favouring interaction with Rn-Tre (Mitra et al. 2011).

Eps8 therefore has a number of identified roles in the cell and has interactions with numerous other signalling molecules to facilitate these effects. Activation of EGFR, and possibly other RTKs, appears responsible for activating Eps8, both directly by phosphorylation and via Ras-triggered assembly of the Rac-activating tricomplex (Scita et al. 1999; Innocenti et al. 2002).

The contextual mechanisms regulating Eps8's location and interactions at any time are still to be fully elucidated, but it has been shown that transient downregulation of Eps8 is required for proper mitosis in Hela cells (Werner et al. 2013). Downregulation is mediated in G2 phase by the ubiquitin E3 ligase $SCFF^{bxw5}$ and is followed by re-expression of Eps8 at the mid-zone and cortical

membrane of dividing cells. Other factors regulating Eps8 expression, and mechanisms terminating its activity, are unclear. One potential mechanism of Eps8 deactivation may be through dimerization. Analysis of the SH3 domain suggests that Eps8 may dimerize between SH3 binding sites preventing binding of proteins such as Abi1 and RN-tre, effectively de-activating the protein (P. P. Di Fiore & Scita 2002). Sequence analysis also reveals numerous phosphorylation sites which may regulate its activity under normal physiological conditions and which may become constitutively activated in cancers (Cunningham et al. 2013). In cancer cells Eps8 degradation, at least in part, appears to occur by chaperone-mediated autophagy (Welsch et al. 2010). Over-expression of human Intersectin 2 (ISTN2) has been shown to target Eps8 for lysosomal degradation but whether this is relevant with physiological ISTN levels is unclear (Ding et al. 2012).

Interestingly, other proteins with partial sequence homology to Eps8 have been identified and are regarded as other members of the 'Eps8 family' (Offenhauser et al. 2004). 'Eps8-like 1,2 and 3 (Eps8L1/2/3)' are expressed in mammals, but *Drosophila* express only two members of the family, and *C elegans* express none beyond Eps8.

In vitro Eps8L2 shows very similar functional characteristics to Eps8. It can bind F-actin, and also binds Abi1, binds and activates SOS-1, and thereby produces Rac1-activating activity. While Eps8L1 also does this, albeit less avidly, Eps8L3 has much less homology in its C terminal domain and resultantly lacks the ability to bind F-actin, SOS-1, or activate Rac1 (Offenhauser et al. 2004). As a result of the sequence of their C-terminal domain, Eps8L1 and Eps8L2 localise to collections of actin, such as at a membrane ruffle, while the distribution of Eps8L3 appears more consistent with a role in vesicle trafficking.

1.2.3 *In vivo* roles

Despite the fundamental importance of Eps8 in actin remodelling and cell motility, the Eps8 knockout mouse is viable and fertile. It has been shown to possess shortened intestinal microvilli resulting in improved metabolic baseline and it has an extended lifespan. It also demonstrated a resistance to alcohol intoxication but was discovered to be profoundly deaf (Scita et al.

1999; Offenhauser et al. 2006; Tocchetti et al. 2010). Recently a group of humans have also been identified with non-functional Eps8 and they too exhibit profound deafness (Behlouli et al. 2014; Olt et al. 2014). Other roles of Eps8 have been identified in synaptic plasticity and learning, macrophage phagocytosis, dendritic cell-mediated immunity, and spermatozoa development (Chen et al. 2012; Frittoli et al. 2011; Menna et al. 2013; Cheng & Mruk 2011). While Eps8 is expressed throughout the body, subtle variations in expression within tissues are now being observed, including variation in different types of neurons. The significance of these findings is currently unclear (Huang et al. 2014).

Several of the known functions of Eps8 are mediated by its interaction with the actin cytoskeleton. Indeed the Eps8 knockout mouse shows markedly reduced actin-based propulsion highlighting the importance of the protein in actin remodelling (Disanza et al. 2004). This was shown to have particular significance in dendritic cells which migrated towards lymph nodes significantly more slowly in Eps8 knockout mice (Frittoli et al. 2011).

Little is known about the role of the other Eps8-like proteins *in vivo.* In the mouse Eps8 is necessary for the initial generation of stereocilia while Eps8L2 is required for hair cell stereocilia maintenance (Furness et al. 2013). The presence of redundancy of Eps8-like proteins in mammals has been used to explain the relative paucity of deleterious effects observed in the Eps8 knockout mouse. However, mouse embryonic fibroblasts have been shown to express no detectable mRNA for Eps8-like proteins and in the adult the relative expression of the different family members varies between tissues (Offenhauser et al. 2004). It therefore seems unclear as to what extent Eps8-like proteins can substitute for Eps8.

1.2.4 Eps8 in cancer

Elevated expression of Eps8 has been documented in the epithelial compartment of a range of tumour types including OSCC, oesophageal, thyroid, pancreatic carcinoma, and glioma but a subset of colonic carcinomas and adenomas downregulate Eps8 expression (Ding et al. 2013; Chu et al. 2012; Abdel-Rahman et al. 2012; Bashir et al. 2010; Welsch et al. 2007; Griffith et al. 2006). The increased expression of Eps8 in tumour specimens can

correlate with the presence of regional metastases, and in haematological and solid malignancies inversely correlates with overall patient survival and outcome (Yap et al. 2009; Bashir et al. 2010; M. Xu et al. 2009; Welsch et al. 2010; Ding et al. 2013; Chu et al. 2012; Kang et al. 2012). Tyrosine phosphorylation of Eps8, to a level consistent with persistent mitogenic signalling, is also observed in a range of tumour specimens and may be as significant as Eps8 overexpression in generating a proliferative and pro-invasive signal (Matoskova et al. 1995).

Head and neck tumour cell lines demonstrating comparatively limited migratory behaviour and expressing low levels of Eps8 can be induced to become more proliferative and invasive by increasing their Eps8 expression, while the migration of lines expressing higher levels of Eps8 can be reduced by its downregulation (Wang et al. 2009). Eps8 has been shown to be essential for mediating αvβ6 and α5β1-integrin dependant migration in oral squamous cell carcinoma lines and so down-regulation of Eps8 is seen as a potential therapeutic tool (Yap et al. 2009). Interestingly, the Rac1-activating tricomplex has been shown to be essential for metastasis in ovarian cancer, where removal of any member of the complex prevents metastatic spread (Chen et al. 2010).

Overexpression of Eps8 in pituitary cell lines also increases proliferation and protects cells from serum-starvation-induced apoptosis. The latter effect was shown to be abrogated by blockade of the PI3K pathway (M. Xu et al. 2009). Elevated Eps8 expression also increases the activity of the transcription factor FOXM1, contributing to cell proliferation and migration, the latter of which could be inhibited by PI3K inhibitors (Wang et al. 2010).

Reduction of Eps8 expression in tumour cell lines by the use of siRNA can reduce cancer cell proliferation and migration (Cattaneo et al. 2012; Ding et al. 2013). Eps8 mRNA and protein levels can effectively also be reduced by the antibiotic Mithramycin A providing a potential for therapeutic use (Yang et al. 2010). A similar effect has been noted for Daunorubicin on AML-derived macrophages (Gan et al. 2013). Other treatments targeting Eps8 expression include the use of vaccination against Eps8 which has proven of some benefit in inhibiting the growth of mouse mammary tumours and improving organism survival (He et al. 2013). Recently Eps8 has also been shown to act as a

prognostic biomarker in AML. Here, elevated levels correlate with disease presence and drop in response to chemotherapy when remission is induced (L. Wang et al. 2013). Response to Cisplatin chemotherapy has also been shown to be improved by Eps8 knockdown or the use of Mithramycin A in five lung cancer cell lines, while Eps8 knockdown also increases Cisplatin and Paclitaxel sensitivity in cervical cancer cell lines (Gorsic et al. 2013; Chen et al. 2008).

The role of Eps8 in tumour stroma, by contrast, has been the focus of comparatively little research.

1.3 Summary

Myofibroblasts and other activated fibroblasts play pivotal roles in the development and progression of both fibrotic disease and tumorigenesis. Despite heterogeneity in their site of origin and expression profile, the most significant marker of their activation remains the *de novo* expression of αSMA and its incorporation into stress fibres. Extracellular matrix and tissue tension are essential for myofibroblast development and the positive feedback loop resulting in further tension generation escalates the pro-fibrotic response. During both surgical and non-surgical wound healing removal of tissue tension reduces the fibrotic signal seemingly by myofibroblast apoptosis.

While there are several identified factors that can prevent *in vitro* myofibroblast transdifferentiation, these are of limited benefit in human disease where in many cases the fibrotic response is already well established prior to diagnosis. Reversal and deactivation of truly transdifferentiated myofibroblasts remains one of the 'holy grails' of stromal research but its use may still be limited to cancer and relatively early fibrotic disease, before the stroma becomes acellular and the volume of secreted matrix determines patient fate. While searching for the 'magic bullet' to reverse myofibroblast transdifferentiation, efforts to further understand the mechanisms of myofibroblast transdifferentiation may further inform preventative strategies that can be employed to avoid inadvertent stromal activation by other treatments. This is especially relevant as we move into an era of personalised treatments in cancer and other diseases where many more therapeutic agents are brought to market for use in a targeted manner in individual patients.

The potential role of Eps8 in myofibroblast transdifferentiation is attractive to investigate. Although Eps8 is a key protein in actin and cytoskeletal re-modelling its role in myofibroblast transdifferentiation had not been investigated. Additionally, in cancer cells, Eps8 has also been shown to influence cell proliferation and apoptosis which, if paralleled in the myofibroblast, could prove therapeutically useful for terminating the myofibroblast response. Furthermore, the overexpression of Eps8 in cancer cells, and evidence of correlation with metastatic potential, have generated the search for Eps8-targetting pharmacological and immunotherapy treatments. Understanding how these treatments may affect the tumour stroma is therefore of great significance.

1.4 Hypothesis

Given the importance of Eps8 as an adaptor protein for actin re-organisation, we hypothesised that it would be required for, and possibly up-regulated during, myofibroblast transdifferentiation.

1.5 Aims

In this project we aimed to specifically investigate:

- the expression of Eps8 in fibrotic disease and cancer stroma.
- the modulation of Eps8 expression during fibroblast-to-myofibroblast transdifferentiation *in vitro*.
- the regulation of fibroblast-to-myofibroblast differentiation by Eps8-dependent signalling pathways *in vitro* and *in vivo*.

Chapter 2: Methods

2.1 Cell culture

2.1.1 Origins of cells used

Human Fetal Foreskin Fibroblasts (HFFF2)

HFFF2s are a non-immortalised cell line derived from a 14-18 week Caucasian human fetus. They were purchased from Public Health England.

Primary Skin Fibroblasts 2/3 (PSF2 & PSF3)

PSF2 and PSF3 are fibroblasts grown out from tissue samples from areas of clinically healthy skin in adult patients. They were isolated using the technique described in section 2.1.5. PSF3 cells were harvested by myself, whereas PSF2 cells were kindly provided by Dr M Mellone.

Primary Oral Fibroblasts (POF)

Primary oral fibroblasts were previously isolated using the same outgrowth method and kindly provided by members of the Experimental Pathology Group.

Normal Oesophageal Fibroblasts (NOF) & Cancer Associated Fibroblasts (CAF)

NOF and CAF cells and lysates were kindly provided by Mr Underwood's group. Normal oesophageal fibroblasts were grown out from oesophageal tissue excised from sites distant from tumour in oesophageal cancer patients. Cancer associated fibroblasts were grown out from stroma immediately surrounding the oesophageal tumour. In some instances, matched pairs originating from the same patient were available.

Human Tongue Squamous Cell Carcinoma cell line (SCC25)

This is a cancer cell line derived from a tongue SCC of a 70-year old male and is commercially available from the ATCC.

UM-SCC-5PT Head & Neck Cancer cell line (5PT)

This is a head & neck cancer cell line developed with cisplatin resistance (Bauer et al. 2005). It has been previously used in our group in mouse xenograft experiments.

2.1.2 Cell culture medium

Fibroblasts were grown routinely in Dulbecco's Modified Eagles Medium (DMEM) with 10% Fetal Bovine Serum (FBS) and 2mM L-glutamine. 1% Penicillin/Streptomycin was added to the medium for early passage primary fibroblasts but was not routinely added otherwise.

SCC25 cells were grown in 'SCC25 medium'. This contained 1:1 mixture of Hams F12 medium and DMEM, with added 10% FBS and 2mM L-glutamine. Serum-free SCC25 medium comprised DMEM with 2mM L-glutamine.

5PT cells were grown in KGM (αMEM with 10% FBS, 2.2mg/ml $NaHCO_3$, 1% L-glutamine, 10ng/ml EGF, 0.4μg/ml hydrocortisone, 5μg/ml insulin, and $1.8x10^{-4}$M adenine).

All media were sterile filtered using a 0.22µm filter when first prepared and were kept in the refrigerator at 4˚C between experiments.

2.1.3 Routine principles

All *in vitro* cell culture was performed in Class II laminar flow hoods. Cells were routinely cultured in 75 or 175cm^2 flasks (Corning). Cells were grown in a humidified incubator at 5-10% CO_2 at 37˚C. Cell culture medium was routinely replaced on cells twice per week. When cell monolayers achieved 100% confluence medium was removed, the monolayer washed with sterile-filtered phosphate-buffered saline (PBS), and 1% trypsin-EDTA (Sigma Aldrich) was added to the flasks. Once the cells had detached the trypsin was neutralised with serum-containing medium, and following thorough mixing, the suspension was divided into new flasks and diluted in the appropriate medium for that cell type. Fibroblasts were split in a ratio of 1:3 or 1:4 while SCC25 were split 1:5.

Cell stocks were maintained by regularly freezing down cells. Following trypsinisation and its neutralisation cells were centrifuged at 1250min^{-1} for three minutes to produce a cell pellet. The medium was removed and the pellet re-suspended in fresh growth medium containing 10% DMSO (Sigma-Aldrich). Aliquots of cells containing approximately 1x10^{6} cells in 1ml were then placed in cryovials in a Nalgene™ cryo-freezing container with isopropanol in the -80°C freezer. These were then transferred to liquid nitrogen for long-term storage.

2.1.4 Mycoplasma PCR

HFFF2 fibroblasts were regularly examined by means of PCR to exclude mycoplasma contamination.

10-15ml of medium was collected from confluent cells grown in antibiotic-free medium for at least two weeks. Medium was spun at 4500 min^{-1} for 5min, and the majority of the supernatant was discarded leaving the last 500μl. 1μl of re-suspended sample was added to a master mix containing, per sample, 16.7μl 'mastermix', 0.3μl formamide, 1μl forward primer 1(100pmol/μl) and 1μl reverse primer (100pmol/μl). In addition to the samples being tested, positive controls and negative controls (containing RNAse-free water) were run.

Thermal cycling conditions were 95°C for 30s, followed by 35 cycles of (95°C for 30s, 55°C for 30s, 72°C for 1min), followed by 72°C for 1min. 1μl of the PCR product was then used again in a fresh reaction mixture containing, per sample, 17μl mastermix, 1μl forward primer (100pmol/μl) and 1μl reverse primer (100pmol/μl). Identical cycling conditions were used for the second round as the first.

10μl of the PCR product was then run on a 1% agarose gel, prepared in a Fisherbond horizontal gel plate, at 120V for 60min along with a 25 base pair DNA ladder (Promega). The gel was then imaged on a UVP GelDoc-It™ imaging system.

Table 2 Sequences of primers for mycoplasma PCR

Name	Sequence
forward 1	ACTCCTACGGGAGGCAGCAGTA
forward 2	CTTAAAGGAATTGACGGGAACCCG
reverse	TGCACCATCTGTCACTCTGTTAACCTC

2.1.5 Isolation of primary dermal fibroblasts

Ethics approval for the isolation of primary fibroblasts from patients' tissues was granted (REC No. 09/H0501/90) and patient consent to the provision of tissue samples was explicitly provided on the hospital operation consent forms. Dermal primary fibroblasts were isolated from skin taken from sites distant from a primary skin tumour (eg. the edge of a donor graft site) from patients undergoing procedures at University Hospital Southampton. Following excision, tissue was immediately placed into 7-10ml of PBS with 1% Penicillin/Streptomycin and Amphotericin B (250ng/ml; Gibco) and then washed three times in the same solution.

The section of dermis was then cut into small pieces, each measuring approximately 2mm. A cross was then scored with a scalpel in the bottom of a 12-well plate and the tissue squashed gently onto it with the scalpel to allow it to adhere.

750μl of DMEM, containing 20% fetal bovine serum (FBS), 1% glutamine, 1% Penicillin/Streptomycin and 250ng/ml Amphotericin B was carefully added to each well. Each plate was minimally disturbed and medium replaced every two days.

After approximately 3-4 weeks, and when there was sufficient fibroblast outgrowth, medium was removed, the wells gently washed with PBS and trypsinised with 750μl trypsin-EDTA per well to allow the contents of all the wells to be pooled into a single 25cm^2 tissue culture flask. This was then expanded to a 75cm^2 and then a 175cm^2 flask.

2.2 siRNA transfection

Initial experiments were performed to optimise the plating density for HFFF2 and primary dermal fibroblasts in preparation for transfection and to optimise the Eps8 siRNA concentration (Appendix A, fig 6-12).

Transfection of fibroblasts with short interfering RNA was performed using the Oligofectamine (life Technologies) delivery system according to the manufacturer's protocol. Cells were counted using a Casy® counter (Roche Innovatis AG) and were plated in 6-well plates, in 2ml 10% DMEM, at a density of 100 000 cells per well for HFFF2 and between 50 000 and 75 000 cells per well for primary fibroblasts. Cells were then incubated at 37˚C overnight to adhere and spread. Following removal of 10% DMEM from the wells, cells were rinsed with 1ml Opti-MEM and then 800µl Opti-MEM was placed in each well. SiRNA was diluted from 20µM stocks in Opti-MEM® (Life technologies) with 1211µl Optimem added to 9.9 µl siRNA per 6-well plate. After 10min the siRNA was mixed with Oligofectamine solution diluted in Opti-MEM (1:5, 95µl total solution per 6-well plate). After a further 20min the mixture was pipetted drop-wise (200µl/well) into the wells resulting in a final siRNA concentration of 30nM.

After incubation at 37˚C 5% CO_2 for 4 hours, 500µl of DMEM containing 30% FBS was added to each well. In some experiments inhibitors (TGFβ-RI kinase IV (Calbiochem) or GKT137831 (Genkyotex)) were added prior to the serum-containing medium to inhibit activation of serum-stimulated pathways. Further treatments, which included the replacement of the medium with serum-free DMEM (+/- TGFβ1), took place 24h post-transfection. Quantitative assays were performed 72-96h after transfection. Functional assays were performed either 24h or 72h after transfection.

Table 3 siRNAs used

SiRNA	Working concentration	Manufacturer
Silencer negative control #1 siRNA	30nM	Ambion
Eps8	30nM	Ambion
Flexitube GeneSolution for Eps8	30nM	Qiagen
On-target Plus human Abi1	30nM	Thermo Scientific
On-target Plus human SOS-1	30nM	Thermo Scientific
Silencer Select Rac-1	30nM	Ambion

2.3 Protein quantification

2.3.1 Protein extraction & total protein quantification

For cells plated in a monolayer, medium was removed and the monolayer washed with PBS, which was subsequently aspirated off to dryness. Cells were either lysed at this point or stored at -80°C as a dry monolayer and lysed later. To lyse the cells, they were scraped on ice in NP40 lysis buffer (50mM Tris pH7.5, 1% Nonidet P40, 5mM EDTA, 5mM EGTA, 50mM NaCl, 5mM NaF) with 1% added protease inhibitor cocktail (Set1, Calbiochem). Where phosphorylated proteins were being assessed 1% phosphatase inhibitor cocktail (Halt phosphatase inhibitor cocktail (Thermo Scientific)) was included in the buffer. The lysate was pipetted several times to mix fully and then centrifuged at 13000rpm for 5min to precipitate the non-soluble fraction. The supernatant was then retained and total protein quantification performed. To do this, 5μl of sample was compared against 5μl of pre-prepared bovine serum albumin (BSA) standards in NP40 buffer using the DC™ protein assay kit (Bio-Rad) according to the manufacturer's instructions. The absorbance of the microplate was measured using a plate-reader (Varioskan) at 650nm.

2.3.2 Polyacrylamide gel electrophoresis

8,10 or 12% gels were cast according to the molecular weight of the proteins of interest (Table 3). Samples were diluted as required with NP40 buffer to create equal total amounts of protein across comparable samples. 5X Laemmli buffer (625mM Tris pH6.8, 10% SDS, 25% glycerol, 0.015% bromophenol blue, 5% β-mercaptoethanol) was added, providing reducing conditions, and the samples were boiled at 95°C for 8min before briefly centrifuging. Samples were loaded into the gel alongside protein marker lanes (Page Ruler Pre-stained Protein ladder 26616 (Thermo Scientific)) and were separated at 100-150V.

2.3.3 Western blotting

Proteins were transferred for 1h at 90V on ice or overnight at 20V at room temperature onto polyvinylidene-difluoride (PVDF) membrane (Millipore) using a mini Trans-Blot®cell (Bio-Rad). PVDF membranes were pre-activated with 100% methanol. When comparison of protein expression was required across

several gels the TE62 tank transfer unit (Amersham) was used which facilitates even, synchronous transfer of several gels overnight. Membranes were then blocked in 5% milk in TBST (0.15M NaCl, 0.01M TrisHCl, 0.05% Tween 20) for at least 45 minutes on an electronic tilting table at room temperature. Following two brief washes in TBST the membranes were placed in primary antibody in 2.5-5% BSA in PBST (2.5-5% BSA in PBS with 0.05-0.1% Tween 20) (see Table 4 for antibody working concentrations). Primary antibody incubation was normally performed in a 50ml Falcon tube on a roller overnight at 4˚C or for 2h at room temperature. Membranes were then washed three times for 5min in TBST and incubated with horseradish-peroxidase-conjugated secondary antibodies (Dako) on a roller for 1h at room temperature (see Table 4 for antibody working concentrations). Membranes were then washed again three times for 5min in TBST, briefly dried and exposed to chemiluminescence solution (Supersignal West Pico or Femto ECL, Thermo Scientific), with visualisation performed using a Chemidoc imager and software (UVP). If stripping of the membrane was required prior to addition of a different primary antibody the Reblot Plus Strong antibody stripping solution (Millipore) was used according to the manufacturer's protocol.

Relative densitometry was performed, where appropriate, using Image J software (National Institute of Health).

Table 4 Antibodies used in Western blotting

Antibody	Manufacturer	Catalogue #	Working dilution	Target MW
HSC70	Santa Cruz	72953	1:1000	70kDa
GAPDH	Cell signalling	14C10	1:1000	37kDa
αSMA	Sigma-Aldrich	A2547	1:1000	42kDa
Palladin	Novus	125959	1:1000	85kDa
Eps8	BD Transduction	610144	1:5000	97kDa
Abi1	Prof Scita, Milan	n/a	1:200	75kDa
SOS1	Santa Cruz	17793	1:200	170kDa
Rac1	Millipore	05-389	1:5000	21kDa
AKT	Cell Signalling	9272	1:1000	60kDa
pAKT (ser473)	Cell Signalling	D9EXP	1:1000	60kDa

SMAD2	Cell Signalling	D43B4	1:500	60kDa
SMAD3	Cell Signalling	C67H9	1:500	52kDa
pSMAD2/3 (ser465/467)	Cell Signalling	138D4	1:500	60/52kDa
pSMAD3 (ser423/425)	Cell Signalling	C25A9	1:500	52kDa
Nox4	Novus	NB110-58849	1:500	67kDa
Shb	R&D systems	AF7036	1:500	55 kDa
polyclonal Rabbit anti-mouse	DAKO	P0260	1:5000	n/a
polyclonal swine anti-rabbit	DAKO	P0217	1:5000	n/a

2.4 Real-Time Quantitative Polymerase Chain Reaction (qRT-PCR)

2.4.1 RNA extraction

RNA extraction was performed using the RNEasy mini kit (Qiagen). Fresh cell monolayers washed with PBS, or dry, previously washed monolayers stored at -80˚C underwent extraction at room temperature according to the manufacturers protocol. β-mercaptoethanol was added to the RLT buffer and optional DNAse digestion steps were performed using the RNAse-free DNAse set (Qiagen). Once extracted, RNA samples were kept on ice and quantification was performed on the Nanodrop spectrophotometer (Thermo Scientific). If 260/280 ratios were ≤1.8, RNA clean-up was performed using the RNEasy Minielute Cleanup kit (Qiagen). Samples were then stored at -80˚C.

2.4.2 cDNA synthesis

cDNA was reverse transcribed from RNA samples using the High Capacity cDNA Reverse Transcription Kit (Applied Biosystems) according to the manufacturer's protocol. The optional addition of RNAse inhibitors was not required. 1µg RNA was reverse transcribed in a 20µl reaction mixture on a thermal cycler with parameters as outlined in the kit's instructions. The synthesised cDNA was stored at -80˚C.

2.4.3 Quantitative real-time PCR

Real time PCR was performed using Power SYBR® Green reagents (Life Technologies) and a 7500 Real time PCR system (Applied Biosystems). Target oligonucleotide sequences were either (1) already available within the Experimental Pathology Group; (2) published and we checked sequences for non-specific interactions in BLAST nucleotide (http://www.ncbi.nlm.nih.gov/BLAST/Blast.cgi?PROGRAM=blastn&PAGE_TYPE=BlastSearch&LINK_LOC=blasthome); or (3) if sequences were not publically available we used Primer Blast (www.ncbi.nlm.nih.gov/tools/primer-blast) to generate the sequences. A PCR product length of 50-150 base pairs was selected, and wherever possible we included an exon-exon junction to exclude erroneous amplification of DNA sequences. Two sets of primer pairs were selected per target, from different locations on the gene. These were then also checked to include that they recognised all known splice variants of the gene. Oligonucleotides were also checked to ensure low self-complementarity. Following their design, primers were manufactured by Sigma-Aldrich and supplied desalted (for specific primer sequences see Table 4).

Primer concentration optimisation was performed for each new primer pair using a mixture of cDNA generated from HFFF2 treated with or without TGFβ1 from previous experiments. Serial dilutions of forward and reverse primer mixes were performed to generate working concentrations in 2-fold dilutions at 0.4, 0.2, 0.1 and 0.05μM. These were then used in PCR reaction mixes with the pooled cDNA. Amplification plots and melt curves were then analysed and the most dilute concentration of primer pair that did not markedly reduce the amplitude of the melt curve were selected. If the first primer pair for each target worked adequately the second pair was not tested.

The relative standard curve technique was used to quantify target mRNA normalised to GAPDH. This facilitates accurate analysis, and is recommended particularly for small fold change differences between samples.

For each experiment standard curves for target and endogenous control genes were prepared against 1:5 serial dilutions of a stock cDNA from a mix of TGFβ1-treated and untreated HFFF2. At least 4 serial dilutions were prepared and wells were plated at least in duplicate (creating 8 points per standard curve). Each experimental sample that was prepared for the plate was run in

triplicate and any gross statistical outliers that were identified by the Applied Biosystems software were excluded. Using analysis of the standard curve the PCR software provided the quantity of target gene in each well. For each sample we could then normalise the mean target gene quantity across the triplicate wells against the mean quantity of GAPDH across the triplicate wells to produce a 'mean normalised target' value, without units. These were then compared between samples to generate a fold-change value.

For the time course experiments, when there were more samples than could be analysed on a single plate, aliquoted pooled cDNA was used for each plate to allow consistent standard curves and therefore analysis between plates. This technique is recommended by Applied Biosystems.

Table 5 Oligonucleotides used for qRT-PCR

Target	Forward	Reverse	Working [ ] (μM)
Eps8	CGACCAAGGGGACTTTGAGA	GCACATCTCTGTCAATGCGG	0.2
Abi1	GGGAACACTGGGACGGAATA	GCTGACTTCCAAGCCTAGCA	0.2
SOS1	AGCAGAGGAACTGGCATTTGA	GCAAATAAAGTGCTGCCCCA	0.4
ACTA2	GACAATGGCTCTGGGCTCTGTAA	ATGCCATGTTCTATCGGGTACTT	0.2
Col1α1	ACGAAGACATCCCACCAATCACCT	AGATCACGTCATCGCACAACACCT	0.2
CTGF	CCCTCGCGGCTTACCGACTG	GGCGCTCCACTCTGTGGTCT	0.2
SMAD2(1)	TTTGCTGCTCTTCTGGCTCA	ACCGTCTGCCTTCGGTATTC	0.2
SMAD3(2)	TGACTGTGGATGGCTTCACC	TGACTGTGGATGGCTTCACC	0.4
SMAD4(1)	CCAGCTCTGTTAGCCCCATC	TACTGGCAGGCTGACTTGTG	0.4
SMAD6(1)	CAAGCCACTGGATCTGTCCGA	TTGCTGAGCAGGATGCCGAAG	0.4
SMAD7(2)	TGCTCCCATCCTGTGTGTTAAG	TCAGCCTAGGATGGTACCTTGG	0.4
NOX4(1)	GCTGACGTTGCATGTTTCAG	CGGGAGGGTGGGTATCTAA	0.4
GAPDH	AGCAATGCCTCCTGCACCACCAAC	CCGGAGGGGCCATCCACAGTCT	0.4

2.5 Indirect immunofluorescence

The day after transfection (as described in Section 2.2), cells were plated in 8 well chambers slides (Sigma-Aldrich) at both 2 500 and 5 000 cells in 200μl 10% DMEM per chamber. Excess cells were re-plated in wells of 6-well plates in order to confirm protein knockdown using Western blotting. After incubation overnight TGFβ1 was added to appropriate chambers at a final concentration of 10ng/ml.

After 3 days the medium was removed and the cells washed three times in PBS. Cells were then fixed by addition of 400μl 4% formaldehyde solution per chamber for 20min at room temperature and subsequently washed three times in 0.1% Triton X solution (0.1% TX100 in PBS) and permeabalised by replacement with 0.5% Triton X solution (0.5% TX100 in PBS) for 10min at room temperature. Triton X was then removed and neutralised with 50mM NH_4Cl for 10min. Following a further three washes in 0.1% Triton X chambers were treated with 150μl blocking solution (2% BSA in 0.1% Triton X) for 2h at room temperature or overnight at 4°C. After removal of the blocking solution mouse anti-smooth muscle actin was added at a concentration of 1:750 in blocking solution and incubated for 1h at room temperature. Following a further set of three 5min washes in 0.1% Triton X solution, fluorescently-labelled secondary antibody at a dilution of 1:250 in blocking buffer was added. From this point onwards the slides were kept in the dark. After 45min the chambers again underwent three washes in wash solution and were then incubated in DAPI (1:1000 in wash solution) with/without FITC-conjugated phalloidin (1:200) (Sigma) for 10min. Following a further three washes in PBS and two washes in distilled water chambers were aspirated to dryness, chambers walls removed, and a coverslip was placed on top on fluorescent mounting solution (Dako). The slides with coverslips were then kept overnight at room temperature in the dark to polymerise.

The slides were subsequently visualised using an Olympus IX81 fluorescent microscope using Xcellence imaging software (Olympus). In addition to slides for each condition, an additional slide was prepared with cells exposed only to secondary antibody to ensure specificity of secondary antibody binding. DAPI nuclear staining was used to select fields of view with a similar number of cells, and following saturation adjustment for the highest signal these parameters were used to capture the images for all conditions, allowing direct comparison. A macro, previously designed by Chris Hanley, was used in Image J to subtract the background signal and quantify the signal per field of view in each channel.

2.6 Proliferation assays

An xCELLigence Real-Time Cell Analyser DP instrument (Roche/ACEA) was used to quantify fibroblast proliferation via measurement of electrical impedance across the floor of specially manufactured tissue culture wells. Transfected HFFF2 were, the following day, trypsinised, counted on a Casy counter and re-suspended in 10% serum DMEM before plating in at least quadruplicate wells of an 'E-plate16' for use on the xCELLigence instrument. For each well, 10 000 cells suspended in 100μl of medium were added to 100μl of medium had already been equilibrating in each well in the incubator. After 6h of measurement, the plate was examined under the microscope to ensure that cells had adhered, and the medium in each well was exchanged for DMEM with/without 10% fetal bovine serum and with/without 5ng/ml human recombinant TGFβ1. After a few minutes of re-equilibration in the incubator measurement was recommenced for up to 4 days. The xCELLigence software could be used to calculate a normalised cell index and average doubling times for groups of wells containing cells in the same condition. Proliferation rates in serum-containing medium were analysed for consideration in the gel contraction assay (see below) and in serum-free conditions for analysis alongside the Transwell migration assays.

2.7 Gel contraction assay

Fibroblasts were plated in 6-well plates and transfected as described in section 2.2. The day after transfection cells were trypsinised and cell suspensions prepared containing 500 000 cells per 100μl of 10% DMEM per condition. Two mastermixes were prepared containing 7 parts rat tail collagen (Millipore), 1 part 10x DMEM (1.35g DMEM, 0.37g $NaHCO_3$, in 10ml H_2O) and 1 part fetal calf serum, neutralised with 0.1M NaOH. One mastermix contained TGFβ1 (5ng/ml) and the other did not. 1.08ml of the required mastermix was mixed with the 120μl of cell suspension per condition (in the ratio of 9:1) and mixed thoroughly. 1ml of the final solution was then plated in a 24 well plate and placed in the incubator at 37°C for 1h. After 1h, 1ml 10% DMEM with or without TGFβ1 (5ng/ml) was added to the gels, which were loosened from the base and sides of the well with a sterile spatula. Wells were monitored on a daily basis for contraction. Gel contraction was quantified by weighing the

gels, comparing the gel weight in each condition with that of the control treatment.

2.8 Transwell migration assay

HFFF2 fibroblasts were transfected as per section 2.2. The following day the medium was changed to 1.2ml of serum-free DMEM with or without TGFβ1 at 5ng/ml. After 48h the medium was aspirated, each well washed with 1ml PBS, and then 2ml of serum-free DMEM was added to each well as a collection media. After 24h the conditioned medium was collected and centrifuged at 1250min^{-1} for 3min to remove any cells or cell debris. The cell monolayers were trypsinised and counted. The medium was then frozen at -80°C or used immediately.

SCC25 cells were split 1:2 the day before being used in the migration assay. On the day the assay was set up, the conditioned medium from the HFFF2 was normalised for HFFF2 cell number by diluting where required with serum-free DMEM. 200μl of normalised collection medium was then placed, for each condition, in the lower well of a Transwell® (Costar) 24-well plate and an 8μm permeable Transwell® insert was then placed in each well. Conditions were set up in triplicate within each experiment. SCC25 cells were trypsinised, counted on the Casy counter and, following re-suspension, 50 000 cells in 100μl of serum-free DMEM were plated in the upper compartment of each Transwell. This produced a confluent monolayer, minimizing mixing of the separated solutions.

After 24h, medium was removed from the lower compartment, cell monolayers were carefully washed with 1ml PBS, and then 500μl of trypsin-EDTA was added to the lower compartment of each well. After 1h incubation at 37°C, detached SCC25 cells were counted on the Casy counter providing results in triplicate per condition.

The volume of collection media, the timing of commencement of collection, and the duration of collection were optimised prior to use.

2.9 TGFβ activation assay

The ability of transfected fibroblasts to secrete or activate TGFβ from the extracellular matrix was assessed using a Mink Lung Epithelial Cell (MLEC) bioassay. MLEC cells had been stably transfected with an expression construct containing a truncated plasminogen activator inhibitor type I (PAI-1) promoter, fused to a firefly luciferase reporter gene. Exposure of these MLEC cells to TGFβ results in a dose-dependent increase in luciferase enzyme activity which can be quantified using the Luciferase assay kit (Promega) and a plate-reader (Varioskan).

In our experiments MLEC cells were plated at 50 000 cells per well in 100μl of medium (DMEM with 10% FCS, 2mM L-glutamine, 400μg/ml Geneticine) which was replaced with serum-free DMEM the following day. After at least 4h of equilibration, the media was removed and the monolayer washed with PBS. Transfected HFFF2 were trypsinised and counted using the Casy counter and, for each condition, 20 000 cells were placed on top of the MLEC monolayer. Additional MLEC containing wells did not receive HFFF2 but instead were treated with fixed doses of TGFβ1 to generate a reference standard curve. The following morning media was removed from all wells, the cells were washed with PBS and then processed in accordance with the protocol of the Promega Luciferase Assay kit. Generated light from each well was measured using the Varioskan plate reader.

2.10 Tissue microarray (TMA) and immunohistochemistry

Tissue microarrays were already in existence within the group for 124 Oral Squamous Cell Carcinoma (OSCC) specimens between 2000-2005 and for 27 specimens of fibrosis in a range of tissues (breast, lung, pleura, kidney, gall bladder, colon). TMAs had previously been prepared from archival paraffin-embedded tissue with triplicate cylindrical cores (1mm in diameter) sampled from selected areas of specimens and arrayed onto a new recipient paraffin block using a tissue arrayer (Alphelys MiniCore® 3). Unstained slides were then cut from the TMA block for immunohistochemical staining.

Immunohistochemical staining was performed by the Department of Histopathology at University Hospital Southampton. Generally, slides were

stained through the automated equipment, but where this was not possible the following manual staining procedure was used:

Sections were de-waxed through xylene and then taken through an alcohol gradient to water. Sections were then placed on a tray and freshly prepared Endogenous Peroxidase Blocking Solution (200μl hydrogen peroxide, 11.8ml methanol) was applied for 10min. Slides were then washed in reverse-osmosis (RO) water for 2min followed by TBST for 2min. Primary antibody was then applied at the required dilution and incubated at room temperature under a plastic cover for 30min. Three 2min washes in TBST were then performed. Slides were then incubated for 30min in diluted biotinylated secondary antibody solution. This was prepared by diluting serum and secondary antibody 1:100 in buffer. Whilst this was incubating Vectastain ABC reagent was prepared by mixing reagents A and B 1:100 in 10mM sodium phosphate pH7.5 0.9% saline. After the 30min incubation had elapsed slides were washed three times in TBST for 2min each before incubation at room temperature for 30min. Wash steps were repeated before incubation in Diaminobenzidine solution (5mg Diaminobenzidine, 10ml Tris HCl buffer pH7.6 and 100μl hydrogen peroxide solution) for 10min. Following a rinse in RO water slides were then counter-stained with haematoxylin for 1min. After a final 5min wash and then blue step in running water slides were dehydrated and mounted. For IHC staining of mouse tumours the Vector® M.O.M™ immunodetection kit was used to minimise background staining. For collagen detection in mouse tumours the Masson's trichrome stain kit (Dako, 235642) was used in accordance with the manufacturer's instructions.

Table 6 Primary antibodies used in IHC

Primary Antibody	Manufacturer	Catalogue #	Working dilution
αSMA (mouse)	Sigma-Aldrich	A2547	1:100
Eps8 (mouse)	BD Transduction	610144	1:20
SMAD2 (Rabbit)	Cell Signalling	D43B4	1:20

Assessment of the TMAs and full sections was performed by Prof G. Thomas, Consultant Pathologist, who also captured the images. For SMAD2 staining, images were analysed using a macro in Image J developed by Dr C. Hanley to enable quantification and statistical analysis.

2.11 Head & neck cancer xenograft mouse model

All animal experiments were performed under appropriate Home Office personal and project licenses. Viral work was performed in Biosafety level 2 tissue culture facilities and local policies were strictly adhered to. HFFF2 fibroblasts were infected with either control lentiviral particles (with a copGFP coding construct) or Eps8 shRNA lentiviral particles (both Santa Cruz) using the manufacturer's protocol. Our group has previously optimised the use of polybrene at a concentration of 8μg/ml in HFFF2 and this was applied to the cells in 10% serum-containing DMEM before the addition of $1x10^6$ viral particles. The following day, and every 3-4 days medium was refreshed with 10% serum-containing DMEM. Populations were expanded before being placed in selection media containing 0.75μg/ml puromycin. Infection in the control group was confirmed by visualisation of the cells under the fluorescent microscope. Non-infected HFFF2 from the same batch and passage were exposed to the selection media and were appropriately eradicated within 24h.

Mcherry-labelled 5PT cancer cells were provided by Dr M Mellone and were expanded to generate sufficient numbers for the mouse experiment. Mcherry signal was confirmed under the fluorescent microscope in the TRITC channel.

Cell suspensions were then generated containing a mixture of $3x10^6$ HFFF2 and $1x10^6$ 5PT cells in 100μl/tumour. The left flank of each of 13 RAG1-/- partially immunocompromised mice was sub-dermally injected with a mixture containing control (copGFP) transfected HFFF2 with 5PT cells, while the right was injected with Eps8 knockdown HFFF2 mixed with 5PT cells. Injections were performed by experienced animal house staff. Over the next month serial electronic calliper assessments of tumour volume were undertaken by a member of the team blinded to the flank allocation. Mice were then culled. Tumours were excised and the mcherry and GFP signal were measured in a paired fashion per mouse on an IVIS imager (IVIS lumina III, Living Image 4.3.1 software) with auto settings. Flank lymph nodes were also excised and imaged.

Following imaging, tumours and lymph nodes initially underwent haematoxylin & eosin stains before the tumours underwent Masson's trichrome staining and immunohistochemistry for αSMA.

2.12 RNA-seq data analysis

The earliest RNA-seq experiments examining the effect of TGFβ1 and γ irradiation on HFFF2 fibroblasts were performed by my co-workers. For TGFβ1-induced myofibroblast transdifferentiation, HFFF2s were treated with TGFβ1 (2ng/ml) in 10% DMEM for three days and then transferred to 10% DMEM alone for a further 4 days. To generate senescent fibroblasts HFFF2 cells were detached using trypsin-EDTA, irradiated with 10Gy ϒ-irradiation and re-plated in 10% DMEM. Control cells were merely trypsinised and then re-plated. After 7 days RNA was extracted. RNA-seq libraries were prepared for each RNA sample and sequenced using an Illumina HiSeq 2500 platform, yielding 35-bp long reads at an average sequencing depth of 42.2 million raw sequencing reads per sample (range 37.4-48.5 million). An average of 87.9% aligned to the hg19 reference genome file (range 85.6%-89.7%). Mappings were then converted to gene-specific read count values using the script HTSeq-count, producing read count values for 23,368 annotated genes. All genes associated with less than 3 total read counts were excluded, providing data for 12,216 genes.

Genes were analysed for differential expression between control and TGFβ1-treated and control and ϒ-irradiated fibroblasts using the RNA-seq-specific function 'voom' in the Limma R package (Law et al. 2014). This analysis yielded a total of 598 differentially expressed genes with a Benjamini-Hochberg adjusted p-value lower than 0.001. STRING v10 network analysis software was used to report interactions between commonly down/upregulated genes (Szklarczyk et al. 2015).

The second set of RNA-seq experiments were designed to examine earlier mRNA expression changes as a result of Eps8 knockdown and TGFβ1 treatment. Early passage HFFF2 were transfected with either Eps8 or non-targeting siRNA as outlined in section 2.2. After 4h the monolayers were washed and the medium replaced with serum-free DMEM containing/free from TGFβ1 (5ng/ml). After a further 20h RNA was harvested as outlined in section 2.4.1(including the optional DNAse step) and RNA quantity along with 260/280

and 260/230 ratios were checked on the spectrophotometer. The experiment was repeated with successive passages of the same batch of HFFF2 to generate data in triplicate. Additional wells for each condition were maintained in serum-free media for 72h prior to western blotting to ensure that Eps8 knockdown augmented TGFβ1-induced αSMA expression. RNA samples were processed externally at UCL genomics where initial QC was performed on a bioanalyser. 43 base pair, paired end sequencing of mRNA was then performed on the Illumina NextSeq 500 system producing ~18 million read pairs per sample. The FASTQC v1.0.0 application (Basespace labs) in the Illumina platform was used to check the quality on the samples. The RNA-seq alignment application V1.0.0 (Illumina) was then used to generate count files which were imported into Chipster where differential expression was assessed with the DESeq pipeline using count normalisation including the parametric method of dispersion estimation and multiple testing correction for statistical analysis (Kallio et al. 2011). Differentially expressed genes ($p<0.05$) were imported into the KEGG pathway mapper to assess pathway modulation. VST normalised count data was also imported into Qlucore where PCA analysis, and heat maps based on hierarchical clustering were produced (Wood et al. 2016).

2.13 Statistics

Figures were prepared using GraphPad Prism software and statistical analysis was performed in GraphPad Prism.

For comparison between a single pair of samples in repeated independent experiments paired t-tests were performed (two-tail with significance set at a p-value of 0.05), assuming a Gaussian distribution of the differences in sample means. Where control values had been pinned to a fixed value across experiments (eg. 1 for mRNA fold change, or 100% for percentage of control gel weight) then unpaired t-tests were performed against control. If comparison was being made between treatment groups then paired t-tests were required since values for neither treatment were pinned to a fixed value and between groups, as well as within groups differences existed. If only 2 repeats had been performed a two-sample t-test was performed.

When comparisons were made between a control and two or more conditions a one-way ANOVA repeated measures analysis was performed with Fisher's Least

Significance Difference (LSD) analysis. No correction was made for multiple comparisons as in our case a maximum of 3 pairs of data were compared in each analysis, and these had been selected in advance.

Unless stated otherwise bar charts portray means with error bars displaying the standard error of the means (SEM). Significance values are marked with asterisks as follows: $P \geq 0.05$ (ns); $0.01 \leq P < 0.05$ (*); $0.001 \leq P < 0.01$ (**); $0.0001 \leq P < 0.001$ (***); $P < 0.0001$(****).

Chapter 3: The Effect of Eps8 on myofibroblast transdifferentiation

The generation of force within fibroblasts is essential for the initial development of the myofibroblast precursor termed the protomyofibroblast (Höner et al. 1988; Chrzanowska-Wodnicka & Burridge 1996). Subsequent acquisition of a full myofibroblast phenotype requires the generation of higher tensile forces, delivered through the development of more mature and developed focal adhesions in direct connection with the extracellular matrix (Goffin et al. 2006). This highly contractile status is accompanied by cytoplasmic recruitment of αSMA to filamentous actin filaments, which has been identified as a defining feature of the myofibroblast (Eyden 2008). Additionally, the transmission of contractile forces releases TGFβ1 from a latent bound state on the extracellular matrix and the released, activated cytokine additionally contributes to myofibroblast transdifferentiation (Murphy-Ullrich & Poczatek 2000).

Given that Eps8 has recognised roles in both the prevention of actin branching and the promotion of actin fibre bundling (Disanza et al. 2004) it may be necessary in order to build the actin and αSMA-containing scaffold necessary for myofibroblast transdifferentiation. If this hypothesis is correct, Eps8 expression may either remain constant or even be upregulated during myofibroblast transdifferentiation within fibrotic tissues or cancer stroma. Furthermore, suppression of Eps8 protein levels may prevent fibroblast-to-myofibroblast transdifferentiation. In this chapter we investigated these hypotheses.

3.1 The modulation of Eps8 expression during myofibroblast transdifferentiation

3.1.1 Eps8 mRNA expression in HFFF2 is down-regulated by TGFβ1 treatment

In a recent study by our group RNA-seq technology was used to assess gene expression changes resulting from treatment of HFFF2 fibroblasts with TGFβ1 as described in Section 2.12.

We analysed the RNA-seq data extracting the fold change and adjusted p-values of a number of genes known to be upregulated during myofibroblast transdifferentiation. As can be seen from fig 3-1(a) ACTA2 (encoding αSMA protein), COL1A1 (encoding alpha 1 type I collagen) and CTGF (encoding connective tissue growth factor) all increased in response to TGFβ1 treatment consistent with changes known to occur during myofibroblast transdifferentiation (Tobar et al. 2014; Mia et al. 2014). The changes seen in the expression of these genes are highly significant with an adjusted p- value between 10^{-8} and 10^{-18}. Under the same conditions, Eps8 gene expression was shown to be downregulated with a fold change value of 0.715. This result was also highly significant with an adjusted p value of 1.86×10^{-5}.

The 497 down-regulated genes with an adjusted p-value of $<1 \times 10^{-8}$ were analysed in STRING 10 software to assess the strength of predicted relationships between their respective coded proteins. Although the role of Eps8 as an important protein in TGFβ-induced myofibroblast transdifferentiation is not recognised in the literature, it can be seen at the edge of a central core of proteins known or predicted to interact with each other (figure 3-1(b)).

The RNA-seq data therefore provided initial evidence that myofibroblast transdifferentiation is associated with a reduction in Eps8 mRNA expression and that this may be a potentially important, unrecognised factor in myofibroblast transdifferentiation.

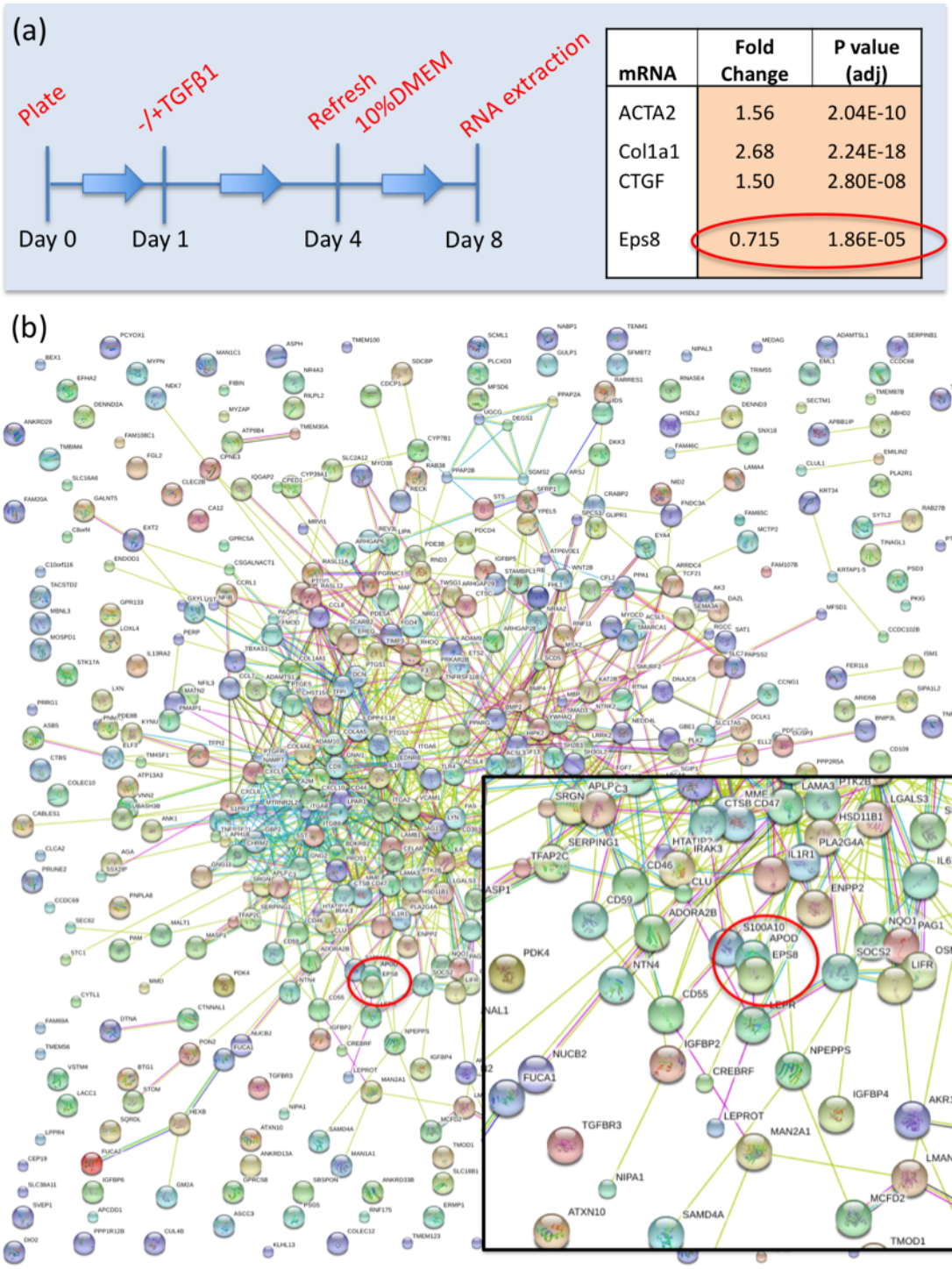

mRNA	Fold Change	P value (adj)
ACTA2	1.56	2.04E-10
Col1a1	2.68	2.24E-18
CTGF	1.50	2.80E-08
Eps8	0.715	1.86E-05

Figure 3-1 Eps8 is downregulated in fibroblasts as a result of TGFβ1 treatment, and lies amongst a core network of downregulated genes.

(a) Fold change and adjusted p-values of Eps8 and three marker genes of myofibroblast transdifferentiation resulting from TGFβ1-treatment for 72h compared to controls in HFFF2 (synchronous n=3) (b) STRING 10 association network resulting from the 497 most significantly down-regulated genes from the RNAseq analysis. Different coloured lines represent the types of evidence used in predicting the associations (red = fusion, green = neighborhood; blue = co-occurrence; purple = experimental; yellow = textmining; light blue = database; and black = coexpression evidence.

We further confirmed these changes using qRT-PCR. HFFF2 fibroblasts were treated with human recombinant TGFβ1 at a final concentration of 5ng/ml or left without treatment in serum-free DMEM for 72h. Following RNA extraction quantitative real-time PCR was performed on the samples using the relative standard curve technique to analyse the change in normalised target quantities resulting from TGFβ1 treatment.

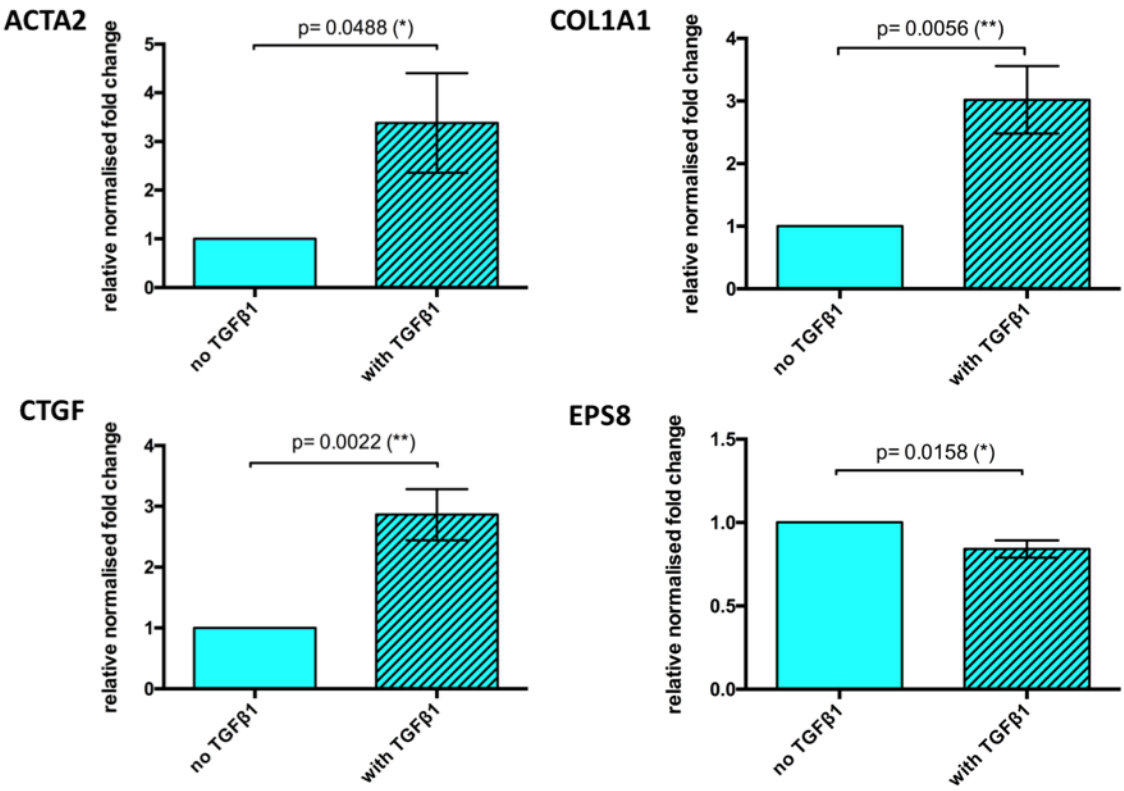

Figure 3-2 TGFβ1 reduces Eps8 mRNA expression in fibroblasts.

Relative fold change of ACTA2, Col1α1, CTGF and Eps8 mRNA in control-transfected HFFF2 treated with/without TGFβ1 (5ng/ml) for 72h (independent n=5). Error bars represent SEM; p value generated using two-tailed unpaired t-test). This formed part of a larger experiment, which is why in both conditions, cells were first transfected with control siRNA.

We can see from the combined results of five independent experiments (figure 3.2) that while ACTA2, CTGF and Col1a1 expression all significantly increase with TGFβ1 treatment (confirming myofibroblast transdifferentiation), Eps8 expression is significantly reduced. Furthermore, the fold change in Eps8 expression is similar to that seen in the RNA-seq experiment.

3.1.2 TGFβ1 reduces Eps8 expression at the protein level and this precedes complete myofibroblast transdifferentiation

We subsequently assessed Eps8 expression changes resulting from TGFβ1 treatment at the protein level, and the temporal relation of those changes to myofibroblast transdifferentiation. As previously, HFFF2 fibroblasts were plated in 10% DMEM and left to adhere overnight. The following day the medium was replaced with serum-free DMEM with or without 5ng/ml TGFβ1. At the designated time points the cells were washed, then lysed, and Eps8 and αSMA expression was analysed by Western blotting.

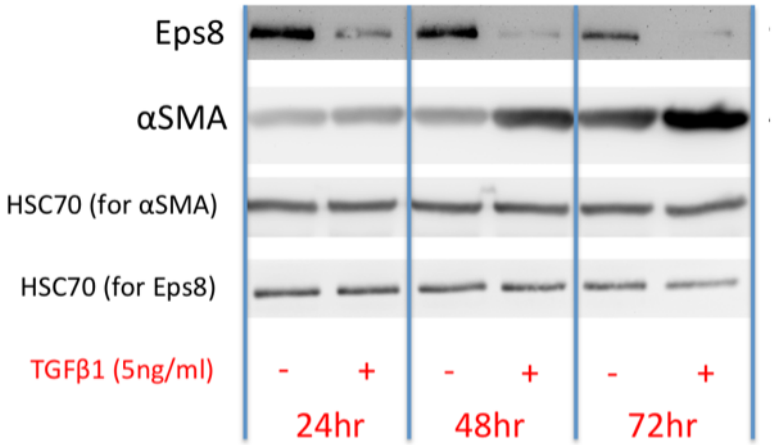

Figure 3-3 In response to TGFβ1 treatment Eps8 downregulation occurs early, before αSMA upregulation.

HFFF2 fibroblasts harvested 24, 48 and 72h post treatment with 5ng/ml human recombinant TGFβ1. Eps8 and αSMA expression were analysed by Western blotting. Hsc70 was used as a loading control. Differing amounts of total protein were run for Eps8 and αSMA so each has its own Hsc70 loading control. The experiment was performed in duplicate and was also independently repeated - a representative blot is shown.

Eps8 expression is reduced within 24h in TGFβ1-treated compared to untreated HFFF2. The effect on Eps8 expression precedes the TGFβ1-induced upregulation of αSMA, which is seen more reliably at 48h and beyond. Since Eps8 levels are reduced before αSMA upregulation and subsequent completion of myofibroblast architectural transdifferentiation, it suggests that Eps8 down-regulation might be involved in the mechanism of fibroblast-to-myofibroblast transdifferentiation.

3.1.3 Stromal Eps8 expression inversely correlates with αSMA expression in human tissue samples of Oral Squamous Cell Carcinoma (OSCC) and organ fibrosis

In order to assess whether the reciprocal stromal expression pattern between Eps8 and αSMA is observable i*n vivo* as well as in fibroblast cultures *in vitro* we analysed a series of tissue micro arrays (TMAs) of oral squamous cell carcinoma (OSCC) cases and fibrotic specimens from a range of different tissues (breast, lung, pleura, kidney, gall bladder, colon). In total 124 OSCC specimens and 27 fibrotic specimens were included in the analysis. Sections from fibroepithelial polyps were used as controls. Fibroepithelial polyps are stromal and fibroblast-rich lesions that contain few myofibroblasts and hence, conversely to the other specimens, express little or no αSMA. They can arise in many different anatomical locations, including the tongue, female urogenital tract and the anus. We used 11 sections of fibroepithelial polyps, one of which was from skin, one from tongue and the other 9 originated from oral mucosa.

Microarray sections were immunostained for Eps8 and αSMA and compared with the 'full-face' sections of fibroepithelial polyps. Holistic scoring of Eps8 expression using a standard scoring technique was not technically feasible due to its comparatively slight expression in the stroma (despite high antibody concentrations), and the variation in expression between stromal cell types. Endothelial cells particularly demonstrated significant Eps8 expression compared to fibroblasts. Our observations therefore had to take into account the stromal cell types being examined within the sections, and are therefore qualitative rather than quantitative.

Cores from various fibrotic organs expressed high levels of αSMA in their stroma, as did most of the cores from OSCC. In contrast, there was almost no αSMA staining in the fibroepithelial polyp sections, which acted as our controls. Analysis of Eps8 staining demonstrated that fibroblasts within the fibrotic and OSCC specimens demonstrated less Eps8 staining compared to the fibroblasts from fibroepithelial polyps. This is clearly demonstrated in the sample images (figure 3-4). Endothelial staining of Eps8 was particularly prominent in all sections and had to be carefully excluded when evaluating fibroblast-related Eps8 expression in the stroma.

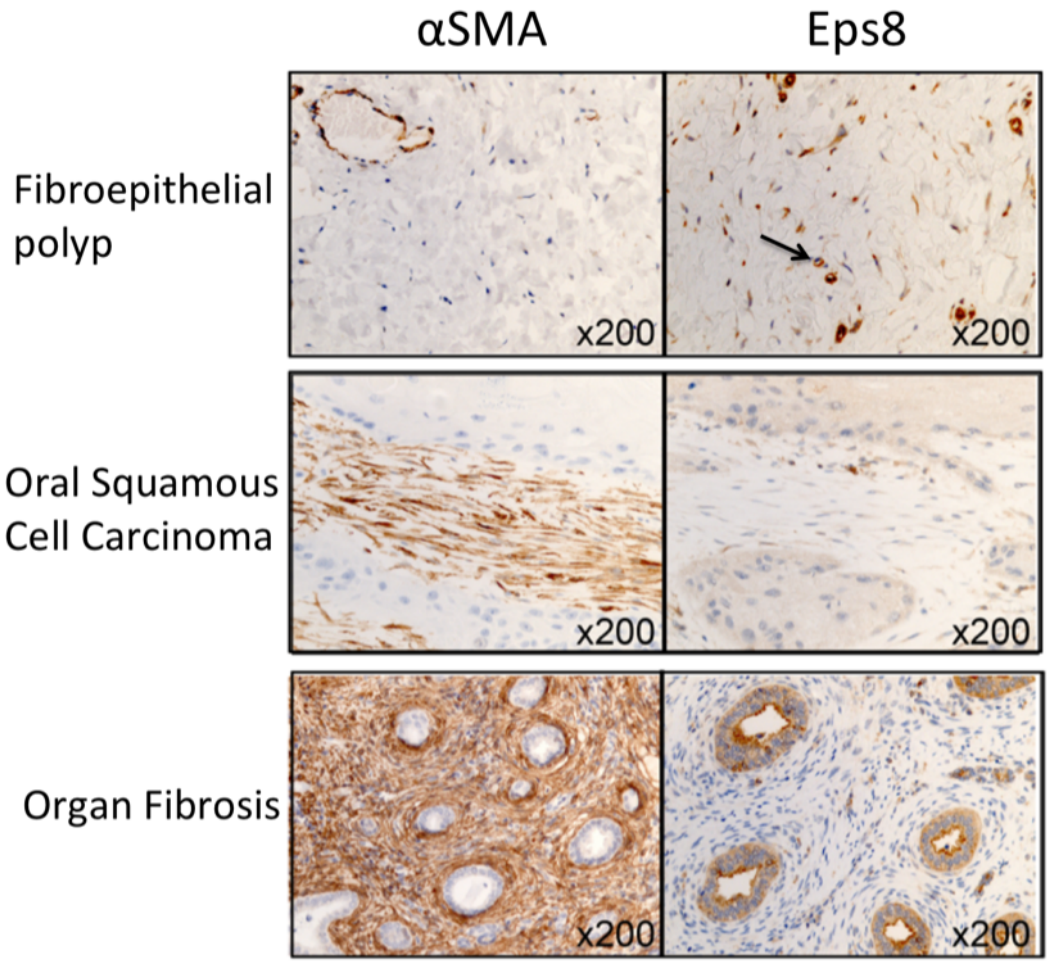

Figure 3-4 Eps8 expression is reduced in the myofibroblast rich stroma of head & neck cancers and within organ fibrosis from a range of tissues.

Representative images from cores of oral squamous cell carcinoma, fibrotic tissues and fibroepithelial polyps, immunostained for smooth muscle actin (1:100) and Eps8 (1:20) and viewed at 200x magnification. Note the marked staining of endothelial cells for Eps8 (arrow).

These findings support the Western blot data and indicate an inverse relationship between stromal Eps8 and αSMA expression in fibroblasts and myofibroblasts within human tissue. These observations hold across a range of human pathologies in which myofibroblasts are known to play critical roles, including organ fibrosis in a range of tissues and oral squamous cell carcinoma.

3.1.4 Myofibroblast transdifferentiation induced by irradiation, hydrogen peroxide or replicative senescence may also reduce Eps8 expression

Senescence is a state in which cells are unable to replicate but also fail to undergo apoptosis. A number of stimuli can induce fibroblast senescence, including γ-irradiation (causing genotoxic stress) and repeated hydrogen peroxide administration (causing oxidative stress) (Gadbois et al. 1997; Chen & Ames 1994). Our group has previously demonstrated that senescent fibroblasts share a number of features with myofibroblasts including augmented expression of αSMA, increased functional contractility and the ability to augment cancer cell migration (Mellone et al. 2016). They also, however, show some distinct differences in their gene expression profiles with senescent fibroblasts demonstrating less upregulation of some extracellular matrix proteins such as secreted collagens (Mellone et al. 2016).

RNA-seq data had previously been generated in our group from γ-irradiation-induced senescent fibroblasts and control fibroblasts (as described in section 2.12). As described in section 3.1.1 we initially extracted the gene expression data for Eps8 along with other recognised myofibroblast markers. I inserted the commonly down-regulated genes resulting from TGFβ1 and irradiation treatment into STRING 10 software and generated a predicted network of relationships between the coded proteins.

We can see in figure 3-4(a) that ACTA2 and CTGF expression levels were significantly elevated following ϒ-irradiation, confirming the development of the myofibroblast-like phenotype observed as a result of fibroblast senescence. The senescent profile differs from the myofibroblast profile by lacking the induction of Col1α1 expression. We can observe that Eps8 mRNA expression is downregulated by γ-irradiation-induced senescence as was demonstrated during TGFβ1-induced myofibroblast transdifferentiation.

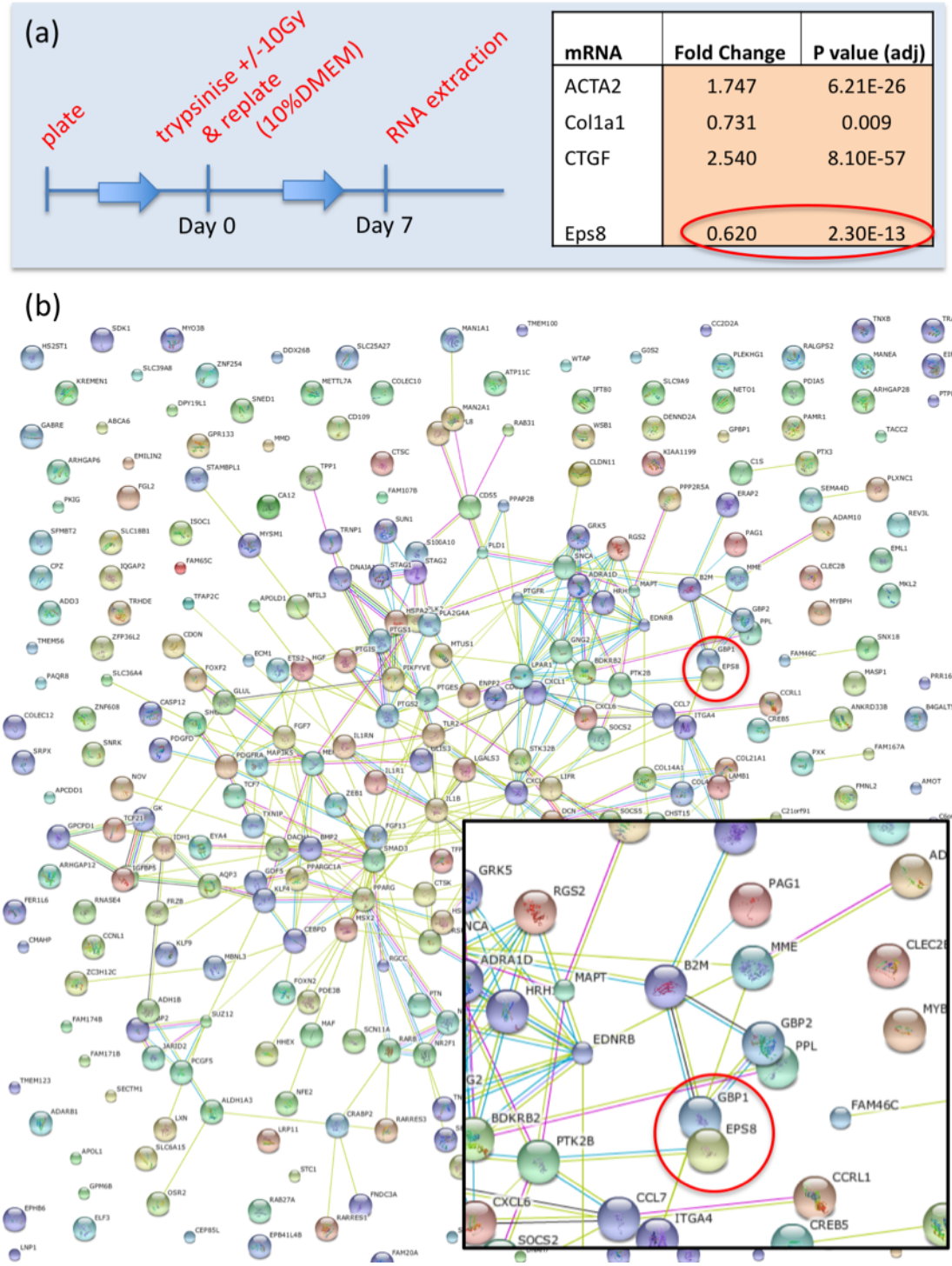

Figure 3-4 Eps8 is downregulated by irradiation-induced fibroblast senescence and lies within a central core of genes whose expression is downregulated by both TGFβ1 and ϒ-irradiation.

(a) Experimental timeline and resultant RNA-seq data displaying fold change and adjusted p-values for myofibroblast markers ACTA2, Col1α1, and CTGF along with Eps8. (b) STRING protein interaction network using commonly down-regulated genes (both $p<0.001$) resulting from TGFβ1 and ϒ-irradiation treatment. Eps8 is circled in red.

The STRING network (figure 3-4(b)) demonstrates that while most proteins encoded by genes in the commonly down-regulated list are not evidenced to be linked to each other, Eps8 lies within a core of proteins that have predicted associations within the group. This provides supportive evidence that Eps8 is an important protein in both senescence and myofibroblast transdifferentiation.

Eps8 expression was also examined at the protein level in HFFF2 fibroblasts undergoing senescence induction by either hydrogen peroxide treatment or repeated passage (aka replicative senescence).

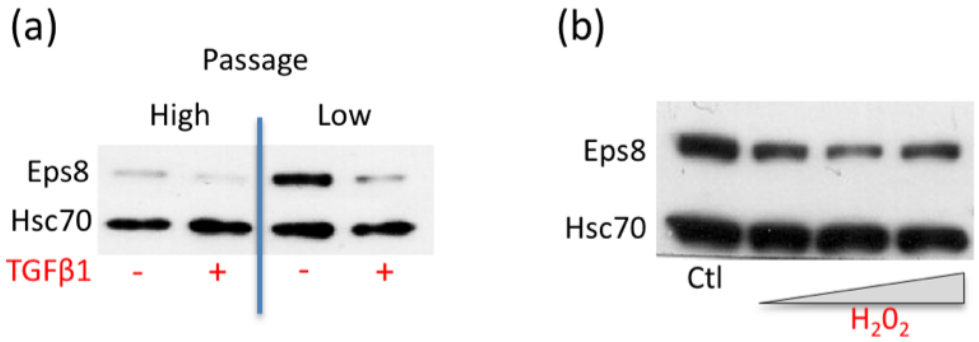

Figure 3-5 Senescence resulting from hydrogen peroxide treatment or repeated passage is associated with Eps8 downregulation

(a) Basal and TGFβ1-induced Eps8 expression in low versus high passage (>20) fibroblasts (b) Eps8 expression in HFFF2 either untreated or treated with 1000μM followed by a further dose of between 500 and 2000μM hydrogen peroxide to induce senescence. Hsc70 has been used as a loading control. Blots produced by another member of our group.

Our preliminary results indicate that the induction of senescence by either serial passage (figure 3.5(a)) or the use of serial doses of hydrogen peroxide (figure 3.5(b)) may also result in a reduction in Eps8 expression. Along with previous results these indicate that Eps8 expression is reduced at both transcriptional and protein levels during both TGFβ-induced fibroblast-to-myofibroblast transdifferentiation and potentially also senescence induction using a variety of stimuli.

3.2 The effect of Eps8 knockdown on TGFβ1-induced myofibroblast transdifferentiation

Our results presented in the previous section demonstrate that myofibroblast transdifferentiation induced by TGFβ1 is associated with a reduction in Eps8 mRNA expression and an early reduction in Eps8 protein levels. Eps8 expression also appears to be downregulated in senescent fibroblasts, which share functional similarity with TGFβ1-induced myofibroblasts. Given that the reduction in Eps8 expression resulting from TGFβ1 treatment preceded αSMA upregulation and the development of the full myofibroblast phenotype (figure 3-3) we next considered whether the reduction of Eps8 was part of the mechanism rather than merely a consequence of myofibroblast transdifferentiation.

3.2.1 Eps8 knockdown induces αSMA protein expression and potentiates its induction by TGFβ1

Initial experiments were performed to optimise the plating density for HFFF2 and primary dermal fibroblasts for transfection experiments and to optimise the Eps8 siRNA concentration (appendix A figure 6-12).

In order to assess the effect of Eps8 knockdown on myofibroblast transdifferentiation, fibroblasts were plated and allowed to adhere overnight before transfection the next morning with 30nM Eps8 or control siRNA. The following day the medium was replaced with serum-free DMEM with or without 5ng/ml TGFβ1 and the cells were incubated for 72h before harvesting. The same experiment was performed with primary dermal, oral and oesophageal fibroblasts, as well as HFFF2, to investigate the role of Eps8 in fibroblasts from different anatomical sites.

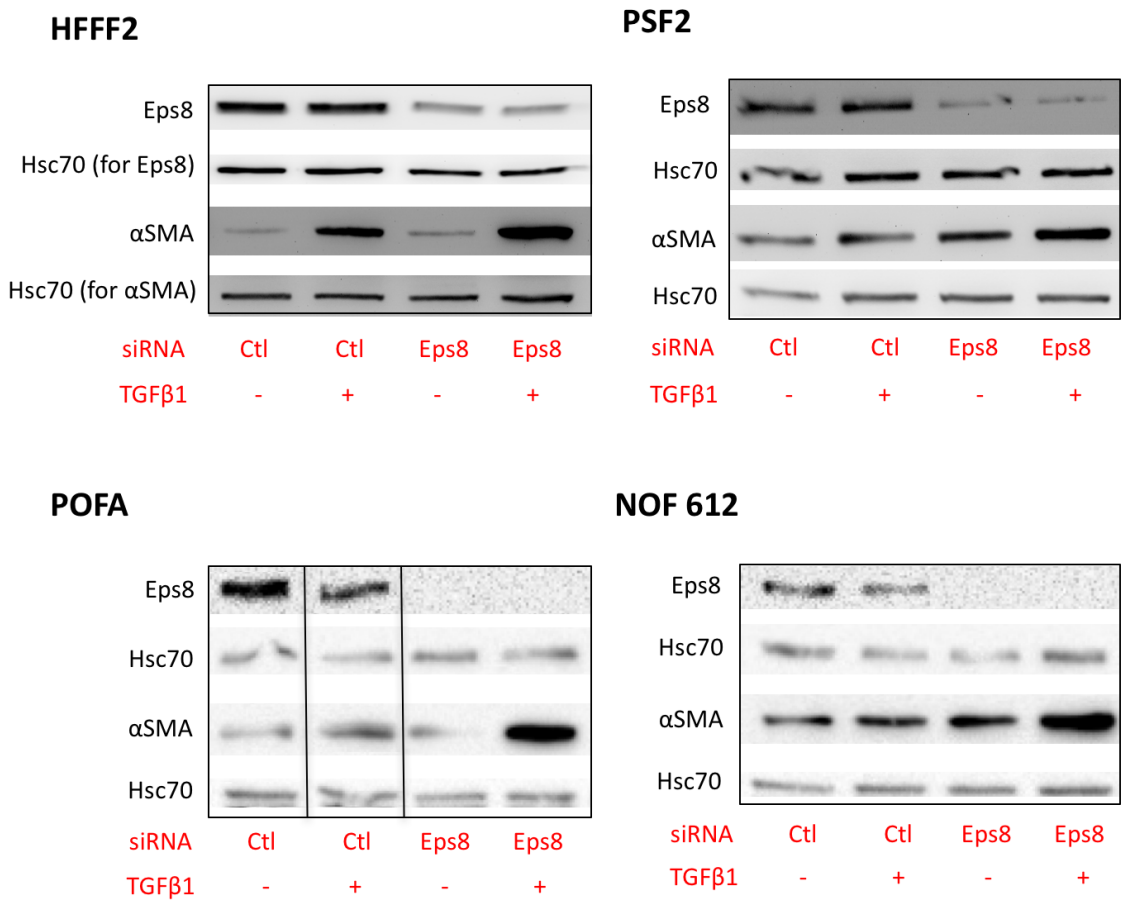

Figure 3-6 Eps8 knockdown augments TGFβ1-induced αSMA expression.

αSMA expression was analysed by Western blotting in (a) HFFF2, (b) PSF2 primary dermal, (c) POFA primary oral, and (d) NOF 612 primary oesophageal fibroblasts following Eps8 knockdown, with and without 5ng/ml human recombinant TGFβ1for a further 72h. Eps8 downregulation was confirmed in the same samples. Differing amounts of total protein were loaded for examining Eps8 and αSMA expression so they each have their associated Hsc70 loading control. Representative blots shown.

In the absence of TGFβ1 treatment, Eps8 knockdown caused a variably sized increase in αSMA levels compared to cells transfected with non-targeting siRNA. However, in all four cell types Eps8 knockdown followed by TGFβ1 treatment produced a significant increase in αSMA expression compared to non-targeting siRNA combined with TGFβ1 treatment.

The effect observed using the Eps8 siRNA does not appear to be an off target effect of the siRNA since a similar pattern was seen in an initial experiment testing siRNAs targeting alternative sequences within Eps8. As shown in figure 3-7 the targeting of alternate sequences similarly augmented the induction of αSMA expression by TGFβ1(in order to display the full range of αSMA

expression on the blot, the induction of αSMA expression by TGFβ1 in the control arm appears quite small).

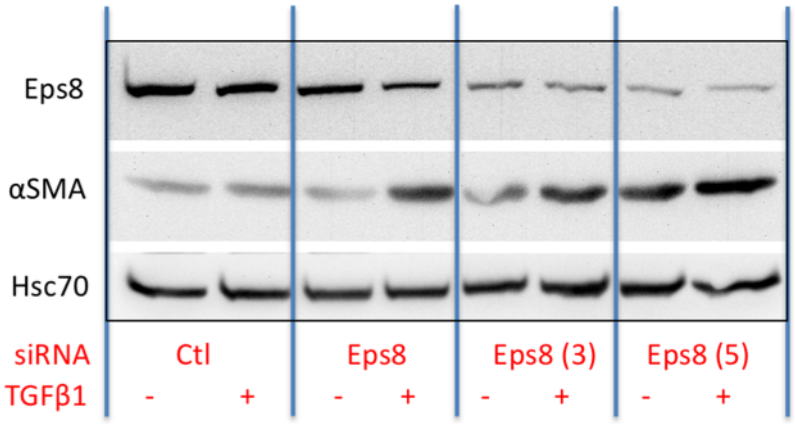

Figure 3-7 Alternative Eps8 siRNA sequences appear to similarly augment TGFβ-induced αSMA expression (single experiment).

HFFF2 were transfected with either non-targeting (control), Eps8 (as used previously) or alternative Eps8 siRNA sequences (3, 5). The following day media was replaced with serum-free medium with/without 5ng/ml human recombinant TGFβ1. After 72h treatment, cells were lysed and processed for Western blotting. Eps8 and αSMA were assessed with the same loaded lanes so only one loading control band was required. Alternative Eps8 sequences produced effective knockdowns of their target and increased basal and TGFβ-induced αSMA.

The potential for a role of Eps8 in the process of myofibroblast transdifferentiation was raised as a result of its observed early downregulation before αSMA induction. We have demonstrated here that the loss of Eps8 increases the efficacy of TGFβ1-induced fibroblast-to-myofibroblast transdifferentiation, indicating that the presence of Eps8 inhibits the process. The fact that Eps8 levels are promptly down-regulated as a result of TGFβ1 treatment suggest that Eps8 down-regulation is likely to be part of the mechanism of TGFβ1-induced transdifferentiation, increasing the sensitivity of fibroblasts to TGFβ1. This identifies a completely novel function of Eps8.

3.2.2 Eps8 knockdown augments TGFβ1-induced expression of COL1A1, another myofibroblast marker

Myofibroblasts are characterised by a marked increase in the expression of various intracellular and secreted proteins. Besides changes in αSMA expression, increases in connective tissue growth factor (CTGF) and collagen alpha-1 type I expression have also been demonstrated as a result of TGFβ1-induced myofibroblast transdifferentiation (Tobar et al. 2014; Mia et al. 2014).

We therefore investigated whether the changes demonstrated in αSMA protein expression were mirrored by similar changes at the mRNA level in ACTA2 (coding for αSMA), COL1A1 (coding for alpha-1 type I collagen) and CTGF expression. HFFF2 cells were transfected with either non-targeting or Eps8 siRNA, and were treated with or without 5ng/ml TGFβ1 in the absence of serum 24h post-transfection. Cells were harvested 72h after TGFβ1 treatment. As shown in Figure 3-8(d), Eps8 knockdown resulted in a highly significant reduction in Eps8 mRNA expression confirming the efficacy of the knockdown.

As has been shown previously at both the mRNA and protein level (sections 3.1.1-2), TGFβ1-treatment results in a reduction in Eps8 expression although this did not achieve statistical significance in this set of experiments containing only 3 repeats (figure 3-8). ACTA2 expression was slightly (but statistically significantly) increased by TGFβ1 or Eps8 knockdown alone while Eps8 knockdown produced a statistically significant augmentation of TGFβ1-induced ACTA2 expression, consistent with results in section 3.2.1. COL1A1 and CTGF expression increased with TGFβ1 treatment alone, correlating with both our RNA-seq data (figure 3.1) and the literature (Mia et al. 2014; Tobar et al. 2014). While Eps8 knockdown alone causes a trend to increased COL1A1 and CTGF expression, in the presence of TGFβ1 Eps8 knockdown causes a significant increase in COL1A11 expression over controls. Given that the trends in CTGF are the same as those seen with ACTA2 and COL1A1, we might expect the augmentation of TGFβ1-induced CTGF expression by Eps8 knockdown to become statistically significant with further experimental repeats.

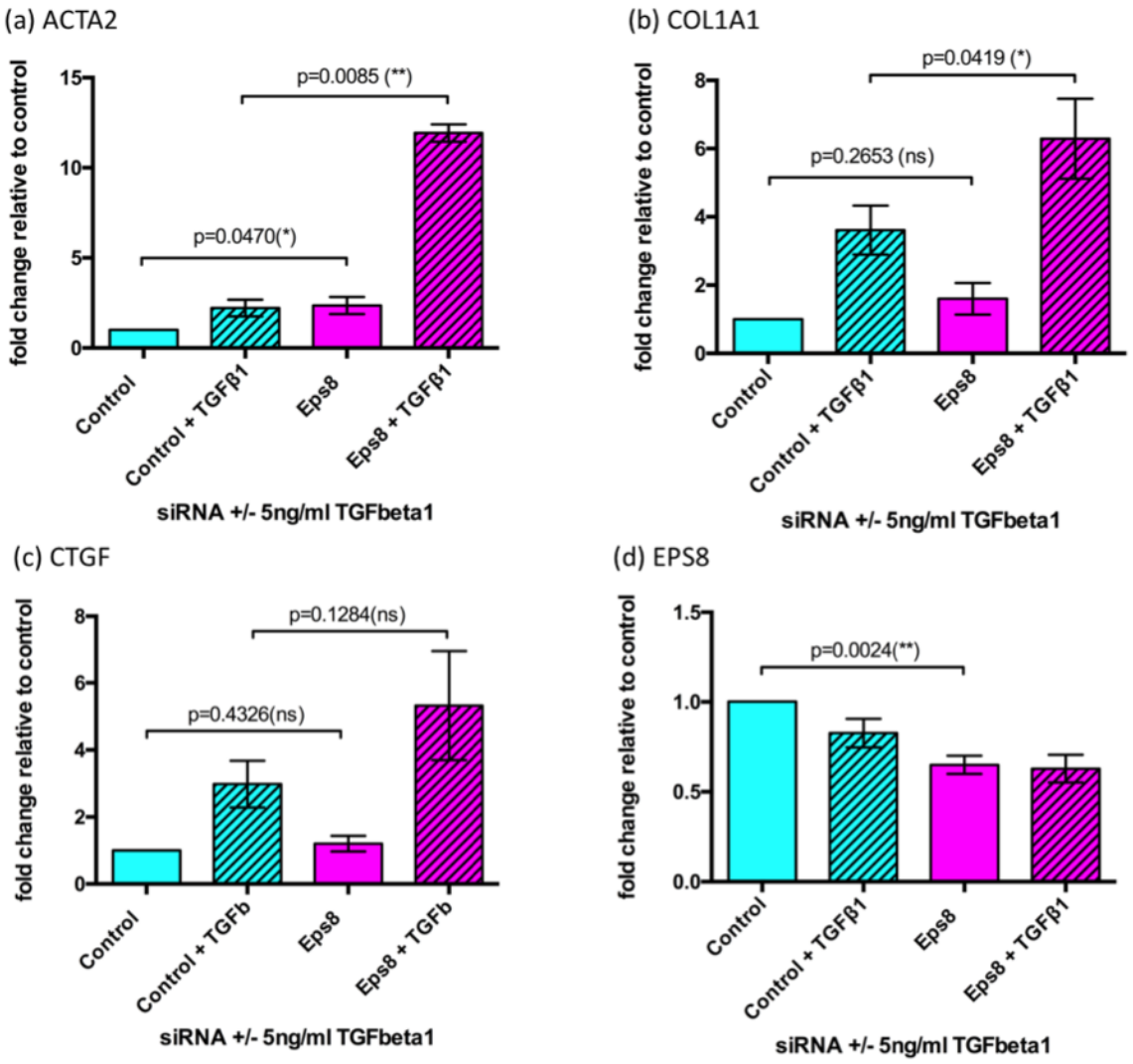

Figure 3-8 Eps8 knockdown augments TGFβ1-induced ACTA2, and COL1A1 expression, and possibly also CTGF mRNA expression in HFFF2.

HFFF2 were transfected with control / Eps8 siRNA and after 24h were converted to serum-free DMEM +/- 5ng/ml TGFβ1 for 72h before mRNA extraction. Fold changes are normalised to GAPDH and relative to the TGFβ1-untreated control-transfected group. Results are presented from 3 independent experiments, displaying means and SEM. Eps8 expression was also analysed to ensure efficacy of knockdown. Unpaired 2-tailed t tests were performed between control and Eps8 groups (due to normalisation to control), and paired 2-tailed t tests were performed between TGFβ1-treated groups.

These results indicate that Eps8 knockdown augments TGFβ1-induced expression of ACTA2 and other markers of myofibroblast transdifferentiation. This provides further evidence that the effect of Eps8 knockdown is not limited purely to an effect on αSMA expression.

3.2.3 Eps8 knockdown induces incorporation of αSMA into bundled stress fibres

An increase in αSMA expression may not necessarily indicate its uptake into bundled stress fibres with a consequent increase in functional contractility. Given that the definition of myofibroblasts is partially architectural and requires the accumulation of αSMA into functional stress fibres (Eyden 2008), we examined the effect of Eps8 knockdown on the development of αSMA-positive stress fibres using immunocytochemistry (and immunofluorescence microscopy).

HFFF2 fibroblasts were transfected with non-targeting (control) or Eps8-targeting siRNA and the following day the cells were re-plated in chambers slides to facilitate subsequent immunofluorescence. Remaining cells were re-plated in multi-well plates to confirm the efficacy of Eps8 knockdown (appendix A figure 6-13). Cells were then treated with human recombinant TGFβ1 for at least 72h. Filamentous actin and αSMA-positive stress fibres were visualised by phalloidin-FITC and αSMA antibody, respectively.

As shown in the sample images and quantitative analysis in figure 3-9, TGFβ1 induced moderate increases in filamentous actin and αSMA stress fibre production, but the prior knockdown of Eps8 resulted in a significantly greater degree of both filamentous actin and αSMA-positive stress fibre development in response to TGFβ1 treatment. This is consistent with the effect of Eps8 knockdown on TGFβ1-induced myofibroblast transdifferentiation that we have observed in previous sections and demonstrates that the increased production of αSMA is utilised for stress fibre production.

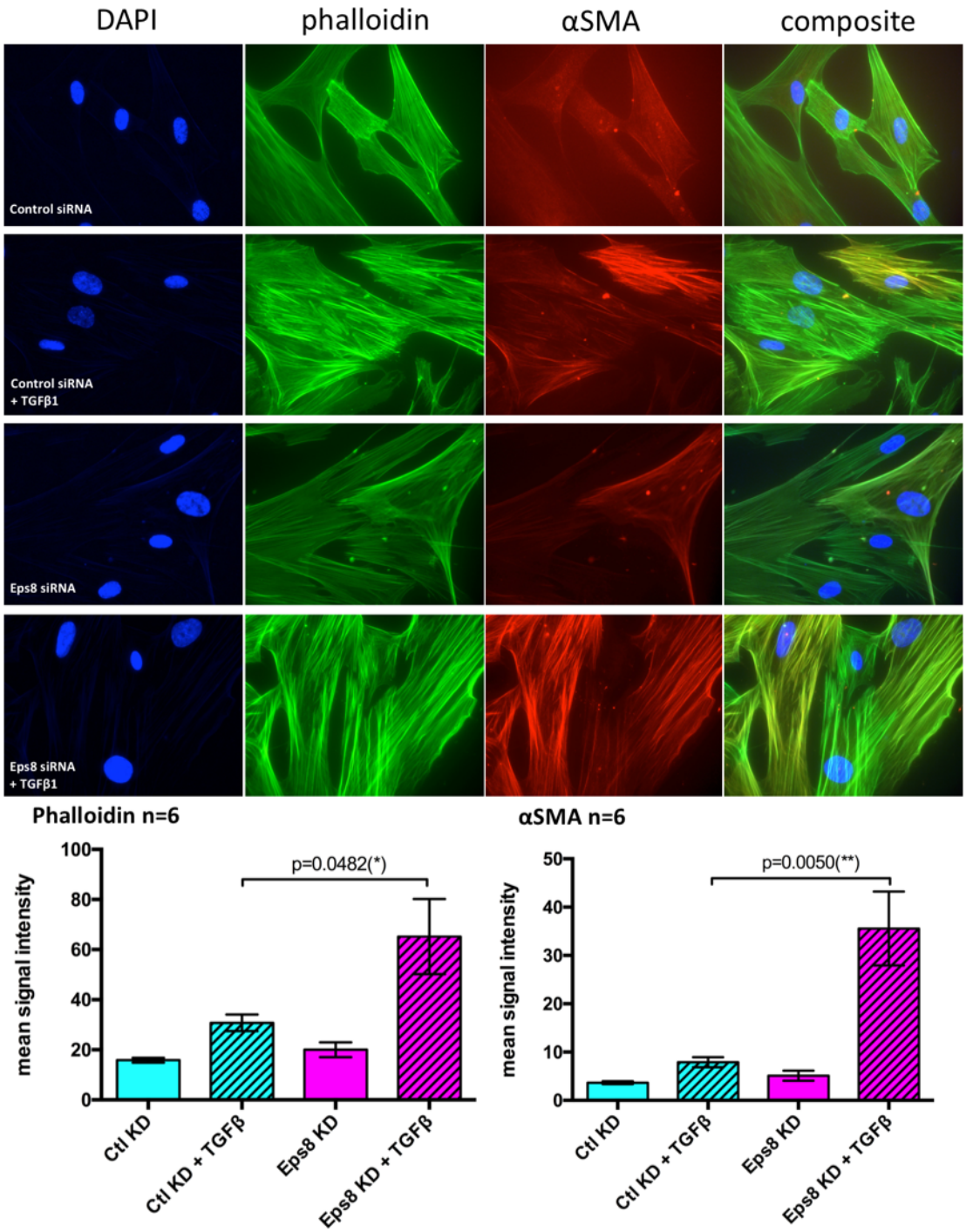

Figure 3-9 Eps8 knockdown augments TGFβ1-induced production of filamentous actin and αSMA stress fibres

HFFF2 were transfected with either non-targeting (control) or Eps8 siRNA and re-plated the next day in chambers slides. The following day cells were treated with 10ng/ml TGFβ1 in serum-free medium for just over 3 days. Immunocytochemistry was performed using a DAPI nuclear stain, a two-stage antibody process for αSMA, and FITC-conjugated phalloidin for filamentous actin. 6 images were captured per condition, encapturing 4 nuclei per field. A sample image from each condition is shown in the uppermost panels while quantitative analysis in Image J (n=6 per condition), is shown below (means and SEM, two-tailed paired t test).

The same experiment has also independently been performed qualitatively in HFFF2 and PSF2 fibroblasts assessing αSMA stress fibre formation (without phalloidin staining) in response to the same treatments. The results were consistent with those above.

3.2.4 Eps8 knockdown increases fibroblast contractility within collagen gels

The formation of αSMA stress fibres as fibroblasts differentiate into myofibroblasts leads to the development of highly contractile cells. To further confirm that Eps8 knockdown induces the development of functional myofibroblasts we performed collagen gel contraction assays to measure fibroblast contractility (Bogatkevich et al. 2001; Marsh et al. 2011). Fibroblasts were transfected with non-targeting (control) or Eps8 siRNA and the following day were incorporated into collagen gels with or without 5ng/ml TGFβ1. When sufficient differences in gel contraction had occurred between TGFβ1-treated and untreated control wells the gels were weighed and photographed (usually between 24-72h).

Figure 3-10(a-b) demonstrates that using either HFFF2 or primary skin fibroblasts (PSF3), Eps8 knockdown in the presence of TGFβ1results in a significant decrease in gel weight compared to controls. As collagen gels contract, water is expelled from the matrix resulting in smaller, lighter gels (Tingstrom et al. 1992). The reduced weight of gels containing Eps8 knockdown fibroblasts compared to control fibroblasts indicates that they have demonstrated greater functional contractility in a three dimensional matrix.

In order to help clarify that the observed increase in gel contraction resulted purely from differences in fibroblast contractility and not increased fibroblast proliferation, we also assessed HFFF2 proliferation in serum-containing medium using xCELLigence® (Roche) technology (figure 3-10c-d). Our results demonstrate that Eps8 knockdown did not have a significant effect on cell proliferation either in the presence or absence of TGFβ1. To further support these observations no statistically significant difference was seen between the same groups using an automated cell counter (CASY counter, Roche).

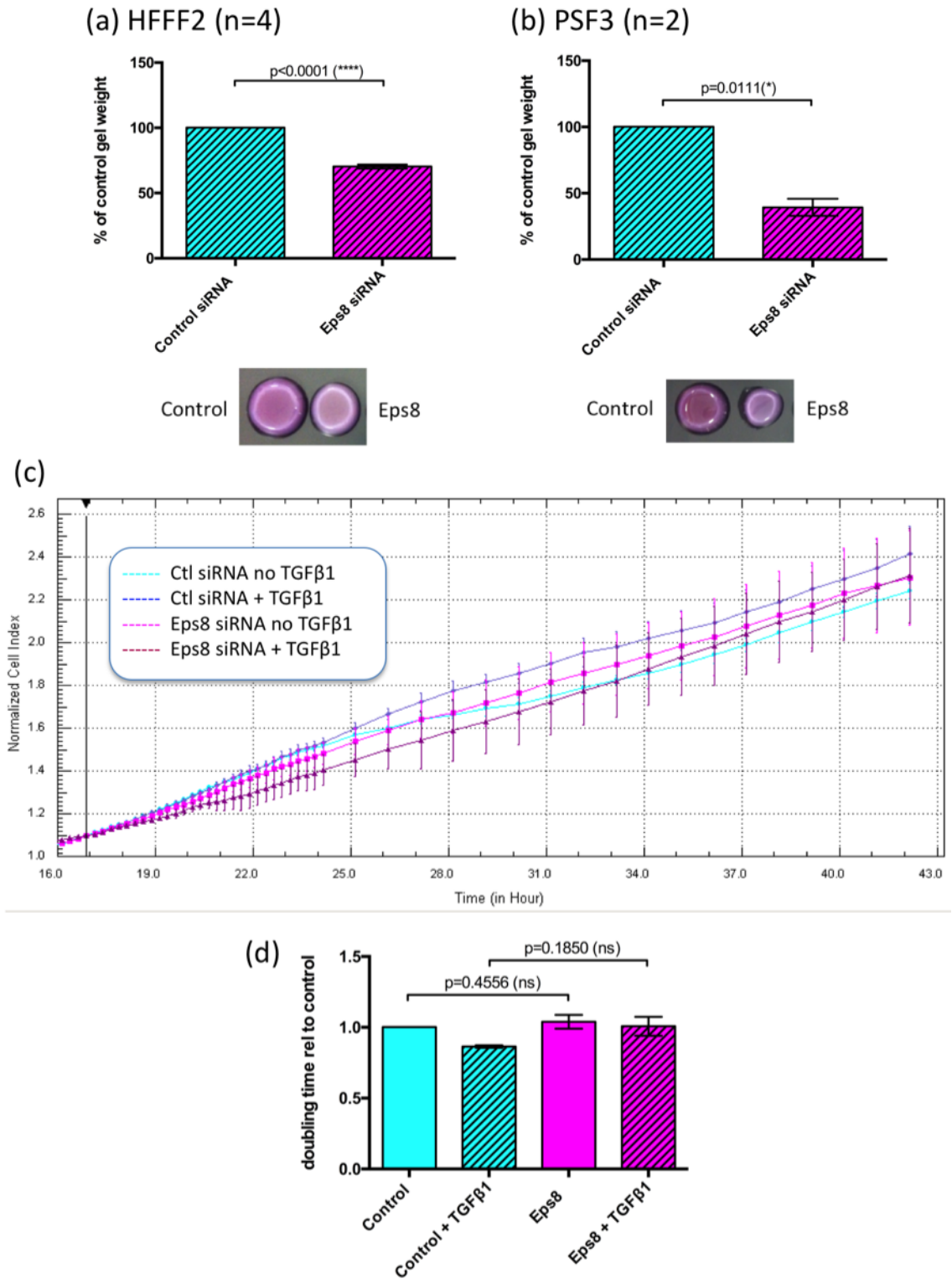

Figure 3-10 Eps8 knockdown increases fibroblast contractility

(a) HFFF2 or (b) PSF3 primary dermal fibroblasts, each transfected with non-targeting (control) or Eps8 siRNA, were incorporated into collagen gels with 5ng/ml TGFβ1. In the figures, gel weights following Eps8 knockdown are expressed as a percentage of the weight of the control gel. *n* is the number of independent experiments performed contributing to the figures and error bars display means and SEM. Photographs of gels from a representative experiment are shown below

the graphs. (c) Cell proliferation in 10% serum DMEM was assessed using the xCELLigence real-time cell analyser. Normalised cell index values are shown from a representative experiment with HFFF2 fibroblasts. (d) Relative doubling times of treated HFFF2 fibroblast populations were calculated across 4 independent experiments. Mean and SEM of doubling times are displayed. Statistical significance was tested using unpaired t-tests (2 tail, 5%).

Together these results indicate that Eps8 knockdown results in increased contractility in both HFFF2 and primary fibroblasts and that the differences observed in the functional assays are not accounted for by differences in cell proliferation.

3.2.5 Eps8 Knockdown increases the ability of conditioned media collected from fibroblasts to enhance cancer cell migration

We have so far demonstrated that Eps8 knockdown not only augments TGFβ1-induced αSMA expression at mRNA and protein levels, but also results in increased incorporation of the αSMA into stress fibres, which enhance the contractile myofibroblast phenotype. Eps8 therefore appears to provide tonic inhibition of the TGFβ pathway in resting, non-activated fibroblasts.

We have additionally demonstrated that downregulation of Eps8 augments the TGFβ1-induced expression of secreted proteins important for myofibroblast function such as type I collagen, and also possibly CTGF. Myofibroblasts are known to promote tumour progression by a variety of mechanisms, including by cell-cell contact (Flaberg et al. 2011), modification of the extracellular matrix (Goetz et al. 2011), and by the secretion of a variety of factors (Orimo et al. 2005; Wheeler et al. 2014). Furthermore, conditioned media from myofibroblasts, which contains these secreted factors, has been shown to augment cancer cell migration compared to media collected from non-activated fibroblasts (Wheeler et al. 2014).

In the following experiments we therefore intended to assess whether Eps8 knockdown augmented another TGFβ-induced myofibroblast characteristic – the ability to increase cancer cell migration. Using Transwell™ migration assays we compared the ability of conditioned media taken from fibroblasts transfected with either Eps8 or non-targeting siRNA to induce migration of SCC25 oral squamous cell carcinoma cells.

In figure 3-11(a) we demonstrated that in serum-free medium there is no *statistically* significant difference in fibroblast proliferation as a result of

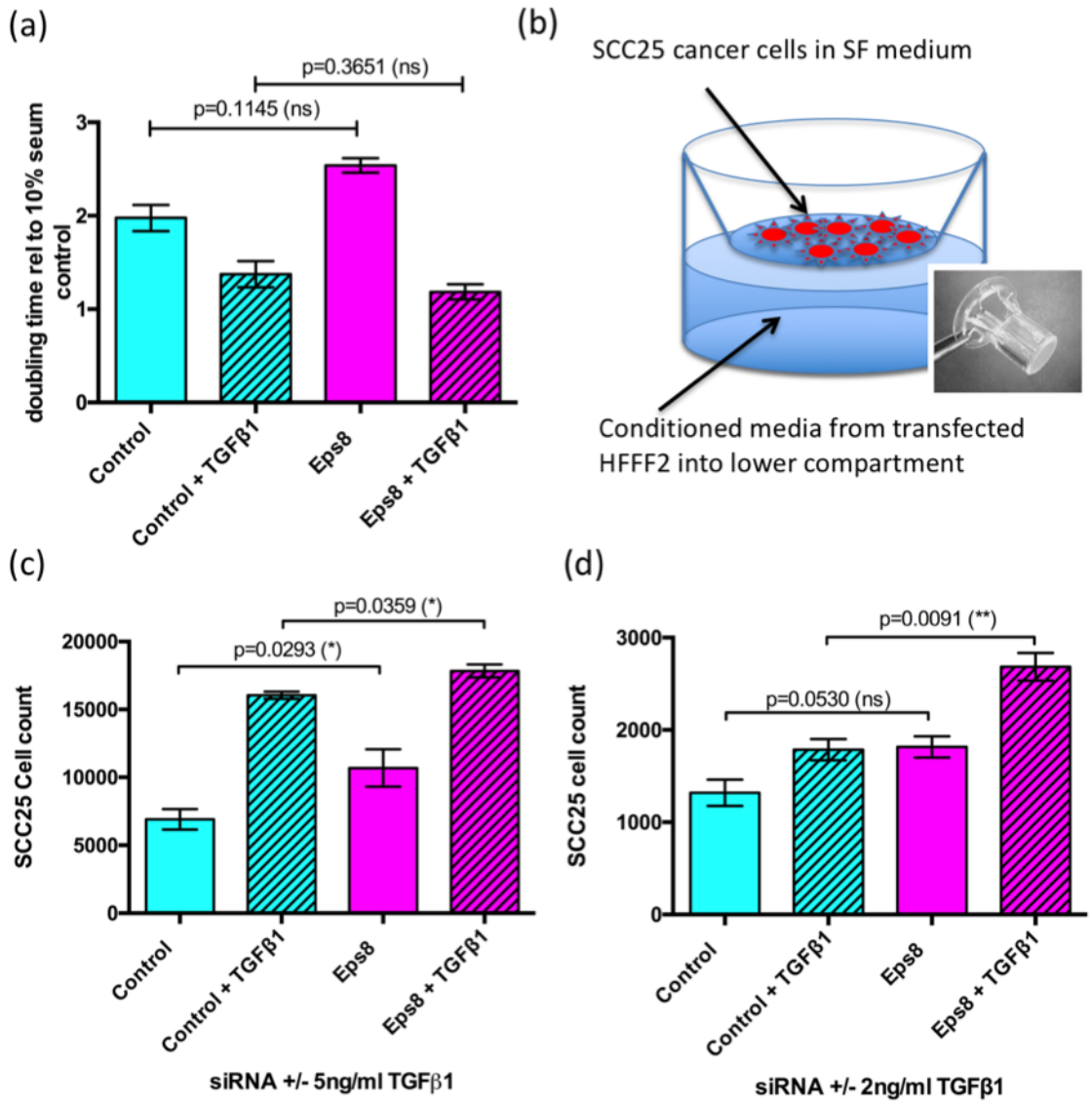

Figure 3-11 Conditioned media from Eps8 knockdown fibroblasts augments cancer cell migration.

(a) Fibroblast proliferation in serum-free medium was assessed using the xCELLigence analyser following transfection +/- TGFβ1 treatment (5ng/ml). (b-d) HFFF2 fibroblasts were transfected with either Eps8 or non-targeting siRNA and media was replaced with serum-free DMEM +/- TGFβ1 for 48h. Conditioned media was collected for a subsequent 24h and dilution was corrected for fibroblast number. (c) SCC25 cell migration following 24h exposure to conditioned media from treated fibroblasts. Data represent the mean number of migrated cells from triplicate wells (duplicate for Eps8 + TGFβ1) during a single representative experiment (of 3); error bars display SEM. Two-tailed paired t-tests were performed between groups. (d) Results as per (c) except this was a single experiment with conditions in triplicate and TGFβ1 treatment concentration was 2ng/ml rather than 5ng/ml.

Eps8 knockdown; there was however a greater difference than was observed using DMEM with 10% serum. In order to negate any *biologically* significant effect of differential fibroblast proliferation on the pro-migratory effect of the conditioned media we counted the fibroblasts in the monolayer following collection of the conditioned media and corrected the concentration by dilution with serum-free media.

Figure 3-11(c) demonstrates that conditioned media taken from control-transfected, TGFβ1-treated fibroblasts induces greater cancer cell migration than that from control-transfected non-TGFβ1-treated fibroblasts (p=0.0118*, not displayed). This correlates well with results from previous sections that confirm, by a variety of methods, the induction of myofibroblast transdifferentiation by TGFβ1 treatment, and that myofibroblasts induce greater cancer cell migration than non-activated fibroblasts. Conditioned media from TGFβ1-untreated Eps8-knockdown fibroblasts was also seen to induce an increase in the migration of SCC25 cells compared to that from TGFβ1-untreated controls (p=0.0293*). Eps8 knockdown in the presence of TGFβ1 also caused a statistically significant additional pro-migratory effect over control-transfected cells, but the size of the difference between these latter two conditions was perhaps smaller than expected (p=0.0359*). We therefore considered whether the maximum migration capacity of the SCC25 cells was being reached. By reducing the TGFβ1 dose to 2ng/ml as shown in figure 3-11(d) we observed a larger difference between these two groups, with even higher statistical significance (p=0.0091**) suggesting that this may have been the case.

Overall our results demonstrate that Eps8 knockdown in HFFF2 fibroblasts produces conditioned media that induces a similar degree of cancer cell migration to conditioned media generated by TGFβ1 treatment of fibroblasts. Furthermore, Eps8 knockdown prior to TGFβ1 treatment of fibroblasts enhances the ability of the conditioned media to increase cancer cell migration provided that the maximum migratory ability of the cancer cell has not been achieved. This suggests that maintenance of fibroblast Eps8 expression could potentially reduce cancer cell migration and may potentially limit metastatic behaviour.

3.2.6 Fibroblast Eps8 knockdown increases tumour growth in a Head & Neck Cancer xenograft mouse model

The results from the previous sections have shown that Eps8 expression is important in preserving the fibroblast phenotype. Loss of Eps8 expression sensitises fibroblasts to the transdifferentiating effect of TGFβ1, resulting in increased αSMA expression, bundling of αSMA into stress fibres, and increased cell contractility. Furthermore, loss of Eps8 expression in fibroblasts results in a secretome that increases cancer cell migration, and also augments the ability of TGFβ to induce a pro-migratory secretome.

In order to assess whether the loss of Eps8 expression in fibroblasts affects *in vivo* tumour growth, we utilised a murine co-injection xenograft model that our group has previously used to implant solid tumours from the Head and Neck and oesophagus into subcutaneous areas on the flanks of mice (Underwood et al. 2015).

Early passage HFFF2 fibroblasts were transduced with either Eps8 shRNA or GFP-linked non-targeting viral particles. Following puromycin selection fibroblasts from each treatment arm were mixed with mcherry-labelled 5PT oral cancer cells and injected subcutaneously into opposing flanks of RAG1-/- immunocompromised mice. An independent scientist, blinded to the treatment allocation, used electronic callipers to measure the tumours at five time points over the next month.

Calculated volumes of subcutaneous flank tumours over the 28 days post-injection are charted in figure 3-12(a) for each mouse. We can see in figure 3-12(b) that pooled 'area under the curve' analysis of the tumour volumes for all nine mice reveals a statistically significant difference in tumour volume with 5PT cells co-injected with Eps8shRNA-transduced HFFF2 producing larger tumours than when they were co-injected with controlGFP-transduced HFFF2. This demonstrates that fibroblasts with suppressed Eps8 expression have a greater tumour-promoting effect *in vivo* compared to fibroblasts where Eps8 expression has not been suppressed.

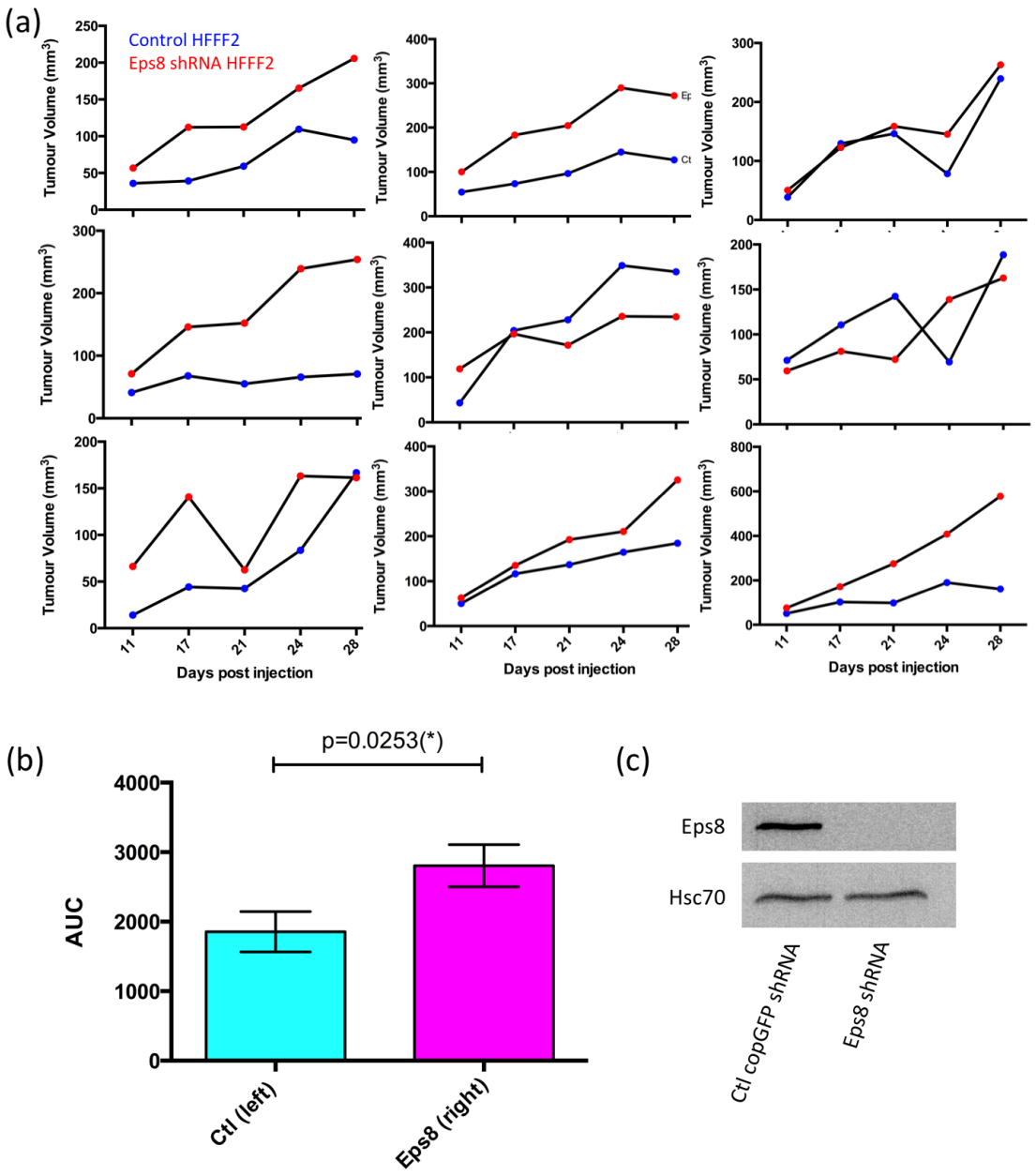

Figure 3-12 Fibroblast Eps8 knockdown increases xenograft tumour volume

Thirteen RAG1-/- mice were injected in their left flank with $3x10^6$ controlGFP-transduced HFFF2 and $1x10^6$ mcherry5PT, and in their right flank with $3x10^6$ Eps8shRNA HFFF2 and $1x10^6$ mcherry5PT. Bilateral measurements of tumour diameter were made over the next month by a colleague blinded to flank allocation. Four mice were excluded from the analysis with likely injection misplacement – two were observed to have intramuscular rather than subcutaneous tumours and two had no discernable tumours at all in one flank suggesting fluid extravasation at the time of injection. Calculated tumour volumes for the remainder were plotted and AUC analysis performed. (a) are tumour volume measurements for each mouse plotted over time (control blue, Eps8shRNA red). (b) displays mean and SEM of AUC measurements across the 9 mice, with a paired two tail t-test to assess statistical significance. (c) Downregulation of Eps8 was confirmed by Western blotting from cell lysates of transduced fibroblasts at the time of injection. Hsc70 was used as a loading control.

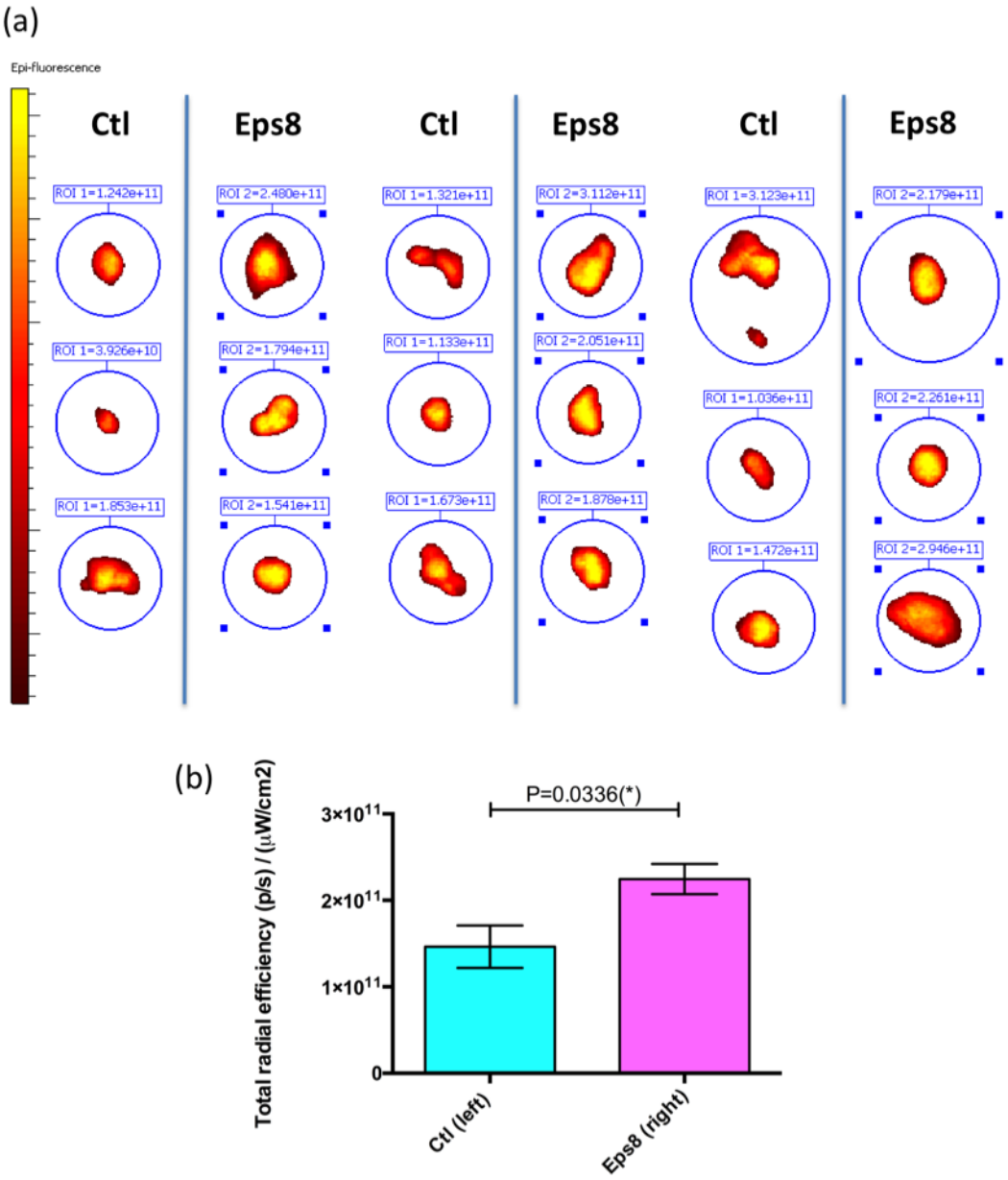

Figure 3-13 Fibroblast Eps8 knockdown results in increased xenograft tumour volume measured by fluorescent signal from co-injected labelled cancer cells

Fluorescence intensity (excitation 520nm, measurement 640nm) was measured for each mouse's pair of tumours immediately after excision. The images for the paired tumours for all 9 mice are collated and shown in (a). The pooled data is presented in the bar chart in (b) (mean, SEM) and a paired 2-tail t-test was performed to compare groups.

In order to measure cancer proliferation by a method independent of tumour volume we also measured the intensity of the fluorescent signal produced by the mCherry marker, linked to the 5PT cancer cells. Excised tumours and associated flank lymph nodes were immediately imaged at appropriate

wavelengths using a fluorescent imager (IVIS lumina III, Living Image 4.3.1 software).

As shown in figure 3-13(b) the mCherry signal intensity was significantly greater in tumours resulting from co-injection of Eps8shRNA fibroblasts with 5PT cells, than in those resulting from co-injection of control-transduced fibroblasts with 5PT cells. The increased mCherry signal suggests that greater cancer cell proliferation has occurred in these tumours. This data correlates with the direct measurement of tumour size and adds further weight to the argument that fibroblasts with suppressed Eps8 expression have a greater tumour promoting effect on 5PT oral cancer cells *in vivo*.

To assess αSMA and collagen expression in the tumour stroma following Eps8 knockdown, tissue sections from each tumour were stained for either αSMA or for collagen (using Masson's trichrome protocol) (Figure 3-14). Our results demonstrate that there is greater αSMA and collagen presence in tumours arising from co-injection with Eps8shRNA-transduced fibroblasts than in those arising from co-injection with control fibroblasts. The difference is highly statistically significant for αSMA but does not attain significance at the 5% level for collagen with 9 paired tumours.

Based on these results we can conclude that downregulation of fibroblast Eps8 expression augments cancer cell proliferation and tumour growth in this xenograft model. We therefore demonstrate that in this model fibroblast Eps8 expression has an important tumour-restraining effect on cancer cells.

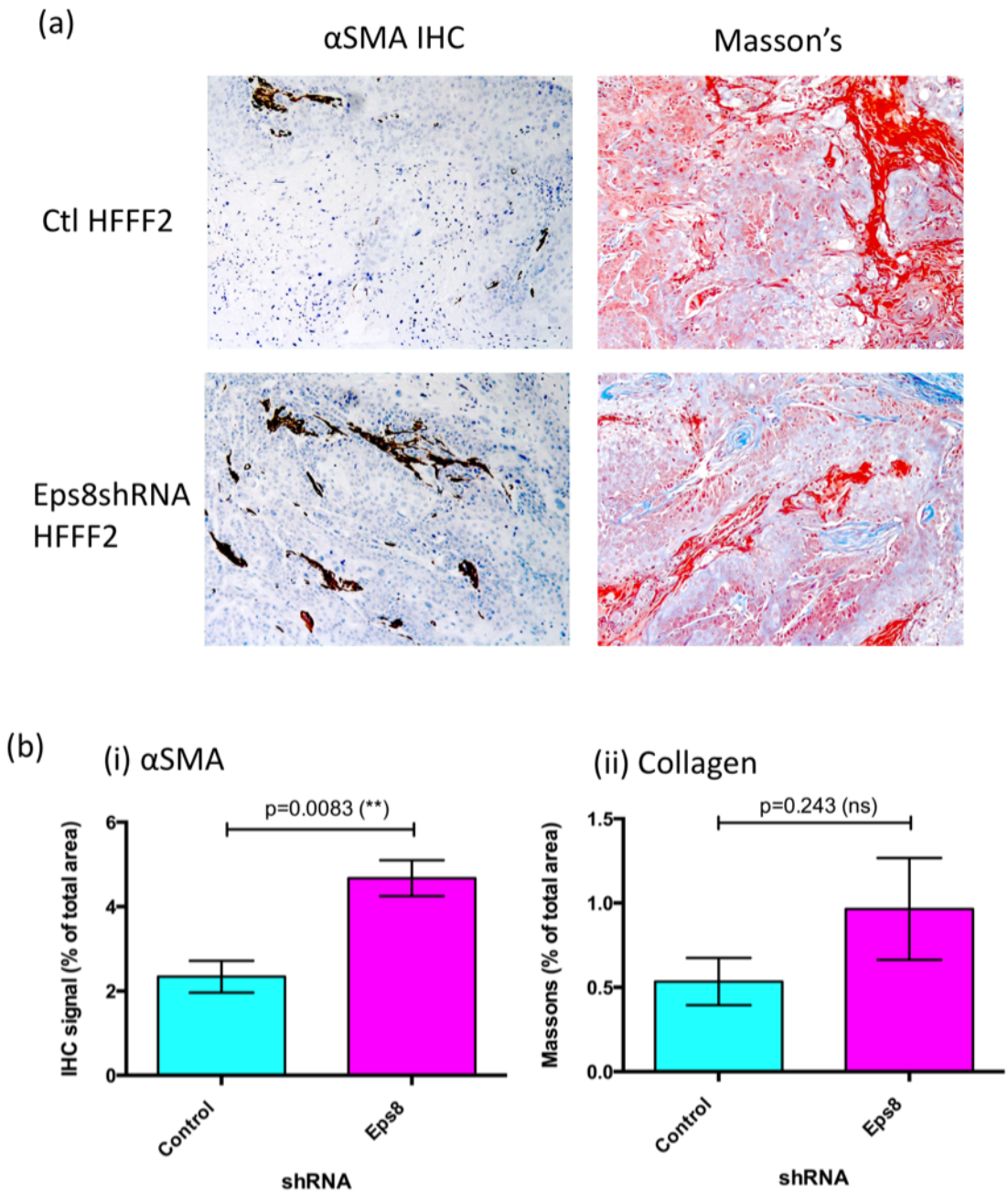

Figure 3-14 Fibroblast Eps8 knockdown increases *in vivo* αSMA and collagen expression in tumour stroma

Halved tumour specimens were formalin fixed and paraffin embedded before sections underwent immunohistochemistry for αSMA or Masson's trichrome staining. Representative images (100x) are shown from (a) one mouse and (b) following quantification, results were pooled across all mice (n=9, mean and SEM shown, 2-tailed paired t-test).

3.2.7 Discussion

Our initial interest in the role of Eps8 in fibroblast biology stemmed from analysis of RNAseq data produced in our group from fibroblasts treated with or without human recombinant TGFβ1- the most well-characterised and potent stimulant of fibroblast-to-myofibroblast transdifferentiation (De Wever et al. 2008). Eps8 was one of the proteins whose mRNA expression in HFFF2 fibroblasts was noted to be significantly downregulated as a result of TGFβ1 treatment. Furthermore, analysis of known interaction networks using data from a range of sources suggested that Eps8 was shown to be within a central core of interacting proteins whose mRNAs were downregulated during TGFβ1-induced myofibroblast transdifferentiation.

From what was previously understood of Eps8 biology the RNA-seq finding perhaps appeared counter-intuitive. In fibroblasts, Eps8 is known to perform effective bundling of filamentous actin, which is necessary for the generation of stress fibres and myofibroblast transdifferentiation (Disanza et al. 2006; Hinz 2016). Through its role, via the tricomplex, in activating Rac1 Eps8 also promotes lamellipodial actin polymerisation via regulation of WAVE complex-dependent nucleation and cofilin family-mediated depolymerisation (Disanza et al. 2005). Furthermore, Eps8 has been shown to bind palladin, another cytoskeletal regulator and marker of myofibroblast transdifferentiation, with co-localisation at active sites of actin polymerisation in vascular smooth muscle cells (Goicoechea et al. 2006). While this literature would suggest a necessary role of Eps8 in the processes of myofibroblast transdifferentiation our data at both mRNA and protein levels suggest that Eps8 expression is actually downregulated early in the process of myofibroblast transdifferentiation and senescence. Furthermore, all of our results convincingly demonstrate that downregulation of Eps8 augments TGFβ1-induced fibroblast-to-myofibroblast transdifferentiation, indicating that Eps8 acts as an inhibitor of this process.

An explanation for this may lie in the actin-capping role of Eps8. The literature is unclear as to the net effect of this function of Eps8 on actin polymerisation in fibroblasts. Some authors postulate that targeted capping of actin side-branches may produce more linear actin structures that are more readily bundled (Disanza et al. 2005), implying that Eps8 end-capping *promotes* stress fibre production. Other literature indicates that capping is likely to prevent

main actin filament extension and regard Eps8's capping and bundling functions as conflicting factors in actin polymerisation. The overall effect of Eps8 on filopodia formation appear to vary by cell-type with Eps8 knockdown decreasing filopodia formation in HeLa cells but increasing their formation in hippocampal neurons and this may be influenced by factors such as the relative expression of co-factors such as IRSp53 and Abi1(Vaggi et al. 2011). It may be the case that in fibroblasts the predominant function of Eps8 is capping rather than bundling, and so the net effect of Eps8 downregulation is to increase actin polymerisation.

Interestingly, a sustained downregulation of Eps8 has also been observed during the terminal differentiation of mouse skeletal muscle myoblasts to myotubes and this proved to be maintained despite the stimulus of serum, which normally increases Eps8 expression (Gallo et al. 1997). In the case of our RNA-seq data the transcriptional downregulation of Eps8 was similarly maintained three days after removal of TGFβ1, suggesting that following myofibroblast transdifferentiation Eps8 mRNA downregulation is autonomously maintained by myofibroblasts. Given the similarity in observations between myofibroblasts and differentiated muscle cells it is possible that similar mechanisms of Eps8 downregulation are involved in the differentiation of both cell types.

Although our RNA-seq and qRT-PCR data provide evidence that TGFβ1 treatment downregulates Eps8 expression at the transcriptional level, we cannot exclude the possibility that Eps8 may additionally be regulated at the protein level by the regulation of translation or degradation. Little information regarding the regulation of Eps8 expression is reported in the literature. Overexpression of the protein Shb (SH2 domain-containing adapter protein B) has been shown to downregulate both the mRNA and protein expression of Eps8 in mouse 3T3 fibroblasts (Karlsson et al. 1995), but an initial experiment that we performed showed only minimal, if any, increase in Shb expression as a result of TGFβ1 treatment (appendix A figure 6-14). Shb has also been shown to bind directly to focal adhesion kinase (FAK), regulating its phosphorylation and enhancing cell spreading (Holmqvist et al. 2003), and to modulate PI3K signalling (Karlsson & Welsh 1997); Akt phosphorylation (Welsh et al. 2002); and Rac1 activation (Lu et al. 2002) in other cell types. Modulation of Shb

expression might also therefore additionally affect myofibroblast transdifferentiation by other mechanisms.

In human embryonic kidney cells enhanced lysosomal degradation of Eps8 has been demonstrated as a result of overexpression of Intersectin 2 (Ding et al. 2012) but it is unclear whether this observation is relevant at physiological levels and in fibroblasts. In addition, studies in v-Src transformed cells demonstrated that Trichostatin A, a histone deacetylase inhibitor, can also reduce Eps8 expression at the mRNA level (Leu et al. 2004).

Our results, demonstrating decreased Eps8 expression upon TGFβ1 treatment, are supported by a study using lung epithelial cells where a downregulation of Eps8 mRNA expression was observed in response to TGFβ1 treatment (Zhang et al. 2011). Using gene microarray techniques Zhang and co-workers demonstrated a reduction in Eps8 gene expression within 12h of TGFβ1 treatment and further reduction at their latest time point, 24h, which correspond with our observation of reduced protein expression 24h post TGFβ1 treatment. The use of a specific SMAD3 inhibitor (SIS3), preventing SMAD3 phosphorylation, partially reduced the size of the TGFβ1-induced reduction in Eps8 expression. Meanwhile, TGFβ1 treatment was shown to increase SMAD3 binding to the Eps8 promoter. Taken together, these results suggest that in lung epithelial cells TGFβ1-activated SMAD3 effects a repression of Eps8 mRNA expression by direct binding to its promoter. Although the results are visible in the figures of the paper, they were not commented on in the text and there is no evidence of an interaction between SMAD3 and the Eps8 promoter elsewhere in the literature. It remains to be seen whether a similar effect is observed in fibroblasts and whether incompleteness of SMAD3 inhibition or an additional mechanism accounts for the continued partial Eps8 repression in the presence of SIS3.

Having observed the downregulation of Eps8 with myofibroblast transdifferentiation *in vitro* we assessed whether this was clinically observable *in vivo*. Although the overexpression of Eps8 has been observed in the tumour compartment of a range of tumour types (Bashir et al. 2010; Chu et al. 2012; Ding et al. 2013; Griffith et al. 2006; Welsch et al. 2007), correlating with increased risk of metastasis (Yap et al. 2009) and worse overall survival (Chu et al. 2012) the expression in the stroma has not previously been examined.

Meanwhile, stromal αSMA expression, predominantly from myofibroblasts, has been shown to be inversely proportional to survival in a number of solid tumours ((Marsh et al. 2011; Chen et al. 2014; Horn et al. 2013). We therefore used immunohistochemical techniques to examine stromal αSMA and Eps8 expression in tissue microarrays from patients with oral cancer and a variety of fibrotic processes, to compare how Eps8 expression varied in myofibroblastic stroma compared to control tissue.

We observed that αSMA expression was elevated in the stroma of both OSCC specimens and a range of fibrotic disorders, compared to that in fibroepithelial polyps, and this finding is supported by the work of a number of other authors (Barth et al. 2004; Lomas et al. 2012; Hewitson & Becker 1995; Chan et al. 2013; Hartmann et al. 1990). Eps8 immunostaining in fibroblasts was comparatively weak compared to endothelial and epithelial cells, consistent with observations in the literature (Gallo et al. 1997). Additionally, in stromal areas exhibiting myofibroblast transdifferentiation, identified by a dense αSMA-staining pattern, we visualised a further reduction in Eps8 staining. The correlation in our findings across both tumour specimens and a range of fibrotic conditions indicates that there is a reproducible and reliable association between Eps8 downregulation and fibroblast-to-myofibroblast transdifferentiation.

We also demonstrated in section 3.1.4 that the downregulation of fibroblast Eps8 mRNA expression is similarly observed during the process of senescence induction. Senescence can be initiated in fibroblasts by a range of stimuli including hydrogen peroxide, ϒ-irradiation and repeated passage (Gadbois et al. 1997; Chen & Ames 1994). Senescent fibroblasts contribute to the heterogenous sub-populations of Cancer-Associated Fibroblasts (CAFs) and are present in approximately 16% of Head and Neck SCCs (Mellone et al. 2016). Although they demonstrate increased contractility *in vitro* and increased tumour promotion in xenograft models, senescent fibroblasts do not upregulate extracellular matrix protein production unlike myofibroblasts (Mellone et al. 2016). The observation that Eps8 is similarly downregulated in both myofibroblasts and γ-irradiation-induced senescent fibroblasts, and that it lies in an association cluster within the subset of downregulated mRNAs in both processes suggests that it may be an important regulator of the contractile, tumour-promoting phenotype. Furthermore, the initial findings of

Eps8 protein downregulation following senescence induction by either serial passage or hydrogen peroxide treatment indicates that the effect is not restricted to a specific senescing agent. Given that tumour stroma has been demonstrated to contain both traditional myofibroblasts and senescent fibroblasts, both with tumour-promoting abilities, it is important for us to understand the role of Eps8 in both of these cell types (Witkiewicz et al. 2011).

In this chapter we have provided evidence that maintenance of Eps8 expression plays an important inhibitory role in myofibroblast transdifferentiation induced by its most potent stimulus, TGFβ. Our time course experiment examining the effect of TGFβ1 treatment on Eps8 and αSMA expression demonstrated that downregulation of Eps8 at the protein level occurs early in the process of TGFβ1-induced myofibroblast transdifferentiation. It precedes αSMA upregulation and incorporation into stress fibres, without which there is insufficient tension for the protomyofibroblast to transdifferentiate into the myofibroblast (Eyden 2008; Gabbiani et al. 2012). This raised the initial possibility that Eps8 downregulation might be actively involved in the mechanism of transdifferentiation, rather than merely being a downstream consequence of it.

To further assess the importance of Eps8 in the mechanism of myofibroblast transdifferentiation, we downregulated Eps8 using RNA interference in HFFF2 and primary fibroblasts from a range of tissues. We also confirmed the effect using two alternative Eps8 siRNA sequences, demonstrating that the effects were gene rather than sequence specific. We observed that in the *absence* of TGFβ1, Eps8 knockdown increased αSMA mRNA and protein expression to a variable extent, but that Eps8 knockdown reliably caused significant augmentation of TGFβ1-induced αSMA expression. These results were independent of the origin of the fibroblasts, providing further support to the potential central role of Eps8 in fibroblast-to-myofibroblast transdifferentiation. These observations also raised the possibility that Eps8 knockdown might increase myofibroblast transdifferentiation by sensitising fibroblasts to TGFβ signalling.

In order to ensure that the effect of Eps8 knockdown resulted in augmentation of the myofibroblast phenotype and not just αSMA expression we also examined the mRNA expression of CTGF and COL1A1, secreted factors known

to be up-regulated during fibroblast-to-myofibroblast transdifferentiation (Mia et al. 2014; Tobar et al. 2014). These were also shown to be upregulated in our group's RNA-seq experiment. In this chapter we see that Eps8 knockdown augmented the TGFβ1-induced increase in COL1A1 and CTGF mRNA expression although the marked increase observed in CTGF did not quite reach statistical significance at the 5% level with only 3 independent experimental repeats.

The *de novo* production of αSMA-containing stress fibres is a defining feature of fibroblast-to-myofibroblast transdifferentiation (Eyden 2008). We therefore used immunocytochemistry to assess whether the observed increase in αSMA expression following Eps8 knockdown correlated with augmentation of TGFβ1-induced αSMA stress fibres. Our results confirmed that Eps8 knockdown augmented the TGFβ1-induced production of both filamentous actin and αSMA stress fibres. The qualitative reproduction of the results using both HFFF2 and primary dermal fibroblasts indicates that this result is reliable and reproducible across different populations of fibroblasts.

Gel contraction assays are commonly used to confirm the functional augmentation of the contractile phenotype (Bogatkevich et al. 2001; Underwood et al. 2015). We also utilised this technique to demonstrate that Eps8 downregulation results in the development of functional myofibroblasts. Eps8 knockdown fibroblasts, implanted in the collagen gels, displayed increased contractility, measured by a significant reduction in collagen gel size and weight compared to controls. These results were highly reproducible (demonstrated by the significance across independent repeats) both between batches of HFFF2 and additionally in primary fibroblasts. Furthermore, our cell proliferation data confirmed that these differences were not explained by variation in fibroblast proliferation as a result of the treatment (Figure 3-10).

Head and neck tumour-associated fibroblasts have been demonstrated to secrete a variety of paracrine factors into their surrounding media that enhance migration, invasion and proliferation of HNSCC cells (Wheeler et al. 2014). The production of secreted factors, influencing tumour behaviour, by activated fibroblasts or myofibroblasts has also been evidenced by a variety of authors in numerous other organ systems (Orimo et al. 2005; Hwang et al. 2008; Hanahan & Coussens 2012; Berdiel-Acer et al. 2014). We therefore sought to

assess whether Eps8 knockdown in fibroblasts resulted in the production of a conditioned media that enhanced HNSCC cell migration. Indeed, conditioned media from Eps8 knockdown fibroblasts augmented Transwell migration of SCC25 oral squamous cell carcinoma cells. Consistent with the findings in previous sections, Eps8 knockdown followed by subsequent TGFβ1 treatment resulted in fibroblast production of conditioned media that generated significantly more migration of SCC25 cancer cells than media produced by control-transfected, TGFβ1-treated fibroblasts. From this we can conclude that fibroblast Eps8 knockdown results in changes in the surrounding media that enhance cancer cell migration, and that Eps8 knockdown significantly enhances the effect of TGFβ1 to produce a pro-migratory fibroblast-conditioned media. The presence of Eps8 in the fibroblast is therefore likely to inhibit the pro-migratory nature of the medium from cancer-associated fibroblasts, myofibroblasts and senescent fibroblasts that has been observed by others *in vivo* and *in vitro* (Berdiel-Acer et al. 2014; Mellone et al. 2016).

While we had assessed the effect of fibroblast-conditioned media on cancer cell migration in vitro we were aware that this would not effectively model other interactions between fibroblasts and cancer cells including cell-cell and cell-matrix interactions through which fibroblasts are known to influence cancer cells (Flaberg et al. 2011; Hanahan & Coussens 2012). The in vivo effect of fibroblast Eps8 downregulation on cancer progression was assessed using a xenograft RAG1-/- murine model, using 5PT oral cancer cells co-injected with fibroblasts. Co-injection xenograft murine models have been published by a number of authors in this field and are therefore well validated (Berdiel-Acer et al. 2014; Orimo et al. 2005; Giannoni et al. 2010). While they are frequently used in the literature, a disadvantage of these models is that while innate immunity remains, the adaptive immune response of the mouse has been necessarily modulated to prevent xenograft rejection. Meanwhile, we are increasingly aware that the immune system plays a critical role in the tumour-host relationship (Puré & Lo 2016). Additionally, these tumours are neither orthotopic nor develop in a manner that is architecturally similar to *de novo* tumour development. They are however a useful model in which to observe a living interaction in a three dimensional physiological environment, between the co-injected cells of interest.

Analysis of tumour size using electronic callipers and of the fluorescent signal from the label on the cancer cells demonstrated that co-injection of Eps8 knockdown fibroblasts resulted in larger tumours, with greater cancer cell abundance, than co-injection with control fibroblasts. As the αSMA antibody is not specific for the human protein we are unable to state whether the observed tumour stromal myofibroblasts were derived directly from injected human fibroblasts or from recruitment of murine fibroblasts. However the histological staining demonstrated significantly more staining for αSMA, indicating greater myofibroblast activation, in tumours arising from the co-injection of Eps8 knockdown fibroblasts than those arising from co-injection of control fibroblasts. A similar pattern was observed with Masson's trichrome staining for collagen but the latter did not achieve statistical significance at the 5% level. Given that we have already demonstrated *in vitro* that Eps8 knockdown sensitises fibroblasts to TGFβ-mediated transdifferentiation our findings are consistent with those of other investigators who, in a variety of co-injection models have shown increased tumour growth in flanks with greater fibroblast activation (Orimo et al. 2005; Berdiel-Acer et al. 2014).

While we might expect larger tumour size to correlate with increased metastases (Kojima et al. 2014), histological assessment of the harvested flank lymph nodes revealed extremely infrequent metastases. The fluorescent signal from the flanks was also 500x less avid than the main tumours and showed no statistically significant difference between treatment arms. It is therefore likely that the experiment was ended too early to accurately assess the effect of fibroblast Eps8 knockdown on tumour metastasis but this would certainly be an interesting topic for further investigation.

An immune-competent Eps8 knockout mouse exists (Tocchetti et al. 2010) and could be considered for use in future experiments. Although this mouse, in its current form, would not be suitable for xenograft experiments, it would have been interesting to see how the Eps8 knockout mice, compared to wild-type, would respond to fibrotic stimuli such as intra-tracheal bleomycin (Jarman et al. 2014). We might expect, given the data acquired above, that Eps8 knockout mice would produce an earlier / more severe fibrotic response to such stimuli, since the fibroblasts would be sensitised to TGFβ-induced myofibroblast transdifferentiation.

In order to assess whether maintenance of Eps8 levels can prevent sensitisation of fibroblasts to TGFβ treatment we have optimised the transfection of HFFF2 fibroblasts with Eps8(mouse)-containing plasmids (appendix A figure 6-15). As a result, we will be able to transfect HFFF2 with mouse Eps8 prior to knockdown, using a human-specific siRNA sequence, of the human Eps8. We also have truncated forms of Eps8 that distinguish the known functions of Eps8, and in the future these could be used to identify which part of the protein is responsible for fibroblast sensitisation to TGFβ signalling.

Of clinical importance, some chemotherapeutic agents have been shown to downregulate Eps8 expression. Plicamycin (aka Mithramycin) is an anti-tumour agent that has historically been used to treat testicular cancer, Paget's disease and Chronic Myeloid Leukaemia (CML) (Dutcher et al. 1997) and is in clinical trial for Ewing's Sarcoma and treatment-resistant solid tumours. Plicamycin has been demonstrated to reduce Eps8 expression in tumour cells, reducing epithelial cell proliferation and migration (Gan et al. 2013; Yang et al. 2010) but its effect on fibroblasts and other myofibroblast precursors has not as yet been investigated. Daunorubicin is an anthracycline antibiotic anti-tumour agent and has also been shown to suppress Eps8 expression in an Acute Myeloid Leukaemia (AML) cell line (Gan et al. 2013). Daunorubicin is in the same family and shares many features with Doxorubicin, which is more widely used in combination chemotherapeutic regimens for a range of tumours including lung, breast, ovarian, gastric, bladder, and thyroid carcinoma as well as for leukaemias, lymphomas, and multiple myeloma.

The effect of these agents on Eps8 expression in the fibroblast has not previously been investigated. If these agents were to reduce Eps8 expression in myofibroblast precursors in addition to tumour cells, this may enhance myofibroblast transdifferentiation and inadvertently enhance stromal promotion of tumorigenesis in solid tumours. This would therefore act to diminish the efficacy of the chemotherapeutic regimes. This is of particular clinical relevance since my colleagues have also demonstrated that irradiation, which is often used in combination with chemotherapy, can also induce fibroblast senescence and myofibroblast transdifferentiation. Initial experiments that we have performed indicate that cisplatin (an agent commonly used in head & neck cancer chemotherapeutic regimens),

plicamycin, and possibly also doxorubicin, at sub-lethal doses, all reduce Eps8 expression in HFFF2 fibroblasts (appendix A figure 6-16). It will be of clinical interest to investigate in the future whether the use of these chemotherapeutic agents also results in enhanced myofibroblast transdifferentiation in response to TGFβ treatment as we have seen with the use of Eps8 siRNA.

3.2.8 Chapter Summary

In this chapter we have demonstrated a previously unrecognised function of Eps8 as a key regulatory protein in the process of myofibroblast transdifferentiation. This process has a critically important role in the pathogenesis of numerous conditions including organ fibrosis and cancer progression. From the evidence that we have, Eps8 is also likely to play a regulatory role in the development of fibroblast senescence, which has emerged as an alternative method by which tumours can be supported.

Maintained Eps8 expression in fibroblasts helps to minimise the effect of TGFβ1 on fibroblast populations. Reducing fibroblast Eps8 expression sensitises the cells to TGFβ1 signalling and results in increased αSMA stress fibre production, cell contractility, secretion of myofibroblast markers and promotion of cancer cell migration *in vitro* and increased tumour growth *in vivo*. Furthermore, we have observed that such downregulation of Eps8 occurs in response to TGFβ1-treatment, driving a dangerous positive feed-forward loop resulting in tissue fibrosis or the development of myofibroblastic cancer stroma supportive of cancer growth.

Further understanding of the molecular mechanism by which Eps8 exerts its tonic inhibitory effect on TGFβ1 signalling may enable us to identify targets, and potentially develop treatments, to limit myofibroblast transdifferentiation in a number of clinical conditions.

Chapter 4: The Role of Eps8 binding partners

4.1 The role of Eps8-binding partners and downstream targets in myofibroblast transdifferentiation

Eps8 is an adapter protein, which interacts with various binding partners within the cell and in many cases affects cell function through the formation of protein complexes. Although some of the functions of Eps8 are mediated independently of effects on cell structure (M. Xu et al. 2009; Wang et al. 2010), several Eps8-containing complexes modulate the actin cytoskeleton. Eps8 acts in a tricomplex with Abi1, SOS1 and PI3K to activate Rac-1, facilitating membrane ruffling, an early step in cell migration (Offenhauser et al. 2004; Scita et al. 1999; Innocenti et al. 2003; Innocenti et al. 2002). Binding of Abi1 is also required to generate a conformational change in Eps8, removing its auto-inhibitory activity, enabling it to cap actin filaments and remodel the actin cytoskeleton (Disanza et al. 2004). The binding of IRSp53 or palladin to Eps8 can further augment the activation of Rac1 and cytoskeletal reorganisation (Funato et al. 2004; Goicoechea et al. 2006). In order to ascertain which binding partners and mechanisms might be involved in the inhibition of myofibroblast transdifferentiation by Eps8, we initially targeted the 'tricomplex' members Abi1 and SOS1.

4.1.1 Knockdown of Abi1 or SOS1 increases αSMA expression and potentiates the effect of TGFβ1 treatment

In order to assess the effect of Abi1 or SOS1 knockdown on αSMA protein expression, HFFF2 and primary fibroblasts from a range of tissues (skin, oral cavity and oesophagus) were transfected with Abi1 or SOS1 siRNA as described in section 2.2. After 24h media was exchanged for serum-free DMEM with or without 5ng/ml recombinant human TGFβ1. Following a further 72h the cells were harvested and processed for Western blotting.

Figure 4-1 demonstrates that downregulation of Abi1, in the absence of TGFβ1, produces small and variable increases in αSMA expression in both HFFF2 and primary adult fibroblasts from differing tissues. Abi1 knockdown however

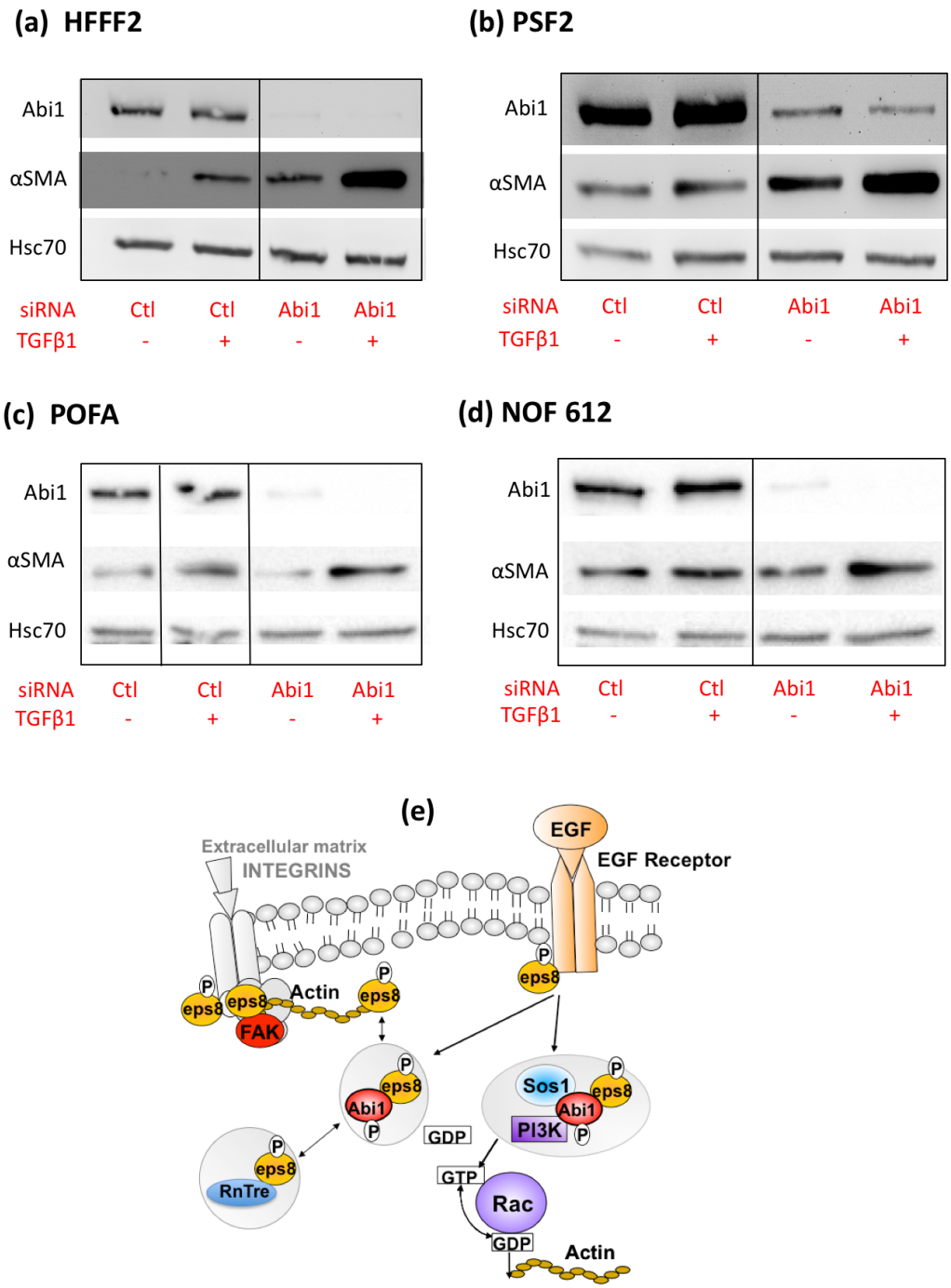

Figure 4-1 Abi1 knockdown augments TGFβ1-induced αSMA expression.

Western blots from (a) HFFF2, and primary fibroblasts: (b) PSF2 dermal, (c) POFA oral, and (d) NOF 612 oesophageal. Fibroblasts were transfected with 30nM Abi1 siRNA and 24h later their medium was exchanged for serum-free DMEM +/- 5ng/ml TGFβ1 for 72h. Hsc70 was used as a loading control. For (a) and (b) each experiment was performed twice, independently; single experiments were performed for (c) and (d). Schematic (e) demonstrates the known interactions of Eps8 with Abi1.

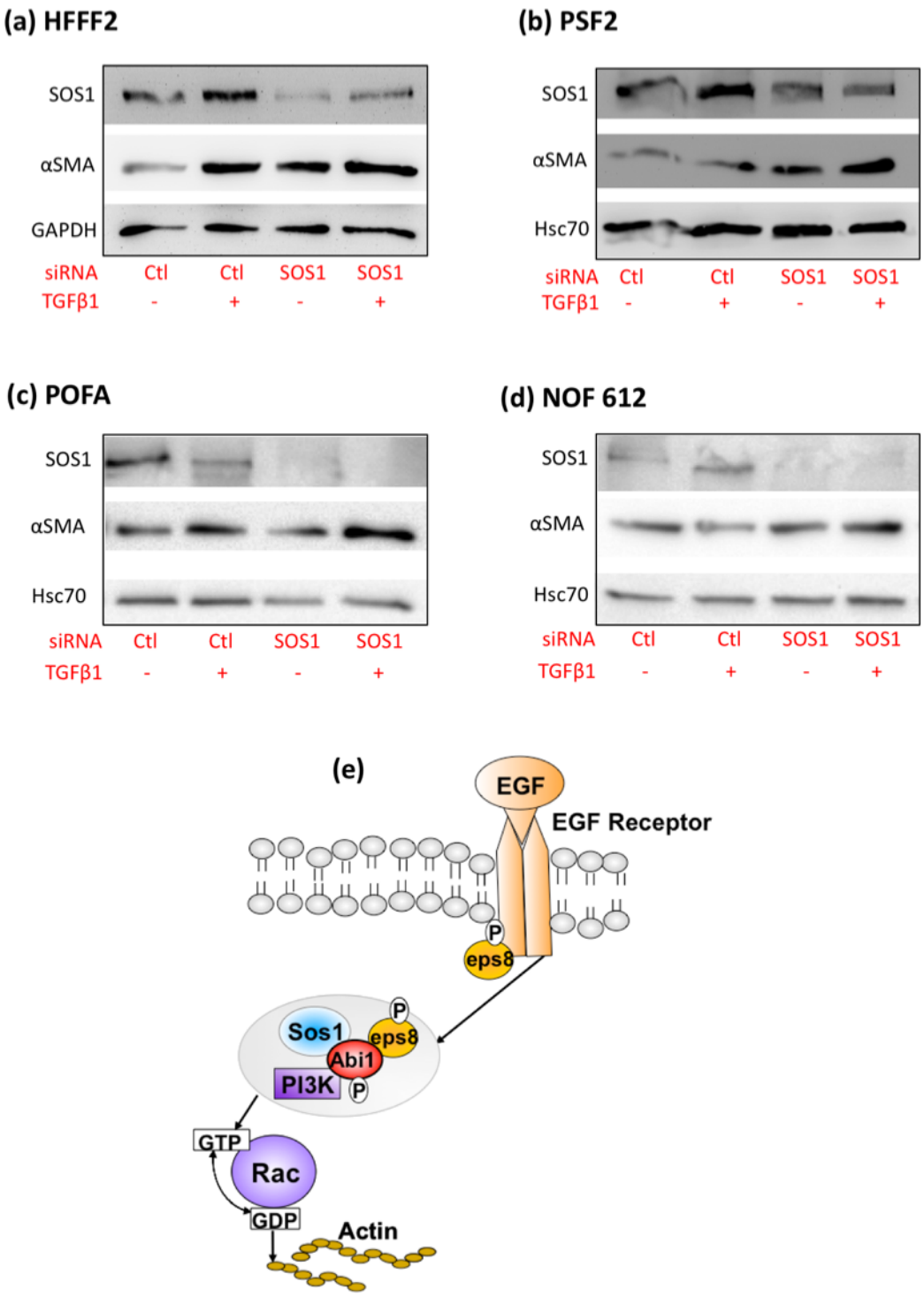

Figure 4-2 SOS1 knockdown augments TGFβ1-induced αSMA expression

Experiments were performed as in figure 4-1 using 30nM SOS1 siRNA. GAPDH or Hsc70 were used as loading controls. Schematic (e) demonstrates the known interactions of Eps8 with SOS1, via the Abi1-containing tricomplex.

consistently potentiates the TGFβ1-induced increase in αSMA expression. The effect is of a similar pattern and magnitude to the effect observed with Eps8 knockdown as demonstrated in section 3.2.1. Given the known interaction between Eps8 and Abi1 and the similarity of the effect seen with Eps8 and Abi1 knockdown, this suggests that they are both required for the regulation of TGFβ-induced fibroblast transdifferentiation and may potentially act in the same pathway.

Given that Eps8 is known, as demonstrated in fig 4-1(e), to form complexes containing Abi1, with or without the additional presence of SOS1, we sought to assess whether the observed effects of Eps8 and Abi1 were mediated via the formation of the Eps8-Abi1-SOS1 tricomplex. In this event we might expect to observe similar effects as a result of SOS1 knockdown to those demonstrated as a result of Eps8 and Abi1 knockdown.

Figure 4-2 demonstrates that in fibroblasts from a range of tissues (fetal and adult skin, oral cavity and oesophagus) SOS1 knockdown, in a similar manner to Eps8 knockdown, causes a variable increase in αSMA expression in the absence of exogenous TGFβ1, but reliably potentiates TGFβ1-induced αSMA expression. Although the similarity of effect resulting from Eps8, Abi1 and SOS1 knockdowns does not prove definitively that the Eps8-Abi1-SOS1 tricomplex is responsible for delivering Eps8's inhibition of myofibroblast transdifferentiation, the requirement for all three members of the tricomplex to inhibit myofibroblast transdifferentiation is consistent with its role in the mechanism.

4.1.2 Abi1 and SOS1 knockdowns augment TGFβ1-induced ACTA2 and COL1A1 mRNA expression

In order to assess whether the transcriptional profile induced by knockdowns of Abi1 and SOS1 was similar to that observed as a result of Eps8 knockdown, we examined ACTA2 and COL1A1 mRNA expression after Abi1 or SOS1 knockdown and 72h in serum-free medium in the presence or absence of human recombinant TGFβ1.

In the absence of exogenous TGFβ1 Abi1 knockdown increases ACTA2 expression slightly, but the knockdown markedly augments ACTA2 induction by TGFβ1 figure 4-3(a) left panel). As a result of one comparative outlier in the

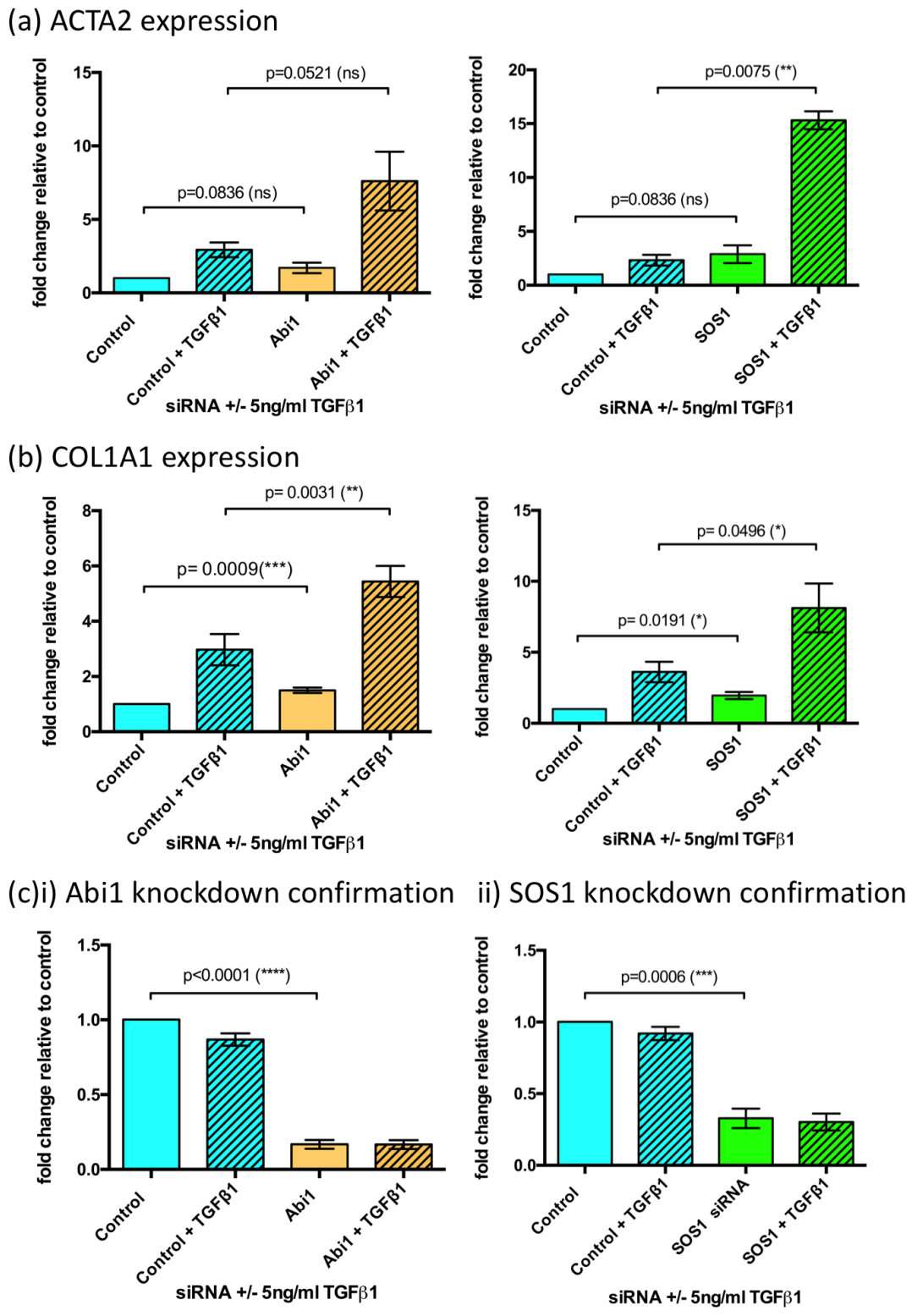

Figure 4-3 Abi1/SOS1 knockdowns increase ACTA2 & COL1A1 expression and augment TGFβ1-induced ACTA2 & COL1A1 expression.

HFFF2 fibroblasts were transfected with Control / Abi1 / SOS1 siRNA, then placed in serum-free DMEM for 72h with or without 5ng/ml TGFβ1. The graphs display, from independent experiments (n=5 for Abi1 and n=3 for SOS1), the mean and SEM of normalised fold change in each treatment group relative to the 'Control transfected no TGFβ1' treatment group.

5 independent repeats, the increase narrowly fails to achieve statistical significance at the 5% level. Knockdown of SOS1 expression similarly produces an increase in ACTA2 expression that does not quite achieve statistical significance at the 5% level but the resultant augmentation of TGFβ1-induced ACTA2 expression is highly statistically significant (figure 4-3(a) right panel).

Abi1 and SOS1 knockdowns also produce a statistically significant increase in COL1A1 expression in both the absence and presence of TGFβ1 (figure 4-3(b). As shown in the lower panels of Figure 4-3(c) Abi1 and SOS1 knockdowns remained effective with high statistical significance at 96h.

The similarity in the ACTA2 and COL1A1 mRNA expression profiles as a result of Eps8, Abi1 and SOS1 knockdowns in either the absence or presence of TGFβ1 suggests that the binding partners may all be involved in a common mechanism inhibiting myofibroblast transdifferentiation. The only known interaction of Eps8 with SOS1 is in the formation of the Rac1-activating tricomplex, which is dependent on Abi1 as an adapter protein. It is therefore possible that Eps8 helps to maintain a non-transdifferentiated state in fibroblasts via signalling through the Eps8-Abi1-SOS1 tricomplex, although we cannot exclude as yet unrecognised interactions between these proteins, or similar, independent effects of all three partners.

4.1.3 Abi1 and SOS1 knockdowns induce incorporation of αSMA into stress fibres

As in section 3.2.3 we aimed to assess whether the increased quantities of αSMA resulting from Abi1 and SOS1 knockdown were incorporated into functional αSMA stress fibres, as had been demonstrated following Eps8 knockdown. HFFF2 fibroblasts were transfected with non-targeting, Eps8, Abi1 or SOS1 siRNA and development of stress fibres was assessed by the use of immunofluorescence after 72h exposure to TGFβ1-treated or untreated serum-free media.

It is evident from the representative images in figure 4-4 that in the absence of TGFβ1, knockdowns of Eps8, Abi1 and SOS1 result in more pronounced αSMA stress fibres than is seen with the use of non-targeting siRNA. In the right-hand panels TGFβ1 is shown to increase the formation of αSMA stress fibres, but following Eps8, Abi1 and SOS1 knockdowns more prominent stress fibres are

produced than are seen with the use of non-targeting siRNA. The pattern of these qualitative observations, consistent with the patterns of quantitative αSMA expression observed in the previous section, suggest that knockdown of individual members of the tricomplex results in similar increases in the production of αSMA stress fibres to that observed with Eps8 knockdown.

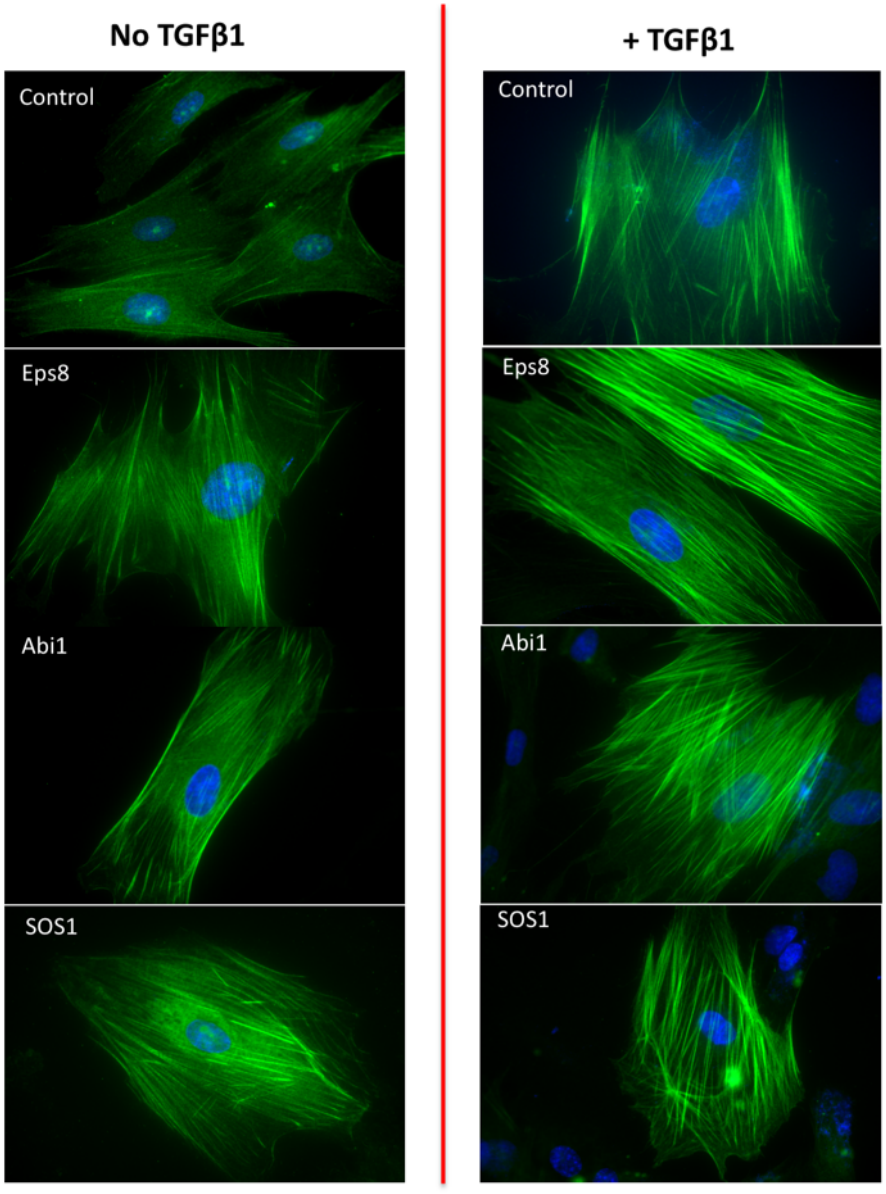

Figure 4-4 Knockdown of tricomplex members increases αSMA stress fibre prominence and augments TGFβ1-induced αSMA stress fibre formation.

Representative immunofluorescent images of αSMA (green) in HFFF2 fibroblasts with DAPI nuclear staining (blue) following non-targeting, Eps8, Abi1 or SOS1 siRNA transfection in the absence (left panel) and presence (right panel) of 10ng/ml TGFβ1. Magnification 400x.

4.1.4 Abi1 or SOS1 knockdown results in increased contractility of fibroblasts

In order to assess whether the additional αSMA stress fibres resulting from knockdown of tricomplex members all correlate with increased fibroblast contractility we performed collagen gel contraction assays using HFFF2 and adult primary dermal fibroblasts (PSF3). Fibroblasts transfected with non-targeting siRNA or siRNA targeting individual members of the tricomplex were incorporated into collagen gels containing 5ng/ml recombinant human TGFβ1. Resultant gel contraction was assessed after 24-72h (figure 4-5).

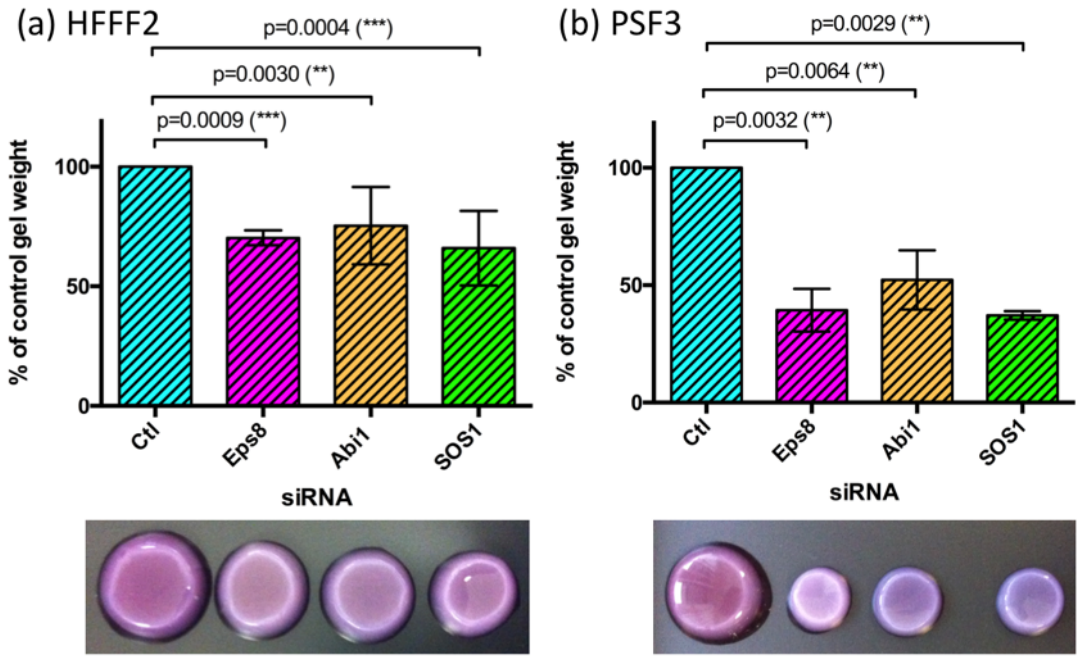

Figure 4-5 Abi1 and SOS1 knockdowns, like Eps8 knockdown, in the presence of TGFβ1 augment fibroblast contractility.

Bar charts display the mean relative weight of collagen gels across independent experiments (HFFF2=4, PSF3=2) following knockdown of Eps8 binding partners in fibroblasts and their incorporation into TGFβ1-contiaining collagen gels. Error bars represent SEM. Statistical analysis utilised a repeated measures ANOVA technique with LSD analysis and a 5% level of significance. Photographs of gels from representative experiments are shown below the bar charts.

Examining the results using both HFFF2 and PSF3 (primary dermal) fibroblasts (figure 4-5) we can see that in the presence of TGFβ1, knockdown of Eps8, Abi1 and SOS1 caused statistically significant reductions in collagen gel weight compared to fibroblasts transfected with non-targeting siRNA. Consistent with our western blot, qRT-PCR and immunofluorescence observations we can

conclude that knockdown of each of the tricomplex binding partners augments fibroblast contractility in the presence of TGFβ1. As noted in previous sections the magnitude of the effects are similar, irrespective of the binding partner targeted, supporting the hypothesis that myofibroblast transdifferentiation is inhibited by the presence of the Eps8-Abi1-SOS1 tricomplex.

In summary, in this chapter so far we have demonstrated that Abi1 and SOS1 knockdowns, similar to Eps8 knockdown, cause an increase in TGFβ1-induced ACTA2 and αSMA expression, and that the increased αSMA is incorporated into stress fibres, resulting in increased fibroblast contractility. Knockdowns of tricomplex binding partners also augment TGFβ1-induced production of COL1A1, another recognised marker of myofibroblast transdifferentiation indicating that this effect is not merely limited to αSMA expression.

4.1.5 Rac1 knockdown augments TGFβ1-induced αSMA and ACTA2 expression.

The Eps8-Abi1-SOS1 tricomplex is currently only known to directly activate the small GTPase Rac1 (Innocenti et al. 2002; Scita et al. 2001; Scita et al. 1999). In order to further assess whether this pathway is involved in the regulation of myofibroblast transdifferentiation we used short interference RNA to knockdown Rac1, reassessing ACTA2 and αSMA expression.

In both HFFF2 and primary adult dermal fibroblasts, Rac1 knockdown causes little, if any, change in αSMA protein expression in the absence of TGFβ1 (figure 4-6(a) and (d)). In the presence of TGFβ1, Rac1 knockdown augmented the induction of αSMA, in a similar manner to knockdowns of Eps8 and other members of the tricomplex.

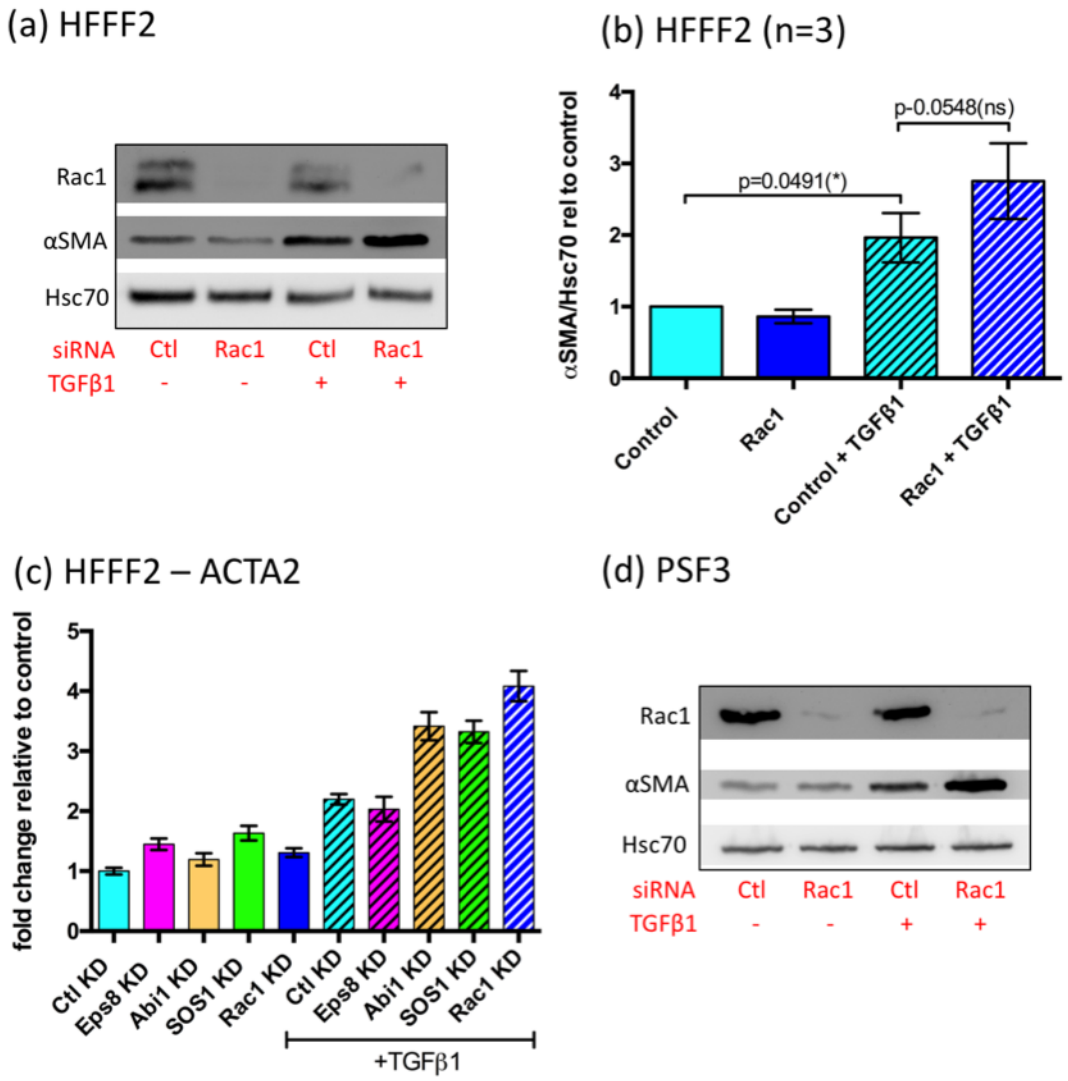

Figure 4-6 Rac1 knockdown augments TGFβ1-induced αSMA expression

HFFF2 fibroblasts were transfected with non-targeting or Rac1 siRNA and were then placed in serum-free DMEM +/- human recombinant TGFβ1 (5ng/ml) for 72h. (a) Displays a representative Western blot. (b) The mean normalised (relative to Hsc70) αSMA protein densitometry is shown relative to the control-transfected TGFβ1-untreated condition in 3 independent experiments (2 of which were also performed in duplicate from which the average densitometry was used). (C) ACTA2 expression measured by qRT-PCR in HFFF2 fibroblasts following Eps8, Abi1, Sos1 and Rac1 knockdown in the absence or presence of human recombinant TGFβ1 for 48h. The normalised (to GAPDH) fold change of ACTA2 expression, relative to the control-transfected TGFβ-untreated group, is demonstrated. Means and SEM of three technical repeats are displayed. (d) A representative blot from 2 additional independent repeats using PSF3 adult primary dermal fibroblasts. Hsc70 was used as a loading control.

At the transcriptional level, the effects of Rac1 knockdown were similar to those observed as a result of Eps8, Abi1 and SOS1 downregulation (figure 4-6(c)). Rac1 knockdown resulted in a small increase in ACTA2 expression in the

absence of TGFβ1, but effected a much larger augmentation of TGFβ1-induced ACTA2 expression. A similar pattern was also observable with COL1A1 expression (appendix B figure 6-17).

4.1.6 Rac1 knockdown augments TGFβ-induced stress fibre formation

In order to assess whether the increased ACTA2 and αSMA expression resulted in the formation of more prominent stress fibres we performed immunocytochemistry to visualise and quantify stress fibre formation following Rac1 knockdown (as per section 3.2.3). Images were captured from 6 randomly selected areas per condition and 4 nuclei were included in the image capture within that field of view to maintain a similar cell density per image. This is demonstrated by the DAPI staining across conditions in the left image stack of figure 4-7. FITC-conjugated phalloidin was used to label filamentous actin and a two-step antibody labelling procedure was used to label αSMA stress fibres.

Quantification of the fluorescent signal was performed per channel for each image and the bar charts in figures 4-7(b) and (c) demonstrate the mean αSMA and phalloidin signal in each condition. The quantification macro subtracted diffuse background signal, so only αSMA incorporated into stress fibres was quantified. The figures demonstrate that TGFβ1 treatment results in a statistically significant increase in filamentous actin and αSMA stress fibre production. Furthermore, knockdown of Rac1 resulted in a highly statistically significant augmentation of the effect of TGFβ1 on αSMA stress fibre production. Compared to the effect observed in section 3.2.3 the magnitude of the effect of Rac1 knockdown was similar to that observed with Eps8 knockdown. The phalloidin staining of filamentous actin followed a similar pattern to αSMA, but the augmentation of TGFβ1-induced filament production as a result of Rac1 knockdown failed to achieve statistical significance at the 5% level.

These findings demonstrate that the presence of both Eps8 and Rac1 are essential to inhibit TGFβ's ability to maximally induce αSMA expression, with resultant incorporation into stress fibres. This adds to the evidence in previous sections that Rac1, like Eps8, has a role in preventing TGFβ-induced myofibroblast transdifferentiation and is consistent with Eps8 mediating an

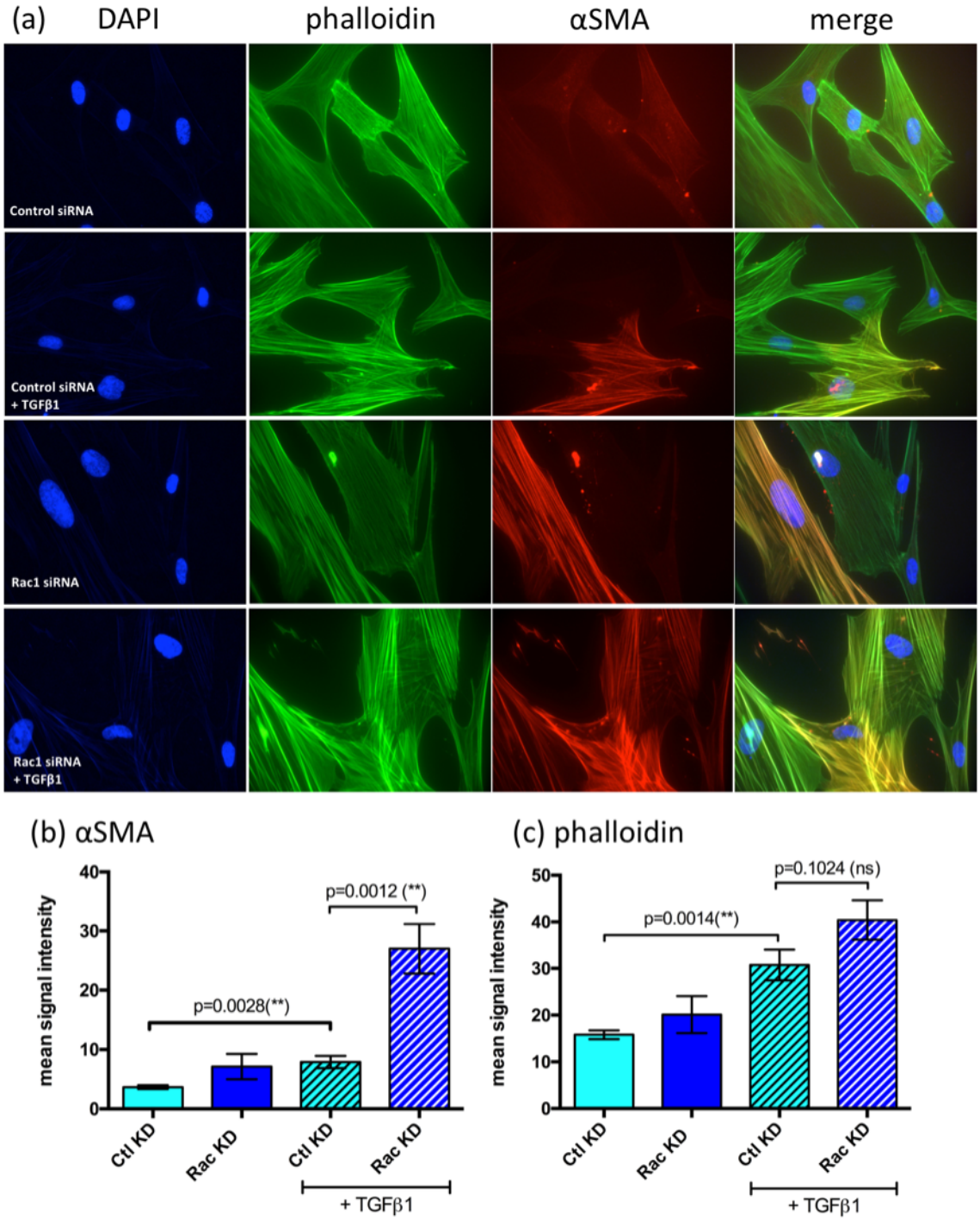

Figure 4-7 Rac1 knockdown augments TGFβ1-induced stress fibres

HFFF2 were transfected with non-targeting / Rac1 siRNA before being re-plated on chamber slides. Media was switched to serum-free medium +/- additional TGFβ1 for 72h before immunocytochemistry was performed. (a) In the upper panels, representative fluorescent images are displayed for phalloidin (green), αSMA (red) and a merged image, with DAPI nuclear stain in blue. 6 fields of view with similar cell density were analysed per condition to quantify the αSMA and phalloidin signal. Image analysis was performed using Image J software. Images for the 'Control siRNA no TGFβ1' arm are also used in figure 3-9. The bar charts display the mean signal intensity across the fields of view within each group for (b) αSMA and (c) phalloidin. Error bars represent SEM (n=6). Unpaired 2-tail t-tests were used. A Western blot confirming downregulation of Eps8 and Rac1 is displayed in the appendix (appendix B figure 6-18).

inhibition of myofibroblast transdifferentiation via the tricomplex and Rac1 signalling.

4.1.7 Rac1 knockdown may reduce fibroblast contractility

We have demonstrated in the previous section that Rac1 knockdown fibroblasts show augmented production of αSMA stress fibres in response to TGFβ1. In order to confirm that these stress fibres are functionally contractile we assessed whether Rac1 knockdown fibroblasts showed increased contractility compared to control transfected fibroblasts when implanted into collagen gels in the presence of TGFβ1.

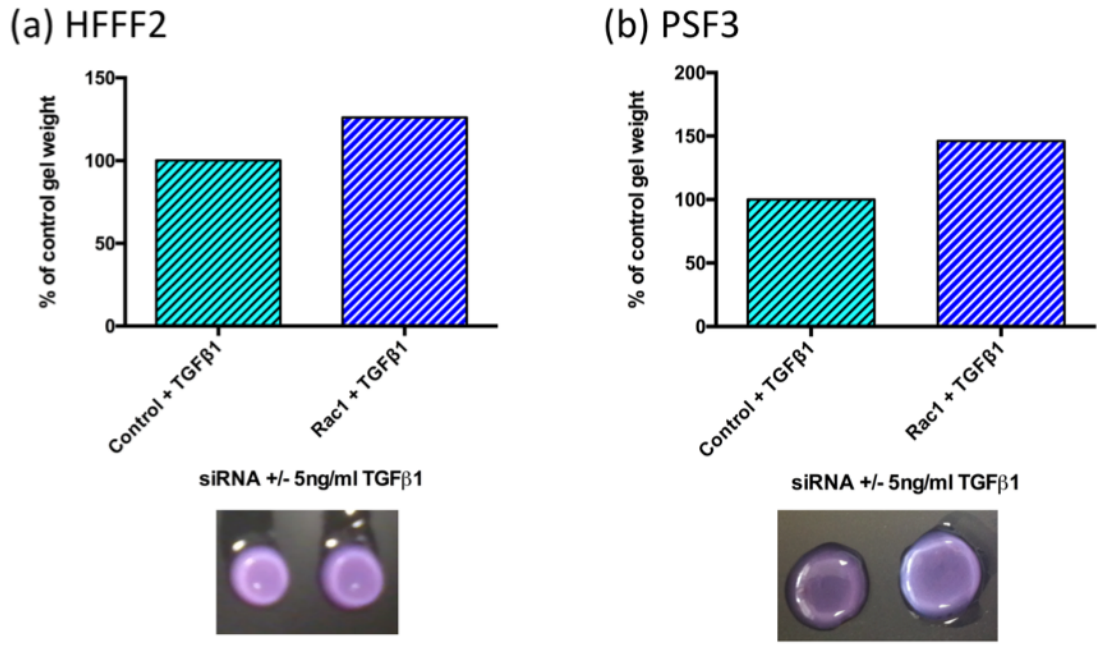

Figure 4-8 Rac1 knockdown, in the presence of TGFβ1, may reduce fibroblast contractility.

Bar charts demonstrate collagen gel weight in each condition as a percentage of the weight of the control-transfected gel using (a) HFFF2 or (b) PSF3 primary dermal fibroblasts. Photographs of the gels are displayed under the graphs. Results displayed are from individual, unrepeated experiments.

The experimental design used for Eps8 in section 3.2.4 was repeated with HFFF2 and PSF3 fibroblasts transfected with either non-targeting or Rac1 siRNA, with fibroblasts then embedded in collagen gels with additional TGFβ1 (5ng/ml). Gels were weighed and photographed after 24 – 72h.

Our results to date demonstrate that, in the presence of TGFβ1, Rac1 knockdown resulted in reduced fibroblast contractility compared to control-transfected fibroblasts. This was observed in both HFFF2 and adult primary dermal fibroblasts. Interestingly, we also prepared gels in parallel in the absence of TGFβ1 and the results showed similar patterns as seen in the presence of TGFβ1 (appendix B figure 6-20). These results are preliminary and require further repetition but if, in response to Rac1 knockdown, there exists a dichotomy between upregulation of αSMA stress fibres and reduced fibroblast contractility exists we would need to investigate reasons for this further.

4.1.8 Discussion

Eps8 is a multi-functional adapter protein with a number of known interactions within the cell. It has many regulatory phosphorylation sites, but the purpose of only a fraction of these are currently understood (Cunningham et al. 2013). Although Eps8 is known also to regulate receptor tyrosine kinase endocytosis via interaction with GTPases (Auciello et al. 2013; Lanzetti et al. 2000), and to modulate a number of integrin-related effects via focal adhesion kinase expression and activation (Maa et al. 2007), the most studied and best understood functions of Eps8 relate to its extensive role in actin reorganisation (Innocenti et al. 2003; Scita et al. 2001; Offenhauser et al. 2004; Disanza et al. 2004). Given the critical involvement of actin cytoskeleton remodelling in the generation of adequate tension for myofibroblast transdifferentiation it was feasible that Eps8 would influence transdifferentiation via this mechanism.

Eps8 is known to influence the actin cytoskeleton in multiple ways. Eps8 binds directly to actin and facilitates the bundling of actin filaments, but the binding of Abi1 to Eps8 is necessary to produce a conformational change to unveil its actin capping function (Disanza et al. 2004; Scita et al. 2001). The bundling activity of Eps8 is further augmented by binding of the adapter protein IRSp53 (Vaggi et al. 2011). The Eps8-IRSp53 interaction generates a conformational change in IRSp53, which recruits the Rho GTPase, Cdc42, known for regulating actin dynamics and filopodia formation (Disanza et al. 2006). The Rac1-activating tricomplex, containing Eps8, Abi1, and SOS1 is also recognised as an important regulator of actin remodelling and the presence of both binding partners, as well as PI3K, in the complex is necessary for its full activity (Scita et al. 1999; Innocenti et al. 2003). The formation of this tricomplex is

regulated by various factors and is promoted by the presence of p66shc, SNTA1 and CIIA proteins (Khanday et al. 2006; Bhat et al. 2014; Hwang et al. 2011). The presence of Eps8 within the complex is not only essential for optimal Rac1 activation but is also responsible for targeting of the tricomplex to the actin cytoskeleton (Scita et al. 2001). IRSp53 also enhances formation of the tricomplex and the subsequent activation of Rac1 (Funato et al. 2004). In order to assess whether or not Eps8 inhibits myofibroblast transdifferentiation via its Abi1-dependent bundling function or by formation of the Abi1 and SOS1-dependent tricomplex, in this chapter we compared the effects of knocking down Abi1, SOS1, and the target of the tricomplex, Rac1, with the effects observed with Eps8 downregulation.

Our results demonstrate that Abi1, like Eps8 knockdown caused a large augmentation of the effect of TGFβ1 on ACTA2 and αSMA expression. This effect was observed not only in fetal foreskin fibroblasts but also in adult primary fibroblasts from a range of tissues including skin, oral cavity and oesophagus suggesting that this was not a cell line or tissue-specific effect. Furthermore, the expression of COL1A1 was affected in a similar manner to ACTA2 suggesting that this is not an isolated effect on ACTA2/αSMA but is a wider effect on fibroblast to myofibroblast transdifferentiation. In the absence of exogenous TGFβ1, Abi1 knockdown produced similar effects to Eps8 knockdown generating small and variably sized increases in ACTA2 mRNA and αSMA protein expression.

Using immunocytochemistry we have shown that the increased expression of αSMA protein resulted in its incorporation into larger and more numerous stress fibres, and we used floating collagen matrices to demonstrate that in the presence of TGFβ1 the stress fibres were functionally contractile, effecting greater contractility than was produced by control transfected fibroblasts. Given that the *de novo* presence of functionally contractile αSMA stress fibres is a defining feature of myofibroblasts our findings demonstrate that Eps8 or Abi1 knockdown augment myofibroblast transdifferentiation and that their maintained expression limits transdifferentiation.

The magnitude of the effects of Abi1 knockdown were strikingly similar to those observed with Eps8, suggesting that Eps8 and Abi1 are both required to prevent fibroblast-to-myofibroblast transdifferentiation, perhaps through a

common mechanism such as the development of a complex. However, we cannot exclude Abi1 producing a similar effect by an Eps8-independent mechanism. Abi1 is centrally involved in actin reorganisation, independently of Eps8, in the actin-modulating WAVE2 complex, mediating Rac1-dependant actin polymerisation and reorganisation (Leng et al. 2005). Furthermore, at least in some cell types Abi1 also regulates PI3K signalling (Kotula 2012) which can itself impact on myofibroblast transdifferentiation (Li et al. 2016). Although Abi1 knockdown is mostly observed in the literature to decrease actin polymerisation (T. Wang et al. 2013; Innocenti et al. 2005), it has also been shown to remove inhibition of mDia2-dependent filopodia formation in HeLa cells, resulting in increased polymerisation within these long, unbranched actin structures (Beli et al. 2008).

The fact that maintained Eps8 and Abi1 levels are required to inhibit TGFβ-induced myofibroblast transdifferentiation raises the possibility that either the actin capping function of Eps8 or the Rac1-activating tricomplex may contribute to the maintenance of the fibroblast phenotype, since both of these functions require Eps8-Abi1 interaction (Scita et al. 1999; Disanza et al. 2006). In an attempt to differentiate between the potential involvement of these two complexes we examined the role of SOS1, a member of the tricomplex that has no recognised role in actin capping. We observed that SOS1 knockdown produced similar effects to that of Eps8 and Abi1 knockdown on ACTA2 / αSMA expression; αSMA incorporation into stress fibres; and cell contractility. It also augmented the TGFβ1-induced expression of COL1A1, providing additional evidence that SOS1 knockdown enhances TGFβ-induced myofibroblast transdifferentiation.

SOS1 is a dual specificity guanine nucleotide exchange factor (GEF), and is only known to activate Ras and Rac1 (Hwang et al. 2011). Although SOS1 does have some intrinsic ability to activate Rac1 alone, phosphorylation by Abl (Sini et al. 2004) or binding of Eps8 and Abi1 (Scita et al. 1999) is necessary for significant Rac1 activation. Given the similarity of effect resulting from SOS1 knockdown compared to that of Eps8 and Abi1 and their disparate functions outside of the tricomplex, our data suggests that the Eps8-Abi1-SOS1 tricomplex may be responsible for limiting TGFβ1-induced fibroblast-to-myofibroblast transdifferentiation.

The RNAseq data from fibroblasts that were either transdifferentiated by treatment with TGFβ1 or senesced by the use of gamma irradiation demonstrated that Abi1 and SOS1 showed no statistically significant change in expression as a result of these processes (appendix B figure 6-19). The fact that only Eps8 is downregulated by TGFβ1 treatment or γ-irradiation in HFFF2 does not exclude the role of the tricomplex in this process. It has been demonstrated by previous research that the relative availability of tricomplex members limits the amount of tricomplex formed and therefore the activation of downstream signalling pathways (Scita et al. 1999). Therefore, irrespective of Abi1 and SOS1 expression, the downregulation of Eps8 upon TGFβ1 treatment would be sufficient to limit tricomplex formation, removing the inhibition of TGFβ-induced myofibroblast transdifferentiation. We would expect this to generate a feed-forward cascade of transdifferentiation as generated myofibroblasts then release further TGFβ from the extracellular matrix as they contribute to further tissue tension (Gabbiani et al. 2012).

Evidencing the involvement of the tricomplex by knocking down its individual members and observing a common effect is imperfect but has been used by other groups (Chen et al. 2010). Using such an approach we cannot exclude the possibility that members of the tricomplex act through independent mechanisms to produce similar effects on αSMA expression, although this would seem unlikely. An ideal way of definitively proving the role of the tricomplex in the suppression of myofibroblast transdifferentiation would be to develop a small molecule inhibitor interrupting the specific interactions between these three proteins without modulating their expression. Such an approach could, if well designed, target only the tricomplex function of these proteins. Although this has been successfully performed for other protein-protein interactions (Spurr et al. 2012) such an inhibitor is not currently available for the Eps8-Abi1-SOS1 tricomplex and given the constraints of time I have not been able to attempt this in this thesis.

PI3Ks are enzymes activated by G-protein coupled receptors, receptor tyrosine kinases, or activated Ras at the plasma membrane, and result in phosphorylation of phosphatidylinositol (4,5)-bisphosphate (PIP2) to generate phosphatidylinositol (3,4,5)-trisphosphate (PIP3) (Conte et al. 2011). Two classes of PI3K have been shown to be recruited into the tricomplex, class 1A, via its regulatory p85 subunit (Innocenti et al. 2003) and class 2β (Katso et al.

2006). Both have been proven to function up-stream of Rac1 and have been shown to drive Rac1-dependent cell migration in both fibroblasts and cancer cells (Innocenti et al. 2003; Katso et al. 2006). PI3Ks have also been shown to function downstream of Rac1 to effect myofibroblast transdifferentiation in renal mesangial cells (Hubchak et al. 2009). Furthermore, PI3Ks additionally signal via the Akt/mTOR pathway, to regulate a range of cellular processes including cell proliferation, metabolism and the avoidance of apoptosis (Cantley 2002). Myofibroblast proliferation and persistence in pathological conditions has been potentially cited as resulting from a failure of apoptosis (Desmouliere et al. 1995) for which activity in the PI3K/Akt pathway may be at least partially responsible.

PI3K phosphorylates and activates PIP and PIP2, which are restricted to the plasma membrane and recruit Akt and phosphoinositide-dependent kinase -1 (PDK1) to themselves (Alessi et al. 1997). PDK1 phosphorylates and activates Akt at Thr308 but further Akt phosphorylation at Ser473 by the TORC2 complex is required for its complete activation (Sarbassov et al. 2005). Dually phosphorylated, fully activated pAkt can then signal downstream.

The role of PI3K signalling has been implicated in fibrosis within many organs including the lungs, liver and heart (Son et al. 2009; Conte et al. 2011; Voloshenyuk et al. 2011; Marra et al. 1997) and fibroblasts isolated from patients with Idiopathic Pulmonary Fibrosis or from the localised fibrosis in Peyronie's disease have demonstrated elevated levels of pAkt (Jung et al. 2013; Xia et al. 2010). It is possible that reduced tricomplex formation, resulting from TGFβ1-induced suppression of Eps8 levels, may release PI3K from the tricomplex to increase Akt phosphorylation and downstream signalling. In a preliminary experiment, using HFFF2 fibroblasts, we observed increased Akt expression and ser473 phosphorylation as a result of knockdowns of Eps8 or other binding partners, all of which would act to limit formation of the tricomplex (appendix B figure 6-21). This is consistent with the literature, where it has also previously been noted that reduced Eps8 expression, resulting from Shb overexpression, is associated with increased PI3K activity using a PI3K assay (Karlsson & Welsh 1997). We also observed an increase in Akt phosphorylation in response to TGFβ1, as has been documented in the literature (Chung et al. 2014). This hypothesis requires further investigation, but could be an alternative mechanism by which Eps8 downregulation, via

reduced tricomplex activity, augments fibroblast to myofibroblast transdifferentiation.

PI3K inhibitors are known to induce apoptosis, reducing activated fibroblast proliferation, and reducing the expression of myofibroblast markers including αSMA and collagen *in vitro* (Jung et al. 2013; Conte et al. 2011). Given the current focus on Akt/mTOR pathway inhibitors in combination therapies for Head and Neck and other cancers (Dorsey & Agulnik 2013; Ando et al. 2014; Fury et al. 2013) it will be interesting to fully investigate the effects of PI3K inhibition on TGFβ or Eps8 knockdown-induced myofibroblast transdifferentiation.

Examination of the roles of Eps8 in cancer and epithelial cells has previously identified a positive correlation with activation of the PI3K pathway, with overexpression of Eps8 leading to increased Akt-dependent proliferation and protection from apoptosis (Ding et al. 2013; Wang et al. 2009; Wang et al. 2010; M. Xu et al. 2009). The tricomplex has even been cited as the likely potential mechanism through which this may occur (M. Xu et al. 2009). Our preliminary results suggest that, in fibroblasts, in contrast to the epithelial compartment, reduction of tricomplex formation increases rather than reduces Akt phosphorylation, which is again a novel finding. If the increase in Akt phosphorylation is shown to produce anti-apoptotic effects in fibroblasts, as in cancer cells, this could represent a mechanism by which transdifferentiated myofibroblasts are protected from apoptosis and persist in fibrotic disease.

The only known target immediately downstream of the Eps8-Abi1-SOS1-PI3K tricomplex, is Rac1 (Innocenti et al. 2002). We demonstrated that knockdown of Rac1, similarly to other members of the tricomplex, results in small effects on ACTA2 and αSMA expression in the absence of TGFβ1, but markedly potentiates TGFβ1-induced expression of ACTA2 and αSMA, and the generation of αSMA stress fibres. In a preliminary experiment we also demonstrated that Rac1 knockdown augments the TGFβ1-induced expression of COL1A1 to a similar extent as knockdowns of other members of the tricomplex.

These results are supported by other studies in the literature. As we have previously discussed, myofibroblasts can be derived from a range of circulating or local precursor cells in different tissues. In renal mesangial cells a reduction

in the expression and activation of Rac1 results in induction of αSMA expression and stress fibre formation, and this effect is reduced by the use of Rho inhibitors (Mondin et al. 2007). Other authors who used the NSC-23766 Rac1 inhibitor in renal fibroblasts, anticipating a reduction in TGFβ1-induced αSMA and fibronectin EIIIA, reported that no effect was seen but their figures clearly demonstrate consistent augmentation of the induction of these proteins by TGFβ1, supporting our results (Manickam et al. 2014). The overexpression of dominant negative Rac1, or the use of a Rac1-inhibitory peptide also have been shown to induce αSMA expression, while overexpression of constitutively active Rac1 inhibits αSMA expression (Mondin et al. 2007; Lakhe-Reddy et al. 2006). Furthermore, liver tissue from inducible Rac1 knockout mice showed increased type I collagen and αSMA mRNA expression when Rac1 knockout was induced (Bopp et al. 2013).

In our experiments with Rac1, despite clear increases in TGFβ-induced ACTA2 expression; αSMA expression; and αSMA stress fibre production following Rac1 knockdown, collagen gels unexpectedly showed reduced contraction when impregnated with Rac1 knockdown compared to control fibroblasts. This experiment was only completed once in 2 different fibroblast lineages but, if reproducible, the observation is supported by other literature, where the use of a Rac1 inhibitor in wild-type fibroblasts has been shown to reduce contractility in floating gel contraction assays (Leask et al. 2008). Given that Rac1 has an important role in cell migration (S. Xu et al. 2009), this may be explained by Rac1 knockdown fibroblasts being less able to spread and settle within the collagen matrix before commencing contraction. Although Rac1 knockdown fibroblasts were re-plated into chamber slides in our immunocytochemistry experiments without any obvious change in cell spreading or cell number over 72h, the requirements for cell adhesion and migration are likely to be very different in a three dimensional collagen matrix (Shih & Yamada 2012) and may be more Rac1-dependent and sensitive. Alternatively, there is a known interaction between Rac1 and Akt signalling (Shen et al. 2014), and Akt signalling is important for avoidance of apoptosis (Kulasekaran et al. 2009). We should perhaps therefore also consider whether Rac1 knockdown fibroblasts are more susceptible than controls to apoptosis when implanted into collagen gels. In addition to repeating the gel contraction assays to confirm the preliminary experiments, sectioning the gels after the assay and examining the

distribution of fibroblasts in the gels could help to address these questions and ascertain whether these issues are masking a true increase in myofibroblast contractility as a result of Rac1 knockdown.

Examining the literature on Rac1 modulation more broadly than solely in relation to TGFβ signalling, there is a body of evidence that the role of Rac1 in fibroblasts is highly dependent on the nature of the applied pro-fibrotic stimulus. For example, bleomycin-induced dermal fibrosis is abrogated by the use of fibroblast-specific Rac1knockout mice (Liu et al. 2008), but Rac1 knockout worsens sub-acute doxorubicin-induced liver fibrosis (Bopp et al. 2013). Additionally, certain pathologies appear to be more dependent on abnormal Rac1 signalling than others. Fibroblasts from scleroderma patients express Rac1 in normal quantities but this Rac1 has been shown to be highly activated (S. Xu et al. 2009). In these scleroderma fibroblasts, the use of Rac1 inhibitors markedly reduces the expression of αSMA and other myofibroblast markers and the formation of stress fibres (S. Xu et al. 2009). In our experiments, using non-scleroderma fibroblasts and Rac1 siRNA, we observed the opposite effect - supporting the hypothesis that the role of Rac1 in myofibroblast transdifferentiation may vary between diseases, as well as between the type of pro-fibrotic stimulus and the cell type and tissue of origin (D'Ambrosi et al. 2014).

Classically and most simply, RhoA has been the Rho GTPase identified most responsible for stress fibre formation, while Rac activity governs lamellipodia formation, and Cdc42 filopodia formation (Richerioux et al. 2012). While RhoB and C can also maintain stress fibre presence RhoA is the most physiologically relevant (Pellegrin & Mellor 2007). RhoA promotes stress fibre contractility via the activity of protein kinase ROCK (Leung et al. 1996) and mDia1(Watanabe et al. 1999). The threonine/serine kinase ROCK is activated by RhoA binding and augments stress fibre formation and contractility by phosphorylating myosin light chain and a number of regulatory proteins (Pellegrin & Mellor 2007; Leung et al. 1996). Actin polymerisation and bundling is critical for stress fibre formation and mDia1 activity is necessary for the production of the required linear actin polymers, appropriately localising actin nucleation at focal adhesions (Butler et al. 2006). Interactions between the Rho GTPases have been identified and, critically, Rac has been shown to inhibit Rho activity directly at the GTPase level in fibroblasts (Sander et al. 1999). The protein kinase p21-

activated kinase (PAK1) is a recognised effector of Rac in fibroblasts and has been shown to inhibit RhoA-dependent stress fibre formation via inhibition of the exchange factor NET1in fibroblasts (Alberts et al. 2005). PAK1 also phosphorylates actin and causes dissolution of stress fibres in kidney epithelial cells and fibroblasts (Papakonstanti & Stournaras 2002; Manser et al. 1997) and phosphorylates MLCK, reducing its activity and actomyosin assembly in kidney epithelial and HeLa cells (Sanders et al. 1999). It is potentially via this mechanism that Eps8 downregulation, via reduced tricomplex and Rac1 activity, increases RhoA activity and reduces stress fibre disassembly. This would resultantly increase stress fibre formation in response to TGFβ1 as we have observed in our results.

4.1.9 Chapter Summary

In this chapter we have provided evidence that supports the involvement of both Abi1 and SOS1, and therefore the Eps8-Abi1-SOS1 tricomplex, in the mechanism by which Eps8 inhibits myofibroblast transdifferentiation. Tricomplex activity results in Rac1activation, and is likely therefore to inhibit RhoA activity and stress fibre formation. Further investigation in this section will include performing repeats of the gel contraction assays, assessing PAK1 activation using phospho-antibodies, and RhoA activity using pulldown assays. The evidence provided is currently supportive rather than conclusive, and the future development of a small molecule inhibitor to specifically interrupt formation of the tricomplex would provide definitive evidence of its role inhibiting myofibroblast transdifferentiation.

Chapter 5: Eps8 Regulation of Canonical SMAD signalling

5.1 Modulation of TGFβ signalling by Eps8

We observed in previous sections that while knockdown of Eps8 and other members of the tricomplex result in small, and variably sized increases in αSMA, they markedly augmented the transdifferentiating effects of exogenous TGFβ1. Considerable cross talk has been recognised between canonical TGFβ signalling and other cell signalling pathways (see section 1.1.6.1.4), but an interaction between Eps8 and canonical TGFβ1 signalling has not previously been proposed. In this chapter we sought to investigate the potential interaction between Eps8 and TGFβ1 signalling.

5.1.1 αSMA upregulation resulting from Eps8 knockdown appears dependent on TGFβ receptor function

We previously demonstrated that the effects of Eps8, Abi1 or SOS1 knockdowns on αSMA expression were varied in magnitude when exogenous TGFβ was withheld from fibroblasts. The observed increases in αSMA expression were larger and more consistent when knockdowns preceded treatment with TGFβ1, indicating a possible interaction between the tricomplex members and TGFβ signalling. In our experimental design, even in the absence of exogenous TGFβ1, TGFβ is available to fibroblasts from both autocrine secretion and is additionally contained in the fetal calf serum applied overnight following transfection, before exchange for serum-free media.

Firstly, we aimed to block canonical TGFβ1 signalling from these sources by the addition of a TGFβ receptor inhibitor prior to fetal calf serum addition to the media, and again when it was replaced with serum-free media. Fibroblasts were transfected with control / Eps8 siRNA and before the addition of serum, 4h after transfection, we added TGFβR1 inhibitor kinase IV (Calbiochem), at a final concentration of 1μM, to specific wells. The following day media was replaced with serum-free DMEM in the absence or presence of TGFβR1 inhibitor. Fibroblasts were harvested 72h post-transfection and lysates assessed by Western blotting.

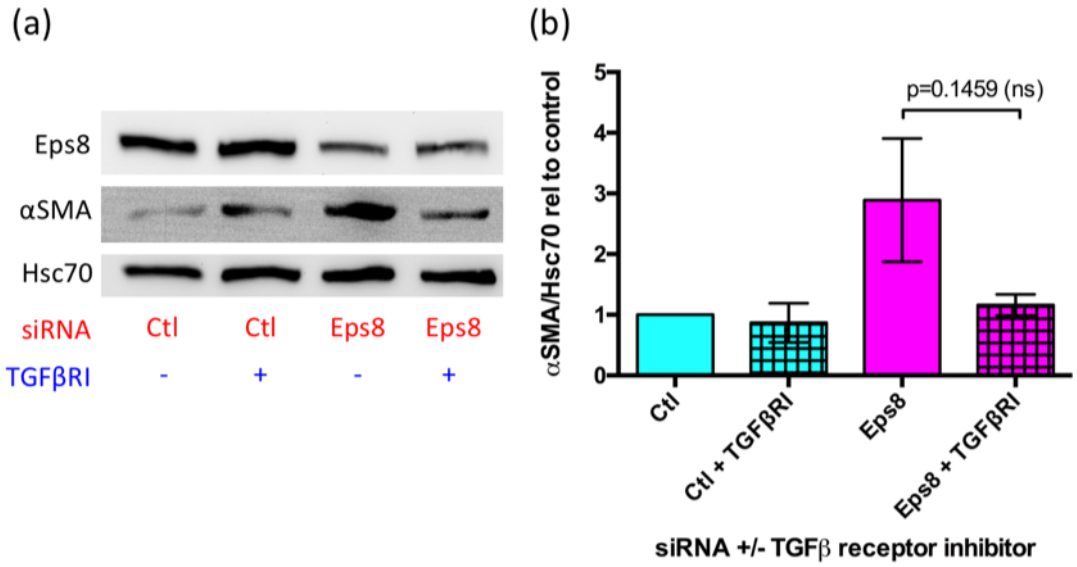

Figure 5-1 Use of a TGFβR1 inhibitor appears to reduce Eps8 knockdown-induced αSMA expression.

HFFF2 fibroblasts were transfected with control / Eps8 siRNA and after 24h were placed in serum-free medium for a further 48h. Cells in TGFβRI+ groups additionally received 1μM TGFβR1 inhibitor prior to serum treatment post-transfection, and again in the serum-free medium. A Western blot from a representative experiment is shown in (a) while (b) displays normalised αSMA densitometry relative to control across 4 independent experiments. Error bars display SEMs and a 2-tailed paired t-test was used to assess differences between groups.

In order to ensure that the ALK5 TGFβ receptor inhibitor was effective at the concentration used we demonstrated its inhibition of αSMA induction by 5ng/ml exogenous human recombinant TGFβ1 (appendix C figure 6-22).

As shown in figure 5-1, Eps8 knockdown compared to transfection with non-targeting siRNA effects a mean trebling of αSMA expression when TGFβ signalling is uninhibited. Use of the TGFβR1 inhibitor results in a very small reduction in αSMA expression in control-transfected fibroblasts, but the increased αSMA expression resulting from Eps8 knockdown is almost completely abrogated by the use of the TGFβ receptor inhibitor. This suggests firstly that autologous TGFβ stimulation and the TGFβ contained in fetal calf serum only have negligible transdifferentiating effects on control-transfected fibroblasts. It also confirms that Eps8 knockdown sensitizes fibroblasts to low levels of TGFβ, resulting in augmented αSMA expression, and that this augmentation is heavily dependent on TGFβ signalling.

Although statistical significance did not reach the 5% level with 4 independent experiments this is largely because of the comparative variability in the extent of Eps8 knockdown-induced αSMA in the absence of exogenous TGFβ1 as we have seen in previous sections. Statistical significance is likely to improve with further independent repeats.

5.1.2 Eps8 knockdown up-regulates total SMAD2 protein levels and potentiates TGFβ1-dependent phosphorylation

Since Eps8 knockdown appeared to sensitise fibroblasts to TGFβ signalling we proceeded to directly examine the effect of Eps8 knockdown on members of the canonical TGFβ signalling pathway.

Receptor SMADs (SMAD2 and SMAD3) are downstream mediators of canonical TGFβ1 signalling (Massagué 2012). SMAD3 expression and activity has been shown to be necessary for the development of a number of fibrotic conditions, and SMAD3 knockout mice display reduced fibrosis as a result of radiation, bleomycin or carbon tetrachloride compared to controls (Flanders 2004). SMAD2 is seen by some as having a comparatively modulatory role on canonical signalling compared to SMAD3, but others recognise both distinct and overlapping roles for SMAD2 and SMAD3 in TGFβ1 signalling, which are currently only partially understood (Brown et al. 2007). Due to the crucial role of SMAD2 and SMAD3 in canonical TGFβ1 signalling, we first examined the effect of Eps8 knockdown on the expression and phosphorylation of these receptor SMADs.

As previously, HFFF2 fibroblasts were transfected with non-targeting or Eps8 siRNA, and the next day media was replaced with serum-free DMEM +/- 5ng/ml TGFβ1 for 72h. Figure 5-2 demonstrates that the induction of αSMA expression resulting from Eps8 knockdown was accompanied by an increase in total SMAD2, but not total SMAD3, expression. Furthermore, while TGFβ1 treatment of control-transfected fibroblasts induced an expected increase in the phosphorylation of SMAD2, this was further potentiated by prior downregulation of Eps8 expression.

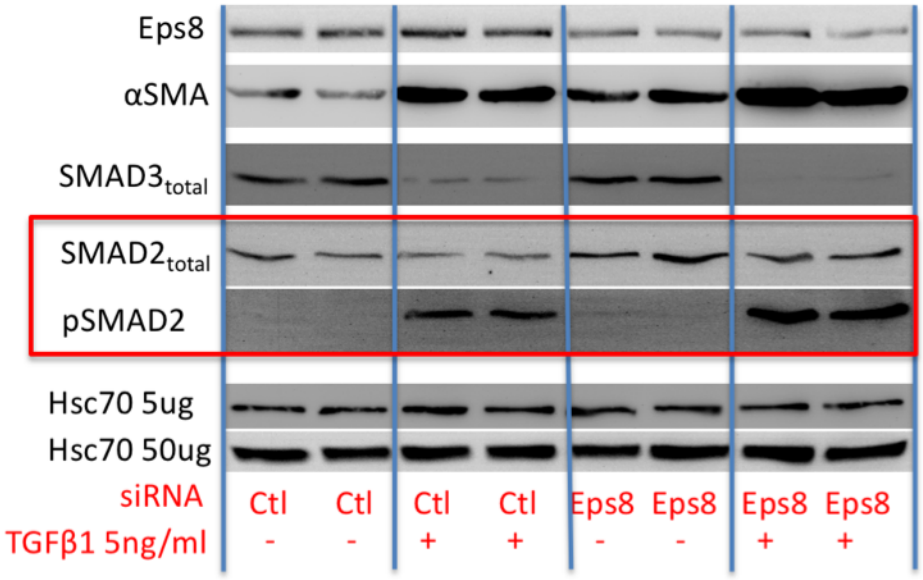

Figure 5-2 Eps8 knockdown increases SMAD2 protein levels and TGFβ1-induced SMAD2 phosphorylation

HFFF2 fibroblasts were transfected with control / Eps8 siRNA and the following day medium was changed to serum-free DMEM +/- 5ng/ml TGFβ1 for 72h. Duplicate lanes were prepared in the Western blot using lysates from independent wells within the same experiment. Hsc70 was used as a normaliser both for Eps8 (5ug total protein) and for αSMA / SMAD2/3 (50ug total protein). This experiment was undertaken independently twice demonstrating the same pattern of results.

These results demonstrate that Eps8 knockdown results in an upregulation of SMAD2 protein levels and increased abundance of phosphorylated SMAD2 in response to TGFβ1 stimulation. Given that SMAD2 phosphorylation is an important mediator of TGFβ signalling this identifies a potential mechanism by which Eps8 can modulate canonical TGFβ signalling. Furthermore, it suggests that maintained Eps8 expression in fibroblasts acts to inhibit SMAD2 protein levels, limiting the ability of TGFβ1 stimulation to signal through the canonical pathway.

5.1.3 Eps8 knockdown up-regulates SMAD2 mRNA expression, but does not modulate that of SMAD3, SMAD4, SMAD6 or SMAD7

Having shown that Eps8 knockdown results in an increase in SMAD2 protein expression we next investigated whether the same increase could be detected at the transcriptional level.

A time course experiment was performed assessing SMAD2 expression in HFFF2 fibroblasts transfected with either Eps8 or non-targeting siRNA, and subsequently treated with human recombinant TGFβ1. In addition to the above experiment, we also analysed the effect of Eps8 knockdown on SMAD2 expression in both the absence and presence of TGFβ1.

As shown in Figure 5-3(a), from the first time point (24h post transfection and 30min after TGFβ1 treatment) onwards, Eps8 knockdown fibroblasts displayed increased SMAD2 mRNA expression compared to controls. This was irrespective of whether TGFβ1 had been applied. The difference between control and Eps8 transfected groups persisted at later time-points up to and including the latest time point, 72h post TGFβ1 treatment. This indicates that Eps8 knockdown results in elevated mRNA and protein levels of SMAD2 and suggests that the increase in mRNA expression occurs within 24h of Eps8 knockdown. Statistical analysis confirms a significant difference in SMAD2 expression between control and Eps8 knockdown conditions, both in the absence ($p=0.0014^{**}$) and presence ($p=0.0472^{*}$) of TGFβ1 treatment.

Further support for the upregulation of SMAD2 mRNA expression with Eps8 knockdown is presented in figure 5-3(b). Examination of SMAD2 levels following Eps8 knockdown in three independent experiments reveals that SMAD2 expression is higher in Eps8 knockdown groups compared to control both in the absence and presence of TGFβ1. With only three independent repeats the differences are highly statistically significant in the presence of TGFβ1, and approach significance at the 5% level in the absence of TGFβ1 treatment.

Finally in 5-3(c) SMAD2 mRNA levels are displayed for a single experiment where fibroblasts were transfected with either Eps8 / Abi1 / SOS1 / Rac1 or non-targeting siRNA, with or without subsequent treatment with TGFβ1. It is shown that elevated levels of SMAD2 appear to arise from knockdown of any member of the tricomplex or downstream Rac1, although this experiment has only been performed once and requires independent repetition. Building on the results in chapter 4 this provides additional supportive evidence for the role of the tricomplex and Rac1 in the modulation of TGFβ signalling by Eps8.

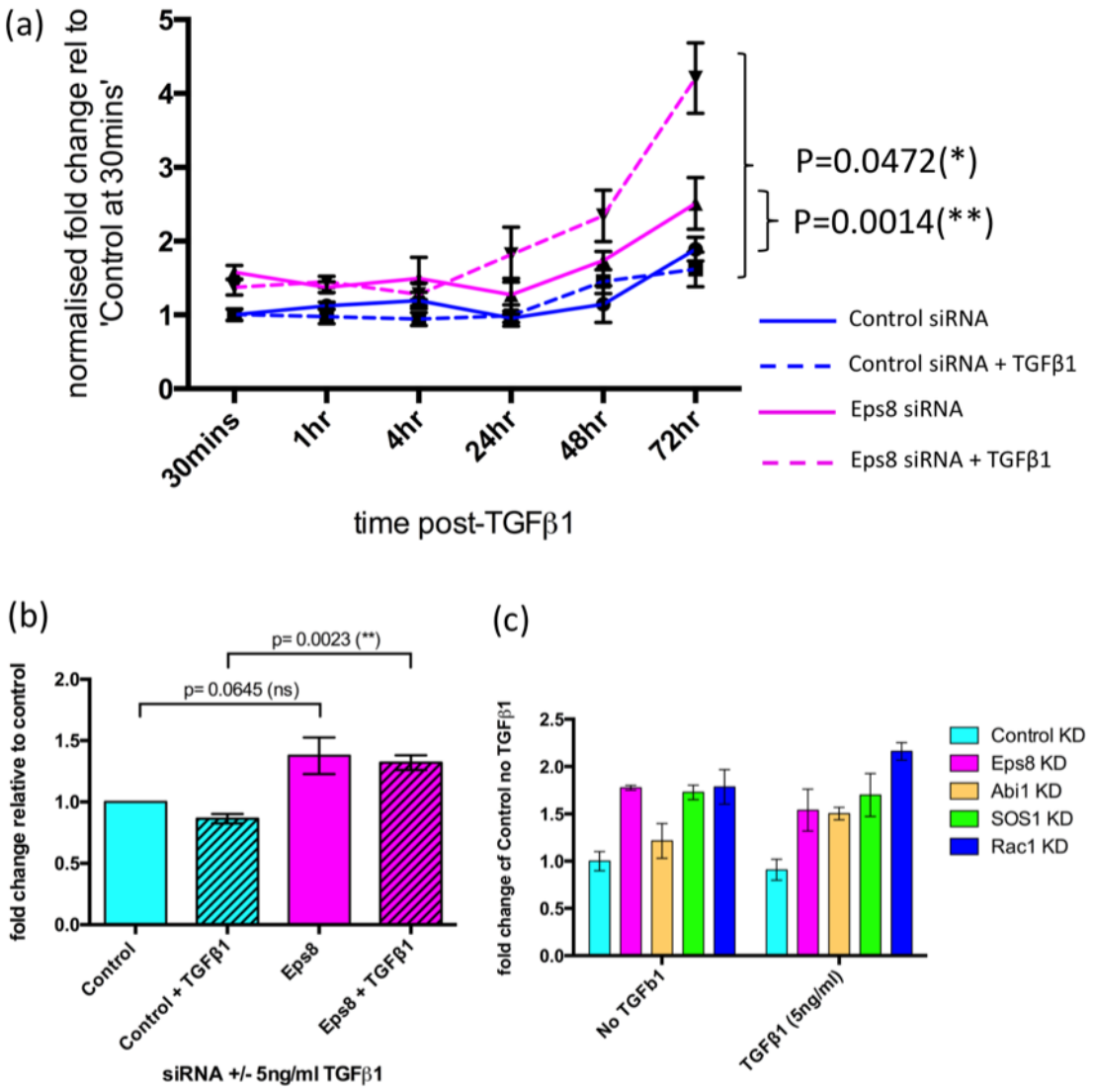

Figure 5-3 Knockdown of Eps8, tricomplex members or Rac1result in increased SMAD2 mRNA expression

(a) HFFF2 fibroblasts were transfected with control / Eps8 siRNA and after 24h medium was replaced with serum-free DMEM +/- 2ng/ml TGFβ1. At the time points shown after switching media, RNA was extracted and analysed for SMAD2 by qRT-PCR. Fold change of SMAD2, normalised against GAPDH, is graphed for each condition relative to the control-transfected, TGFβ1-untreated condition at 30min. Error bars indicate SD of three technical replicates. P values result from paired 2-tailed t-tests. (b) HFFF2 fibroblasts were transfected with control or Eps8 siRNA and changed to serum-free DMEM +/- TGFβ1 (5ng/ml) after 24h for 72h. RNA was extracted and analysed using qRT-PCR. The mean normalised fold change of SMAD2 relative to the control transfected, TGFβ1-untreated condition is displayed from three independent experiments. Error bars represent SEM of the data. T-tests were performed with significance level set at 5%. (c) HFFF2 were transfected with non-targeting / Eps8 / Abi1 / SOS1 or Rac1 siRNA and after 24h medium was replaced with SFM +/- TGFβ1 (5ng/ml) for 72h. RNA was extracted, and analysed for SMAD2. Normalisation against GAPDH was performed and relative fold change is

displayed against the control-transfected TGFβ1-untreated condition. Error bars indicate the SD of 3 technical replicates.

Although we have previously indicated that SMAD3 protein expression was not greatly altered by Eps8 knockdown in the absence of TGFβ1 treatment (section 5.1.2), we sought to confirm this finding at the mRNA level and used RNA from the time course experiment in figure 5-3(a). In figure 5-4 we can see that until 48h after media change to serum-free media (ie 72h post transfection) there is no observable difference between SMAD3 mRNA levels in control vs Eps8 knockdown conditions. In both conditions that received TGFβ1 treatment it can be seen that following 4 hours of TGFβ1 treatment a clear temporary reduction in SMAD3 expression develops. This negative feedback loop of SMAD3 expression as a result of TGFβ stimulation is supported by the published findings of others (Zhao & Geverd 2002), and the associated depression of total SMAD3 protein levels is visible in figure 5-2. Eps8 knockdown increases TGFβ1-dependent suppression of SMAD3 at the protein level (figure 5-2), and augments slightly the suppression of SMAD3 mRNA levels induced by TGFβ1 treatment (figure 5-4). This is also supported by later data in figure 6-2.

Activation of the TGFβ receptor results in phosphorylation of SMAD2 and SMAD3, their binding to SMAD4, and subsequent translocation of the complex to the nucleus effecting changes in gene expression (Massagué 2012). Because of the crucial role of SMAD4 in canonical TGFβ signalling we also investigated the effect of Eps8 downregulation on SMAD4 mRNA expression. As shown in figure 5-4 we observed no marked change in its expression as a result of either Eps8 knockdown or TGFβ1 treatment. Although this experiment has only been performed once, it is additionally supported by the findings of the independent RNA-seq experiment, with data shown in figure 6-2.

We also investigated the expression patterns of the inhibitory SMADs: SMAD6 & SMAD7. SMAD7 is recognised as having the most important inhibitory influence on TGFβ signalling, enabling negative feedback in response to TGFβ (Nakao et al. 1997). We can see from the single experiment in figure 5-4 that in the absence of TGFβ1 treatment (solid lines), Eps8 knockdown has no detectable effect on fibroblast SMAD7 expression compared to control transfected fibroblasts. In response to TGFβ1 treatment control-transfected fibroblasts respond by increasing SMAD7 expression, which peaks between 1

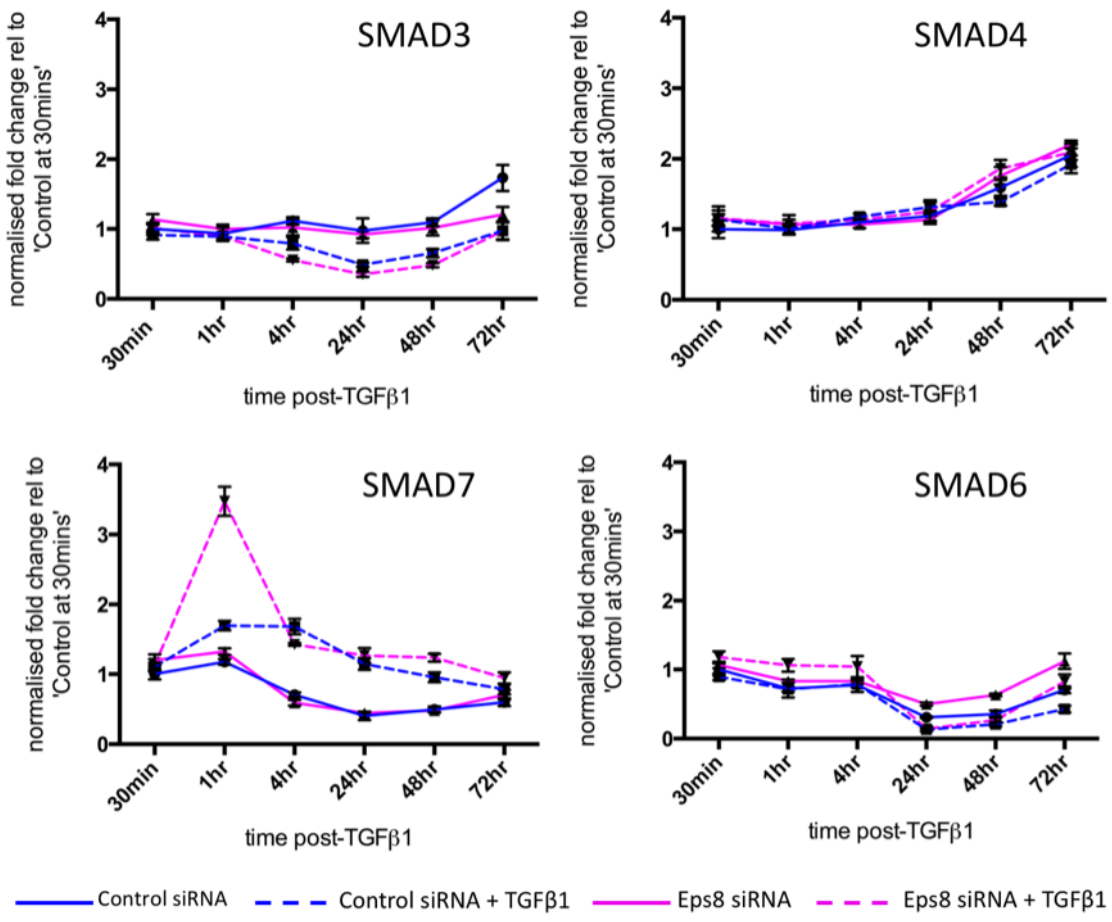

Figure 5-4 Eps8 knockdown has no effect on the expression of SMAD3, 4, 6 or 7 mRNA but augments TGFβ1-induced SMAD7 mRNA expression.

HFFF2 fibroblasts were transfected with control / Eps8 siRNA and after 24hrs were switched to serum-free DMEM +/- 2ng/ml TGFβ1. At the time points shown post TGFβ1 treatment, fibroblasts were harvested and RNA extracted and analysed by qRT-PCR. Expression of SMADs is graphed as fold change, normalised to GAPDH, and relative to the expression within fibroblasts transfected with non-targeting siRNA, 30mins after changing to serum-free medium. Error bars indicate SD of three technical replicates, from a single experiment.

and 4h post treatment, consistent with the literature (Nakao et al. 1997). When Eps8-transfected fibroblasts were treated with TGFβ1, the quantity of induced SMAD7 at least doubled compared to that in control-transfected fibroblasts. Given that we have demonstrated an augmentation of SMAD2 expression as a result of Eps8 knockdown, and have observed that TGFβ1 stimulation results in elevated canonical signalling via phosphorylated SMAD2, it is logical that this would induce a greater negative feedback signal by augmenting TGFβ-induced SMAD7 induction. This experiment does however require further repetition to substantiate these observations.

SMAD6 is a less potent inhibitor of canonical TGFβ signalling than SMAD7 (Miyazono 2000) and we observe no marked difference in its mRNA expression levels in response to either Eps8 knockdown or TGFβ1 treatment.

Overall we can conclude that Eps8 knockdown results in an upregulation of SMAD2 protein levels, sensitising fibroblasts to TGFβ stimulation, and resulting in increased SMAD2 phosphorylation as a result of TGFβ1 signalling. The increased SMAD2 protein levels are at least partially accounted for by increased expression of SMAD2 mRNA, which remains elevated compared to controls for at least 96h after Eps8 transfection. Our results indicate that Eps8 knockdown augments TGFβ signalling by modulation of SMAD2 expression while SMAD3 and 4 levels are unchanged as a result of Eps8 knockdown. Initial experiments indicate that basal levels of the inhibitory SMADs 6 & 7 do not appear to be modulated by Eps8 knockdown but the augmentation of TGFβ signalling by Eps8 knockdown results in greater induction of SMAD7 expression in response to TGFβ1, providing greater negative feedback. It appears that in resting fibroblasts maintenance of Eps8 expression limits SMAD2 expression and thus the sensitivity of the canonical signalling pathway to TGFβ.

5.1.4 SMAD2 expression in human Head & Neck Cancer stroma

Using cores of tissue from microarrays of human head & neck cancer we have previously observed diminished Eps8 immunohistochemical staining in myofibroblast-rich compared to myofibroblast deplete stroma (section 3.1.3). Meanwhile, we have demonstrated *in vitro* that Eps8 downregulation occurs early in the process of fibroblast transdifferentiation and that knockdown of Eps8 increases SMAD2 expression, augmenting TGFβ1-induced SMAD2 phosphorylation. Eps8 knockdown also results in augmentation of TGFβ1-induced ACTA2 and αSMA expression, stress fibre formation and functional contractility. Given the *in vitro* evidence of SMAD2 upregulation by Eps8 knockdown it was important to assess whether SMAD2 expression was

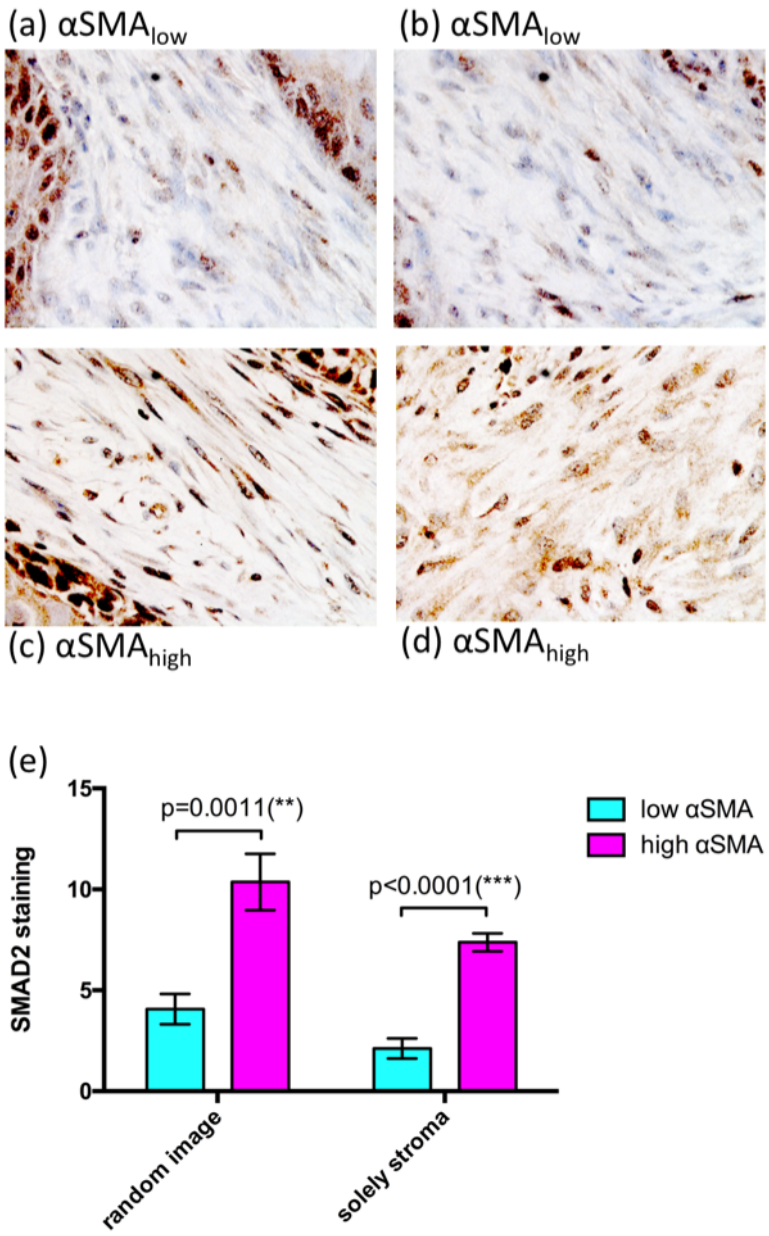

Figure 5-5 In human head & neck cancers stromal SMAD2 protein expression is greater with tumours with marked associated myofibroblast transdifferentiation

Cores from TMAs of human oral cancers underwent SMAD2 immunohistochemical staining, image-capture and analysis using Image J. 9 cores were chosen with low stromal αSMA expression to compare with 9 with high αSMA expression. Images were taken from randomly selected areas of the slide. If an image contained non-stromal tissue both the whole image and stroma-only area were analysed. Sample images of SMAD2 immunohistochemical staining are shown for stroma with (a-b) low and (c-d) high αSMA expression (x400). (e) SMAD2 staining density is displayed in low versus high αSMA cohorts comparing both whole images (left two bars) and stroma-only areas (right two bars). Means and SD of the data are shown with results of unpaired t-tests between groups.

also upregulated *in vivo* in myofibroblast-rich, Eps8-deplete stromal areas of head and neck cancers.

Figure 5-5 demonstrates that images randomly taken from cores of human oral cancer demonstrate greater SMAD2 staining when cores have high αSMA staining than when they have low αSMA staining. This difference was highly statistically significant. Furthermore, when images were selected to only include stromal tissue the difference between SMAD2 staining in αSMA high versus low groups became even more pronounced.

This data demonstrates that myofibroblast-rich tumour stroma, which we previously indicated displays reduced Eps8 expression, expresses greater levels of SMAD2 than myofibroblast-deplete stroma. This provides supportive evidence that Eps8 knockdown results in elevated SMAD2 expression and indicates that this is the case *in vivo* as demonstrated *in vitro*.

5.1.5 Eps8 knockdown augments TGFβ1-induced NOX4 and αSMA expression

NOX4 is known to be upregulated by TGFβ1 (Barnes & Gorin 2011) and its expression has been shown to be elevated in a number of fibrotic conditions (Amara et al. 2010). Indeed it has been shown to drive myofibroblastic differentiation in a number of organ systems (Cucoranu et al. 2005; Bondi et al. 2010; Amara et al. 2010; Jiang et al. 2012). Our group has recently demonstrated that NOX4 induction, as a result of TGFβ1 treatment, is responsible for a peak in reactive oxygen species and that inhibiting the induction of NOX4 can prevent αSMA induction and fibroblast-to-myofibroblast transdifferentiation (Mellone et al. 2016). Given the augmentation in TGFβ1 signalling that we have observed as a result of Eps8 knockdown we decided to investigate to what extent this was dependent on NOX4 induction.

Initially we examined NOX4 and ACTA2 mRNA expression in a time course experiment. In response to TGFβ1treatment, we observed that NOX4 induction (Figure 5-6b) preceded ACTA2 induction (Figure 5-6a), consistent with our knowledge of the role of NOX4 in ACTA2 expression. In addition, we observed that Eps8 knockdown resulted in an augmentation of NOX4 as well as ACTA2 induction in response to TGFβ1. This augmentation of NOX4 expression was also observed at the protein level (figure 5-6c). Given the documented role of

NOX4 in ACTA2 induction these results suggested that Eps8 knockdown might augment αSMA induction at least partly via a NOX4-dependent mechanism.

In order to assess the role of NOX4 in this process, in a preliminary experiment we used a novel small molecule inhibitor of NOX4, GKT137831 (Genkyotex), immediately post-transfection to assess whether this abrogated the effect of Eps8 knockdown on αSMA induction by TGFβ1. HFFF2 fibroblasts were transfected with control or Eps8 siRNA and, before the addition of serum at 4h, GKT137831 at a final concentration of 20μM was added to the medium. When medium was replaced with serum-free DMEM the next day the GKT137831 was refreshed. After a further 48h the cells were lysed and processed for Western blotting.

As shown in Figure 5-6d, GKT13781 had no effect on αSMA expression in the absence of TGFβ1 treatment, suggesting that there was negligible NOX4-dependent αSMA expression in the absence of TGFβ1. However, TGFβ1-induced αSMA expression was almost completely abrogated by the use of GKT13781, confirming previous results from our laboratory that NOX4 is indeed responsible for a significant proportion of TGFβ1-induced myofibroblast transdifferentiation. Eps8 knockdown, in the absence of TGFβ1, produced a slight induction of αSMA expression, as we have shown previously, but this was not reduced by GKT13781 suggesting that it is NOX4-independent. The augmenting effect of Eps8 knockdown on TGFβ1-induced αSMA expression however was partially reduced by the NOX4 inhibitor GKT13781. While this experiment requires further repetition to confirm the results, they suggest that while TGFβ-induced augmentation of αSMA expression is NOX4-dependent, at least some of the effect of Eps8 knockdown to induce αSMA expression occurs via NOX4-independent mechanisms.

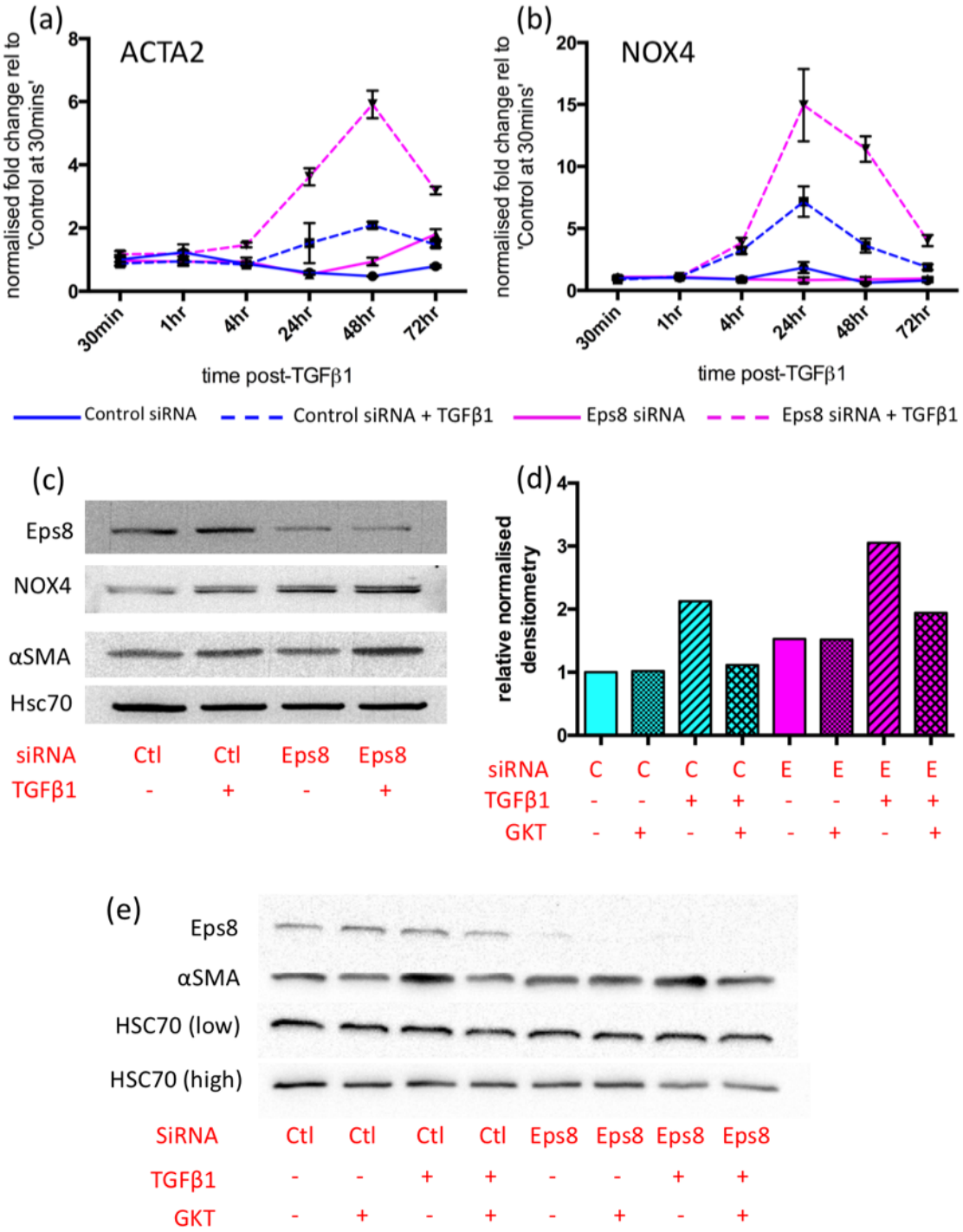

Figure 5-6 Eps8 knockdown augments NOX4 induction by TGFβ1

(a–b) cDNA that had been analysed for SMAD expression in figures 5-3(a) and 5-4 was analysed for NOX4 and ACTA2 expression. Error bars represent SD of three technical repeats at each time point. (c) HFFF2 were transfected with non-targeting / Eps8 siRNA and after 24h media was changed to serum-free media with / without added TGFβ1for 48h. Hsc70 was used as a loading control. (d-e) GKT137831, a NOX4 inhibitor, was used to assess the dependency of the Eps8 knockdown effect on the NOX4 signal. HFFF2 were transfected with control / Eps8 siRNA and after 4h were treated with or without 20μM GKT13781 prior to the addition of serum. GKT13781

was replenished when the medium was changed to serum-free DMEM +/- TGFβ1 after 24h. After a further 48h the cells were lysed and processed using Hsc70 as a loading control. Densitometry was performed and normalised against Hsc70.

5.1.6 Discussion

Results from preceding chapters have demonstrated that maintained expression of the tricomplex members Eps8, Abi1 and SOS1 and their downstream target Rac1 limits the ability of TGFβ1 to induce αSMA expression and myofibroblast transdifferentiation.

In the absence of TGFβ1 treatment, downregulation of tricomplex members results in a small increase in myofibroblast transdifferentiation. In this chapter, initial results indicate that almost all of this increase is dependent on signalling through TGFβR1, and that Eps8 and possibly also the tricomplex partners may minimise myofibroblast transdifferentiation via an effect on TGFβ receptor-dependent signalling. Variability in the extent of autocrine fibroblast TGFβ secretion between different batches or passages of HFFF2, or variation in the concentration of TGFβ1 in the serum added following transfection is likely to account for the variability between experiments in the extent of transdifferentiation in the absence of exogenous TGFβ1.

One of our co-workers identified that Eps8 knockdown produces a shift in the ratio of surface integrins, and it is possible that this might affect fibroblasts' ability to activate latent TGFβ, bound to the extracellular matrix. To test the hypothesis that Eps8 knockdown, in the absence of exogenous TGFβ1, generates the small increase in αSMA expression via this method, we performed a TGFβ activation assay in Eps8 knockdown versus control HFFF2 fibroblasts. We discovered, by analysis of 4 independent experiments, that Eps8 siRNA-transfected fibroblasts activated (via secretion or tension-mediated activation) no more TGFβ than control-transfected fibroblasts (appendix C figure 6-23). This supports the hypothesis that Eps8 knockdown primarily sensitises fibroblasts to TGFβ signalling by a mechanism at, or downstream of, the TGFβ receptor.

TGFβ receptors have been shown to interact with a number of downstream signalling pathways (Mu et al. 2012) but the bulk of the signal via the TGFβR1/R2 heterodimer is mediated via the canonical signalling pathway. This

requires phosphorylation of SMAD2 and SMAD3, their formation of a hetero-oligomer with SMAD4 and their subsequent translocation to the nucleus to regulate SMAD-dependent transcription (Massagué 2012). Given the dependence we had observed of Eps8 knockdown-induced myofibroblast transdifferentiation on TGFβ signalling we decided to investigate whether the mechanism involved upregulation of SMAD-dependent signalling.

Our results confirm that Eps8 knockdown increases SMAD2 mRNA and protein expression and, in response to TGFβ1, subsequent production of phosphorylated SMAD2. Although it is evident from our qRT-PCR data that the increase in SMAD2 protein is at least partially a consequence of upregulated mRNA transcription we have yet to assess whether modulation of protein degradation also contributes to the observed increase in protein levels. Given that this has been observed as an additional mechanism of regulation of SMAD3 levels (Poncelet et al. 2007) this would be an interesting avenue for further investigation.

The role of Eps8 as an inhibitor of the canonical TGFβ signalling is not previously described and is, therefore, a completely novel observation. Although not directly relevant for the subject of this thesis, our group also looked more widely at the effect of Eps8 on SMAD2 expression in pancreatic cell lines, as a result of the fibroblast observations described above, and confirmed that the same effect of Eps8 on SMAD2 mRNA and protein expression was observed in two pancreatic cancer cell lines (appendix C figure 6-24). Given that these results were observed in cells of completely independent origin this suggests that the regulatory mechanism of Eps8 on TGFβ signalling may be conserved across cell types, and such conservation is normally reserved for functionally important mechanisms.

In contrast to our findings with SMAD2, total SMAD3 levels appear unaffected by Eps8 knockdown. They do however reduce within 24h of TGFβ1stimulation, an observation that is additionally supported by RNAseq data generated by our group (appendix C figure 6-25) and the published work of others (Poncelet et al. 2007; Zhao & Geverd 2002). Poncelet and co-workers observed an increase in SMAD3 protein degradation and a reduction in SMAD3 mRNA expression in mesangial cells in response to 24h of TGFβ1 treatment, with no observed change in the levels of SMAD2 or SMAD4. Zhao demonstrated downregulation

of SMAD3 mRNA expression in lung fibroblasts in response to TGFβ1 *in vitro*, and also *in vivo* using a bleomycin-induced model of pulmonary fibrosis. Interestingly, our qRT-PCR results (and later RNA-seq data in figure 6-2) suggest that Eps8 knockdown slightly augments the TGFβ1-induced reduction in SMAD3 mRNA expression. If the TGFβ-induced reduction in SMAD3 expression acts to provide a negative feedback loop on canonical TGFβ signalling, as proposed by others (Zhao & Geverd 2002), the increased suppression following Eps8 knockdown provides further support that SMAD2 upregulation carries an augmented signal through the canonical TGFβ pathway.

A number of studies have suggested that SMAD2 and SMAD3 have distinct transcriptional roles in the fibroblast. SMAD2 knockouts, unlike SMAD3 knockouts are embryonically lethal in mice (Brown et al. 2007), and SMAD2 has been shown to be necessary for TGFβ1-induced PAI-1 and MMP2 expression in mouse fibroblasts (Piek et al. 2001). Reduction of SMAD2 phosphorylation and translocation to the nucleus has been shown to result in reduced expression of αSMA and pro-collagen in NIH3T3 mouse fibroblasts (Lim et al. 2014), consistent with our findings of SMAD2 upregulation being associated with increased αSMA expression. However one author, using SMAD2 and SMAD3 expression plasmids in fetal lung fibroblasts, found that overexpression of SMAD3 but not SMAD2 resulted in increased αSMA expression (Gu et al. 2007).

Some authors have suggested that SMAD3 essentially relays the core canonical signal while SMAD2 provides regulatory modulation (Brown et al. 2007; Yang et al. 2003). Studies using SMAD2 or SMAD3-deficient mouse fibroblasts have indicated that SMAD3 is necessary for TGFβ1 auto-activation and the expression of some pro-fibrotic genes, but SMAD2 knockout mice also demonstrate a blunted response to TGFβ1 stimulation (Piek et al. 2001; Flanders 2004). In our experiments, we have provided supporting evidence that elevated SMAD2 levels, resulting from Eps8 downregulation, are associated with increased expression of the TGFβ-induced profibrotic genes ACTA2 and COL1A1, as well as an augmentation of TGFβ-induced negative feedback via SMAD7 expression. SMAD3 expression, which may be required at a basal level to permissively transmit the canonical signal, is not modulated by Eps8 downregulation in our experiments.

SMAD4 expression is known to be modulated by MAPK signalling in some cell types providing cross-talk between the signalling pathways. In intestinal epithelial cells oncogenic Ras reduces SMAD4 expression, reducing SMAD complex formation and TGFβ-dependent protein expression (Saha et al. 2001). Given that Abi1 (via tricomplex formation) competes with Grb2 to generate SOS1-dependent activation of Rac1 rather than Ras, we might expect knockdown of Eps8 or Abi1, and hence reduced tricomplex formation, to increase Grb2-SOS1 binding and Ras activation (Innocenti et al. 2002). If the same mechanism occurred in fibroblasts as intestinal epithelial cells this might act to reduce SMAD4 expression. In fibroblasts however, overexpression of Abi1 in NIH3T3/EGFR fibroblasts has been observed to increase EGFR-dependent Rac1 activation, but this did not affect EGF-induced Ras activation (Jenei et al. 2005) and in our experiments we have also shown no modulation of SMAD4 expression levels as a result of Eps8 downregulation. This suggests that in the fibroblast Rac activation does not affected Ras activation or result in a reduction in the expression of SMAD4.

SMAD7 mRNA expression is rapidly induced in response to TGFβ activation via the canonical signalling pathway (Nakao et al. 1997), due to SMAD complex activation of the SMAD7 promoter (Nagarajan et al. 1999). Increases in SMAD7 protein levels rapidly ensue. Consistent with this we observed an early induction in SMAD7 mRNA within an hour of TGFβ1 treatment. We also demonstrate that this induction is greatly augmented by prior Eps8 knockdown, but that Eps8 knockdown alone does not alter SMAD7 levels, albeit in a single time course experiment. Some authors have demonstrated that SMAD3 is required for TGFβ-induced SMAD7 upregulation (Nagarajan et al. 1999; Piek et al. 2001), but given our observation that Eps8 knockdown upregulates SMAD2 levels but not SMAD3 levels, our data suggests that SMAD2 levels also determine the extent of SMAD7 induction by TGFβ. SMAD7 resultantly acts at multiple points in the TGFβ pathway to provide negative feedback to signalling. In the nucleus SMAD7 interferes with DNA binding by the SMAD complex while in the cytoplasm it competes with receptor SMADs (2 & 3) for binding sites on the TGFβ receptor, reducing their subsequent activation (Emori et al. 2012). Additionally SMAD7 recruits SMURF2 to TGFβ receptors (Datta & Moses 2000) facilitating receptor ubiquitination and degradation, inhibiting ongoing TGFβ signalling.

In our time course experiment we observed, in response to TGFβ1, an increase in NOX4 expression emerging after 1 to 4h and peaking at approximately 24h, consistent with the work of my colleagues (Mellone et al. 2016). We know that NOX4 is an important mediator of fibroblast-to-myofibroblast transdifferentiation (Cucoranu et al. 2005; Bondi et al. 2010; Amara et al. 2010; Jiang et al. 2012) and that it increases canonical signalling by augmenting TGFβ-mediated phosphorylation of SMAD2/3 (Jiang et al. 2014; Cucoranu et al. 2005; Amara et al. 2010).

NOX4 is constitutively active and therefore its regulation is primarily at the transcriptional level (Serrander et al. 2007). Our results indicate that Eps8 knockdown does not in itself alter basal NOX4 expression but it does augment the induction of NOX4 expression observed in response to TGFβ. It appears that the augmentation of TGFβ signalling is responsible for amplification of NOX4 expression which, in turn, catalyses further SMAD phosphorylation and TGFβ1 signalling. It is plausible that the upregulation of SMAD2 expression by Eps8 knockdown sufficiently primes TGFβ1 signalling to trigger this amplification cascade via NOX4.

In order to assess the relative contribution of NOX4 to the Eps8 knockdown-induced augmentation of TGFβ1 signalling we used the NOX4 inhibitor GKT137831 (Genkyotex) to inhibit TGFβ1-induced NOX4 expression. We observed that in control transfected fibroblasts GKT137831 prevented almost all αSMA expression in response to TGFβ1. In the presence of Eps8 knockdown, while GKT137831 abrogated much of the TGFβ-induced increase in αSMA expression, a smaller proportion of αSMA expression remained suggesting that a degree of TGFβ1-induced αSMA expression was generated by NOX4-independent mechanisms. In this preliminary experiment, however, saturation of GKT137831 could not be excluded and this will need to be addressed in future experiments by the use of an additional group subjected to a higher concentration of GKT137831. This initial experiment has only been performed once, but the results are consistent with previous results in our group using GKT13781 on TGFβ1-treated fibroblasts.

Our group has also now accomplished generation of a stable knockdown of NOX4 in HFFF2 by viral transduction of NOX4 shRNA. It will be useful to repeat our experiments using these to assess whether, in the absence of NOX4, Eps8

knockdown results in augmented TGFβ signalling to any significant extent. This will obviate concerns regarding adequate dosing of the NOX4 inhibitor or dose timing issues. Although Eps8 clearly acts to limit SMAD2 expression, phosphorylation and NOX4 induction, regulating receptor SMAD phosphorylation and canonical signalling, it will be interesting to further assess whether Eps8 limits αSMA expression and myofibroblast transdifferentiation through other mechanisms, including the many other signalling pathways downstream of the TGFβ receptor (Mu et al. 2012).

5.1.7 Chapter Summary

In this chapter we have demonstrated a novel function of Eps8 as an inhibitor of SMAD2 transcription and protein expression. Eps8 also modulates TGFβ-induced NOX4 expression and perhaps thereby regulates its catalysis of receptor SMAD phosphorylation, the induction of pro-fibrotic genes, and subsequent myofibroblast transdifferentiation.

We have also provided evidence that this is clinically relevant *in vivo* using human head and neck cancer specimens. Not only did we assess that Eps8 was downregulated in cases of head and neck cancer with myofibroblast-rich stroma, but assessment of SMAD2 expression confirmed that this is significantly upregulated in such cases.

Given that we have demonstrated that TGFβ (produced by numerous cancers), several chemotherapeutic agents, and γ-irradiation all downregulate Eps8 expression in fibroblasts, the regulation of SMAD2 expression and TGFβ signalling by Eps8 is potentially extremely important for cancer biology and its treatment.

Chapter 6: Future Directions & Conclusions

6.1 Bioinformatics

We have demonstrated in the previous chapters that Eps8 has a previously unrecognised role in regulating fibroblast to myofibroblast transdifferentiation. Downregulation of Eps8 occurs early in the process of myofibroblast transdifferentiation (irrespective of the inducing agent), and the downregulation of Eps8 appears to augment transdifferentiation by a process involving upregulation of SMAD2 and sensitization of fibroblasts to TGFβ1.

In order to identify, for further study, potential mechanisms via which Eps8 regulates myofibroblast transdifferentiation, we performed RNA-seq analysis on HFFF2 fibroblasts that had undergone either Eps8 or non-targeting siRNA transfection, followed by 20 hours in serum-free media with/without the addition of 5ng/ml TGFβ1.

6.1.1 Quality control and validation against previous results

The quality of the output following sequence alignment was assessed prior to further data analysis (appendix D figures 6-26 to 6-37). A principal component analysis (PCA) plot of the data (figure 6-1(a)) demonstrates that each of the four conditions were cleanly separated, and the repeats with subsequent passages were generally tightly clustered to each other. Most of the variance between all samples was generated by TGFβ1 treatment alone (27%) as we might expect, while Eps8 downregulation alone accounted for a further 10%. As shown in figure 6-1(b) there was no significant effect of passage number on variation in gene expression with repeats in each condition clustering reasonably well. Additionally, when hierarchical clustering was performed across all the samples, considering all genes, the resultant dendrogram naturally separated between the sample conditions, and indicated that the greatest effect was due to TGFβ1(figure 6-1(c)). Finally, when heat maps were generated comparing the expression profiles of the 8000 most variant genes between samples, both in the absence (figure 6-1d) and presence of

TGFβ1(figure 6-1e) there was a clear differential between the expression profiles as a results of Eps8 knockdown.

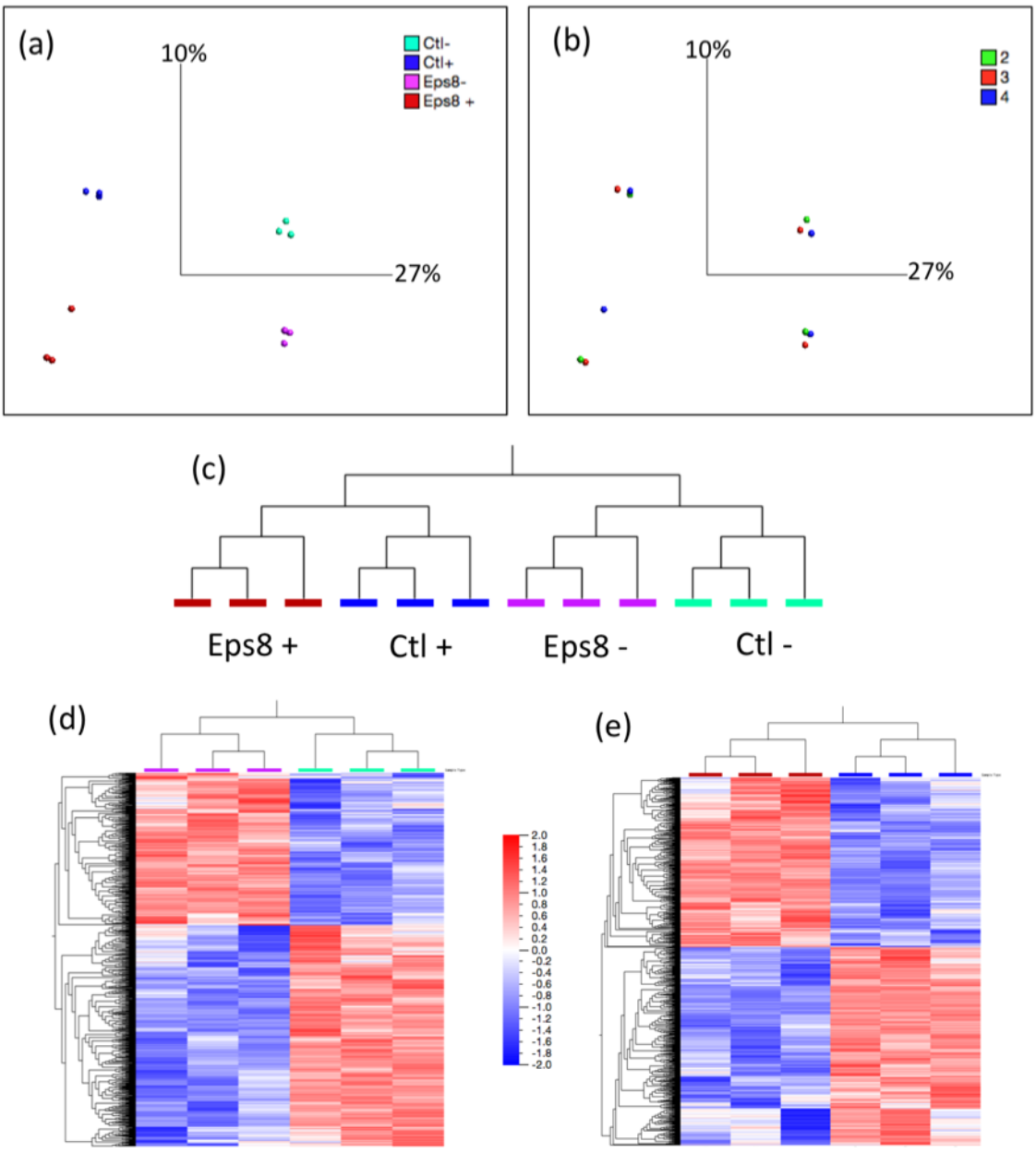

Figure 6-1 RNAseq data separates well between conditions and not experimental repeats

HFFF2 were transfected with Eps8 or non-targeting siRNA. After 4h medium was replaced with serum free DMEM +/- 5ng/ml TGFβ1. After 20h cells' RNA was extracted. Repeats were performed with two sequential passages of HFFF2 to generate 3 repeats per condition. RNAseq was performed and from normalised read counts for each condition PCA plots were generated using the top 8000 genes filtered by variance. (a) demonstrates that each of the 4 conditions separate well with the two defined variables: Eps8 knockdown and TGFβ1 treatment accounting for 37% of the variability between genes. (b) Passage number had minimal effect on variability of

gene expression. (c) A dendrogram using the top 8000 genes generated clean separation between treatment groups. (d-e) Heat maps of the 50 most variant genes between conditions comparing Control versus Eps8 KD in the absence (d) and presence (e) of TGFβ1.

(a)

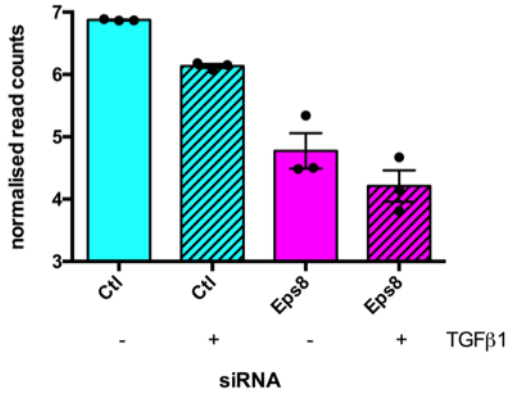

(b)

	Ctl- vs Ctl+	
	fold change	padj
ACTA2	3.51	0.00E+00
COL1A1	1.93	0.00E+00
CTGF	6.57	0.00E+00
EPS8	0.60	0.00E+00
ABI1	1.07	4.38E-01
SOS1	0.99	9.61E-01
RAC1	1.10	3.02E-02
EPS8L1	0.89	9.03E-01
EPS8L2	0.62	7.98E-10

(c)

	Ctl- vs Eps8-			Ctl+ vs Eps8+	
	fold change	padj		fold change	padj
SMAD2	1.69	7.82E-12	SMAD2	1.67	7.22E-11
SMAD3	0.9	1.90E-01	SMAD3	0.78	7.98E-03
SMAD4	1.01	9.98E-01	SMAD4	0.93	7.43E-01
SMAD6	1.22	6.54E-01	SMAD6	1.31	7.07E-01
SMAD7	0.95	8.86E-01	SMAD7	1.3	9.12E-04
NOX4	1.02	9.98E-01	NOX4	1.67	6.41E-05
EPS8	0.23	1.86E-10	EPS8	0.26	8.58E-13
EPS8L1	1.24	8.74E-01	EPS8L1	0.57	8.17E-01
EPS8L2	1.1	4.26E-01	EPS8L2	1.08	7.08E-01

Figure 6-2 RNA-seq data correlates with previous data

(a) VST-normalised read counts were plotted for Eps8 expression in each condition. (b) mRNA fold change resulting from TGFβ1 treatment in a selection of genes of interest. (c) DESeq differential gene expression resulting from Eps8 knockdown compared to controls both in the absence and the presence of TGFβ1. Fold change and adjusted p values are displayed.

We then sought to validate the RNAseq output against results that we have reported in previous chapters. As shown in figure 6-2(a), Eps8 mRNA was downregulated within 20h as a result of TGFβ1 treatment, confirming the data previously displayed in figures 3-3 and 3-8(d). It was also effectively downregulated by the use of Eps8 siRNA, confirming that the transfection of Eps8 siRNA had been effective. Figure 6-2(b) validates the RNA-seq results

against data that we have observed in other experiments. Although the time point is a shorter than for our groups' previous RNAseq experiment (figure 3-1(a)) we still observe upregulation of ACTA2, COL1A1 and CTGF mRNA, confirming that the fibroblasts, in response to TGFβ1, were producing a myofibroblastic expression profile. Furthermore, treated cells that we ran in parallel during the experiment and harvested for western blotting 72h after TGFβ1 treatment (appendix D figure 6-38) displayed protein profiles in keeping with previous experiments. This reassures us that early changes seen in the RNAseq data resulting from Eps8 knockdown preceded an enhanced myofibroblast phenotype in *this* experiment.

Figure 6-2(b) also confirms that, as in our previous experiments, TGFβ1 does not significantly alter Abi1 or SOS1 mRNA expression (appendix B figure 6-19). A small increase in Rac1 expression was observed in response to TGFβ1 treatment but this was markedly less statistically significant than the other changes and may not be biologically significant. TGFβ1additionally downregulated the expression of Eps8L2, while Eps8L1 remained unchanged suggesting that the downregulation of Eps8 is not compensated by an increase in expression of either of these other family members.

In figure 6-2(c) we demonstrate that the RNA-seq data also supports our previous qRT-PCR data from previous chapters. As in figures 5-3 and 5-4, Eps8 downregulation increases SMAD2 expression but has no effect on SMAD3/4/6/7 in the absence of TGFβ1. Eps8 knockdown also augments TGFβ1-induced suppression of SMAD3 and induction of SMAD7 expression. The RNA-seq data also supports our observation, using qRT-PCR and western blotting, that Eps8 knockdown augments TGFβ1-induced NOX4 induction (figure 5-6). The expression of the other Eps8 family members, Eps8L1 and Eps8L2 are unchanged as a result of Eps8 downregulation indicating that their expression is not upregulated to functionally compensate for Eps8.

6.1.2 New Insights into SMAD2 signalling

We have observed that Eps8 downregulation results in an upregulation of SMAD2 expression and increased generation of c-terminal phosphorylated SMAD2 (ser465/7) in response to TGFβ1(figures 5-2 and 5-3). We know that SMAD2 signalling is regulated by a number of factors including TGFβ receptor

degradation; receptor-SMAD linker phosphorylation and subsequent ubiquitin ligase-mediated degradation; and nuclear SMAD complex disruption (Kavsak et al. 2000; Gao et al. 2009; Stroschein 1999; Lönn et al. 2010). Analysis of the

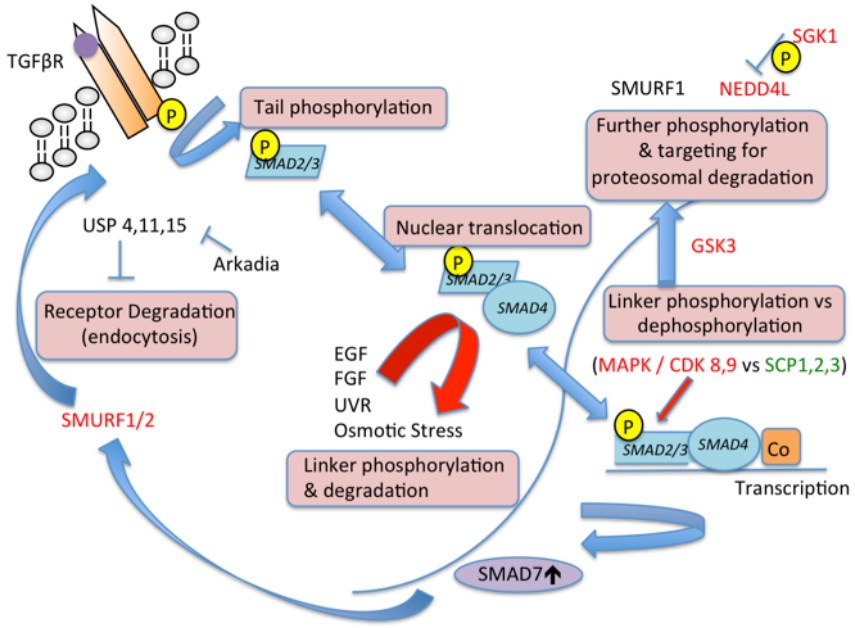

	Ctl- vs Eps8-		Ctl+ vs Eps8+		
	fold change	padj		fold change	padj
MAPK1	0.93	4.86E-01	MAPK1	0.96	8.06E-01
MAPK3	2.05	0.00E+00	MAPK3	1.91	0.00E+00
MAP3K1/MEKK-1	1.05	9.29E-01	MAP3K1/MEKK-1	0.93	8.95E-01
CDK4	0.86	1.62E-01	CDK4	0.81	6.01E-03
CDK8	1.02	9.79E-01	CDK8	0.91	8.43E-01
CDK9	0.92	7.04E-01	CDK9	0.9	6.09E-01
YAP1	0.83	3.11E-04	YAP1	0.89	6.81E-02
GSK3B	0.93	5.92E-01	GSK3B	0.92	5.63E-01
NEDD4L	0.83	1.71E-02	NEDD4L	0.72	6.51E-04
SGK1	0.98	9.57E-01	SGK1	1.16	1.81E-01
PARP1	0.99	9.91E-01	PARP1	0.93	7.13E-01
SKIL	0.99	9.92E-01	SKIL	1.31	7.27E-04
SKI	0.93	4.77E-01	SKI	0.94	5.69E-01

Figure 6-3 RNA-seq data related to SMAD2 regulation

The table displays fold change and adjusted p values for mRNA of the identified genes in response to Eps8 knockdown, both in the absence (-) and presence (+) of TGFβ1. The expression of genes highlighted in green was significantly affected by Eps8 knockdown in both conditions, while those in blue were only affected by Eps8 knockdown in the presence of TGFβ1. Genes in white were not significantly altered by Eps8 knockdown.

RNA-seq data indicates that the expression of CDK4/8/9, MEKK-1, and MAPK1 (ERK2) does not significantly alter as a result of Eps8 knockdown. MAPK3 (ERK1) is significantly upregulated by Eps8 knockdown in both the absence and presence of TGFβ1, but this is unlikely to account for the observed increase in SMAD2 expression and phosphorylation, since linker phosphorylation by ERK1 is known to inhibit SMAD2 phosphorylation, and help to target the protein for degradation (Kretzschmar et al. 1999; Schievenbusch et al. 2009).

YAP is a transcriptional activator thought to interact with CDK8/9 linker-phosphorylated SMAD2 (Chen & Wang 2009) and although it was differentially expressed as a result of Eps8 knockdown, it was downregulated rather than upregulated. This also therefore does not help to explain the increased SMAD2 phosphorylation. SKIL codes for a nuclear repressor factor that binds to SMAD-responsive elements (Wu et al. 2002). It was only differentially expressed in response to Eps8 if TGFβ1 was also applied but the upregulation rather than downregulation of this repressor factor again cannot explain the observed effect of Eps8 knockdown on SMAD2 signalling.

Following linker phosphorylation, resulting in augmentation or inhibition of SMAD2's activity (depending on the agent and site of phosphorylation), further phosphorylation by GSK3β targets SMAD2 for ubiquitin ligase-mediated degradation by NEDD4L (Gao et al. 2009). Although GSK3β expression was not altered by Eps8 knockdown, NEDD4L levels were significantly downregulated both in the absence and presence of TGFβ1. If the reduction in mRNA levels translated into a similar reduction in NEDD4L protein levels, the resultant effective inhibition of SMAD2 degradation could account for the increase in both total and phosphorylated SMAD2 levels. We have subsequently acquired the NEDD4L antibody and this is an exciting avenue for further investigation.

While a reduction in degradation could account for an increase in SMAD2 protein levels, we also sought to assess whether any transcription factors associated with the SMAD2 promoter were differentially expressed as a result of Eps8 downregulation. The differentially expressed gene list ($p<0.05$) resulting from Eps8 knockdown in the absence of TGFβ1 was compared against lists of known transcription factors for the SMAD2 promoter from the Genecards and Qiagen databases (figure 6-4(a)).

(a)

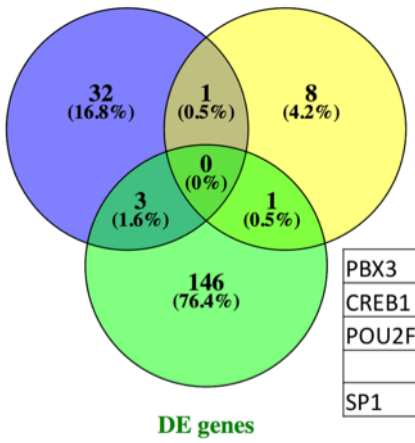

	no TGF		with TGF	
	fold change	adj p	fold change	adj p
PBX3	0.71	1.51E-06	0.80	4.98E-02
CREB1	0.82	4.62E-02	0.8	4.31E-02
POU2F2	0.41	0.00E+00	0.43	0.00E+00
SP1	0.70	7.12E-10	0.67	1.76E-11

(b)

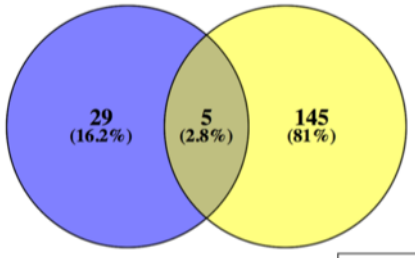

	no TGF		with TGF	
	fold change	adj p	fold change	adj p
YY1	0.82	8.11E-03	0.88	1.79E-01
JUND	1.18	5.37E-03	1.05	7.54E-01
IRF1	0.62	2.68E-03	0.54	1.26E-05
PTTG1	0.79	3.54E-04	0.76	2.35E-02
KLF13	0.46	1.52E-10	0.49	0.00E+00

Figure 6-4 Differentially expressed transcription factors with binding sites within SMAD2's promoter or enhancer sequences.

The list of differentially expressed genes ($p<0.05$) resulting from Eps8 knockdown in the absence of TGFβ1 were screened for transcription factor function, identifying 150 candidates. This list was then compared with known transcription factor binding sites on the (a) SMAD2 promoter sequence (Genecards and Qiagen) or (b) the principal enhancer sequence housed on the Genecards website. Transcription factors common with at least one database are shown in the table with their fold change resulting from Eps8 knockdown both in the absence and presence of TGFβ1.

Out of the 150 candidate differentially-expressed transcription factors, binding sites for 3 were present in the SMAD2 promoter sequence on the Genecards database while one was present on the Qiagen database. Pre-B-Cell leukaemia homeobox 3, CAMP responsive element binding protein 1, POU2 class homeobox 2, and SP1 transcription factors all lie in the promoter sequence of SMAD2 and were downregulated as a result of Eps8 knockdown. We similarly

assessed the main enhancer region associated with the SMAD2 promoter using the GeneHancer database within Genecards. Although 5 transcription factors with known binding sites in this region were differentially expressed as a result of Eps8 knockdown in the absence of TGFβ1, 2 of these lost differential expression in the presence of TGFβ1. IRF1, PTTG1 and KLF13 would therefore be worthy of early investigation, with the larger fold change and greatest statistical significance attached to KLF13.

6.1.3 Wider analysis of the mechanism of regulation of myofibroblast transdifferentiation by Eps8

Firstly, using the normalised gene read counts for Eps8 knockdown and control samples in the absence of TGFβ1 we generated a heat map of the 50 most variant genes with Qlucore software. As demonstrated in figure 6-5 there was a clear differential between conditions and hierarchical clustering between experimental repeats indicating that these genes were consistently differentially expressed as a result of Eps8 downregulation. It can be seen that the bulk of the differentially expressed genes were down rather than upregulated as a result of Eps8 knockdown.

The 50 genes are then displayed in figure 6-6. Genes were highlighted in green if their recognised function and the direction of their change in expression (up/down regulated) were consistent with augmentation of the myofibroblast phenotype. Growth differentiation factor 11 (GDF11) codes for BMP 11, a member of the TGFβ receptor superfamily and could be involved in modifying the transduction of the signal from applied TGFβ1. Interestingly, TGFBR2, coding for the TGFβR2 subunit which contributes to the canonical signal receptor complex, was downregulated as a result of Eps8 knockdown but expression of the mRNA of the TGFβR1subunit was significantly upregulated. It may be the case that altering the balance of the receptor subunits modulates signal transmission (Bandyopadhyay et al. 2011). Transmembrane protein 184B (TMEM184B), upregulated in our heat map, is little understood but

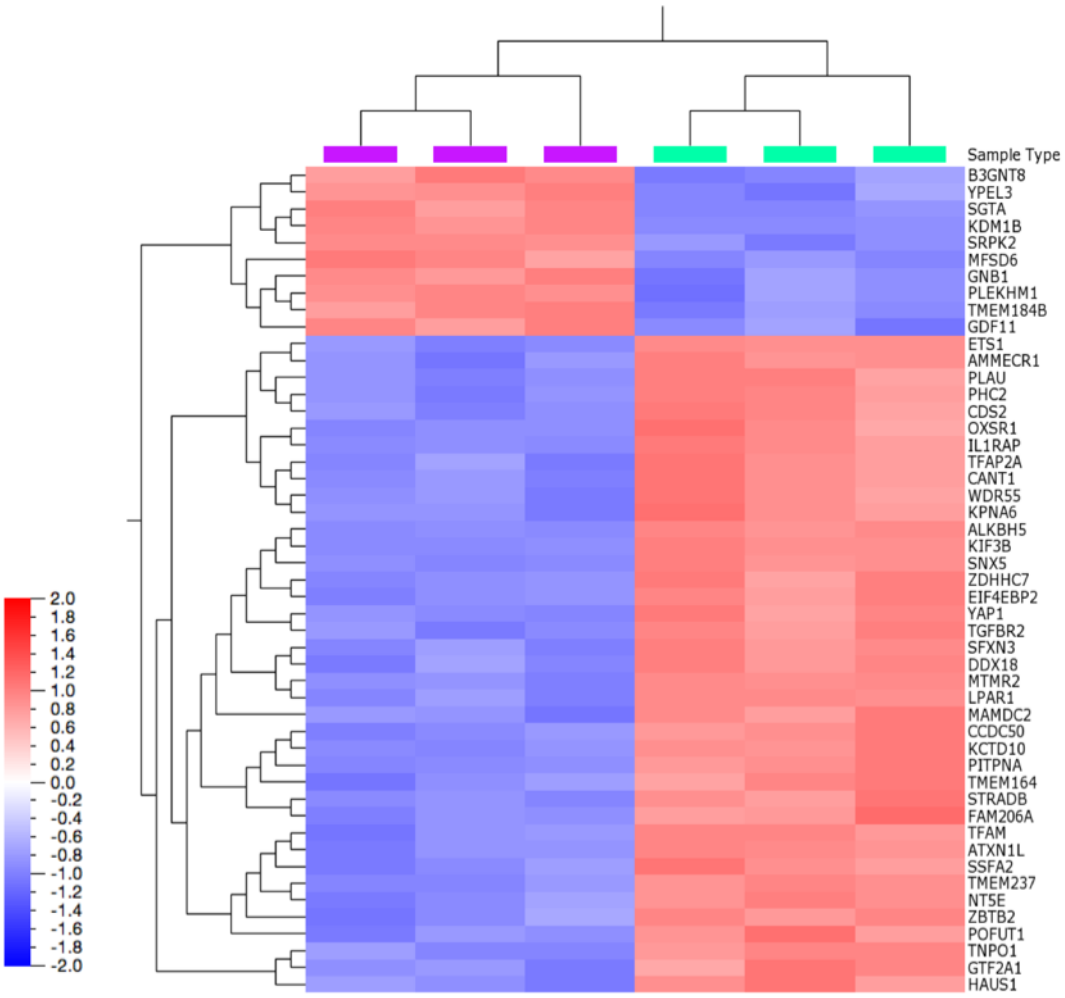

Figure 6-5 Heat Map with hierarchical clustering of 50 most variant genes resulting from Eps8 knockdown in the absence of TGFβ1.

Qlucore-derived heat map filtered to the top 50 genes with the most variant expression. The FDR-adjusted p-value threshold was decreased to limit the gene list from the filtered 8000 to the top 50 most variant genes. Eps8 knockdown samples are labelled with magenta bars and control samples with turquoise labels.

thought to potentially activate MAPK signalling and so also may be worthy of further study. MAPK signalling is known to both enhance and inhibit TGFβ signalling. Oxidative stress responsive 1 (OXSR1) was downregulated as a result of Eps8 knockdown. It regulates kinases in response to environmental stress and is postulated to have a function in regulating the actin cytoskeleton which may be of relevance in the regulation of myofibroblast transdifferentiation. Eukaryotic translation initiation factor 4E binding protein 2 (EIF4EBP2) inhibits translation initiation, regulating protein translation by growth factors and other stimuli that signal through the MAP kinase and

GENE ID	GENE NAME	Log2fold change
B3GNT8	UDP-GlcNAc:BetaGal Beta-1,3-N-Acetylglucosaminyltransferase 8	1.3
MFSD6	Major Facilitator Superfamily Domain Containing 6	1.1
GDF11	Growth Differentiation Factor 11	0.9
PLEKHM1	Pleckstrin Homology And RUN Domain Containing M1	0.8
SRPK2	SRSF Protein Kinase 2	0.8
GNB1	G Protein Subunit Beta 1	0.8
SGTA	Small Glutamine Rich Tetratricopeptide Repeat Containing Alpha	0.7
TMEM184B	Transmembrane Protein 184B	0.7
KDM1B	Lysine Demethylase 1B	0.6
YPEL3	Yippee Like 3	0.5
ALKBH5	AlkB Homolog 5, RNA Demethylase	-0.3
YAP1	Yes Associated Protein 1	-0.3
PITPNA	Phosphatidylinositol Transfer Protein Alpha	-0.3
LPAR1	Lysophosphatidic Acid Receptor 1	-0.3
WDR55	WD Repeat Domain 55	-0.4
TNPO1	Transportin 1	-0.4
GTF2A1	General Transcription Factor IIA Subunit 1	-0.4
OXSR1	Oxidative Stress Responsive 1	-0.4
TFAP2A	Transcription Factor AP-2 Alpha	-0.4
POFUT1	Protein O-Fucosyltransferase 1	-0.4
CCDC50	Coiled-Coil Domain Containing 50	-0.4
ZDHHC7	Zinc Finger DHHC-Type Containing 7	-0.4
ZBTB2	Zinc Finger And BTB Domain Containing 2	-0.4
SSFA2	Sperm Specific Antigen 2	-0.4
KPNA6	Karyopherin Subunit Alpha 6	-0.5
EIF4EBP2	Eukaryotic Translation Initiation Factor 4E Binding Protein 2	-0.5
CDS2	CDP-Diacylglycerol Synthase 2	-0.5
CANT1	Calcium Activated Nucleotidase 1	-0.5
SFXN3	Sideroflexin 3	-0.5
KCTD10	Potassium Channel Tetramerization Domain Containing 10	-0.5
TMEM237	Transmembrane Protein 237	-0.6
SNX5	Sorting Nexin 5	-0.6
PHC2	Polyhomeotic Homolog 2	-0.6
TGFBR2	Transforming Growth Factor Beta Receptor 2	-0.7
FAM206A	Family With Sequence Similarity 206 Member A	-0.7
PLAU	Plasminogen Activator, Urokinase	-0.8
STRADB	STE20-Related Kinase Adaptor Beta	-0.8
MTMR2	Myotubularin Related Protein 2	-0.9
HAUS1	HAUS Augmin Like Complex Subunit 1	-0.9
TFAM	Transcription Factor A, Mitochondrial	-0.9
DDX18	DEAD-Box Helicase 18	-1.0
TMEM164	Transmembrane Protein 164	-1.0
ATXN1L	Ataxin 1 Like	-1.0
KIF3B	Kinesin Family Member 3B	-1.0
IL1RAP	Interleukin 1 Receptor Accessory Protein	-1.1
ETS1	ETS Proto-Oncogene 1, Transcription Factor	-1.2
MAMDC2	MAM Domain Containing 2	-1.4
AMMECR1	Alport Syndrome, Mental Retardation, Midface Hypoplasia And Elliptocytosis Chromosomal Region Gene 1	-1.4
NT5E	5'-Nucleotidase Ecto	-1.5

Figure 6-6 The 50 genes with the greatest variance across samples as a result of Eps8 knockdown in the absence of TGFβ1.

Log_2fold change displayed. Genes in red were also in the 50 most variant genes as a result of Eps8 knockdown in the presence of TGFβ1. Genes highlighted in green have known functions derived from Entrez gene and UniProtKB/Swiss-Prot that may be consistent with a role in sensitizing fibroblasts to myofibroblastic transdifferentiation.

mTORC1 pathways. It was also significantly downregulated in our heat map and may be responsible for priming cells in anticipation of TGFβ signalling. It also remains downregulated as a result of Eps8 knockdown in the presence of TGFβ1. Potassium Channel Tetramerization Domain Containing 10 (KCTD10) is an adapter protein for E3 ubiquitin ligases and so suppression of its expression may have a role in the downregulation of NEDD4L-mediated SMAD2 degradation. Finally, ETS Proto-Oncogene 1 is a transcription factor involved in the activation or repression of cytokine and chemokine genes in a variety of different cellular contexts, including senescence, and so will be interesting to study further in the context of Eps8 downregulation.

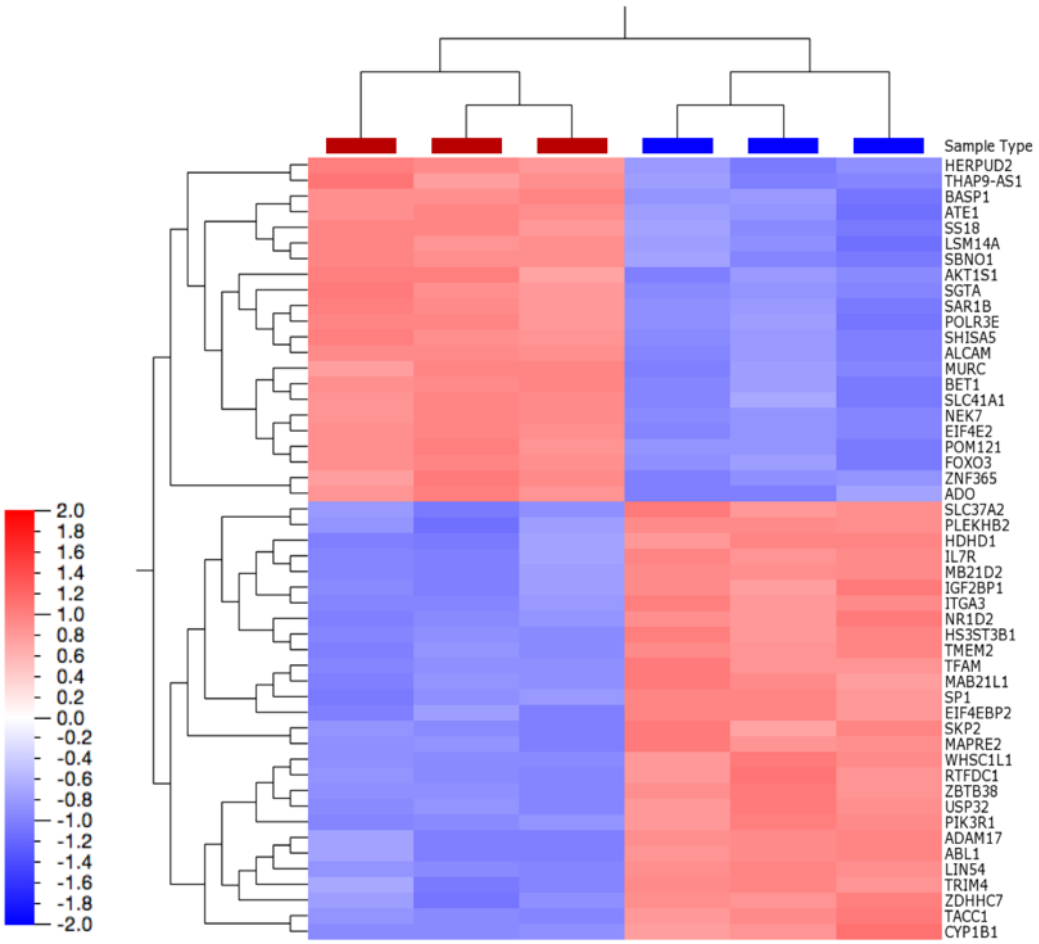

Figure 6-7 Hierarchical clustering heat map of differentially expressed genes resulting from Eps8 knockdown (in the presence of TGFβ1)

Qlucore-derived heat map filtered to the top 50 genes with the most variant expression. The FDR adjusted p-value threshold was decreased to limit the gene list from the filtered 8000 to the top 50 most variant genes. Eps8 Knockdown sample columns are labelled in red and control in blue.

GENE ID	GENE NAME	Log2fold change
SLC41A1	Solute Carrier Family 41 Member 1	1.6
POLR3E	Polymerase (RNA) III Subunit E	1.3
ALCAM	Activated Leukocyte Cell Adhesion Molecule	1.2
ZNF365	Zinc Finger Protein 365	1.1
LSM14A	MRNA Processing Body Assembly Factor	1.1
SAR1B	Secretion Associated Ras Related GTPase 1B	1.1
NEK7	NIMA Related Kinase 7	1.1
BASP1	Brain Abundant Membrane Attached Signal Protein 1	1.0
FOXO3	Forkhead box O3	1.0
SBNO1	Strawberry Notch Homolog 1 (Drosophila)	0.9
MURC	Muscle Related Coiled-Coil Protein	0.9
HERPUD2	HERPUD Family Member 2	0.9
SGTA	Small Glutamine Rich Tetratricopeptide Repeat Containing Alpha	0.8
BET1	Bet1 Golgi Vesicular Membrane Trafficking Protein	0.7
ATE1	Arginyltransferase 1	0.7
THAP9-AS1	THAP9 Antisense RNA 1	0.7
POM121	POM121 Transmembrane Nucleoporin	0.6
EIF4E2	Eukaryotic Translation Initiation Factor 4E Family Member 2	0.6
SS18	NBAF Chromatin Remodeling Complex Subunit	0.5
SHISA5	Shisa Family Member 5	0.5
AKT1S1	AKT1 Substrate 1	0.5
ADO	2-Aminoethanethiol (Cysteamine) Dioxygenase	0.3
ZBTB38	Zinc Finger And BTB Domain Containing 38	-0.2
RTFDC1	Replication Termination Factor 2 Domain Containing 1	-0.3
ITGA3	Integrin Subunit Alpha 3	-0.3
PLEKHB2	Pleckstrin Homology Domain Containing B2	-0.3
WHSC1L1	Wolf-Hirschhorn Syndrome Candidate 1-Like 1	-0.4
TRIM4	Tripartite Motif Containing 4	-0.4
ABL1	ABL Proto-Oncogene 1, Non-Receptor Tyrosine Kinase	-0.4
ZDHHC7	Zinc Finger DHHC-Type Containing 7	-0.4
IGF2BP1	Insulin Like Growth Factor 2 MRNA Binding Protein 1	-0.5
EIF4EBP2	Eukaryotic Translation Initiation Factor 4E Binding Protein 2	-0.5
MAPRE2	Microtubule Associated Protein RP/EB Family Member 2	-0.5
MB21D2	Mab-21 Domain Containing 2	-0.5
HS3ST3B1	Heparan Sulfate-Glucosamine 3-Sulfotransferase 3B1	-0.6
SP1	SP1 transcription factor	-0.6
TMEM2	Transmembrane Protein 2	-0.6
LIN54	Lin-54 DREAM MuvB Core Complex Component	-0.6
TACC1	Transforming Acidic Coiled-Coil Containing Protein 1	-0.6
MAB21L1	Mab-21 Like 1	-0.7
ADAM17	ADAM Metallopeptidase Domain 17	-0.8
PIK3R1	Phosphoinositide-3-Kinase Regulatory Subunit 1	-1.0
IL7R	Interleukin 7 Receptor	-1.1
USP32	Ubiquitin Specific Peptidase 32	-1.1
TFAM	Transcription Factor A, Mitochondrial	-1.3
NR1D2	Nuclear Receptor Subfamily 1 Group D Member 2	-1.3
SKP2	S-Phase Kinase-Associated Protein 2, E3 Ubiquitin Protein Ligase	-1.3
SLC37A2	Solute Carrier Family 37 Member 2	-1.9
HDHD1	Pseudouridine 5'-Phosphatase	-2.2
CYP1B1	Cytochrome P450 Family 1 Subfamily B Member 1	-2.9

Figure 6-8 The 50 genes with the greatest variance across samples as a result of Eps8 knockdown in the presence of TGFβ1.

Log_2fold change displayed. Genes in red were also in the 50 most variant genes as a result of Eps8 knockdown in the absence of TGFβ1. Genes highlighted in green have functions, derived from Entrez gene and UniProtKB/Swiss-Prot, that may be consistent with a role in sensitizing fibroblasts to myofibroblastic transdifferentiation.

In the presence of TGFβ1 (figures 6-7 and 6-8), Eps8 knockdown upregulated the expression of the mRNA for Muscle-related coiled-coil protein (MURC) whose encoded protein promotes Rho/ROCK (Rho-kinase) signalling in cardiac muscles cells, and is thought to facilitate myofibrillar organization. Wolf-Hirschhorn syndrome candidate 1-like 1 (WHSC1L1) codes for a histone methyltransferase, which represses gene transcription and is downregulated by Eps8 knockdown, potentially facilitating expression of a range of genes suppressed in the presence of Eps8. Finally, Eps8 knockdown results in the downregulation of S-phase kinase-associated protein 2 (SKP2), a substrate recognition component of the E3 ubiquitin ligase complex whose targets include CDK9. Given that CDK9 is known to phosphorylate the linker region of SMAD2, augmenting canonical signalling, reduction of its degradation is likely to increase TGFβ1-induced myofibroblast transdifferentiation.

In order to analyse the effects of Eps8 downregulation on a network level, the list of differentially expressed genes produced via the DESeq pipeline were mapped using the KEGG pathway mapper. In figures 6-9, 6-10 and 6-11 the differentially expressed genes as a result of Eps8 knockdown (in the absence of TGFβ1) were imposed on the 'pathways in cancer', 'TGF-beta signalling' and 'regulation of actin cytoskeleton' KEGG pathways.

In figures 6-9 and 6-10 the SMAD2/3 box erroneously failed to highlight, but it can be seen that members of the TGFβ signalling pathway were significantly differentially expressed as a result of Eps8 knockdown. TGFβ1 mRNA itself was upregulated by Eps8 knockdown (fold change(fc) 1.18, p_{adj} $1.18x10^{-3}$), as was TGFβ2 (fc 2.01, $1.81x10^{-4}$), while TGFβ3 was not significantly altered. Both TGFβ1 and TGFβ2 can induce myofibroblast transdifferentiation, although TGFβ1 is the most potent (Cheifetz et al. 1990). The balance of expression of TGFβR subunits changes, as previously discussed, with an increase in R1 and reduction in R2 subunits, but the biological significance of this is unclear.

PTEN was significantly downregulated (fc 0.78, p_{adj} $2.55x10^{-5}$) by Eps8 downregulation which would increase activity in the PI3K/Akt signalling pathway. This correlates with the increased Akt phosphorylation that we observed as a result of Eps8 knockdown (figure 4-13). Furthermore, increased Akt activity phosphorylates and inhibits GSK-3β which will serve to reduce degradation of activated pSMAD2, prolonging and augmenting TGFβ signalling.

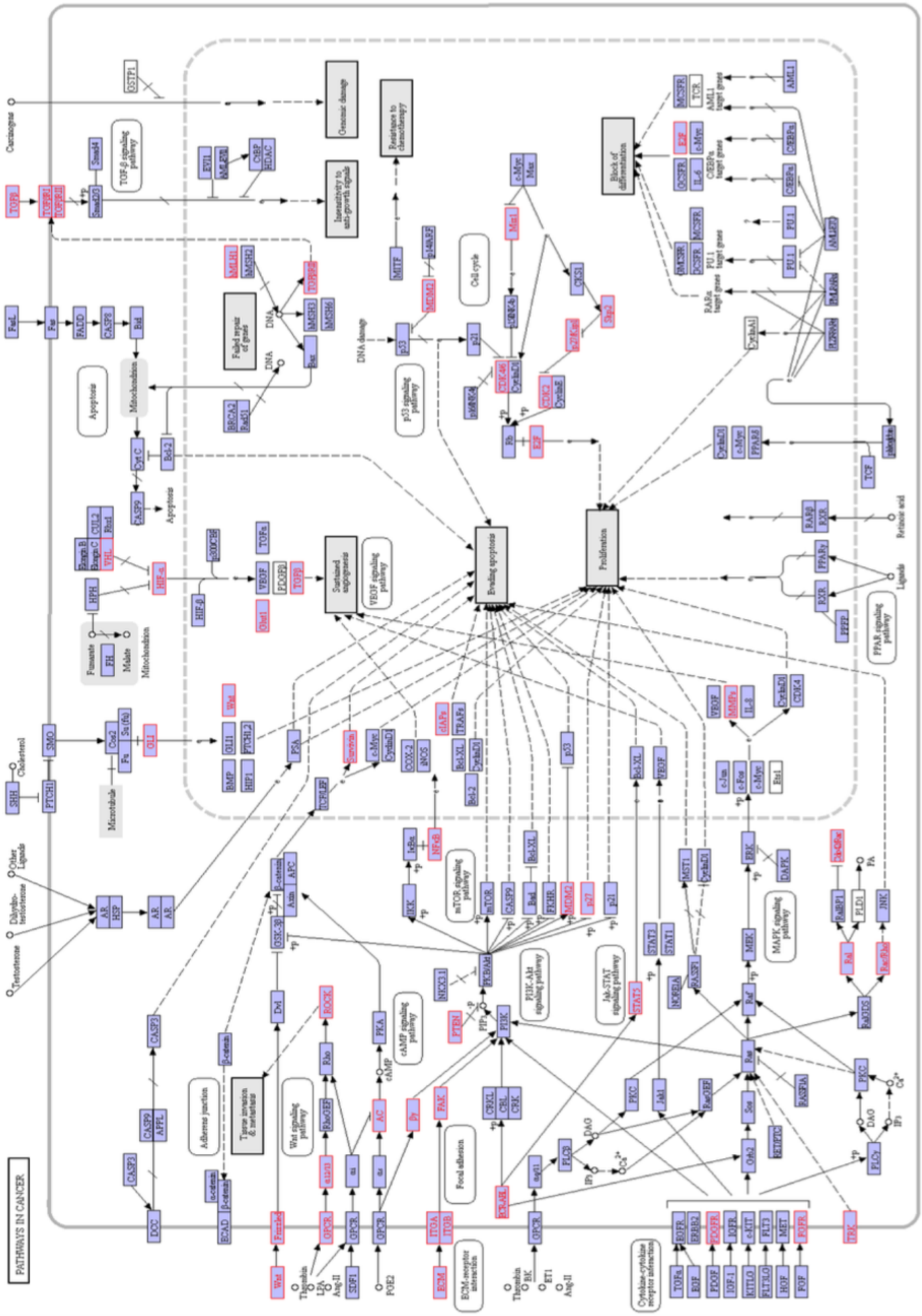

Figure 6-9 KEGG ‘pathways in cancer’

Eps8 knockdown-induced differentially expressed genes (without TGFβ1 treatment) superimposed in red.

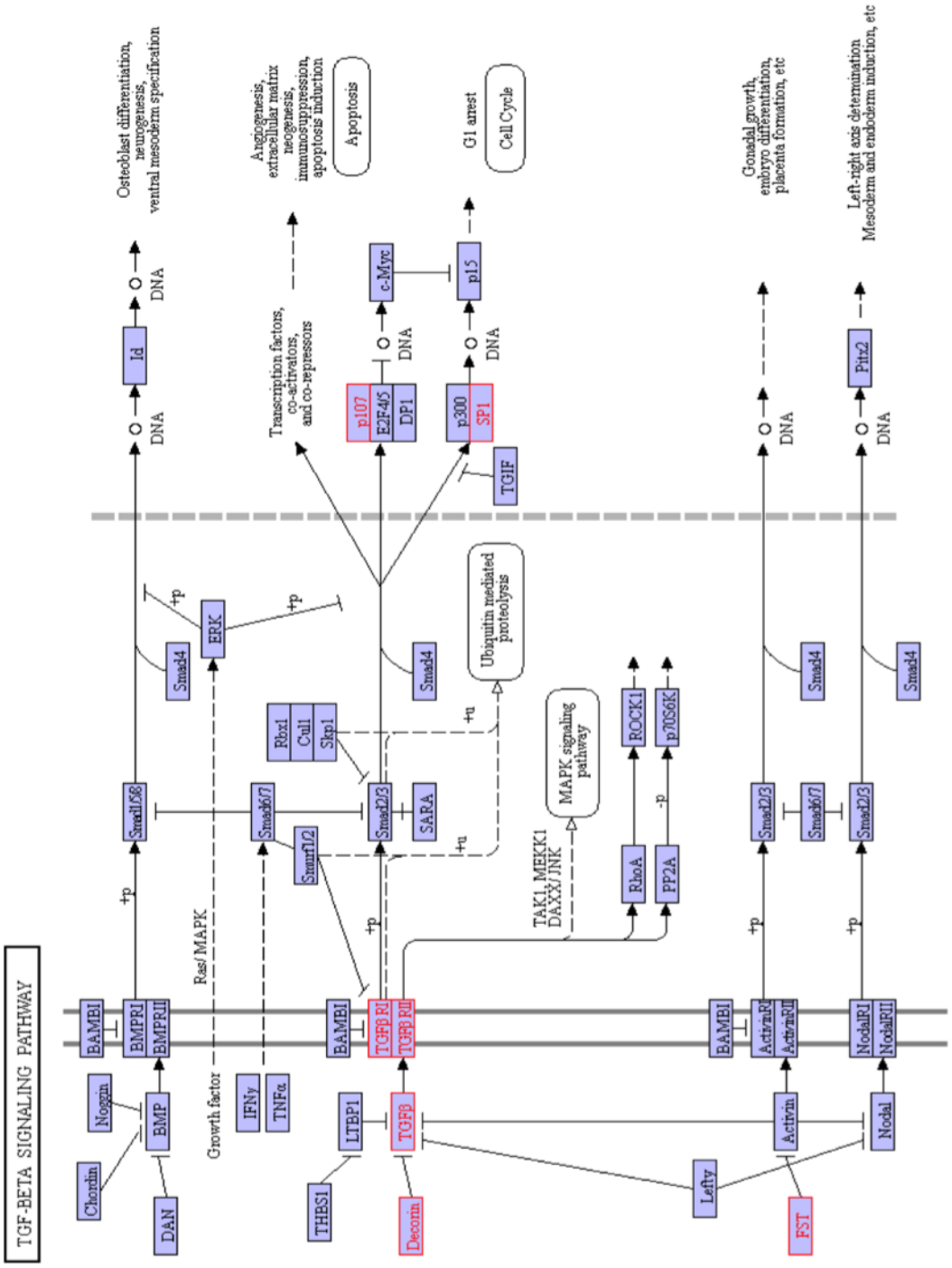

Figure 6-10 KEGG 'TGFβ signalling pathway'.

Eps8 knockdown-induced differentially expressed genes (without TGFβ1 treatment) superimposed in red.

Focal adhesion kinase (FAK) is a key member of the focal adhesion complex and is an important enzyme in the transduction of mechanical tension to

facilitate myofibroblast transdifferentiation (Lagares et al. 2012). Although its mRNA was differentially expressed as a result of Eps8 knockdown, it was downregulated rather than upregulated as a result of Eps8 knockdown (fc 0.76, p_{adj} $1.31x10^{-5}$) which fails to account for the augmentation of TGFβ1-induced myofibroblast transdifferentiation caused by Eps8 downregulation. A range of integrin α and β subunits were also downregulated rather than up regulated by Eps8 knockdown.

Within the 'regulation of actin cytoskeleton' module (figure 6-11) we observed several genes that are differentially expressed as a result of Eps8 downregulation. We have previously mentioned that a small increase in Rac1 mRNA expression was observed. Of the P21 protein-activated kinase (PAK) family, known to link Rho GTPase activity to modifications of the actin cytoskeleton, only PAK4 was significantly differentially expressed, and was downregulated in response to Eps8 knockdown (fc 0.77, p_{adj} $1.25x10^{-3}$). PAK family members are known to inhibit RhoA-dependent stress fibre formation (Alberts et al. 2005); phosphorylate actin, causing stress fibre disassembly (Manser et al. 1997); and phosphorylate MLCK reducing actomyosin assembly (Sanders et al. 1999). It is likely therefore that PAK4 downregulation will aid in stress fibre stabilisation and myofibroblast transdifferentiation.

LIM domain kinase proteins 1 and 2 phosphorylate cofilin, inhibiting its depolymerisation of actin. LIMK2 expression was upregulated as a result of Eps8 downregulation (fc 1.36, p_{adj} $2.56x10^{-2}$) and therefore also stabilises filamentous actin, potentially contributing to maintenance of the myofibroblast phenotype.

While ROCK and mDia1 are central to stress fibre formation and fibroblast contractility, ROCK1 mRNA expression was not significantly altered by Eps8 knockdown and ROCK2 expression was downregulated (fc 0.82, p_{adj} $3.49x10^{-3}$), while mDia1 mRNAs were also either unchanged or downregulated. Myosin light chain kinase (MLCK) was also downregulated at the mRNA level by Eps8 knockdown (fc 0.83, p_{adj} $6.91x10^{-3}$), however myosin light chain 9 was upregulated (fc 1.14, p_{adj} $1.48x10^{-3}$) which may contribute to stress fibre contractility.

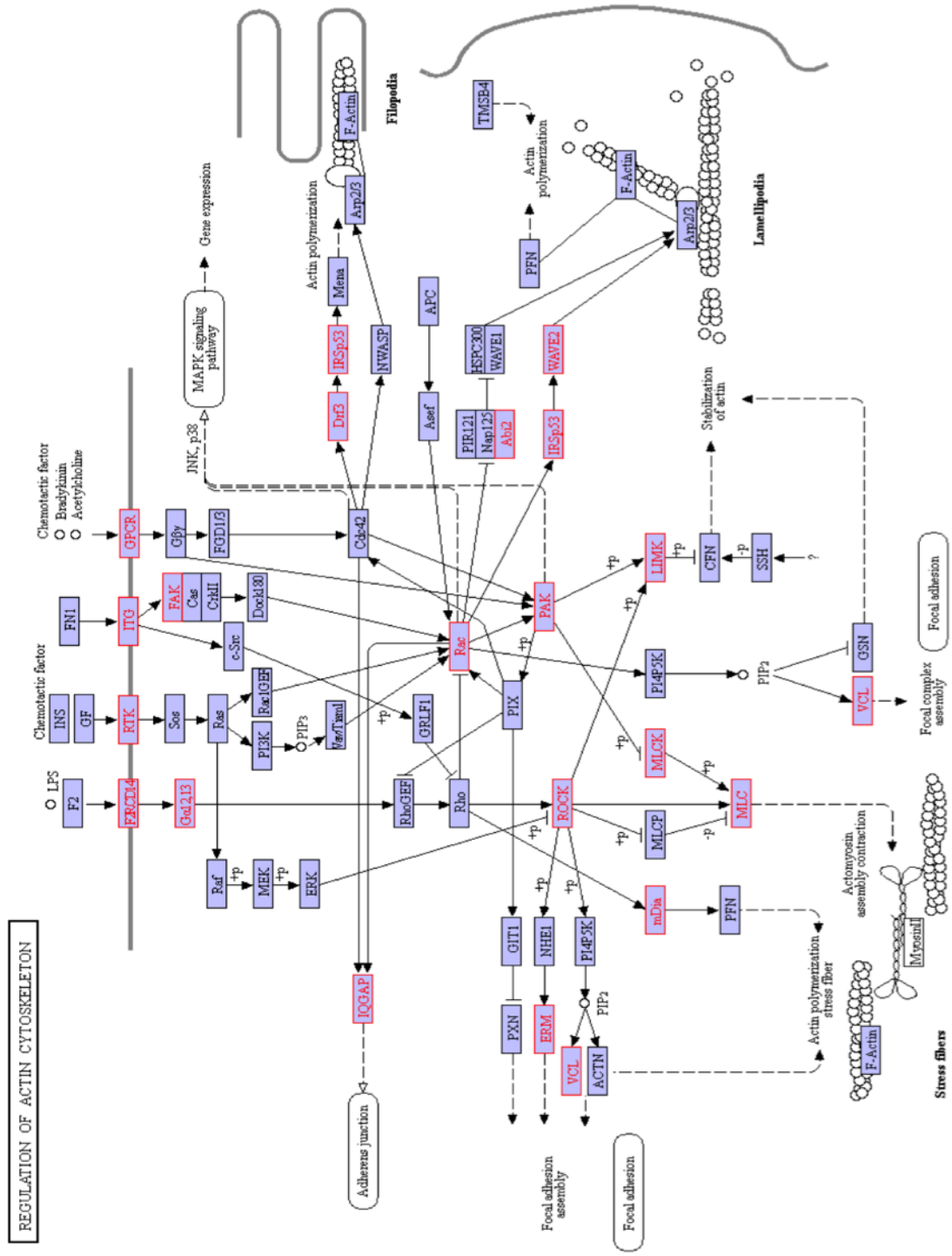

Figure 6-11 KEGG 'Regulation of actin cytoskeleton'

Eps8 knockdown-induced differentially expressed genes (without TGFβ1 treatment) superimposed in red.

6.2 Final Conclusions

In this thesis we have identified a novel function of the protein Eps8 in regulating myofibroblast transdifferentiation. We have demonstrated that *in vitro* Eps8 restricts SMAD2 expression and inhibits TGFβ1-induced NOX4 expression and SMAD2 phosphorylation. Eps8 expression restricts TGFβ1-induced αSMA induction and stress fibre assembly, limiting myofibroblast functional contractility. Fibroblasts with downregulated Eps8 expression induce greater migration in head & neck cancer cells in an *in vitro* assay and greater tumour growth in xenograft animal models using a head & neck cancer cell line.

We have also demonstrated that fibroblasts themselves downregulate Eps8 expression early in the process of myofibroblast transdifferentiation and also downregulate Eps8 during fibroblast senescence, which also generates a myofibroblast phenotype. Examining tissue microarrays has revealed that the expression of Eps8 is inversely correlated with αSMA expression in the stroma of human cancers and in a range of fibrotic conditions, correlating with these *in vitro* observations.

Maintenance of expression of Eps8's tricomplex binding partners, Abi1 and SOS1, is also required to regulate myofibroblast transdifferentiation. This suggests that despite the varied functions of Eps8, its regulation of myofibroblast transdifferentiation is likely to be effected via the tricomplex. It is possible that tricomplex-mediated Rac1 activation limits Rho-mediated stress fibre assembly but this requires further investigation.

Our RNA-seq experiment examining the early effects of Eps8 knockdown has identified new avenues for investigation including potential transcription factors responsible for the induction of SMAD2. It has also provided evidence to support the inhibition of pSMAD2 degradation in response to Eps8 knockdown, which would also serve to augment TGFβ signalling. Clearly the mRNA expression profile only provides information at one level of regulation within the cell, and phosphoproteomics would be a welcome addition to inform us further regarding pathway activation.

Our investigations to date raise the intriguing question as to whether the artificial maintenance of Eps8 levels, or prevention of Eps8 downregulation could significantly limit TGFβ-induced myofibroblast transdifferentiation. We have optimised transfection of a plasmid containing murine Eps8 in an effort to overexpress Eps8 in the fibroblast, but further understanding of the regulation of Eps8 expression during myofibroblast transdifferentiation may enable us to do this chemically.

We have also observed that irradiation and a range of chemotherapeutic agents, both used in cancer treatment, downregulate fibroblast Eps8 expression. We have demonstrated that this downregulation augments tumour-supporting behaviour and the ability of TGFβ1 to induce myofibroblast transdifferentiation. It is possible therefore that our use of these agents in cancer therapies, while targeting tumour cells for destruction, might be inadvertently subverting the cancer stroma into a more tumour-supportive environment and this would be an extremely interesting extension to this work in the future.

References

Abdel-Rahman, W. et al., 2012. Differential roles of EPS8 in carcinogenesis: loss of protein expression in a subset of colorectal carcinoma and adenoma. *World J Gastroenterol*, 18(29), pp.3896–3903.

Adhikari, A. et al., 2007. Ubiquitin-mediated activation of TAK1 and IKK. *Oncogene*, 26(22), pp.3214–26.

Alberts, A. et al., 2005. PAK1 negatively regulates the activity of the Rho exchange factor NET1. *J Biol Chem*, 280(13), pp.12152–61.

Alessi, D. et al., 1997. Characterization of a 3-phosphoinositide-dependent protein kinase which phosphorylates and activates protein kinase Bα. *Curr Biol*, 7(4), pp.261–269.

Alizadeh, N. et al., 2007. Persistent ischemia impairs myofibroblast development in wound granulation tissue: a new model of delayed wound healing. *Wound repair regen*, 15(6), pp.809–16.

Amara, N. et al., 2010. NOX4/NADPH oxidase expression is increased in pulmonary fibroblasts from patients with idiopathic pulmonary fibrosis and mediates TGFbeta1-induced fibroblast differentiation into myofibroblasts. *Thorax*, 65(8), pp.733–8.

Ando, Y. et al., 2014. Phase I dose-escalation study of buparlisib (BKM120), an oral pan-class I PI3K inhibitor, in Japanese patients with advanced solid tumors. *Cancer sci*, 105(3), pp.347–53.

Annes, J. et al., 2003. Making sense of latent TGFbeta activation. *J Cell Sci*, 116(2), pp.217–224.

Aoyama, T. et al., 2012. Nicotinamide Adenine Dinucleotide Phosphate Oxidase (NOX) in Experimental Liver Fibrosis: GKT137831 as a Novel Potential Therapeutic Agent. *Hepatology*, 56(6), pp.2316–2327.

Armstrong, B. & Kricker, A., 2001. The epidemiology of UV induced skin cancer. *J photochem photobiol B,* 63(1–3), pp.8–18.

Asano, Y. et al., 2004. Impaired Smad7-Smurf-mediated negative regulation of

TGF-beta signaling in scleroderma fibroblasts. *J Clin Invest*, 113(2), pp.253–264.

Auciello, G. et al., 2013. Regulation of fibroblast growth factor receptor signalling and trafficking by Src and Eps8. *J Cell Sci*, 126(2), pp.613–24.

Bakin, A. et al., 2000. Phosphatidylinositol 3-kinase function is required for transforming growth factor beta-mediated epithelial to mesenchymal transition and cell migration. *J Biol Chem*, 275(47), pp.36803–10.

Bandyopadhyay, B. et al., 2011. TbetaRI/Alk5-independent TbetaRII signaling to ERK1/2 in human skin cells according to distinct levels of TbetaRII expression. *J Cell Sci*, 124(1), pp.19–24.

Barcellos-Hoff, M. & Dix, T., 1996. Redox-mediated activation of latent transforming growth factor-beta 1. *Mol Endocrinol*, 10(9), pp.1077–83.

Barnes, J. & Gorin, Y., 2011. Myofibroblast differentiation during fibrosis: role of NAD(P)H oxidases. *Kidney Int*, 79(9), pp.944–956.

Barry-Hamilton, V. et al., 2010. Allosteric inhibition of lysyl oxidase-like-2 impedes the development of a pathologic microenvironment. *Nat Med*, 16(9), pp.1009–17.

Barth, P. et al., 2004. CD34+ fibrocytes, alpha-smooth muscle antigen-positive myofibroblasts, and CD117 expression in the stroma of invasive squamous cell carcinomas of the oral cavity, pharynx, and larynx. *Virchows Arch*, 444(3), pp.231–234.

Bashir, M. et al., 2010. P66shc and its downstream Eps8 and Rac1 proteins are upregulated in esophageal cancers. *Cell Commun Signal*, 8, p.13.

Bauer, J. et al., 2005. Reversal of cisplatin resistance with a BH3 mimetic, (-)-gossypol, in head and neck cancer cells: role of wild-type p53 and Bcl-xL. *Mol Cancer Ther*, 4(7), pp.1096–104.

Beanes, S. et al., 2002. Confocal microscopic analysis of scarless repair in the fetal rat : defining the transition. *Plast Reconstr Surg*, 109(1), pp.160–170.

Beeton, C. et al., 2001. Serum TIMP-1 , TIMP-2 , and MMP-1 in patients with systemic sclerosis , primary Raynaud ' s phenomenon , and in normal

controls. *Ann Rheum Dis*, 60(9), pp.846–851.

Behlouli, A. et al., 2014. EPS8, encoding an actin-binding protein of cochlear hair cell stereocilia, is a new causal gene for autosomal recessive profound deafness. *Orphanet J Rare Dis*, 9, p.55.

Beli, P. et al., 2008. WAVE and Arp2/3 jointly inhibit filopodium formation by entering into a complex with mDia2. *Nat Cell Biol*, 10(7), pp.849–57.

Berdiel-Acer, M. et al., 2014. Differences between CAFs and their paired NCF from adjacent colonic mucosa reveal functional heterogeneity of CAFs, providing prognostic information. *Mo Oncol*, 8(7), pp.1290–1305.

Bhat, H. et al., 2014. Role of SNTA1 in Rac1 activation, modulation of ROS generation, and migratory potential of human breast cancer cells. *Br J Cancer*, 110(3), pp.706–14.

Bierie, B. & Moses, H., 2006. Tumour microenvironment: TGFbeta: the molecular Jekyll and Hyde of cancer. *Nat Rev Cancer*, 6(7), pp.506–20.

Bitzer, M. et al., 2000. A mechanism of suppression of TGF-beta/SMAD signaling by NF-kappa B/RelA. *Genes Dev*, 14(2), pp.187–97.

Block, K. et al., 2008. Nox4 NAD(P)H oxidase mediates Src-dependent tyrosine phosphorylation of PDK-1 in response to angiotensin II: role in mesangial cell hypertrophy and fibronectin expression. *J Biol Chem*, 283(35), pp.24061–76.

Bock, O. et al., 2005. Studies of transforming growth factors beta 1-3 and their receptors I and II in fibroblast of keloids and hypertrophic scars. *Acta Derm Venereol*, 85(3), pp.216–20.

Bogatkevich, G. et al., 2001. Thrombin differentiates normal lung fibroblasts to a myofibroblast phenotype via the proteolytically activated receptor-1 and a protein kinase C-dependent pathway. *J Biol Chem*, 276(48), pp.45184–92.

Bondi, C. et al., 2010. NAD(P)H oxidase mediates TGF-beta1-induced activation of kidney myofibroblasts. *J Am Soc Nephrol*, 21(1), pp.93–102.

Bopp, A. et al., 2013. Rac1 modulates acute and subacute genotoxin-induced

hepatic stress responses, fibrosis and liver aging. *Cell Death Dis*, 4(3), p.558.

Boyde, A. & Bailey, A., 1977. Observations on the marginal ruffles of an established fibroblast-like cell line. *Cell Tissue Res*, 179(2), pp.225–34.

Brem, H. & Tomic-Canic, M., 2007. Cellular and molecular basis of wound healing in diabetes. *J Clin Invest*, 117(5), pp.1219–1222.

Brown, J. et al., 1999. MEKK-1, a component of the stress (stress-activated protein Kinase/c-Jun N-terminal kinase) pathway, can selectively activate Smad2-mediated transcriptional activation in endothelial cells. *J Biol Chem*, 274(13), pp.8797–8805.

Brown, K. et al., 2007. A tale of two proteins: differential roles and regulation of Smad2 and Smad3 in TGF-beta signaling. *J Cell Biochem*, 101(1), pp.9–33.

Bruce, D. & Sapkota, G., 2012. Phosphatases in SMAD regulation. *FEBS lett*, 586(14), pp.1897–905.

Butler, B. et al., 2006. Purified integrin adhesion complexes exhibit actin-polymerization activity. *Curr Biol*, 16(3), pp.242–51.

Canady, J. et al., 2013. Fibrosing connective tissue disorders of the skin: molecular similarities and distinctions. *J Dermatol Sci*, 70(3), pp.151–8.

Cantley, L., 2002. The phosphoinositide 3-kinase pathway. *Science*, 296(5573), pp.1655–7.

Carlson, M. et al., 2003. Wound splinting regulates granulation tissue survival. *J Surg Res*, 110(1), pp.304–309.

Castagnino, P. et al., 1995. Direct binding of eps8 to the juxtamembrane domain of EGFR is phosphotyrosine- and SH2-independent. *Oncogene*, 10(4), pp.723–729.

Castella, L. et al., 2010. A new lock-step mechanism of matrix remodelling based on subcellular contractile events. *J Cell Sci*, 123(10), pp.1751–60.

Cattaneo, M. et al., 2012. Silencing of Eps8 blocks migration and invasion in human glioblastoma cell lines. *Exp Cell Res*, 318(15), pp.1901–1912.

Chaffer, C. & Weinberg, R., 2011. A perspective on cancer cell metastasis. *Science,* 331(6024), pp.1559–64.

Chan, M. et al., 2013. Case Report: Giant labial fibroepithelial stromal polyp. *Malays J Pathol*, 35(1), pp.91–94.

Cheifetz, S., Hernandez, H. & Laiho, M., 1990. Distinct transforming growth factor(TGF-beta) receptor subsets as determinants of cellular responsiveness to three TGF-beta isoforms. *J Biol Chem,* 265(33), pp.20533–20538.

Chen, H. et al., 2010. Integrity of SOS1/EPS8/ABI1 tri-complex determines ovarian cancer metastasis. *Cancer Res*, 70(23), pp.9979–9990.

Chen, Q. & Ames, B., 1994. Senescence-like growth arrest induced by hydrogen peroxide in human diploid fibroblast F65 cells. *Proc Natl Acad Sci USA*, 91(10), pp.4130–4134.

Chen, X. & Xu, L., 2010. Specific nucleoporin requirement for Smad nuclear translocation. *Mol Cell Biol*, 30(16), pp.4022–34.

Chen, Y. et al., 2008. Eps8 decreases chemosensitivity and affects survival of cervical cancer patients. *Mol Cancer Ther*, 7(6), pp.1376–1385.

Chen, Y. et al., 2014. Transforming growth factor-β1 and α-smooth muscle actin in stromal fibroblasts are associated with a poor prognosis in patients with clinical stage I-IIIA nonsmall cell lung cancer after curative resection. *Tumour biol*, 35(7), pp.6707–13.

Chen, Y. & Wang, X., 2009. Finale: the last minutes of Smads. *Cell*, 139(4), pp.658–60.

Chen, Y. et al., 2012. Eps8 protein facilitates phagocytosis by increasing TLR4-MyD88 protein interaction in lipopolysaccharide-stimulated macrophages. *J Biol Chem*, 287(22), pp.18806–18819.

Cheng, C. & Mruk, D., 2011. Regulation of spermiogenesis, spermiation and blood-testis barrier dynamics: novel insights from studies on Eps8 and Arp3. *Biochem J*, 435(3), pp.553–562.

Cho, J. et al., 2011. Exosomes from ovarian cancer cells induce adipose tissue-

derived mesenchymal stem cells to acquire the physical and functional characteristics of tumor-supporting myofibroblasts. *Gynecol Oncol*, 123(2), pp.379–86.

Cho, J. et al., 2012. Exosomes from breast cancer cells can convert adipose tissue-derived mesenchymal stem cells into myofibroblast-like cells. *Int J Oncol,* 40(1), pp.130–8.

Chowdhury, R. et al., 2015. Cancer exosomes trigger mesenchymal stem cell differentiation into pro-angiogenic and pro-invasive myofibroblasts. *Oncotarget*, 6(2), pp.715–31.

Chrzanowska-Wodnicka, M. & Burridge, K., 1996. Rho-stimulated contractility drives the formation of stress fibers and focal adhesions. *J Cell Biol*, 133(6), pp.1403–15.

Chu, A. & Prasad, J., 1999. Up-regulation by human recombinant transforming growth factor β-1 of collagen production in cultured dermal fibroblasts is mediated by the inhibition of nitric oxide signaling. *J Am Coll Surg*, 188(3), pp.271–280.

Chu, P. et al., 2012. Expression of Eps8 correlates with poor survival in oral squamous cell carcinoma. *Asia Pac J Clin Oncol*, 8(4), pp.77–81.

Chung, E. et al., 2014. Lithium chloride inhibits TGF-β1-induced myofibroblast transdifferentiation via PI3K/Akt pathway in cultured fibroblasts from Tenon's capsule of the human eye. *Biotechnol lett*, 36(6), pp.1217–24.

Colwell, A. et al., 2003. Fetal wound healing. *Front Biosci*, 8, pp.1240-8.

Conery, A. et al., 2004. Akt interacts directly with Smad3 to regulate the sensitivity to TGF-beta induced apoptosis. *Nat Cell Biol*, 6(4), pp.366–72.

Conte, E. et al., 2014. Effect of pirfenidone on proliferation, TGF-β-induced myofibroblast differentiation and fibrogenic activity of primary human lung fibroblasts. *Eur J Pharm Sci*, 58, pp.13–9.

Conte, E. et al., 2011. Inhibition of PI3K prevents the proliferation and differentiation of human lung fibroblasts into myofibroblasts: the role of class I P110 isoforms. *PloS one*, 6(10), p.24663.

Costa, A. et al., 2014. The role of reactive oxygen species and metabolism on cancer cells and their microenvironment. *Semin Cancer Biol*, 25, pp.23–32.

Crawford, Y. et al., 2009. PDGF-C mediates the angiogenic and tumorigenic properties of fibroblasts associated with tumors refractory to anti-VEGF treatment. *Cancer cell*, 15(1), pp.21–34.

Crider, B. et al., 2012. Myocardin-related transcription factors A and B are key regulators of TGFB1-induced fibroblast-to-myofibroblast transdifferentiation. *J Invest Dermatol.*, 131(12), pp.2378–2385.

Cucoranu, I. et al., 2005. NAD(P)H oxidase 4 mediates transforming growth factor-beta1-induced differentiation of cardiac fibroblasts into myofibroblasts. *Circ Res*, 97(9), pp.900–7.

Cunningham, D. et al., 2013. Novel binding partners and differentially regulated phosphorylation sites clarify Eps8 as a multi-functional adaptor. *PLoS One*, 8(4), p.61513.

D'Ambrosi, N. et al., 2014. Rac1 at the crossroad of actin dynamics and neuroinflammation in Amyotrophic Lateral Sclerosis. *Front Cell Neurosci*, 8, p.279.

Daly, A. et al., 2008. Transforming growth factor beta-induced Smad1/5 phosphorylation in epithelial cells is mediated by novel receptor complexes and is essential for anchorage-independent growth. *Mol Cell Biol*, 28(22), pp.6889–6902.

Datta, P. & Moses, H., 2000. STRAP and Smad7 synergize in the inhibition of transforming growth factor beta signaling. *Mol Cell Biol*, 20(9), pp.3157–67.

Derynck, R. & Zhang, Y., 2003. Smad-dependent and Smad-independent pathways in TGF-beta family signalling. *Nature*, 425(6958), pp.577–584.

Desmouliere, A. et al., 1995. Apoptosis mediates the decrease in cellularity during the transition between granulation tissue and scar. *Am J Pathol*, 146(1), pp.56–66.

Dimanche-Boitrel, M. et al., 1994. In vivo and in vitro invasiveness of a rat

colon-cancer cell line maintaining E-cadherin expression: an enhancing role of tumor-associated myofibroblasts. *Int J Cancer*, 56(4), pp.512–21.

Ding, X. et al., 2013. Eps8 promotes cellular growth of human malignant gliomas. *Oncol Rep*, 29(2), pp.697–703.

Ding, X. et al., 2012. Human intersectin 2 (ITSN2) binds to Eps8 protein and enhances its degradation. *BMB Rep*, 45(3), pp.183–188.

Dingemans, K. et al., 1993. Transplantation of colon carcinoma into granulation tissue induces an invasive morphotype. *Int J Cancer*, 54(6), pp.1010–6.

Disanza, A. et al., 2005. Actin polymerization machinery: the finish line of signaling networks, the starting point of cellular movement. *Cell Mol Life Sci*, 62(9), pp.955–70.

Disanza, A. et al., 2004. Eps8 controls actin-based motility by capping the barbed ends of actin filaments. *Nat Cell Biol*, 6(12), pp.1180–8.

Disanza, A. et al., 2006. Regulation of cell shape by Cdc42 is mediated by the synergic actin-bundling activity of the Eps8-IRSp53 complex. *Nat Cell Biol*, 8(12), pp.1337–47.

Dong, C. et al., 2002. Deficient Smad7 expression: a putative molecular defect in scleroderma. *Proc Natl Acad Sci USA*, 99(6), pp.3908–13.

Dorsey, K. & Agulnik, M., 2013. Promising new molecular targeted therapies in head and neck cancer. *Drugs*, 73(4), pp.315–25.

Douglass, A. et al., 2008. Antibody-targeted myofibroblast apoptosis reduces fibrosis during sustained liver injury. *J Hepatol*, 49(1), pp.88–98.

Duda, D. et al., 2010. Malignant cells facilitate lung metastasis by bringing their own soil. *Proc Natl Acad Sci USA*, 107(50), pp.21677–82.

Dugina, V. et al., 2001. Focal adhesion features during myofibroblastic differentiation are controlled by intracellular and extracellular factors. *J Cell Sci*, 114(18), pp.3285–96.

Dulauroy, S. et al., 2012. Lineage tracing and genetic ablation of ADAM12(+) perivascular cells identify a major source of profibrotic cells during acute

tissue injury. *Nat Med*, 18(8), pp.1262–70.

Dutcher, J. et al., 1997. A pilot study of alpha-interferon accelerated phase of chronic and plicamycin for myeloid leukemia. *Leuk Res*, 21(5), pp.375–380.

Dvorak, H., 1986. Tumors: wounds that do not heal. Similarities between tumor stroma generation and wound healing. *N Engl J Med*, 315(26), pp.1650–9.

Ebisawa, T. et al., 2001. Smurf1 interacts with transforming growth factor-beta type I receptor through Smad7 and induces receptor degradation. *J Biol Chem*, 276(16), pp.12477–80.

Emori, T. et al., 2012. Nuclear Smad7 overexpressed in mesenchymal cells acts as a transcriptional corepressor by interacting with HDAC-1 and E2F to regulate cell cycle. *Biol Open*, 1(3), pp.247–60.

Engel, M. et al., 1999. Interdependent SMAD and JNK signaling in transforming growth factor-beta-mediated transcription. *J Biol Chem*, 274(52), pp.37413–37420.

Erez, N. et al., 2010. Cancer-associated fibroblasts are activated in incipient neoplasia to orchestrate tumor-promoting inflammation in an NF-kappaB-dependent manner. *Cancer cell*, 17(2), pp.135–47.

Eyden, B., 2008. The myofibroblast: phenotypic characterization as a prerequisite to understanding its functions in translational medicine. *J Cell Mol Med*, 12(1), pp.22–37.

Eyden, B. et al., 2009. The myofibroblast and its tumours. *J Clin Pathol*, 62(3), pp.236–249.

Fazioli, F. et al., 1993. Eps8, a substrate for the epidermal growth factor receptor kinase, enhances EGF-dependent mitogenic signals. *EMBO J*, 12(10), pp.3799–808.

Feng, X. & Derynck, R., 2005. Specificity and versatility in tgf-beta signaling through Smads. *Annu Rev Cell Dev Biol*, 21, pp.659–93.

Ferrini, M. et al., 2006. Effects of long-term vardenafil treatment on the

development of fibrotic plaques in a rat model of Peyronie's disease. *BJU Int*, 97(3), pp.625–33.

Di Fiore, P. & Scita, G., 2002. Eps8 in the midst of GTPases. *The International Journal of Biochemistry & Cell Biology*, 34(10), pp.1178–1183.

Di Fiore, P. & Scita, G., 2002. Eps8 in the midst of GTPases. *Int J Biochem Cell Biol*, 34(10), pp.1178–1183.

Flaberg, E. et al., 2011. High-throughput live-cell imaging reveals differential inhibition of tumor cell proliferation by human fibroblasts. *Int J Cancer*, 128(12), pp.2793–802.

Flanders, K., 2004. Smad3 as a mediator of the fibrotic response. *Int J Exp Pathol*, 85(2), pp.47–64.

Forman, H. et al., 2008. The chemistry of cell signaling by reactive oxygen and nitrogen species and 4-hydroxynonenal. *Arch Biochem Biophys*, 477(2), pp.183–95.

Frittoli, E. et al., 2011. The signaling adaptor Eps8 is an essential actin capping protein for dendritic cell migration. *Immunity*, 35(3), pp.388–99.

Fukumoto, J. et al., 2010. Amphiregulin attenuates bleomycin-induced pneumopathy in mice. *Am J Physiol Lung Cell Mol Physiol*, 298(2), pp.131–8.

Funato, Y. et al., 2004. IRSp53 / Eps8 complex is important for positive regulation of Rac and cancer cell motility / invasiveness. *Cancer Res*, 64(15), pp.5237–44.

Furness, D. et al., 2013. Progressive hearing loss and gradual deterioration of sensory hair bundles in the ears of mice lacking the actin-binding protein Eps8L2. *Proc Natl Acad Sci USA*, 110(34), pp.13898–903.

Fury, M. et al., 2013. A phase 1 study of everolimus plus docetaxel plus cisplatin as induction chemotherapy for patients with locally and/or regionally advanced head and neck cancer. *Cancer*, 119(10), pp.1823–31.

Gabbiani, G. et al., 2012. The role of the myofibroblast in tumor stroma remodeling. *Cell Adh Migr*, 6(3), pp.203–219.

Gabbiani, G. et al., 1971. Presence of modified fibroblasts in granulation tissue and their possible role in wound contraction. *Experientia*, 27(5), pp.549–50.

Gabriel, V., 2011. Hypertrophic scar. *Phys Med Rehabil Clin N Am*, 22(2), pp.301–10.

Gadbois, D. et al., 1997. Control of radiation-induced G1 arrest by cell-substratum interactions. *Cancer Res*, 57(6), pp.1151–6.

Gaggioli, C., 2008. Collective invasion of carcinoma cells: when the fibroblasts take the lead. *Cell Adh Migr*, 2(1), pp.45–7.

Galliher, A. & Schiemann, W., 2007. Src phosphorylates Tyr284 in TGF-beta type II receptor and regulates TGF-beta stimulation of p38 MAPK during breast cancer cell proliferation and invasion. *Cancer Res*, 67(8), pp.3752–8.

Gallo, R. et al., 1997. Regulation of the tyrosine kinase substrate Eps8 expression by growth factors, v-Src and terminal differentiation. *Oncogene*, 15(16), pp.1929–36.

Gan, J. et al., 2013. Effects of daunorubicin on KG1a cell proliferation and Eps8 expression. *Zhongguo Shi Yan Xue Ye Xue Za Zhi*, 21(1), pp.49–52.

Gao, S. et al., 2009. Ubiquitin ligase Nedd4L targets activated Smad2/3 to limit TGF-B signalling. *Mol cell*, 36(3), pp.457–468.

Garrison, G. et al., 2013. Reversal of myofibroblast differentiation by prostaglandin E(2). *Am J Respir Cell Mol Biol*, 48(5), pp.550–8.

Georges, P. et al., 2007. Increased stiffness of the rat liver precedes matrix deposition: implications for fibrosis. *Am J Physiol Gastrointest Liver Physiol*, 293(6), pp.1147–54.

Giannoni, E. et al., 2010. Reciprocal activation of prostate cancer cells and cancer-associated fibroblasts stimulates epithelial-mesenchymal transition and cancer stemness. *Cancer Res*, 70(17), pp.6945–56.

Goetz, J. et al., 2011. Biomechanical remodeling of the microenvironment by stromal caveolin-1 favors tumor invasion and metastasis. *Cell*, 146(1),

pp.148–63.

Goffin, J. et al., 2006. Focal adhesion size controls tension-dependent recruitment of alpha-smooth muscle actin to stress fibers. *J Cell Biol*, 172(2), pp.259–68.

Goicoechea, S. et al., 2006. Palladin binds to Eps8 and enhances the formation of dorsal ruffles and podosomes in vascular smooth muscle cells. *J Cell Sci*, 119(16), pp.3316–24.

Gorin, Y. et al., 2005. Nox4 NAD(P)H oxidase mediates hypertrophy and fibronectin expression in the diabetic kidney. *J Biol Chem*, 280(47), pp.39616–26.

Gorsic, L. et al., 2013. EPS8 inhibition increases cisplatin sensitivity in lung cancer cells. *PloS one*, 8(12), p.82220.

Goumans, M. et al., 2003. Activin receptor-like kinase (ALK)1 is an antagonistic mediator of lateral TGFbeta/ALK5 signaling. *Mol Cell*, 12(4), pp.817–28.

Griffith, O. et al., 2006. Meta-analysis and meta-review of thyroid cancer gene expression profiling studies identifies important diagnostic biomarkers. *J Clin Oncol*, 24(31), pp.5043–5051.

Grum-Schwensen, B. et al., 2005. Suppression of tumor development and metastasis formation in mice lacking the S100A4(mts1) gene. *Cancer Res*, 65(9), pp.3772–80.

Gu, L. et al., 2007. Effect of TGF-beta/Smad signaling pathway on lung myofibroblast differentiation. *Acta pharmacol Sin*, 28(3), pp.382–91.

Guido, C. et al., 2012. Mitochondrial fission induces glycolytic reprogramming in cancer-associated myofibroblasts, driving stromal lactate production, and early tumor growth. *Oncotarget*, 3(8), pp.798–810.

Guo, W. & Shan, B., 2009. Abrogation of TGF-β1-induced fibroblast-myofibroblast differentiation by histone deacetylase inhibition. *Am J Physiol Lung Cell Mol Physiol*, 297(5), pp.864–870.

Guyot, C. et al., 2010. Fibrogenic cell phenotype modifications during remodelling of normal and pathological human liver in cultured slices.

Liver Int, 30(10), pp.1529–40.

Hanahan, D. & Coussens, L., 2012. Accessories to the crime: functions of cells recruited to the tumor microenvironment. *Cancer Cell*, 21(3), pp.309–22.

Hart, T. et al., 2002. A mutation in the SOS1 gene causes hereditary gingival fibromatosis type 1. *Am J Hum Genet*, 70(4), pp.943–54.

Hartmann, C. et al., 1990. So-called fibroepithelial polyps of the vagina exhibiting an unusual but uniform antigen profile characterized by expression of desmin and steroid hormone receptors but no muscle-specific actin or macrophage markers. *Am J Clin Path*, 93(5), pp.604–8.

He, Y. et al., 2013. Eps8 vaccine exerts prophylactic antitumor effects in a murine model: a novel vaccine for breast carcinoma. *Mol Med Rep*, 8(2), pp.662–668.

Hecker, L. et al., 2010. NADPH oxidase-4 mediates myofibroblast activation and fibrogenic responses to lung injury. *Nat Med*, 15, pp.1077–81.

Hecker, L. et al., 2014. Reversal of persistent fibrosis in aging by targeting Nox4-Nrf2 redox imbalance. *Sci Transl Med*, 6(231), pp.231–47.

Hertzog, M. et al., 2010. Molecular basis for the dual function of Eps8 on actin dynamics: bundling and capping. *PLoS Biol*, 8(6), p.e1000387.

Hewitson, T. & Becker, G., 1995. Interstitial myofibroblasts in IgA glomerulonephritis. *Am J Nephrol*, 15(2), pp.111–7.

Hill, C., 2009. Nucleocytoplasmic shuttling of Smad proteins. *Cell Res*, 19(1), pp.36–46.

Hill, R. et al., 2005. Selective evolution of stromal mesenchyme with p53 loss in response to epithelial tumorigenesis. *Cell*, 123(6), pp.1001–11.

Hinz, B. et al., 2001. Alpha-Smooth Muscle Actin expression upregulates fibroblast contractile activity. *Mol Biol Cell*, 12(9), pp.2730–41.

Hinz, B. et al., 2001. Mechanical tension controls granulation tissue contractile activity and myofibroblast differentiation. *Am J Pathol*, 159(3), pp.1009–20.

Hinz, B., 2016. Myofibroblasts. *Exp Eye Res*, 142, pp.56–70.

Hinz, B. et al., 2012. Recent developments in myofibroblast biology: paradigms for connective tissue remodeling. *Am J Pathol*, 180(4), pp.1340–55.

Hinz, B. & Gabbiani, G., 2003. Cell-matrix and cell-cell contacts of myofibroblasts: role in connective tissue remodeling. *Thromb Haemost*, 90(6), pp.993–1002.

Holmqvist, K. et al., 2003. The Shb adaptor protein causes Src-dependent cell spreading and activation of focal adhesion kinase in murine brain endothelial cells. *Cell Signal*, 15(2), pp.171–179.

Höner, B. et al., 1988. Modulation of cellular morphology and locomotory activity by antibodies against myosin. *J Cell Biol*, 107;6(1), pp.2181–9.

Horn, L. et al., 2013. CD34(low) and SMA(high) represent stromal signature in uterine cervical cancer and are markers for peritumoral stromal remodeling. *Ann Diag Pathol*, 17(6), pp.531–5.

Horowitz, J. et al., 2004. Activation of the pro-survival phosphatidylinositol 3-Kinase/AKT pathway by transforming growth factor-β1 in mesenchymal cells is mediated by p38 MAPK-dependent induction of an autocrine growth factor. *J Biol Chem*, 279(2), pp.1359–67.

Hu, B. & Phan, S., 2013. Myofibroblasts. *Curr Opin Rheumatol*, 25(1), pp.71–7.

Huang, C. et al., 2014. Cell type-specific expression of Eps8 in the mouse hippocampus. *BMC Neurosci*, 15, pp.26.

Hubchak, S. et al., 2009. Rac1 promotes TGF-beta-stimulated mesangial cell type I collagen expression through a PI3K/Akt-dependent mechanism. *Am J Physiol Renal Physiol*, 297(5), pp.1316–23.

Hubenak, J. et al., 2014. Mechanisms of injury to normal tissue after radiotherapy: a review. *Plast Reconstr Surg*, 133(1), pp.49–56.

Huse, M. et al., 2001. The TGFβ receptor activation process: an inhibitor to substrate-binding switch. *Mol Cell*, 8(3), pp.671–682.

Hwang, H. et al., 2011. CIIA functions as a molecular switch for the Rac1-specific GEF activity of SOS1. *J Cell Biol*, 195(3), pp.377–386.

Hwang, R. et al., 2008. Cancer-associated stromal fibroblasts promote pancreatic tumor progression. *Cancer Res*, 68(3), pp.918–26.

Innocenti, M. et al., 2005. Abi1 regulates the activity of N-WASP and WAVE in distinct actin-based processes. *Nat Cell Biol*, 7(10), pp.969–76.

Innocenti, M. et al., 2002. Mechanisms through which Sos-1 coordinates the activation of Ras and Rac. *J Cell Biol*, 156(1), pp.125–136.

Innocenti, M. et al., 2003. Phosphoinositide 3-kinase activates Rac by entering in a complex with Eps8, Abi1, and Sos-1. *J Cell Biol*, 160(1), pp.17–23.

Ishii, G. et al., 2003. Bone-marrow-derived myofibroblasts contribute to the cancer-induced stromal reaction. *Biochem Biophys Res Commun,* 309(1), pp.232–40.

Jarman, E. et al., 2014. An inhibitor of NADPH oxidase-4 attenuates established pulmonary fibrosis in a rodent disease model. *Am J Respir Cell Mol Biol*, 50(1), pp.158–69.

Jenei, V. et al., 2005. E3B1, a human homologue of the mouse gene product Abi-1, sensitizes activation of Rap1 in response to epidermal growth factor. *Exp Cell Res*, 310(2), pp.463–473.

Jiang, F. et al., 2014. NADPH oxidase-dependent redox signaling in TGF-β-mediated fibrotic responses. *Redox Biol*, 2, pp.267–72.

Jiang, J. et al., 2012. Liver fibrosis and hepatocyte apoptosis are attenuated by GKT137831, a novel NOX4/NOX1 inhibitor in vivo. *Free Radic Biol Med*, 53(2), pp.289–96.

Joannes, A. et al., 2016. FGF9 and FGF18 in idiopathic pulmonary fibrosis promote survival and migration and inhibit myofibroblast differentiation of human lung fibroblasts in vitro. *Am J Physiol Lung Cell Mol Physiol*, 310(7), pp.615–29.

Jobling, M. et al., 2006. Isoform-specific activation of latent transforming growth factor beta (LTGF-beta) by reactive oxygen species. *Radiat Res*, 166(6), pp.839–48.

Jun, J. et al., 2005. Scleroderma fibroblasts demonstrate enhanced activation of

Akt (protein kinase B) in situ. *J Invest Dermatol*, 124(2), pp.298–303.

Jung, K. et al., 2013. A novel PI3K inhibitor alleviates fibrotic responses in fibroblasts derived from Peyronie's plaques. *Int J Oncol*, 42(6), pp.2001–8.

Kallio, M. et al., 2011. Chipster: user-friendly analysis software for microarray and other high-throughput data. *BMC Genomics*, 12(1), p.507.

Kalluri, R. & Weinberg, R., 2009. The basics of epithelial-mesenchymal transition. *J Clin Invest*, 119(6), pp.1420–8.

Kang, H. et al., 2012. Gene expression profiles predictive of outcome and age in infant acute lymphoblastic leukemia: a Children's Oncology Group study. *Blood*, 119(8), pp.1872–1881.

Karaköse, E. et al., 2010. The kindlins at a glance. *J Cell Sci*, 123(14), pp.2353–6.

Karamichos, D. et al., 2014. Reversal of fibrosis by TGF-β3 in a 3D in vitro model. *Exp Eye Res*, 124, pp.31–6.

Karlsson, T. et al., 1995. Molecular interactions of the Src homology 2 domain protein Shb with phosphotyrosine residues, tyrosine kinase receptors and Src homology 3 domain proteins. *Oncogene*, 10(8), pp.1475–83.

Karlsson, T. & Welsh, M., 1997. Modulation of Src homology 3 proteins by the proline-rich adaptor protein Shb. *Exp Cell Res*, 275(231), pp.269–75.

Katso, R. et al., 2006. Phosphoinositide 3-Kinase C2beta regulates cytoskeletal organization and cell migration via Rac-dependent mechanisms. *Mol Biol Cell*, 17(9), pp.3729–44.

Kavsak, P. et al., 2000. Smad7 binds to Smurf2 to form an E3 ubiquitin ligase that targets the TGF receptor for degradation. *Mol Cell*, 6, pp.1365–75.

Kellermann, M. et al., 2007. Myofibroblasts in the stroma of oral squamous cell carcinoma are associated with poor prognosis. *Histopathology*, 51(6), pp.849–53.

Khanday, F. et al., 2006. Sos-mediated activation of rac1 by p66shc. *J Cell Biol*, 172(6), pp.817–22.

Kidd, S. et al., 2012. Origins of the tumor microenvironment: quantitative assessment of adipose-derived and bone marrow-derived stroma. *PloS one*, 7(2), p.30563.

Kim, B. et al., 2006. Smad4 signalling in T cells is required for suppression of gastrointestinal cancer. *Nature*, 441(7096), pp.1015–9.

King, T. et al., 2014. A phase 3 trial of pirfenidone in patients with idiopathic pulmonary fibrosis. *N Engl J Med*, 370(22), pp.2083–92.

Koesters, R. et al., 2010. Tubular overexpression of transforming growth factor-beta1 induces autophagy and fibrosis but not mesenchymal transition of renal epithelial cells. *Am J Pathol*, 177(2), pp.632–43.

Koinuma, D. et al., 2003. Arkadia amplifies TGF-b superfamily signalling through degradation of Smad7. *EMBO J*, 22(24), pp.6458–70.

Kojima, M. et al., 2014. Human subperitoneal fibroblast and cancer cell interaction creates microenvironment that enhances tumor progression and metastasis. *PloS one*, 9(2), p.88018.

Kotula, L., 2012. Abi1, a critical molecule coordinating actin cytoskeleton reorganization with PI-3 kinase and growth signaling. *FEBS lett*, 586(17), pp.2790–4.

Kramann, R. et al., 2013. Understanding the origin, activation and regulation of matrix-producing myofibroblasts for treatment of fibrotic disease. *J Pathol*, 231(3), pp.273–89.

Kretzschmar, M. et al., 1999. A mechanism of repression of TGFbeta/ Smad signaling by oncogenic Ras. *Genes Dev*, 13(7), pp.804–16.

Kulasekaran, P. et al., 2009. Endothelin-1 and transforming growth factor-beta1 independently induce fibroblast resistance to apoptosis via AKT activation. *Am J Respir Cell Mol Biol*, 41(4), pp.484–93.

Kurisaki, A. et al., 2001. Transforming growth factor-beta induces nuclear import of Smad3 in an importin-beta1 and Ran-dependent manner. *Mol Biol Cell*, 12(4), pp.1079–91.

Kurose, K. et al., 2002. Frequent somatic mutations in PTEN and TP53 are

mutually exclusive in the stroma of breast carcinomas. *Nat Genet*, 32(3), pp.355–7.

Lagares, D. et al., 2012. Inhibition of focal adhesion kinase prevents experimental lung fibrosis and myofibroblast formation. *Arthritis Rheum*, 64(5), pp.1653–64.

Lakhe-Reddy, S. et al., 2006. Beta8 integrin binds Rho GDP dissociation inhibitor-1 and activates Rac1 to inhibit mesangial cell myofibroblast differentiation. *J Biol Chem*, 281(28), pp.19688–99.

Lamouille, S. & Derynck, R., 2011. Emergence of the phosphoinositide 3-kinase-Akt-mammalian target of rapamycin axis in transforming growth factor-β-induced epithelial-mesenchymal transition. *Cells Tissues Organs*, 193(1–2), pp.8–22.

Lang, F. & Cohen, P., 2001. Regulation and physiological roles of serum- and glucocorticoid-induced protein kinase isoforms. *Sci STKE*, 2001(108), p.17.

Lanzetti, L. et al., 2000. The Eps8 protein coordinates EGF receptor signalling through Rac and trafficking through Rab5. *Nature*, 408(6810), pp.374–7.

Larson, B. et al., 2010. Scarless fetal wound healing: a basic science review. *Plast Reconstr Surg*, 126(4), pp.1172–80.

Law, C. et al., 2014. Voom: Precision weights unlock linear model analysis tools for RNA-seq read counts. *Genome Biol*, 15(2), p.29.

Leask, A. et al., 2008. Loss of protein kinase Cepsilon results in impaired cutaneous wound closure and myofibroblast function. *J Cell Sci*, 121(20), pp.3459–67.

LeBleu, V. et al., 2013. Origin and function of myofibroblasts in kidney fibrosis. *Nat Med*, 19(8), pp.1047–53.

Lee, M. et al., 2007. TGF-beta activates Erk MAP kinase signalling through direct phosphorylation of ShcA. *EMBO J*, 26(17), pp.3957–67.

Legate, K. et al., 2009. Genetic and cell biological analysis of integrin outside-in signaling. *Genes Dev*, 23(4), pp.397–418.

Leng, Y. et al., 2005. Abelson-interactor-1 promotes WAVE2 membrane

translocation and Abelson-mediated tyrosine phosphorylation required for WAVE2 activation. *Proc Natl Acad Sci USA*, 102(4), pp.1098–103.

Leu, T. et al., 2004. Participation of p97Eps8 in Src-mediated transformation. *J Biol Chem*, 279(11), pp.9875–81.

Leung, T. et al., 1996. The p160 RhoA-binding kinase ROK alpha is a member of a kinase family and is involved in the reorganization of the cytoskeleton. *Mol Cell Biol*, 16(10), pp.5313–27.

Levy, L. et al., 2007. Arkadia activates Smad3/Smad4-dependent transcription by triggering signal-induced SnoN degradation. *Mol Cell Biol*, 27(17), pp.6068–83.

Li, G. et al., 2016. ILK-PI3K/AKT pathway participates in cutaneous wound contraction by regulating fibroblast migration and differentiation to myofibroblast. *Lab Invest*, 96, pp.741–51.

Li, W.et al., 2008. Reversal of Myofibroblasts by Amniotic Membrane Stromal Extract. *J Cell Physiol*, 215(3), pp.657–64.

Lim, M. et al., 2014. Induction of galectin-1 by TGF-β1 accelerates fibrosis through enhancing nuclear retention of Smad2. *Exp Cell Res*, 326(1), pp.125–35.

Liu, C. et al., 2009. TACE-mediated ectodomain shedding of the type I TGF-beta receptor down-regulates TGF-beta signalling. *Mol Cell*, 35(1), pp.26–36.

Liu, G. et al., 2010. miR-21 mediates fibrogenic activation of pulmonary fibroblasts and lung fibrosis. *J Exp Med*, 207(8), pp.1589–97.

Liu, P. et al., 2010. The interplay between Eps8 and IRSp53 contributes to Src-mediated transformation. *Oncogene*, 29(27), pp.3977–89.

Liu, R. et al., 2010. Oxidative modification of nuclear mitogen-activated protein kinase phosphatase 1 is involved in transforming growth factor beta1-induced expression of plasminogen activator inhibitor 1 in fibroblasts. *J Biol Chem*, 285(21), pp.16239–47.

Liu, S. et al., 2008. Role of Rac1 in a bleomycin-induced scleroderma model using fibroblast-specific Rac1-knockout mice. *Arthritis Rheum*, 58(7),

pp.2189–95.

Liu, X. et al., 2013. Reversibility of Liver Fibrosis and Inactivation of Fibrogenic Myofibroblasts. *Curr Pathobiol Rep*, 1(3), pp.209–14.

Liu, Z. et al., 2012. MicroRNA-146a modulates TGF-β1-induced phenotypic differentiation in human dermal fibroblasts by targeting SMAD4. *Arch Dermatol Res*, 304(3), pp.195–202.

Loeffler, M. et al., 2006. Targeting tumor-associated fibroblasts improves cancer chemotherapy by increasing intratumoral drug uptake. *J Clin Invest*, 116(7), pp.1955–62.

Lomas, N. et al., 2012. Idiopathic pulmonary fibrosis: Immunohistochemical analysis provides fresh insights into lung tissue remodelling with implications for novel prognostic markers. *Int J Clin Exp Pathol*, 5(1), pp.58–71.

Lönn, P. et al., 2010. PARP-1 attenuates Smad-mediated transcription. *Mol Cell*, 40(4), pp.521–32.

Lu, L. et al., 2002. Role of the Src homology 2 domain-containing protein Shb in murine brain endothelial cell proliferation and differentiation. *Cell Growth Differ*, 13(3), pp.141–8.

Lyons, R. et al., 1988. Proteolytic activation of latent transforming growth factor-beta from fibroblast-conditioned medium. *J Cell Biol*, 106(5), pp.1659–65.

Maa, M. et al., 2007. Eps8 facilitates cellular growth and motility of colon cancer cells by increasing the expression and activity of focal adhesion kinase. *J Biol Chem,* 282(27), pp.19399–409.

Macieira-Coelho, A., 1998. Markers of cell senescence. *Mech Ageing Dev*, 104, pp.207–211.

Maltseva, O. et al., 2001. Fibroblast growth factor reversal of the corneal myofibroblast phenotype. *Invest Ophthalmol Vis Sci*, 42(11), pp.2490–5.

Manickam, N. et al., 2014. RhoA/Rho kinase mediates TGF-β1-induced kidney myofibroblast activation through Poldip2/Nox4-derived reactive oxygen

species. *Am J Physiol Renal Physiol*, 307(41), pp.159-71.

Manser, E. et al., 1997. Expression of constitutively active alpha-PAK reveals effects of the kinase on actin and focal complexes. *Mol Cell Biol*, 17(3), pp.1129–43.

Marra, F. et al., 1997. Phosphatidylinositol 3-kinase is required for platelet-derived growth factor's actions on hepatic stellate cells. *Gastroenterology*, 112(4), pp.1297–306.

Marsh, D. et al., 2011. Stromal features are predictive of disease mortality in oral cancer patients. *J Pathol*, 223(4), pp.470–81.

Martinez-Outschoorn, U. et al., 2012. Hereditary ovarian cancer and two-compartment tumor metabolism: epithelial loss of BRCA1 induces hydrogen peroxide production, driving oxidative stress and NFκB activation in the tumor stroma. *Cell Cycle*, 11(22), pp.4152–66.

Martinez-Outschoorn, U. et al., 2012. Ketone bodies and two-compartment tumor metabolism: stromal ketone production fuels mitochondrial biogenesis in epithelial cancer cells. *Cell Cycle*, 11(21), pp.3956–63.

Martinu, L. et al., 2002. Endocytosis of epidermal growth factor receptor regulated by Grb2-mediated recruitment of the Rab5 GTPase-activating protein RN-tre. *J Biol Chem*, 277(52), pp.50996–1002.

Massagué, J., 2012. TGFβ signalling in context. *Nat Rev Mol Cell Biol*, 13(10), pp.616–30.

Massagué, J. et al., 2005. Smad transcription factors. *Genes Dev*, 19(23), pp.2783–810.

Matoskova, B. et al., 1995. Constitutive phosphorylation of eps8 in tumor cell lines: relevance to malignant transformation. *Mol Cell Biol*, 15(7), pp.3805–12.

Mellone, M. et al., 2016. Induction of fibroblast senescence generates a non-fibrogenic myofibroblast phenotype that differentially impacts on cancer prognosis. *Aging*. DOI: 10.18632/aging.101127 (epub ahead of print)

Menna, E. et al., 2013. Eps8 controls dendritic spine density and synaptic

plasticity through its actin-capping activity. *EMBO J*, 32(12), pp.1730–44.

Meyer, L. et al., 2000. Reduced hyaluronan in keloid tissue and cultured keloid fibroblasts. *J Invest Dermatol*, 114(5), pp.953–9.

Mia, M. et al., 2014. Interleukin-1β attenuates myofibroblast formation and extracellular matrix production in dermal and lung fibroblasts exposed to transforming growth factor-β1. *PloS one*, 9(3), p.91559.

Miki, H. et al., 2000. IRSp53 is an essential intermediate between Rac and WAVE in the regulation of membrane ruffling. *Nature*, 408(6813), pp.732–5.

Miralles, F. et al., 2003. Actin Dynamics Control SRF Activity by Regulation of Its Coactivator MAL. *Cell*, 113, pp.329–42.

Mirkovic, S. et al., 2002. Attenuation of cardiac fibrosis by pirfenidone and amiloride in DOCA-salt hypertensive rats. *Br J Pharmacol*, 135(4), pp.961–8.

Mitra, S. et al., 2011. c-Jun N-terminal kinase 2 (JNK2) enhances cell migration through epidermal growth factor substrate 8 (EPS8). *J Biol Chem*, 286(17), pp.15287–97.

Miyazono, K., 2000. Positive and negative regulation of TGF- β signaling. *J Cell Sci*, 1109(113), pp.1101–9.

Modarressi, A. et al., 2010. Hypoxia impairs skin myofibroblast differentiation and function. *J Invest Dermatol*, 130(12), pp.2818–27.

Mondin, M. et al., 2007. Alterations in cytoskeletal protein expression by mycophenolic acid in human mesangial cells requires Rac inactivation. *Biochem Pharmacol*, 73(9), pp.1491–8.

Mori, Y. et al., 2003. Expression and regulation of intracellular SMAD signaling in scleroderma skin fibroblasts. *Arthritis Rheum*, 48(7), pp.1964–78.

Moustakas, A. et al., 2001. Smad regulation in TGF-beta signal transduction. *J Cell Sci*, 114(24), pp.4359–69.

Mu, D. et al., 2002. The integrin alpha(v)beta8 mediates epithelial homeostasis through MT1-MMP-dependent activation of TGF-beta1. *J Cell Biol,* 157(3),

pp.493–507.

Mu, Y. et al., 2012. Non-Smad signaling pathways. *Cell Tissue Res*, 347(1), pp.11–20.

Muller, F., 2000. The nature and mechanism of superoxide production by the electron transport chain: its relevance to aging. *J Am Aging Assoc*, 23(16), pp.227–53.

Murad, F., 2006. Nitric oxide and cyclic GMP in cell signaling and drug development. *N Engl J Med*, 355(19) pp.2003–2011.

Murphy-Ullrich, J. & Poczatek, M., 2000. Activation of latent TGF-beta by thrombospondin-1: mechanisms and physiology. *Cytokine Growth Factor Rev*, 11(1–2), pp.59–69.

Nagarajan, R. et al., 1999. Regulation of Smad7 Promoter by Direct Association with Smad3 and Smad4. *J Biol Chem*, 274(47), pp.33412–8.

Nakao, A. et al., 1997. Identification of Smad7, a TGFbeta-inducible antagonist of TGF-beta signalling. *Nature*, 389(6651), pp.631–5.

Ng, C. et al., 2005. Interstitial fluid flow induces myofibroblast differentiation and collagen alignment in vitro. *J Cell Sci*, 118(20), pp.4731–9.

O'Connell, J. et al., 2011. VEGF-A and Tenascin-C produced by S100A4+ stromal cells are important for metastatic colonization. *Proc Natl Acad Sci*, 108(38), pp.16002–7.

Offenhauser, N. et al., 2006. Increased ethanol resistance and consumption in Eps8 knockout mice correlates with altered actin dynamics. *Cell*, 127(1), pp.213–26.

Offenhauser, N. et al., 2004. The eps8 family of proteins links growth factor stimulation to actin reorganization generating functional redundancy in the Ras/Rac pathway. *Mol Biol Cell*, 15(1), pp.91–8.

Olive, K. et al., 2009. Inhibition of Hedgehog signaling enhances delivery of chemotherapy in a mouse model of pancreatic cancer. *Science*, 324(5933), pp.1457–61.

Olsen, A. et al., 2011. Hepatic stellate cells require a stiff environment for myofibroblastic differentiation. *Am J Physiol Gastrointest Liver Physiol*, 301(1), pp.110–8.

Olt, J. et al., 2014. The actin-binding proteins eps8 and gelsolin have complementary roles in regulating the growth and stability of mechanosensory hair bundles of Mammalian cochlear outer hair cells. *PloS one*, 9(1), p.87331.

Olumi, A. et al., 1999. Carcinoma-associated fibroblasts direct tumor progression of initiated human prostatic epithelium. *Cancer Res*, pp.5002–11.

Orimo, A. et al., 2005. Stromal fibroblasts present in invasive human breast carcinomas promote tumor growth and angiogenesis through elevated SDF-1/CXCL12 secretion. *Cell*, 121(3), pp.335–48.

Orr, J. et al., 2004. Mechanism of action of the antifibrogenic compound gliotoxin in rat liver cells. *Hepatology*, 40(1), pp.232-42.

Papakonstanti, E. & Stournaras, C., 2002. Association of PI-3 kinase with PAK1 leads to actin phosphorylation and cytoskeletal reorganization. *Mol Biol Cell*, 13(8), pp.2946–62.

Pardali, E. et al., 2010. Signaling by members of the TGF-beta family in vascular morphogenesis and disease. *Trends Cell Biol,* 20(9), pp.556–67.

Patocs, A. et al., 2007. Breast-cancer stromal cells with TP53 mutations and nodal metastases. *N Engl J Med*, 357, pp.2543–51.

Pavlides, S. et al., 2010. Transcriptional evidence for the 'Reverse Warburg Effect' in human breast cancer tumor stroma and metastasis: similarities with oxidative stress, inflammation, Alzheimer's disease, and 'Neuron-Glia Metabolic Coupling'. *Aging*, 2(4), pp.185–99.

Pellegrin, S. & Mellor, H., 2007. Actin stress fibres. *J Cell Sci*, 120(20), pp.3491–9.

Piek, E. et al., 2001. Functional characterization of transforming growth factor beta signaling in Smad2- and Smad3-deficient fibroblasts. *J Biol Chem*, 276(23), pp.19945–53.

Pietras, K. & Ostman, A., 2010. Hallmarks of cancer: interactions with the tumor stroma. *Exp Cell Res*, 316(8), pp.1324–31.

Polanska, U. & Orimo, A., 2013. Carcinoma-associated fibroblasts: non-neoplastic tumour-promoting mesenchymal cells. *J Cell Physiol*, 228(8), pp.1651–7.

Poncelet, A. et al., 2007. Cell phenotype-specific down-regulation of Smad3 involves decreased gene activation as well as protein degradation. *J Biol Chem*, 282(21), pp.15534–40.

Puré, E. & Lo, A., 2016. Can Targeting Stroma Pave the Way to Enhanced Antitumor Immunity and Immunotherapy of Solid Tumors? *Cancer Immunol Res*, 4(4), pp.269–78.

Rajkumar, V. et al., 2005. Shared expression of phenotypic markers in systemic sclerosis indicates a convergence of pericytes and fibroblasts to a myofibroblast lineage in fibrosis. *Arthritis Res Ther*, 7(5), pp.1113-23.

Räsänen, K. & Vaheri, A., 2010. Activation of fibroblasts in cancer stroma. *Exp Cell Res*, 316(17), pp.2713–22.

Remy, I. et al., 2004. PKB/Akt modulates TGF-beta signalling through a direct interaction with Smad3. *Nat Cell Biol*, 6(4), pp.358–65.

Richerioux, N. et al., 2012. Rho-ROCK and Rac-PAK signaling pathways have opposing effects on the cell-to-cell spread of Marek's Disease Virus. *PloS one*, 7(8), p.44072.

Roberts, A. & Wakefield, L., 2003. The two faces of transforming growth factor in carcinogenesis. *Proc Natl Acad Sci*, 100(15), pp.8621–3.

Roberts, A. et al., 2007. Germline gain-of-function mutations in SOS1 cause Noonan syndrome. *Nat Genet*, 39(1), pp.70–4.

Rønnov-Jessen, L. & Petersen, O., 1993. Induction of alpha-smooth muscle actin by transforming growth factor-beta 1 in quiescent human breast gland fibroblasts. Implications for myofibroblast generation in breast neoplasia. *Lab Invest*, 68(6), pp.696–707.

Rudnicka, L. et al., 1994. Elevated expression of type VII collagen in the skin of

patients with systemic sclerosis. *J Clin Invest*, 93(4), pp.1709–15.

Saha, D. et al., 2001. Oncogenic ras represses transforming growth factor-beta /Smad signaling by degrading tumor suppressor Smad4. *J Biol Chem*, 276(31), pp.29531–7.

Salazar-Montes, A. et al., 2008. Potent antioxidant role of pirfenidone in experimental cirrhosis. *Eur J Pharmacol*, 595, pp.69–77.

Salem, A. et al., 2012. Downregulation of stromal BRCA1 drives breast cancer tumor growth via upregulation of HIF-1α, autophagy and ketone body production. *Cell Cycle,* 11(22), pp.4167–73.

Samarasinghe, V. et al., 2011. Management of high-risk squamous cell carcinoma of the skin. *Expert Rev Anticancer Ther*, 11(5), pp.763–9.

Sambo, P. et al., 2001. Oxidative stress in scleroderma: maintenance of scleroderma fibroblast phenotype by the constitutive up-regulation of reactive oxygen species generation through the NADPH oxidase complex pathway. *Arthritis Rheum*, 44(11), pp.2653–64.

Sampson, N. et al., 2011. ROS signaling by NOX4 drives fibroblast-to-myofibroblast differentiation in the diseased prostatic stroma. *Mol Endocrinol*, 25(3), pp.503–15.

Sander, E. et al., 1999. Rac downregulates Rho activity: reciprocal balance between both GTPases determines cellular morphology and migratory behavior. *J Cell Biol*, 147(5), pp.1009–22.

Sanders, L. et al., 1999. Inhibition of myosin light chain kinase by p21-activated kinase. *Science*, 283(5410), pp.2083–5.

Sanders, Y. et al., 2011. Epigenetic regulation of thy-1 by histone deacetylase inhibitor in rat lung fibroblasts. *Am J Respir Cell Mol Biol*, 45(1), pp.16–23.

Sarbassov, D. et al., 2005. Phosphorylation and regulation of Akt/PKB by the rictor-mTOR complex. *Science*, 307(5712), pp.1098–101.

Sargent, J. & Whitfield, M., 2011. Capturing the heterogeneity in systemic sclerosis wide genome-wide expression profiling. *Expert Rev Clin Immunol*, 7(4), pp.463–473.

Satish, L. et al., 2006. Gene expression patterns in isolated keloid fibroblasts. *Wound Repair Regen*, 14(4), pp.463–70.

Schievenbusch, S. et al., 2009. Profiling of anti-fibrotic signaling by hepatocyte growth factor in renal fibroblasts. *Biochem Biophys Res Commun*, 385(1), pp.55–61.

Scita, G. et al., 2001. An effector region in Eps8 is responsible for the activation of the Rac-specific GEF activity of Sos-1 and for the proper localization of the Rac-based actin-polymerizing machine. *J Cell Biol*, 154(5), pp.1031–44.

Scita, G. et al., 1999. EPS8 and E3B1 transduce signals from Ras to Rac. *Nature*, 401(6750), pp.290–3.

Serini, G. et al., 1998. The fibronectin domain ED-A is crucial for myofibroblastic phenotype induction by transforming growth factor-beta1. *J Cell Biol*, 142(3), pp.873–81.

Serrander, L. et al., 2007. NOX4 activity is determined by mRNA levels and reveals a unique pattern of ROS generation. *Biochem J,* 406(1), pp.105–14.

Shen, L. et al., 2014. Gadolinium promoted proliferation in mouse embryo fibroblast NIH3T3 cells through Rac and PI3K/Akt signaling pathways. *Biometals*, 27(4), pp.753–62.

Shih, W. & Yamada, S., 2012. N-cadherin as a key regulator of collective cell migration in a 3D environment. *Cell Adh Migr*, 6(6), pp.513–7.

Shimizu, T. et al., 1998. Pirfenidone improves renal function and fibrosis in the post-obstructed kidney. *Kidney Int*, 54(1), pp.99–109.

Sini, P. et al., 2004. Abl-dependent tyrosine phosphorylation of Sos-1 mediates growth-factor-induced Rac activation. *Nat Cell Biol*, 6(3), pp.268–74.

Sohara, N. et al., 2002. Reversal of activation of human myofibroblast-like cells by culture on a basement membrane-like substrate. *J Hepatol*, 37(2), pp.214–21.

Son, G. et al., 2009. Inhibition of phosphatidylinositol 3-kinase signaling in hepatic stellate cells blocks the progression of hepatic fibrosis.

Hepatology, 50(5), pp.1512–23.

Sorrentino, A. et al., 2008. The type I TGF-beta receptor engages TRAF6 to activate TAK1 in a receptor kinase-independent manner. *Nat Cell Biol*, 10(10), pp.1199–207.

Spurr, I. et al., 2012. Targeting tumour proliferation with a small-molecule inhibitor of AICAR transformylase homodimerization. *Chembiochem*, 13(11), pp.1628–34.

Steffen, A. et al., 2004. Sra-1 and Nap1 link Rac to actin assembly driving lamellipodia formation. *EMBO J*, 23(4), pp.749–59.

Stover, D. et al., 2007. A delicate balance: TGF-beta and the tumor microenvironment. *J Cell Biochem*, 101(4), pp.851–61.

Straussman, R. et al., 2012. Tumour micro-environment elicits innate resistance to RAF inhibitors through HGF secretion. *Nature*, 487(7408), pp.500–4.

Stroschein, S., 1999. Negative feedback regulation of TGF- signaling by the SnoN oncoprotein. *Science*, 286(5440), pp.771–4.

Sugimoto, H. & Mundel, T., 2006. Identification of fibroblast heterogeneity in the tumor microenvironment. *Cancer Biol Ther,* 5(12), pp.1640–6.

Sun, Q. et al., 2006. Defining the mammalian CArGome. *Genome Res*, 16(2), pp.197–207.

Suzuki, H. et al., 2003. Epidermal growth factor receptor tyrosine kinase inhibition augments a murine model of pulmonary fibrosis. *Cancer Res*, 63(16), pp.5054–9.

Szklarczyk, D. et al., 2015. STRING v10: protein-protein interaction networks, integrated over the tree of life. *Nucleic Acids Res*, 43, pp.447–52.

Thillainadesan, G. et al., 2012. TGF-β-dependent active demethylation and expression of the p15ink4b tumor suppressor are impaired by the ZNF217/CoREST complex. *Mol Cell*, 46(5), pp.636–49.

Tingstrom, A. et al., 1992. Regulation of fibroblast-mediated collagen gel contraction by platelet-derived growth factor, interleukin-1 alpha and

transforming growth factor-beta 1. *J Cell Sci*, 102(2), pp.315–22.

Tobar, N. et al., 2014. c-Jun N terminal kinase modulates NOX-4 derived ROS production and myofibroblasts differentiation in human breast stromal cells. *BMC Cancer*, 14(1), p.640.

Tocchetti, A. et al., 2003. In silico analysis of the EPS8 gene family: genomic organization, expression profile, and protein structure. *Genomics*, 81(2), pp.234–44.

Tocchetti, A. et al., 2010. Loss of the actin remodeler Eps8 causes intestinal defects and improved metabolic status in mice. *PLoS One*, 5(3), p.9468.

Tomasek, J. et al., 2002. Myofibroblasts and mechano-regulation of connective tissue remodelling. *Nat Rev Mol Cell Biol*, 3(5), pp.349–63.

Trachootham, D. et al., 2008. Redox regulation of cell survival. *Antioxid Redox Signal,* 10(8), pp.1343–74.

Troeger, J. et al., 2012. Deactivation of hepatic stellate cells during liver fibrosis resolution in mice. *Gastroenterology*, 143(4), pp.1073–83.

Tsukazaki, T. et al., 1998. SARA, a FYVE domain protein that recruits Smad2 to the TGFbeta receptor. *Cell*, 95(6), pp.779–91.

Ulrich, D. et al., 2010. Matrix metalloproteinases and tissue inhibitors of metalloproteinases in patients with different types of scars and keloids. *J Plast Reconstr Aesthet Surg*, 63(6), pp.1015–21.

Underwood, T. et al., 2015. Cancer-associated fibroblasts predict poor outcome and promote periostin-dependent invasion in oesophageal adenocarcinoma. *J Pathol*, 235(3), pp.466–77.

Vaggi, F. et al., 2011. The Eps8/IRSp53/VASP network differentially controls actin capping and bundling in filopodia formation. *PLoS Comput Biol*, 7(7), p.1002088.

Valente, E. et al., 2003. L-arginine and phosphodiesterase (PDE) inhibitors counteract fibrosis in the Peyronie's fibrotic plaque and related fibroblast cultures. *Nitric Oxide*, 9(4), pp.229–44.

Vancheri, C. et al., 2010. Idiopathic pulmonary fibrosis: a disease with similarities and links to cancer biology. *Eur Respir J*, 35(3), pp.496–504.

Vanhaesebroeck, B. et al., 2001. Synthesis and function of 3- phosphorylated inositol lipids. *Annu Rev Biochem*, 70, pp.535–602.

Vedrenne, N. et al., 2012. The complex dialogue between (myo)fibroblasts and the extracellular matrix during skin repair processes and ageing. *Pathol Biol*, 60(1), pp.20–7.

Vercelino, R. et al., 2010. S-nitroso-N-acetylcysteine attenuates liver fibrosis in cirrhotic rats. *J Mol Med (Berl)*, 88(4), pp.401–11.

Verhaegen, P. et al., 2009. Differences in collagen architecture between keloid, hypertrophic scar, normotrophic scar, and normal skin: An objective histopathological analysis. *Wound Rep Regen*, 17(5), pp.649–56.

Voloshenyuk, T. et al., 2011. Induction of cardiac fibroblast lysyl oxidase by TGF-β1 requires PI3K/Akt, Smad3, and MAPK signaling. *Cytokine*, 55(1), pp.90–7.

de Vries, E. et al., 2005. Predictions of skin cancer incidence in the Netherlands up to 2015. *Br J Dermatol*, 152(3), pp.481–8.

Wang, H. et al., 2010. EPS8 upregulates FOXM1 expression, enhancing cell growth and motility. *Carcinogenesis*, 31(6), pp.1132–41.

Wang, H. et al., 2009. Role for EPS8 in squamous carcinogenesis. *Carcinogenesis*, 30(1), pp.165–174.

Wang, J. et al., 2002. Transcriptional regulation of a contractile gene by mechanical forces applied through integrins in osteoblasts. *J Biol Chem*, 277(25), pp.22889–95.

Wang, L. et al., 2013. Real-time quantitative polymerase chain reaction assay for detecting the eps8 gene in acute myeloid leukemia. *Clin Lab*, 59 (11-12), pp.1261–9.

Wang, T. et al., 2013. Role of the adapter protein Abi1 in actin-associated signaling and smooth muscle contraction. *J Biol Chem*, 288(28), pp.20713–22.

Wang, Y. et al., 2006. Association between enhanced type I collagen expression and epigenetic repression of the FLI1 gene in scleroderma fibroblasts. *Arthritis Rheum*, 54(7), pp.2271–9.

Watanabe, N. et al., 1999. Cooperation between mDia1 and ROCK in Rho-induced actin reorganization. *Nat Cell Biol*, 1(3), pp.136–43.

Van De Water, L. et al., 2013. Mechanoregulation of the myofibroblast in wound contraction, scarring, and fibrosis: opportunities for new therapeutic intervention. *Adv Wound Care (New Rochelle)*, 2(4), pp.122–41.

Webber, J. et al., 2010. Cancer exosomes trigger fibroblast to myofibroblast differentiation. *Cancer Res*, 70(23), pp.9621–30.

Wei, X. et al., 2009. Advanced oxidation protein products induce mesangial cell perturbation through PKC-dependent activation of NADPH oxidase. *Am J Physiol Renal Physiol*, 296(2), pp.427–37.

Welsch, T. et al., 2007. Eps8 is increased in pancreatic cancer and required for dynamic actin-based cell protrusions and intercellular cytoskeletal organization. *Cancer Lett*, 255(2), pp.205–18.

Welsch, T. et al., 2010. Eps8 is recruited to lysosomes and subjected to chaperone-mediated autophagy in cancer cells. *Exp Cell Res*, 316(12), pp.1914–24.

Welsh, N. et al., 2002. Overexpression of the Shb SH2 domain-protein in insulin-producing cells leads to altered signaling through the IRS-1 and IRS-2 proteins. *Mol Med,* 8(11), pp.695–704.

Werner, A. et al., 2013. SCFFbxw5 mediates transient degradation of actin remodeller Eps8 to allow proper mitotic progression. *Nat Cell Biol*, 15(2), pp.179–188.

De Wever, O. et al., 2008. Stromal myofibroblasts are drivers of invasive cancer growth. *Int J Cancer*, 123(10), pp.2229–38.

Wheeler, S. et al., 2014. Enhancement of head and neck squamous cell carcinoma proliferation, invasion, and metastasis by tumor-associated fibroblasts in preclinical models. *Head Neck*, 36(3), pp.385–92.

Wiater, E. et al., 2006. Identification of distinct inhibin and transforming growth factor beta-binding sites on betaglycan: functional separation of betaglycan co-receptor actions. *J Biol Chem,* 281(25), pp.17011–22.

Wick, G. et al., 2013. The immunology of fibrosis. *Annu Rev Immunol*, 31, pp.107-35

Witkiewicz, A. et al., 2011. Association of RB/p16-pathway perturbations with DCIS recurrence: dependence on tumor versus tissue microenvironment. *Am J Pathol*, 179(3), pp.1171–8.

Witt, W. et al., 2014. Reversal of myofibroblastic activation by polyunsaturated fatty acids in valvular interstitial cells from aortic valves. Role of RhoA/G-actin/MRTF signalling. *J Mol Cell Cardiol*, 74, pp.127–38.

Wong, W. et al., 1994. Evolutionary conservation of the EPS8 gene and its mapping to human chromosome 12q23-q24. *Oncogene*, 9(10), pp.3057–61.

Wood, O. et al., 2016. Gene expression analysis of TIL rich HPV-driven head and neck tumors reveals a distinct B-cell signature when compared to HPV independent tumors. *Oncotarget*, 5, p.10788.

Wright, M. et al., 2001. Gliotoxin stimulates the apoptosis of human and rat hepatic stellate cells and enhances the resolution of liver fibrosis in rats. *Gastroenterology*, 121(3), pp.685-98.

Wu, G. et al., 2000. Structural basis of Smad2 recognition by the Smad anchor for receptor activation. *Science*, 287(5450), pp.92–7.

Wu, J. et al., 2002. Structural mechanism of Smad4 recognition by the nuclear oncoprotein Ski: insights on Ski-mediated repression of TGF-beta signaling. *Cell*, 111(3), pp.357–67.

Wynn, T., 2009. Fibrotic disease and the TH 1/TH 2 paradigm. *Nat Rev Immunol*, 4(8), pp.583–94.

Xia, H. et al., 2010. Pathologic caveolin-1 regulation of PTEN in idiopathic pulmonary fibrosis. *Am J Pathol,* 176(6), pp.2626–37.

Xu, M. et al., 2009. Epidermal growth factor receptor pathway substrate 8 is

overexpressed in human pituitary tumors: role in proliferation and survival. *Endocrinology*, 150(5), pp.2064–2071.

Xu, S. et al., 2009. Rac inhibition reverses the phenotype of fibrotic fibroblasts. *PloS one*, 4(10), p.7438.

Yakymovych, I. et al., 2001. Regulation of Smad signaling by protein kinase C. *FASEB J*, 15(3), pp.553–5.

Yamashita, M. et al., 2008. TRAF6 mediates Smad-independent activation of JNK and p38 by TGF-β. *Mol Cell*, 31(6), pp.918–24.

Yang, T. et al., 2010. Mithramycin inhibits human epithelial carcinoma cell proliferation and migration involving downregulation of Eps8 expression. *Chem Biol Interact*, 183(1), pp.181–6.

Yang, Y. et al., 2003. Hierarchical model of gene regulation by transforming growth factor beta. *Proc Natl Acad Sci USA*, 100(18), pp.10269–74.

Yap, L. et al., 2009. Upregulation of Eps8 in oral squamous cell carcinoma promotes cell migration and invasion through integrin-dependent Rac1 activation. *Oncogene*, 28(27), pp.2524–34.

Yi, J. et al., 2005. Type I transforming growth factor beta receptor binds to and activates phosphatidylinositol 3-kinase. *J Biol Chem*, 280(11), pp.10870–6.

Yu, Q. & Stamenkovic, I., 2000. Cell surface-localized matrix metalloproteinase-9 proteolytically activates TGF-beta and promotes tumor invasion and angiogenesis. *Genes Dev*, 14(2), pp.163–76.

Zenzmaier, C. et al., 2010. Attenuated proliferation and trans-differentiation of prostatic stromal cells indicate suitability of phosphodiesterase type 5 inhibitors for prevention and treatment of benign prostatic hyperplasia. *Endocrinology*, 151(8), pp.3975–84.

Zenzmaier, C. et al., 2012. Phosphodiesterase type 5 inhibition reverts prostate fibroblast-to-myofibroblast trans-differentiation. *Endocrinology*, 153(11), pp.5546–55.

Zhang, L. et al., 2016. TGF-β1/FGF-2 signaling mediates the 15-HETE-induced differentiation of adventitial fibroblasts into myofibroblasts. *Lipids Health*

Dis, 15, p.2.

Zhang, Y. et al., 2011. High throughput determination of TGFβ1/SMAD3 targets in A549 lung epithelial cells. *PloS one*, 6(5), p.20319.

Zhao, Y. & Geverd, D., 2002. Regulation of Smad3 expression in bleomycin-induced pulmonary fibrosis: a negative feedback loop of TGF-beta signaling. *Biochem Biophys Res Commun*, 294(2), pp.319–23.

Appendix A

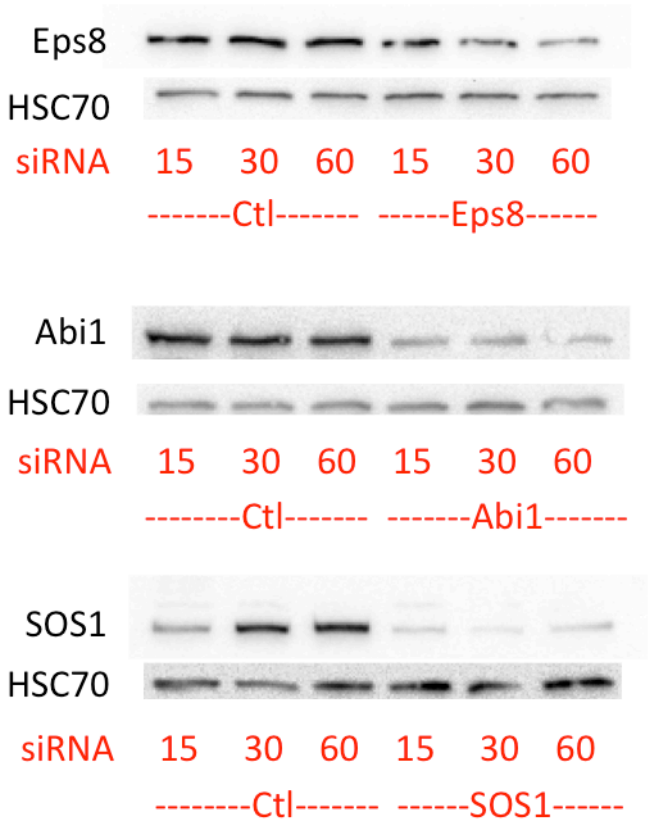

Figure 6-12 Optimisation of Eps8 siRNA concentration

HFFF2 were transfected with 15, 30 and 60nM of Control, Eps8, Abi1 and SOS1 siRNA and returned to serum-free DMEM after 24h. Fibroblasts were harvested at 72h and lysates run on Western blots. Hsc70 was used as a loading control.

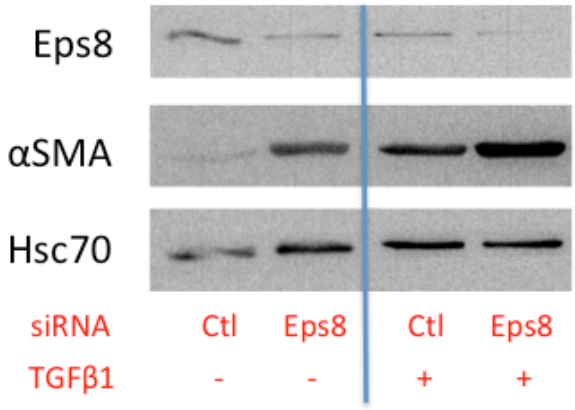

Figure 6-13 Confirmation of Eps8 knockdown (figure 3-9)

At the point of re-plating cells into chambers slides, remaining cells were re-plated in 6 well plates in serum-free medium +/- TGFβ1 and were cultured alongside the cells in chambers wells. They were lysed when the chambers slides were fixed, and subsequently lysates were run on a western blot using Hsc70 as a loading control.

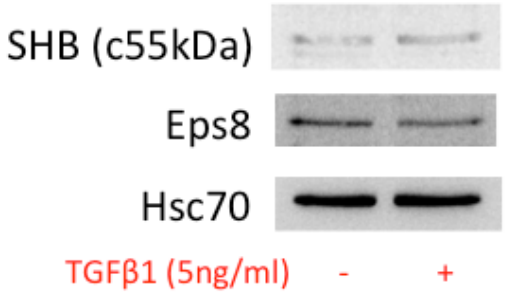

Figure 6-14 Shb expression does not significantly change as a result of TGFβ1 treatment

HFFF2 were plated and after 24h the medium was exchanged for serum-free medium +/- TGFβ1 5ng/ml. After a further 24h cells were lysed and lysates run on a western blot, with Hsc70 used as a loading control.

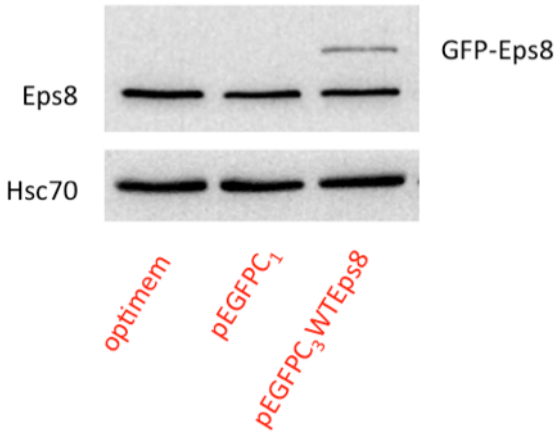

Figure 6-15 Overexpression of mouse Eps8 within human HFFF2 fibroblasts

HFFF2 were either sham-transfected with Optimem alone; with empty vector; or vector containing mouse Eps8. After 72h lysates were harvested and run on a Western blot with Hsc70 as a loading control.

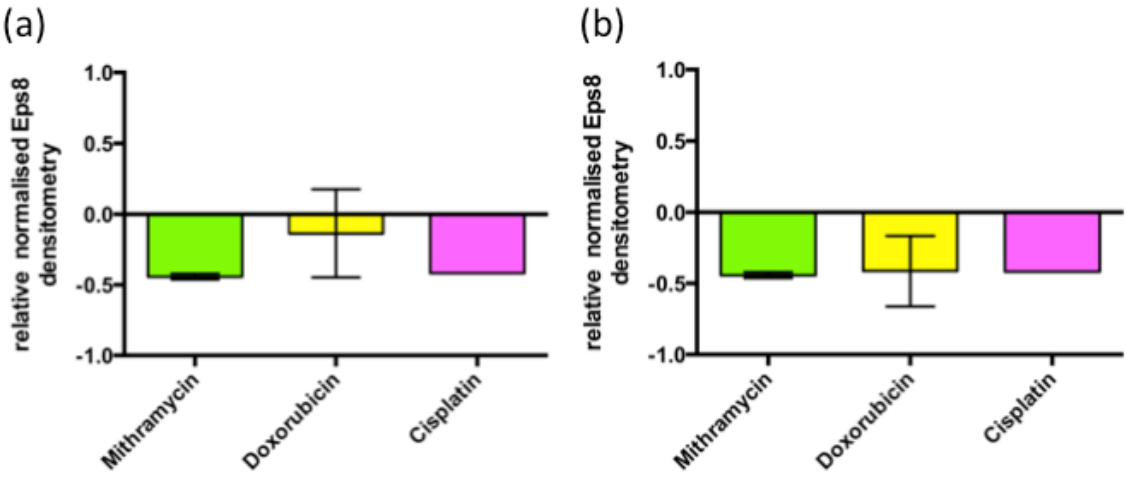

Figure 6-16 Fibroblast Eps8 expression is downregulated in response to various chemotherapeutic agents

HFFF2 were treated with 1uM mithramycin, 500nM doxorubicin or 20uM cisplatin or matched vehicles (PBS or DMSO) in serum-free DMEM for 24h. Medium was then replaced with serum-free DMEM for a further 24h before the cells were lysed and lysates run on Western blots. Hsc70 was used as a loading control. Within each experiment densitometry was performed on Eps8 bands and normalised against Hsc70. Normalised Eps8 relative fold change using the agent compared to the vehicle-only lane is expressed above across n independent experiments. (a) Includes all experiments: n = 2 for mithramycin; 3 for doxorubicin; 1 for cisplatin. (b) Excludes the final experiment using doxorubicin where no reduction was seen, and which may have resulted from reduced efficacy of the agent due to light exposure. Mean values displayed, error bars display SEM where shown.

Appendix B

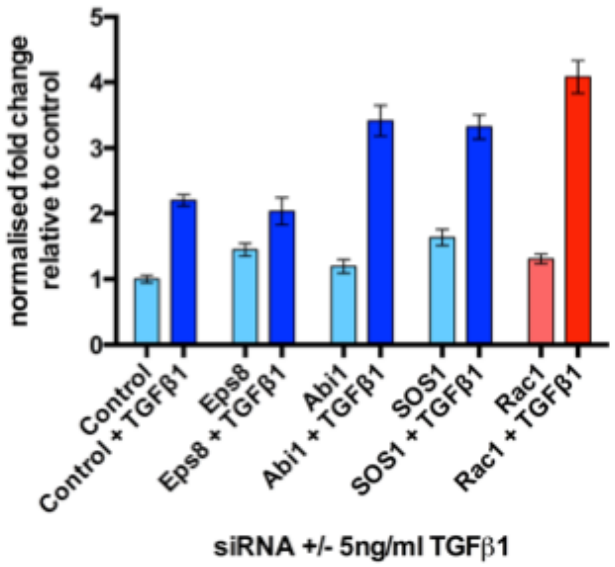

Figure 6-17 Rac1 knockdown augments TGFβ1-induced COL1A1 mRNA expression in HFFF2

HFFF2 fibroblasts were transfected with either non-targeting siRNA, or siRNA targeted against members of the tricomplex or Rac1. The following day medium was exchanged for serum-free medium +/- TGFβ1 (5ng/ml). After 48h mRNA was extracted for qRT-PCR. COL1A1 expression was normalised against GAPDH and is expressed above as fold change relative to the control-transfected, non-TGFβ1-treated condition. Error bars display the SD of 3 technical repeats from the same biological sample.

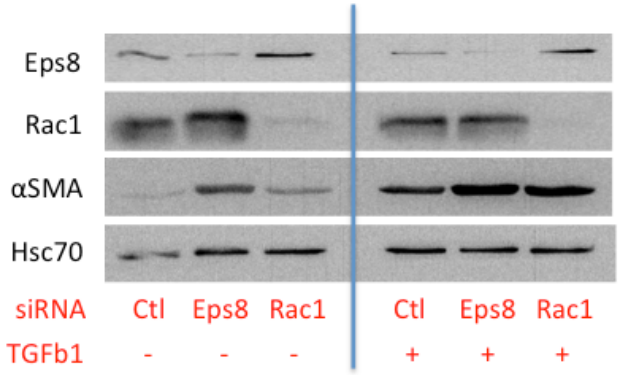

Figure 6-18 Western blot confirming Eps8 and Rac1 knockdowns during immunocytochemistry (figure 4-4)

HFFF2 fibroblasts were transfected with non-targeting / Eps8 / Rac1 siRNA and the next day were trypsinised and re-plated in either chambers slides (for immunocytochemistry) or 6 well plates (for Western blotting). The next day the medium on both the chambers and the 6 well plates was replaced with serum-free media +/- TGFβ1 for 3 days. When the chambers slides underwent immunocytochemistry the HFFF2 in the 6 well plates were lysed. Western blotting was performed using Hsc70 as a loading control.

TGFβ1 treatment

	Fold change	P value (adj)
Eps8	0.715	1.86E-05
Abi1	0.945	0.730
SOS1	0.840	0.143
Rac1	0.974	0.946

γ irradiation

	Fold change	P value (adj)
Eps8	0.620	2.30E-13
Abi1	1.044	0.729
SOS1	1.082	0.441
Rac1	0.920	0.294

Figure 6-19 RNAseq data from TGFβ1-treated and Ɣ-irradiated fibroblasts

Benjamini-Hochberg adjusted p-values and fold changes of mRNAs of interest are displayed. It is evident that both TGFβ1 treatment and Ɣ-irradiation result in statistically significant reductions in Eps8 expression compared to controls. Changes in Abi1, SOS1 and Rac1 expression were smaller and had large p values.

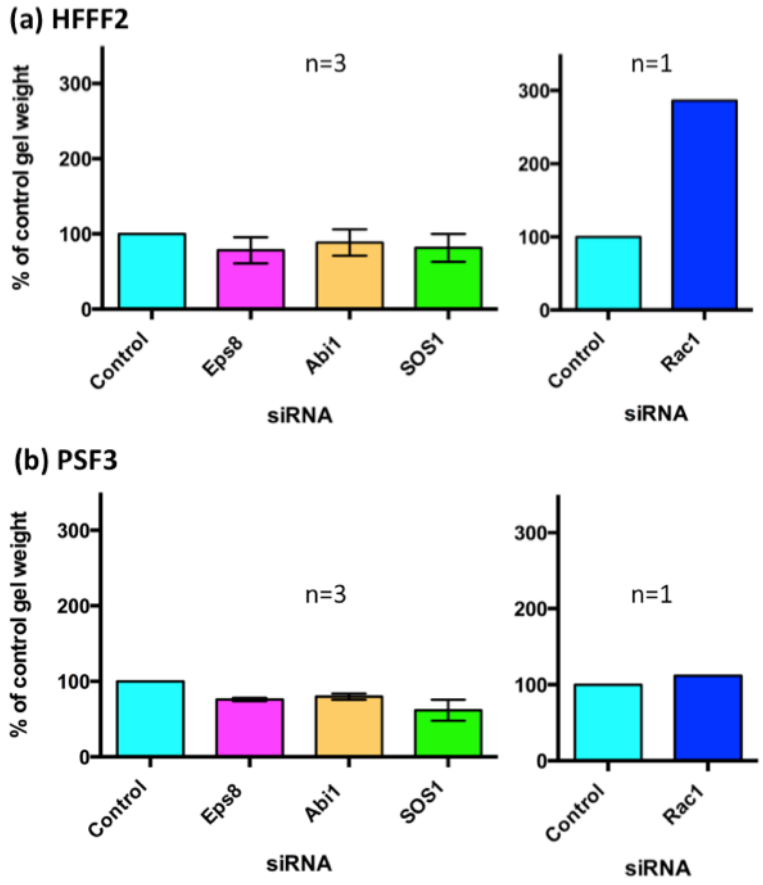

Figure 6-20 In the absence of TGFβ1, Rac1 knockdown may reduce fibroblast contractility

(a) HFFF2 or (b) PSF3 fibroblasts were transfected with siRNA, as labelled, and implanted into collagen gels. Gel weight was measured between 24-72h post-implantation. Knockdown of tricomplex members was undertaken in 3 independent experiments per fibroblast type; Rac1 knockdown was performed only once at time of writing.

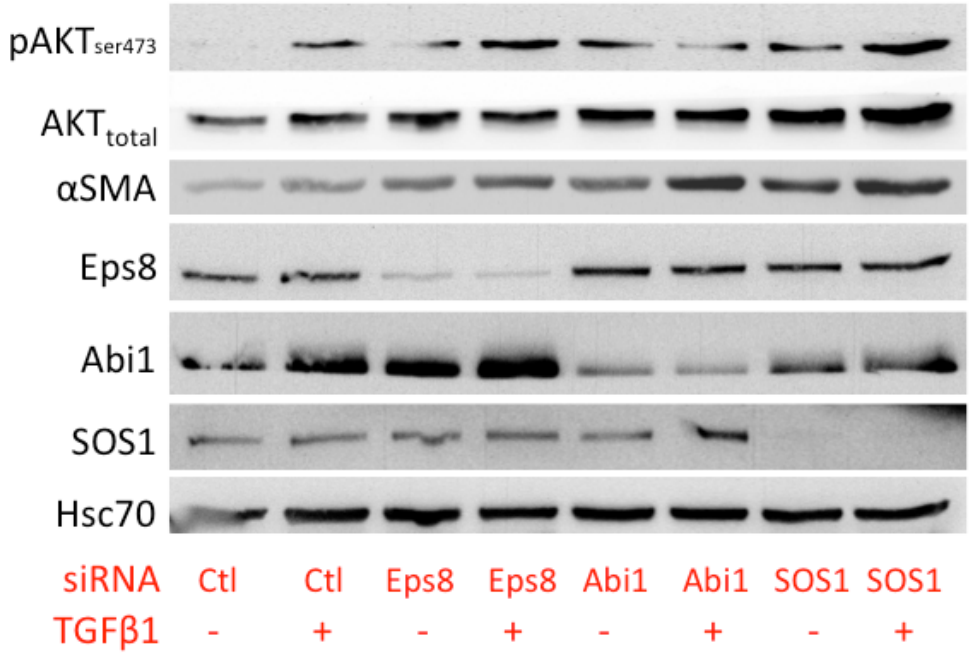

Figure 6-21 Akt ser473 phosphorylation results from knockdowns of Eps8 / binding partners, or treatment with TGFβ1

HFFF2 were transfected with non-targeting / Eps8 / Abi1 / SOS1 siRNA and the next day media was exchanged for serum-free media +/- TGFβ1 (5ng/ml). After 72h lysates were extracted for Western blotting. Hsc70 was used as a loading control.

Appendix C

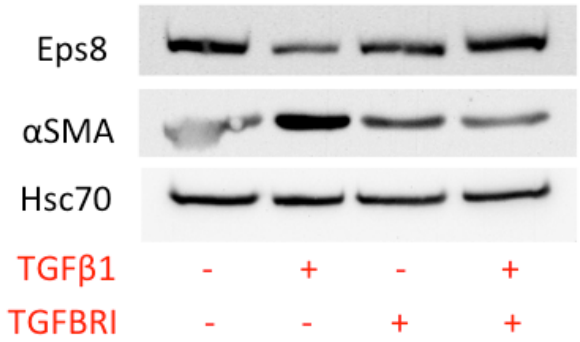

Figure 6-22 Western blot confirming the efficacy of the TGFβR1 (ALK5) inhibitor.

The day following plating, medium on HFFF2 was exchanged for serum-free DMEM +/- 1uM TGFβR1 inhibitor kinase IV. After 1h, human recombinant TGFβ1 (5ng/ml) was added to appropriate wells, cells lysed after 72h, and lysates processed for Western blotting. Hsc70 was used as a loading control.

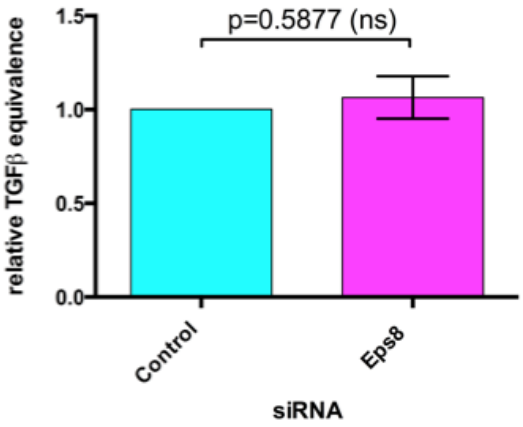

Figure 6-23 TGFβ activation assay demonstrating no significant effect of fibroblast Eps8 knockdown on TGFβ activation

HFFF2 fibroblasts were transfected with either non-targeting or Eps8 siRNA. After 4h the cells were trypsinised and plated on an MLEC monolayer and the cells were incubated overnight. The next day the cells were lysed and the luciferase assay was performed. A reference curve with exogenous TGFβ treatment was performed within each assay, to generate a mean TGFβ-equivalent value. Displayed are mean TGFβ equivalent values for Eps8 knockdown fibroblasts compared to control-transfected fibroblasts across 4 independent experiments. Error bars display SEM and a two-tailed t test was performed to assess statistical significance.

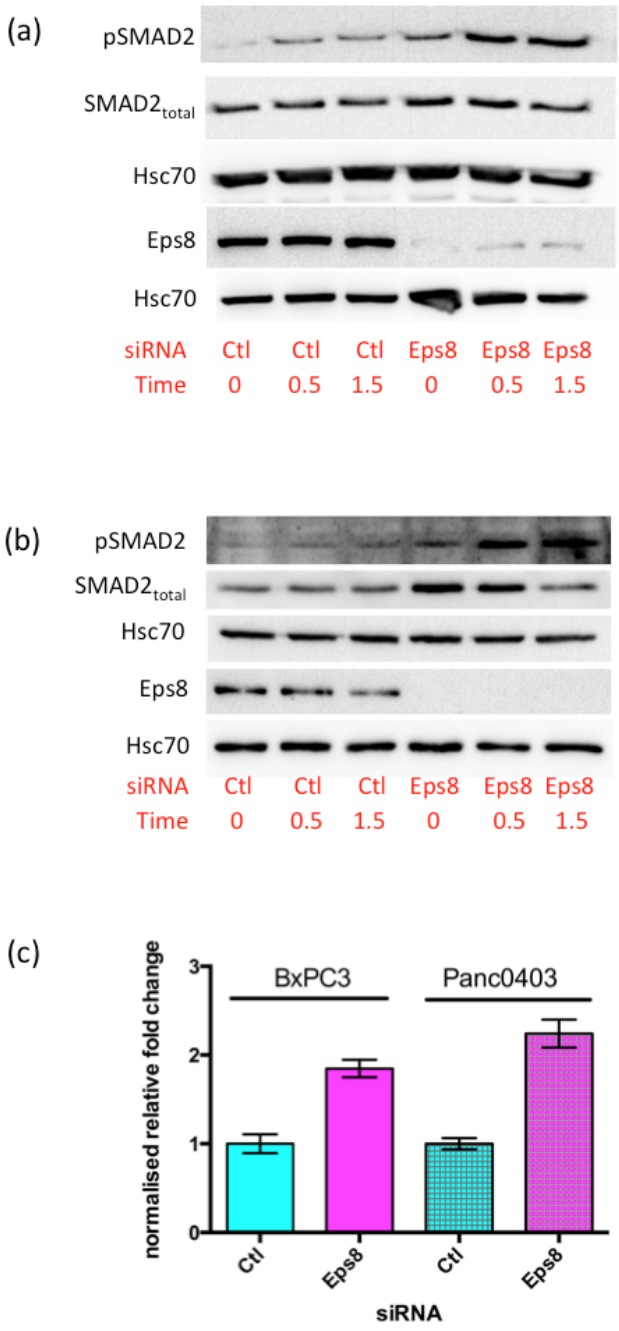

Figure 6-24 Eps8 knockdown in cancer cells increases SMAD2 expression at mRNA and protein levels, and facilitates increased SMAD2 phosphorylation by TGFβ1.

Cells from (a) BxPC3 and (b) Panc0403 pancreatic cancer cell lines were transfected with Eps8 or non-targeting siRNA. After overnight incubation cells were treated with TGFβ1. Cells were then harvested for Western blotting either before (time 0), 0.5 or 1.5h after TGFβ1 treatment. Hsc70 was used as a loading control. (c) mRNA expression was also analysed for cells from each cell line, harvested after transfection, immediately before TGFβ1 treatment. SMAD2 mRNA expression is displayed, normalised against GAPDH and displayed relative to expression in control-transfected cells.

TGFβ1 treatment

	Fold change	P value (adj)
SMAD3	0.515	1.86E-22

γ irradiation

	Fold change	P value (adj)
SMAD3	0.747	3.48E-07

Figure 6-25 RNAseq data confirms SMAD3 downregulation following TGFβ1 treatment / γ-irradiation

For the TGFβ1 treatment experiment HFFF2 fibroblasts were treated with 10% DMEM +/- 2ng/ml TGFβ1 for 3 days, and then 10% DMEM for 4 days. For the irradiation experiment, HFFF2s were trypsinised +/- irradiated with 10Gy γ irradiation before being re-plated for 7 days. Fold change for SMAD3 mRNA compared to controls along with Benjamini-Hochberg adjusted p-values are shown for both experiments performed by my co-workers.

Appendix D

(a)

Primary Analysis Information

	Read 1	Read 2
Read Length	43	43
Number of Reads	22,136,177	22,136,177
Bases (GB)	0.94	0.94
Q30 Bases (GB)	0.90	0.87

Insert Information

Insert Length Mean	136.24
Insert Length S.D.	46.37
Duplicates (% Reads)	12.55%

Alignment Quality

	Read 1	Read 2
Total Aligned Reads (% Reads)	97.80%	95.16%
Abundant Reads (% Reads)	8.43%	8.35%
Unaligned Reads (% Reads)	2.20%	4.84%
Reads with spliced alignment (% Aligned Reads)	15.70%	17.11%
Reads aligned at multiple loci (% Aligned Reads)	2.36%	2.34%

(b)

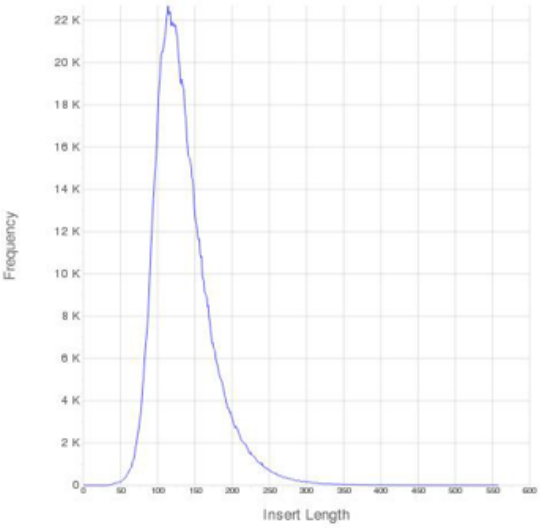

(c)

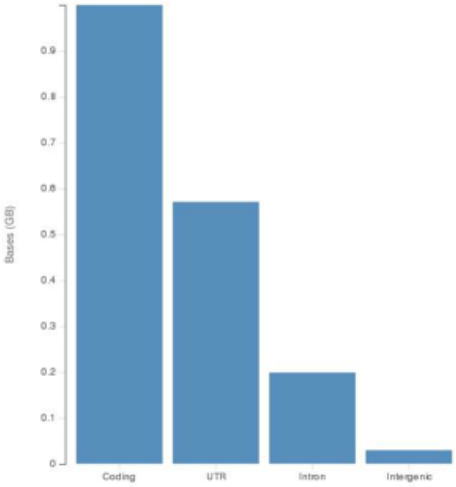

(d)

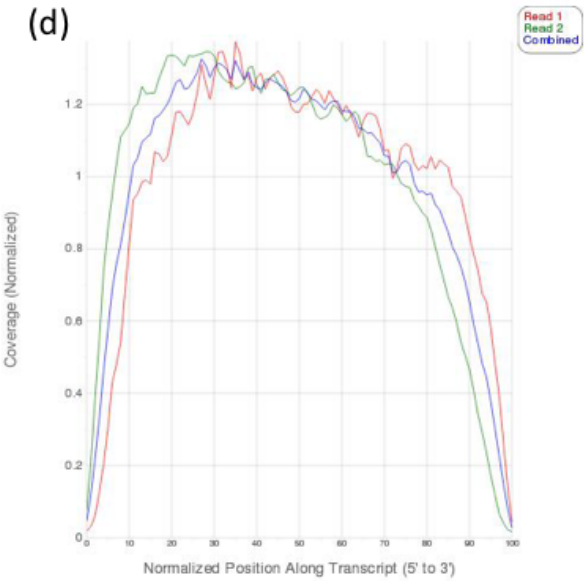

Figure 6-26 Quality assessment of sample following RNA-seq alignment

For the 'Control no TGFβ1 (1)' sample the data report provides an assessment of (a) read length, number of reads, and alignment quality (b) insert length distribution, (c) alignment distribution and (d) transcript coverage, indicating that the data was of good quality.

(a)

Primary Analysis Information

	Read 1	Read 2
Read Length	43	43
Number of Reads	21,428,582	21,428,582
Bases (GB)	0.91	0.91
Q30 Bases (GB)	0.87	0.84

Insert Information

Insert Length Mean	135.94
Insert Length S.D.	46.63
Duplicates (% Reads)	13.13%

Alignment Quality

	Read 1	Read 2
Total Aligned Reads (% Reads)	97.85%	95.10%
Abundant Reads (% Reads)	8.05%	7.97%
Unaligned Reads (% Reads)	2.15%	4.90%
Reads with spliced alignment (% Aligned Reads)	15.83%	17.21%
Reads aligned at multiple loci (% Aligned Reads)	2.27%	2.25%

(b)

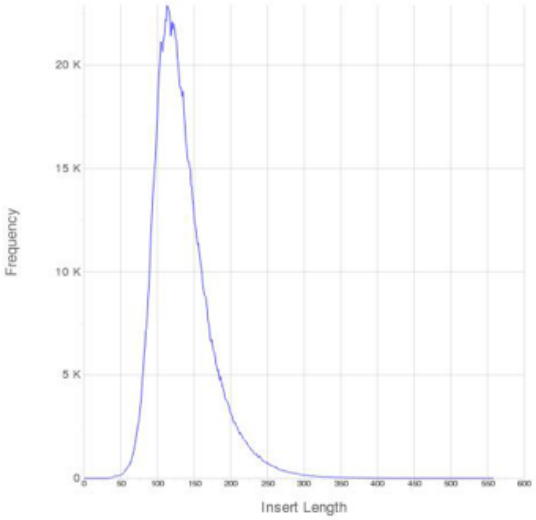

(c)

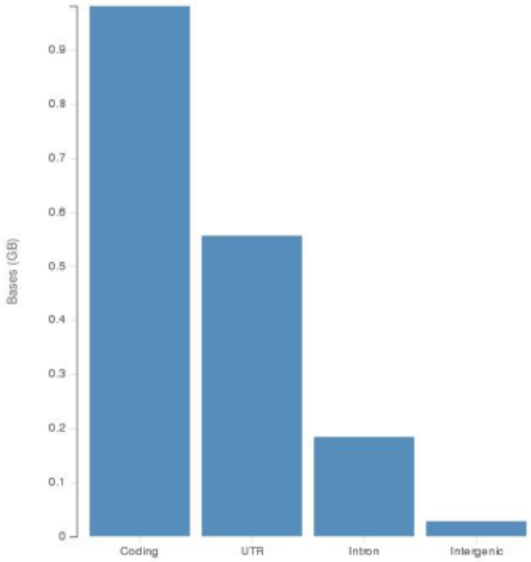

(d)

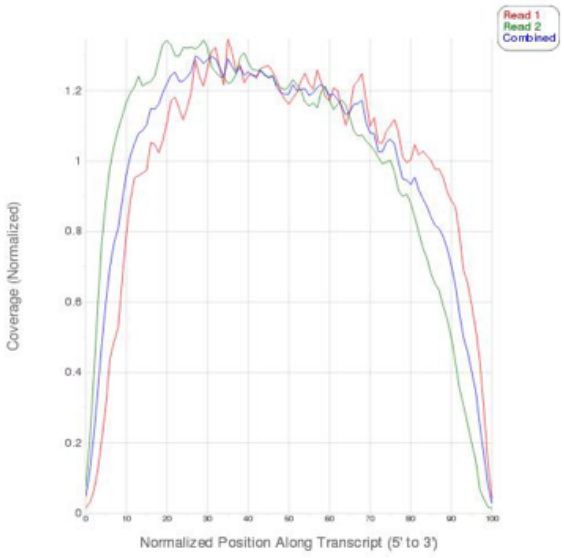

Figure 6-27 Quality assessment of sample following RNA-seq alignment

For the 'Control no TGFβ1 (2)' sample the data report provides an assessment of (a) read length, number of reads, and alignment quality (b) insert length distribution, (c) alignment distribution and (d) transcript coverage, indicating that the data was of good quality.

(a)

Primary Analysis Information

	Read 1	Read 2
Read Length	43	43
Number of Reads	20,600,632	20,600,632
Bases (GB)	0.87	0.87
Q30 Bases (GB)	0.83	0.80

Insert Information

Insert Length Mean	136.59
Insert Length S.D.	47.42
Duplicates (% Reads)	12.81%

Alignment Quality

	Read 1	Read 2
Total Aligned Reads (% Reads)	97.56%	94.45%
Abundant Reads (% Reads)	9.15%	9.09%
Unaligned Reads (% Reads)	2.44%	5.55%
Reads with spliced alignment (% Aligned Reads)	15.49%	16.89%
Reads aligned at multiple loci (% Aligned Reads)	2.36%	2.34%

(b)

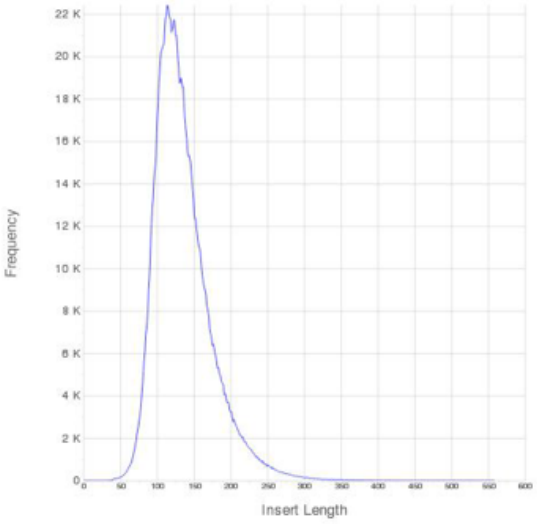

(c)

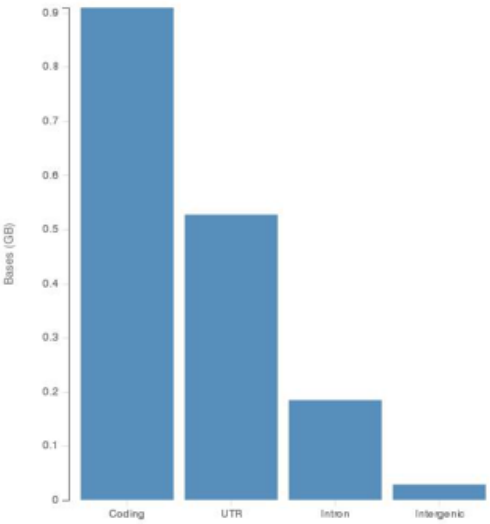

(d)

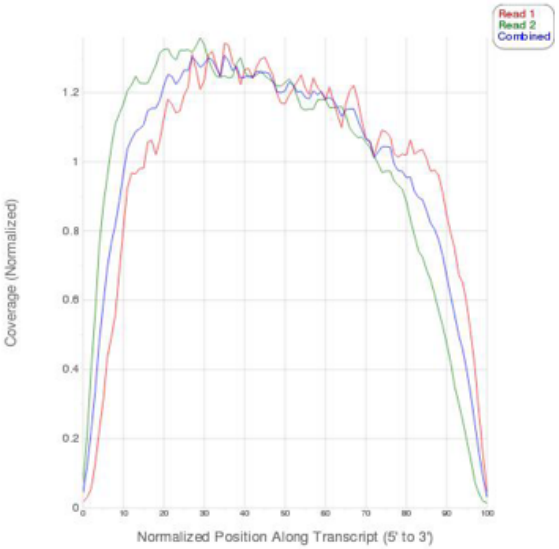

Figure 6-28 Quality assessment of sample following RNA-seq alignment

For the 'Control no TGFβ1 (3)' sample the data report provides an assessment of (a) read length, number of reads, and alignment quality (b) insert length distribution, (c) alignment distribution and (d) transcript coverage, indicating that the data was of good quality.

(a)

Primary Analysis Information

	Read 1	Read 2
Read Length	43	43
Number of Reads	19,600,903	19,600,903
Bases (GB)	0.83	0.83
Q30 Bases (GB)	0.79	0.76

Insert Information

Insert Length Mean	134.01
Insert Length S.D.	47.90
Duplicates (% Reads)	15.48%

Alignment Quality

	Read 1	Read 2
Total Aligned Reads (% Reads)	97.58%	94.64%
Abundant Reads (% Reads)	7.83%	7.77%
Unaligned Reads (% Reads)	2.42%	5.36%
Reads with spliced alignment (% Aligned Reads)	16.38%	17.58%
Reads aligned at multiple loci (% Aligned Reads)	2.10%	2.08%

(b)

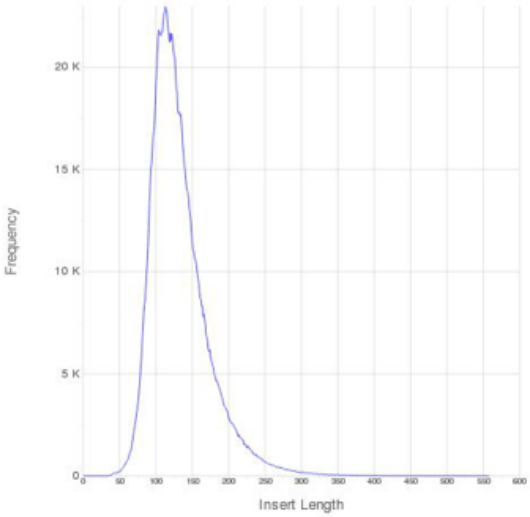

(c)

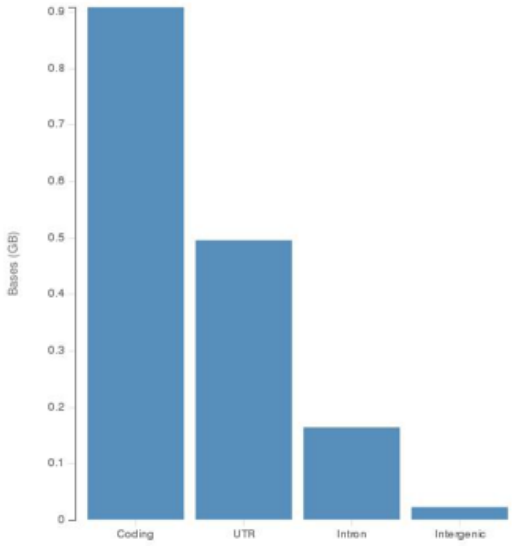

(d)

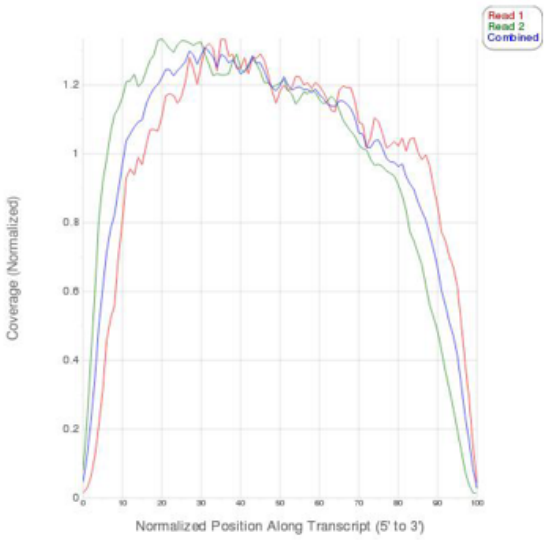

Figure 6-29 Quality assessment of sample following RNA-seq alignment

For the 'Control + TGFβ1 (1)' sample the data report provides an assessment of (a) read length, number of reads, and alignment quality (b) insert length distribution, (c) alignment distribution and (d) transcript coverage, indicating that the data was of good quality.

(a)

Primary Analysis Information

	Read 1	Read 2
Read Length	43	43
Number of Reads	18,279,853	18,279,853
Bases (GB)	0.78	0.77
Q30 Bases (GB)	0.74	0.71

Insert Information

Insert Length Mean	138.19
Insert Length S.D.	50.29
Duplicates (% Reads)	18.17%

Alignment Quality

	Read 1	Read 2
Total Aligned Reads (% Reads)	97.52%	94.40%
Abundant Reads (% Reads)	7.60%	7.72%
Unaligned Reads (% Reads)	2.48%	5.60%
Reads with spliced alignment (% Aligned Reads)	16.37%	17.63%
Reads aligned at multiple loci (% Aligned Reads)	2.12%	2.09%

(b)

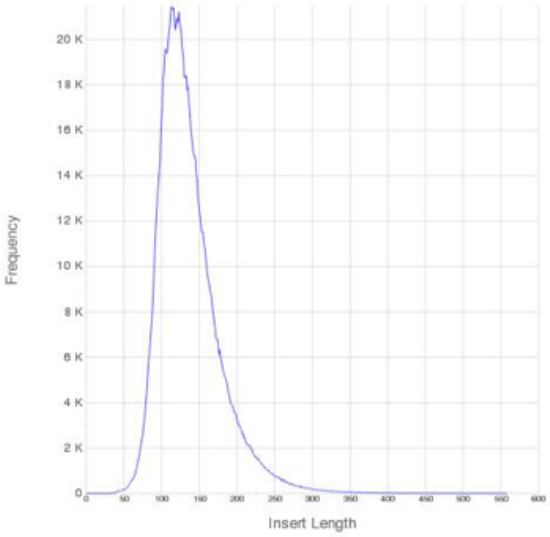

(c)

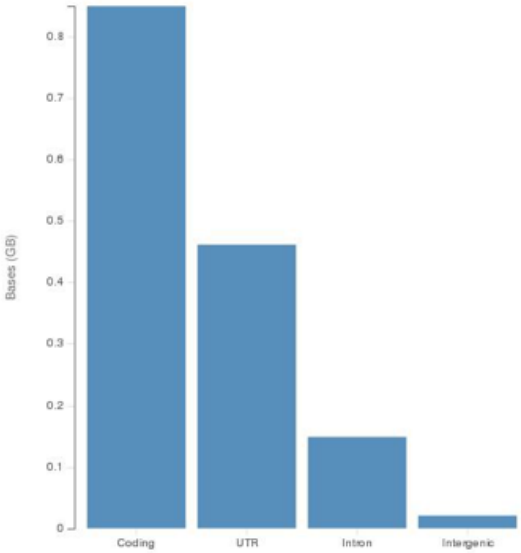

(d)

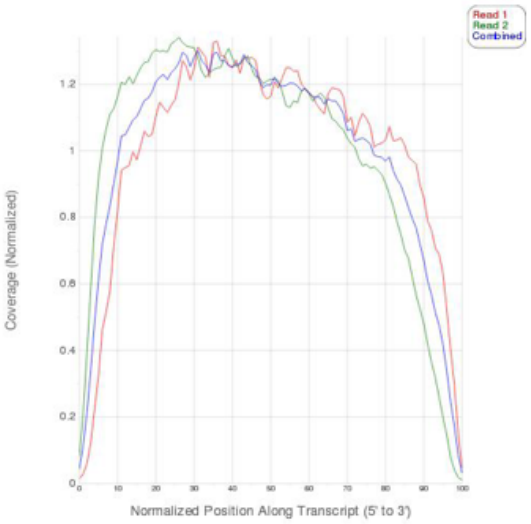

Figure 6-30 Quality assessment of sample following RNA-seq alignment

For the 'Control + TGFβ1 (2)' sample the data report provides an assessment of (a) read length, number of reads, and alignment quality (b) insert length distribution, (c) alignment distribution and (d) transcript coverage, indicating that the data was of good quality.

(a)

Primary Analysis Information

	Read 1	Read 2
Read Length	43	43
Number of Reads	16,752,754	16,752,754
Bases (GB)	0.71	0.71
Q30 Bases (GB)	0.67	0.64

Insert Information

Insert Length Mean	136.78
Insert Length S.D.	48.56
Duplicates (% Reads)	15.49%

Alignment Quality

	Read 1	Read 2
Total Aligned Reads (% Reads)	97.37%	93.80%
Abundant Reads (% Reads)	8.08%	8.05%
Unaligned Reads (% Reads)	2.63%	6.20%
Reads with spliced alignment (% Aligned Reads)	16.19%	17.43%
Reads aligned at multiple loci (% Aligned Reads)	2.15%	2.12%

(b)

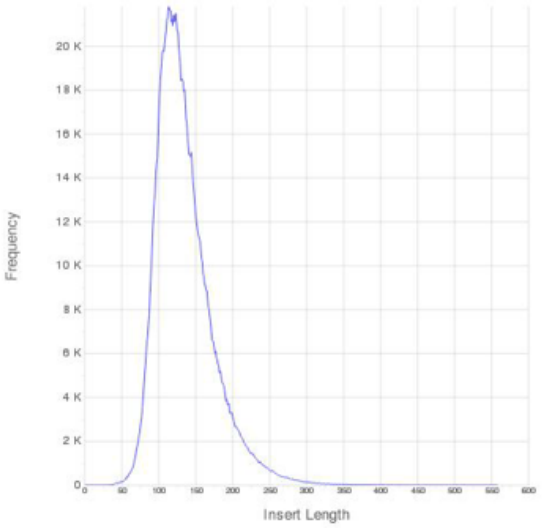

(c)

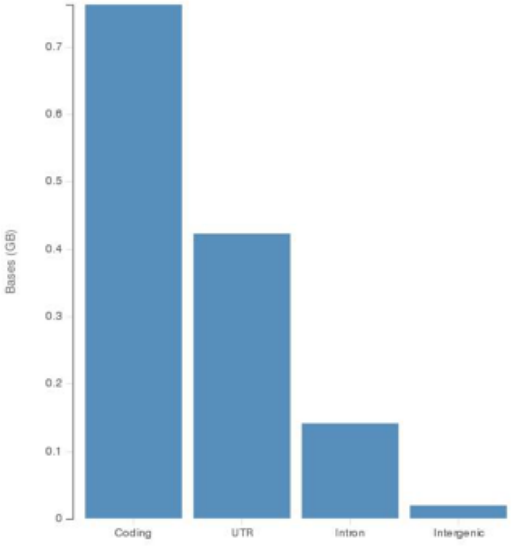

(d)

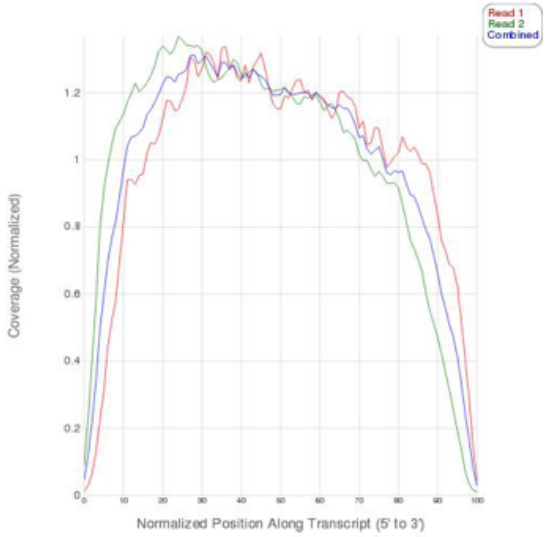

Figure 6-31 Quality assessment of sample following RNA-seq alignment

For the 'Control + TGFβ1 (3)' sample the data report provides an assessment of (a) read length, number of reads, and alignment quality (b) insert length distribution, (c) alignment distribution and (d) transcript coverage, indicating that the data was of good quality.

(a)

Primary Analysis Information

	Read 1	Read 2
Read Length	43	43
Number of Reads	18,658,051	18,658,051
Bases (GB)	0.79	0.79
Q30 Bases (GB)	0.76	0.72

Insert Information

Insert Length Mean	135.09
Insert Length S.D.	49.53
Duplicates (% Reads)	15.95%

Alignment Quality

	Read 1	Read 2
Total Aligned Reads (% Reads)	97.43%	94.12%
Abundant Reads (% Reads)	10.86%	10.93%
Unaligned Reads (% Reads)	2.57%	5.88%
Reads with spliced alignment (% Aligned Reads)	15.25%	16.64%
Reads aligned at multiple loci (% Aligned Reads)	2.48%	2.45%

(b)

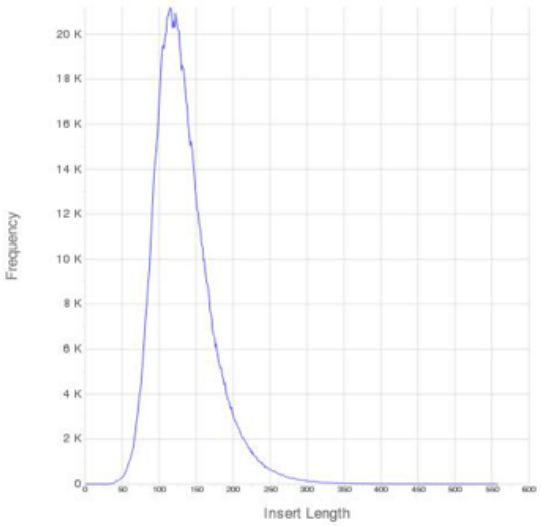

(c)

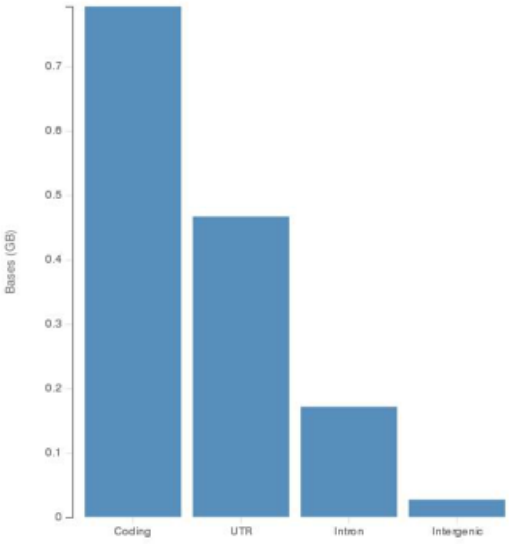

(d)

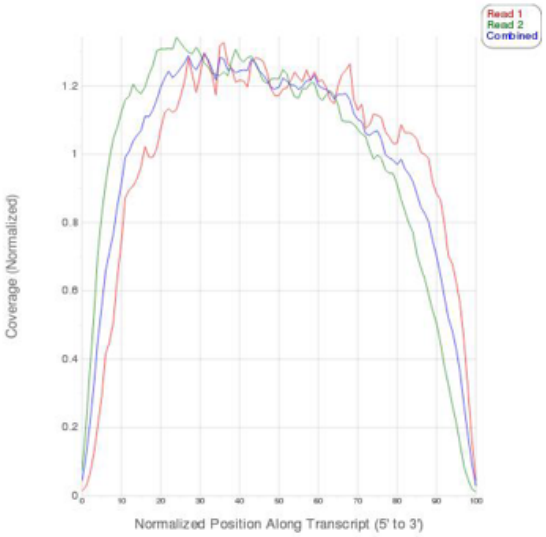

Figure 6-32 Quality assessment of sample following RNA-seq alignment

For the 'Eps8 KD no TGFβ1 (1)' sample the data report provides an assessment of (a) read length, number of reads, and alignment quality (b) insert length distribution, (c) alignment distribution and (d) transcript coverage, indicating that the data was of good quality.

(a)

Primary Analysis Information

	Read 1	Read 2
Read Length	43	43
Number of Reads	17,335,814	17,335,814
Bases (GB)	0.74	0.73
Q30 Bases (GB)	0.70	0.65

Insert Information

Insert Length Mean	139.90
Insert Length S.D.	52.12
Duplicates (% Reads)	14.36%

Alignment Quality

	Read 1	Read 2
Total Aligned Reads (% Reads)	96.89%	92.24%
Abundant Reads (% Reads)	9.86%	10.04%
Unaligned Reads (% Reads)	3.11%	7.76%
Reads with spliced alignment (% Aligned Reads)	15.63%	17.07%
Reads aligned at multiple loci (% Aligned Reads)	2.42%	2.39%

(b)

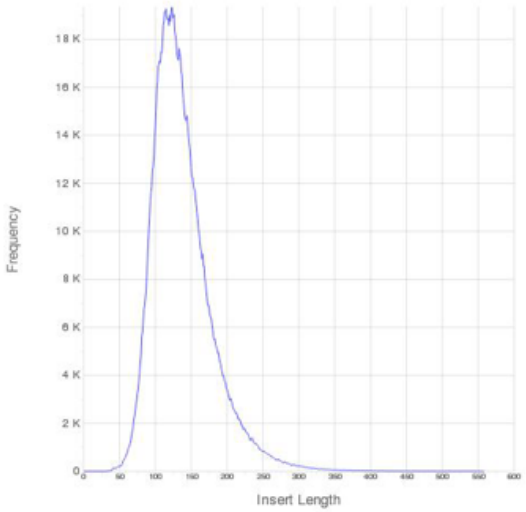

(c)

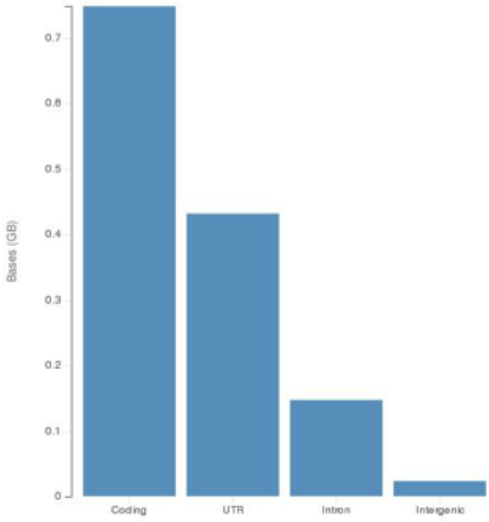

(d)

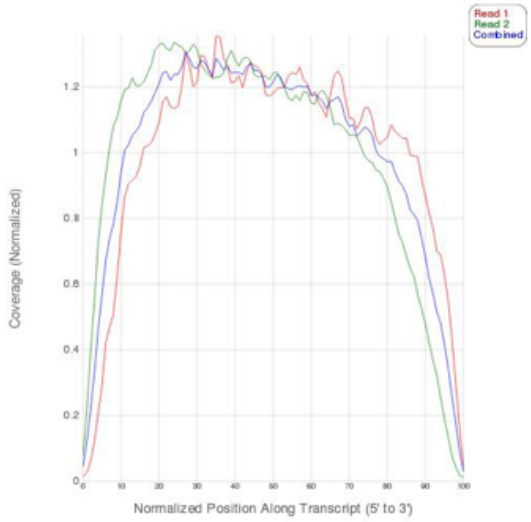

Figure 6-33 Quality assessment of sample following RNA-seq alignment

For the 'Eps8 KD no TGFβ1 (2)' sample the data report provides an assessment of (a) read length, number of reads, and alignment quality (b) insert length distribution, (c) alignment distribution and (d) transcript coverage, indicating that the data was of good quality.

(a)

Primary Analysis Information

	Read 1	Read 2
Read Length	43	43
Number of Reads	19,488,054	19,488,054
Bases (GB)	0.83	0.83
Q30 Bases (GB)	0.79	0.75

Insert Information

Insert Length Mean	135.88
Insert Length S.D.	49.94
Duplicates (% Reads)	16.25%

Alignment Quality

	Read 1	Read 2
Total Aligned Reads (% Reads)	97.21%	93.59%
Abundant Reads (% Reads)	10.32%	10.44%
Unaligned Reads (% Reads)	2.79%	6.41%
Reads with spliced alignment (% Aligned Reads)	15.41%	16.86%
Reads aligned at multiple loci (% Aligned Reads)	2.43%	2.40%

(b)

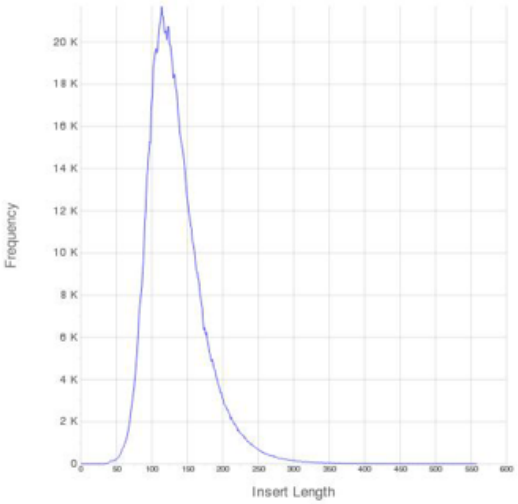

(c)

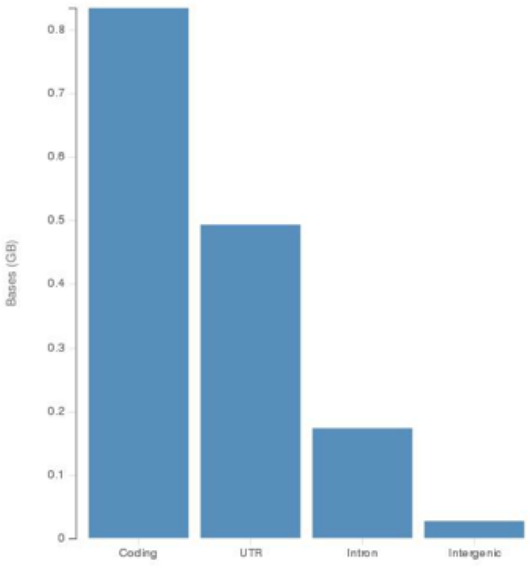

(d)

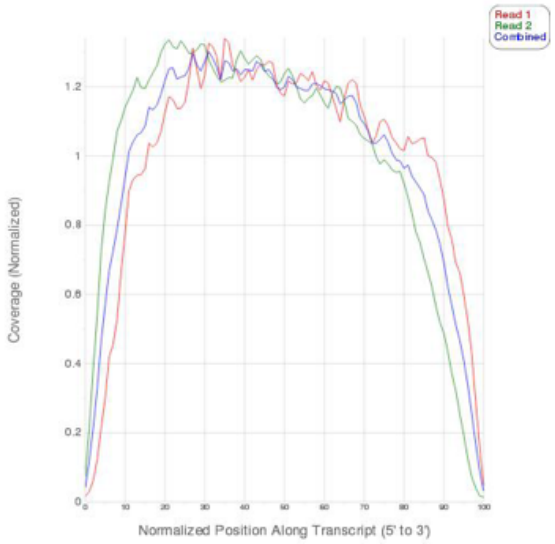

Figure 6-34 Quality assessment of sample following RNA-seq alignment

For the 'Eps8 KD no TGFβ1 (3)' sample the data report provides an assessment of (a) read length, number of reads, and alignment quality (b) insert length distribution, (c) alignment distribution and (d) transcript coverage, indicating that the data was of good quality.

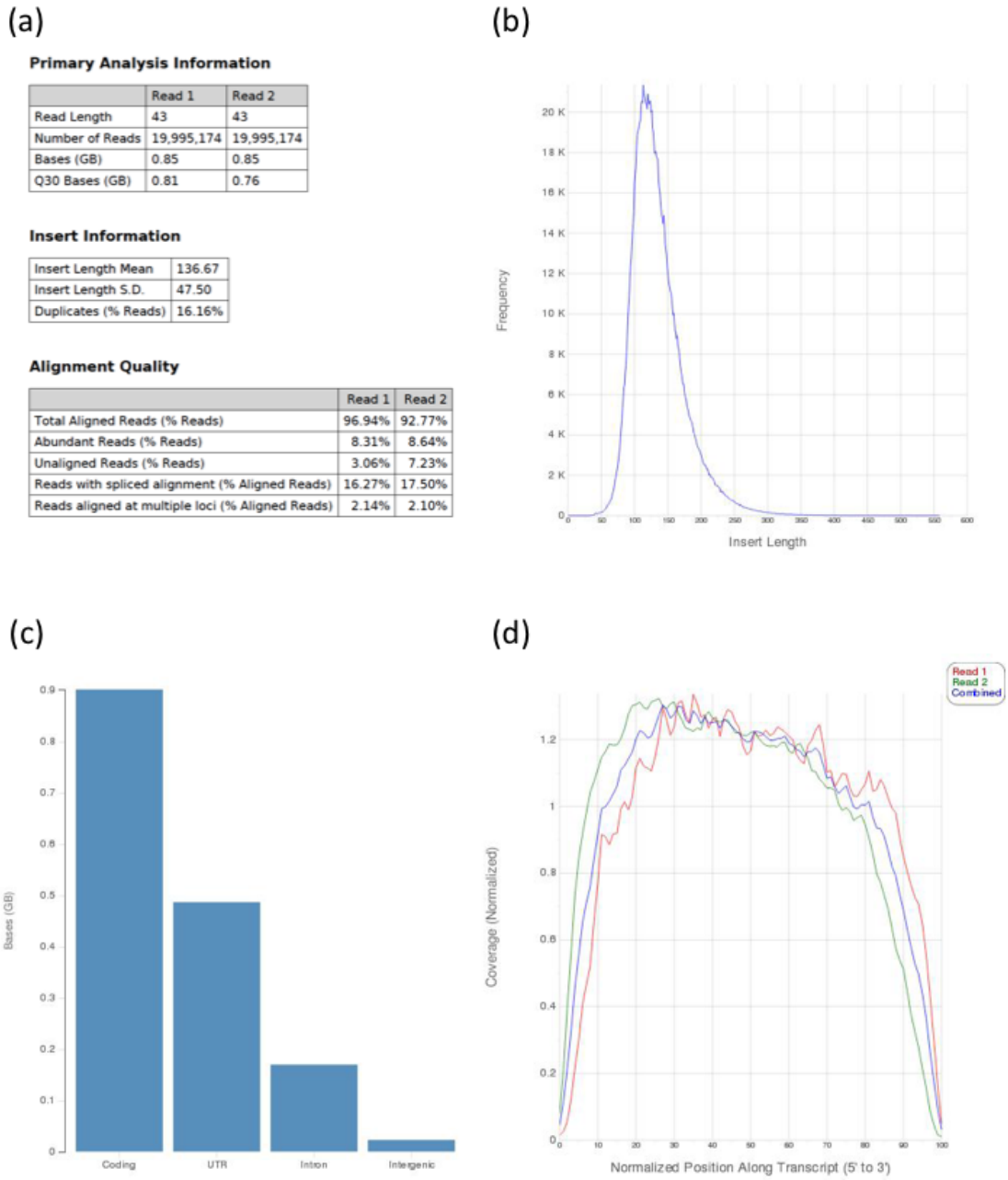

Figure 6-35 Quality assessment of sample following RNA-seq alignment

For the 'Eps8 KD + TGFβ1 (1)' sample the data report provides an assessment of (a) read length, number of reads, and alignment quality (b) insert length distribution, (c) alignment distribution and (d) transcript coverage, indicating that the data was of good quality.

(a)

Primary Analysis Information

	Read 1	Read 2
Read Length	43	43
Number of Reads	19,026,539	19,026,539
Bases (GB)	0.81	0.81
Q30 Bases (GB)	0.77	0.74

Insert Information

Insert Length Mean	136.42
Insert Length S.D.	47.81
Duplicates (% Reads)	17.27%

Alignment Quality

	Read 1	Read 2
Total Aligned Reads (% Reads)	97.62%	94.78%
Abundant Reads (% Reads)	7.26%	7.23%
Unaligned Reads (% Reads)	2.38%	5.22%
Reads with spliced alignment (% Aligned Reads)	16.45%	17.65%
Reads aligned at multiple loci (% Aligned Reads)	2.04%	2.02%

(b)

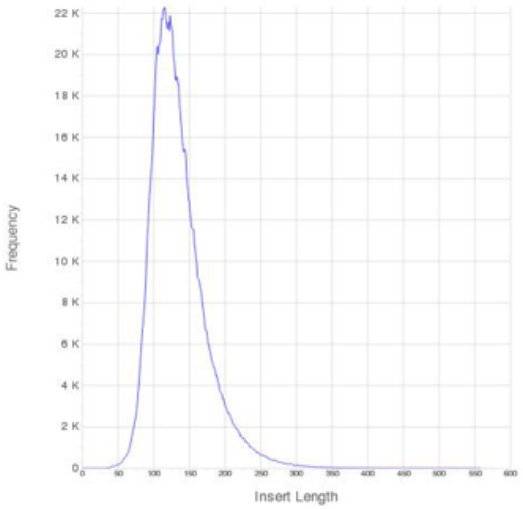

(c)

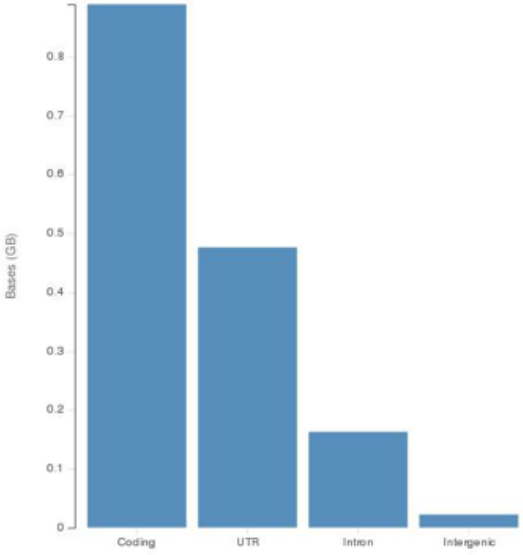

(d)

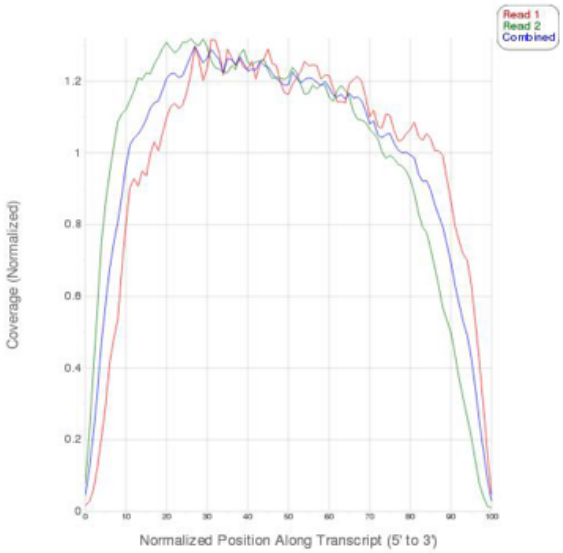

Figure 6-36 Quality assessment of sample following RNA-seq alignment

For the 'Eps8 KD + TGFβ1 (2)' sample the data report provides an assessment of (a) read length, number of reads, and alignment quality (b) insert length distribution, (c) alignment distribution and (d) transcript coverage, indicating that the data was of good quality.

(a)

Primary Analysis Information

	Read 1	Read 2
Read Length	43	43
Number of Reads	18,286,360	18,286,360
Bases (GB)	0.78	0.77
Q30 Bases (GB)	0.74	0.71

Insert Information

Insert Length Mean	138.00
Insert Length S.D.	50.48
Duplicates (% Reads)	16.32%

Alignment Quality

	Read 1	Read 2
Total Aligned Reads (% Reads)	97.66%	94.85%
Abundant Reads (% Reads)	8.83%	8.72%
Unaligned Reads (% Reads)	2.34%	5.15%
Reads with spliced alignment (% Aligned Reads)	16.34%	17.67%
Reads aligned at multiple loci (% Aligned Reads)	2.16%	2.14%

(b)

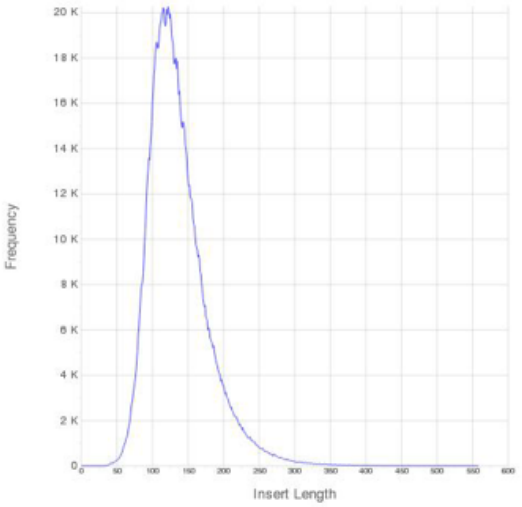

(c)

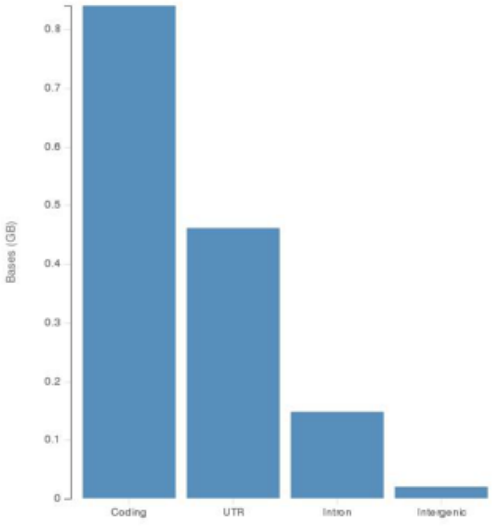

(d)

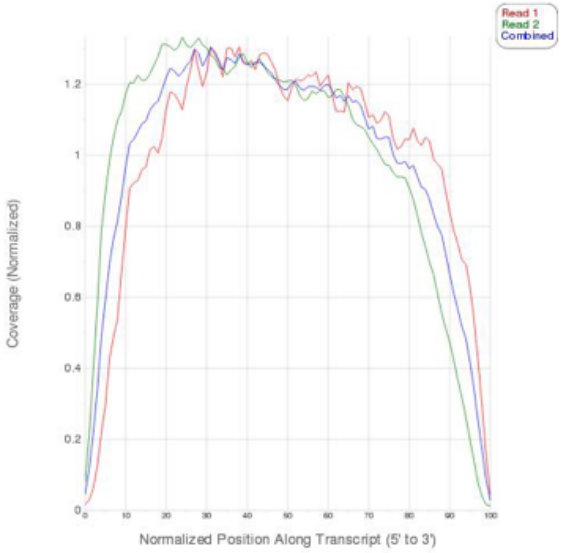

Figure 6-37 Quality assessment of sample following RNA-seq alignment

For the 'Eps8 KD + TGFβ1 (3)' sample the data report provides an assessment of (a) read length, number of reads, and alignment quality (b) insert length distribution, (c) alignment distribution and (d) transcript coverage, indicating that the data was of good quality.

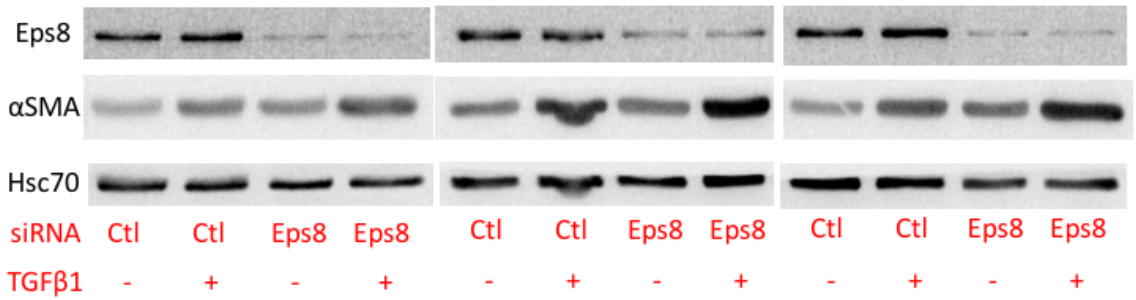

Figure 6-38 Western blotting of parallel samples after 72h of TGFβ1 treatment.

Some 6 well plates were not harvested in the RNA-seq experiment and were maintained in culture with 72h of TGFβ1 treatment (5ng/ml) before lysates were harvested. The western blots confirm continued Eps8 knockdown, effective TGFβ1-induced αSMA induction , and its augmentation by prior Eps8 knockdown. Hsc70 was used as a loading control. The three western blots relate to the three experimental repeats with successive passage of HFFF2.
